# Insulin sensitivity of hepatic glucose and lipid metabolism in animal models of hepatic steatosis

Cover and page design: Maaike Leemreize and Aldo Grefhorst
Printed by Ponsen & Looijen B.V., Wageningen, The Netherlands

**RIJKSUNIVERSITEIT GRONINGEN**

# Insulin sensitivity of hepatic glucose and lipid metabolism in animal models of hepatic steatosis

**Proefschrift**

ter verkrijging van het doctoraat in de
Medische Wetenschappen
aan de Rijksuniversiteit Groningen
op gezag van de
Rector Magnificus, dr. F. Zwarts,
in het openbaar te verdedigen op
woensdag 18 januari 2006
om 16.15 uur

door

**Aldo Grefhorst**

geboren op 25 oktober 1974
te Apeldoorn

**Promotores**
Prof. dr. F. Kuipers
Prof. dr. L.M. Havekes
Prof. dr. J.A. Romijn

**Beoordelingscommissie**
Prof. dr. J.D. Horton
Prof. dr. P.J.J. Sauer
Prof. dr. B. Staels

ISBN papieren versie: 90-367-2469-4
ISBN elektronische versie: 90-367-2470-8

**Paranimfen**
Arnout van der Borden
Ronald Grefhorst

**Research**
The studies described in this thesis were conducted within the Groningen University Institute for Drug Exploration (GUIDE), Center for Liver, Digestive, and Metabolic Diseases, Department of Pediatrics, University Medical Center Groningen, University of Groningen, The Netherlands.

**Funding**
The studies described in this thesis were supported by grant 903-39-291 from the Netherlands Organization for Scientific Research (NWO), Den Haag, The Netherlands.

**Printing of this thesis was financially supported by**
Diabetesfonds Nederland, Amersfoort, The Netherlands
Rijksuniversiteit Groningen, Groningen, The Netherlands
Groningen University Institute for Drug Exploration (GUIDE), Groningen, The Netherlands
Nederlandse Vereniging voor Hepatologie, Haarlem, The Netherlands
Harlan Nederland, Horst, The Netherlands

Their contribution is gratefully acknowledged!

# Table of contents

# Chapter 1

# General introduction

## Hepatic steatosis: definitions, stages, prevalence and association with insulin resistance

Hepatic steatosis refers to the, nowadays common, condition of ectopic accumulation of triglycerides (TG) in parenchymal cells (hepatocytes) of the liver. This condition is therefore also termed "fatty liver". Several forms of hepatic steatosis are generally distinguished, depending on underlying cause of the condition and the progression of the disease. Excessive and chronic alcohol consumption has been known for decades to be associated with alcoholic fatty liver, a condition that is beyond the scope of this thesis. Interested readers are therefore referred to recently published, excellent reviews on this topic (1-4).

In 1980, Ludwig *et al*. (5) were the first to describe the appearance of hepatic steatosis without excessive alcohol usage, a condition they termed nonalcoholic steatohepatitis (NASH). Nowadays, non-alcoholic fatty liver (NAFL) is considered the precursor of NASH and both conditions are non-alcoholic fatty liver diseases (NAFLDs) (6). Table 1.1 shows the major causes of NAFLD, as recently published by Adams *et al.* (7). Especially the association of hepatic steatosis with features of the metabolic syndrome is of interest for this thesis and will be discussed in more detail later in this introduction.

Studies suggest that circa 20% of NASH will finally result in cirrhosis (8). A recent editorial in Gastroenterology (9), however, summarized that 'simple steatosis' itself might be relatively benign: over a 15-20 years period, only 1-2% of the patients with this condition actually developed cirrhosis. In patients with fibrosis and NASH, this percentage might be up to 12% in 8 years. The largest natural history study performed so far in patients with NAFLD (10) showed that mortality in these patients is higher than in patients without NAFLD and associated not only with cirrhosis, but also with age and impaired fasting glucose. When cirrhotic patients were excluded, the overall mortality was not increased. Thus, these human data stress the importance of staging the hepatic steatosis found.

In NAFLD, the liver contains more than normal amounts of TG, the most energy-dense molecules in mammalian physiology. TG molecules consist of three fatty acids esterified to a glycerol backbone (figure 1.1). The fatty acids can either be saturated, monounsaturated, or polyunsaturated, reflecting the amount of double bonds. In NASH, the increased TG content is accompanied by hepatocellular ballooning and lobular inflammation (11). NASH can by graded and staged depending on which hepatocytes are inflamed, *i.e.*, perivenously or periportally located hepatocytes, and whether ballooning of cells is minimal, present or marked (12). The progression of simple hepatic steatosis (NAFL) towards NASH and finally cirrhosis, is thought to involve two "hits", a model first proposed by Day and James in 1998 (13). In this model, the first "hit" is the development of the hepatic steatosis: accumulation of TG in hepatocytes. The second "hit" induces the transition of NAFL to NASH and is the result of the actions of inflammatory molecules, *i.e.*, reactive oxygen species (ROS). The second "hit" might be the result of the increased liver TG levels itself because fatty acids are cytotoxic: fatty acid oxidation in mitochondria and peroxisomes might generate ROS (14). However, one must keep in mind that inflammation itself is the major factor in the transition of NAFL to NASH (15).

It is alarming that the prevalence of NAFLD in the adult population in Western societies is estimated at about 20% (11) and it is therefore suggested that 9.1 million individuals in the United States have NAFLD (16). The risk of NAFLD is almost 5-fold higher in persons with body mass index (BMI) $\geq$ 30 kg/m$^2$ (17). BMI is considered a good index for obesity, but waist-to-hip circumference ratio (WHR) is probably a better marker for fat distribution (18). The World Health Organisation (WHO) defines overweight as BMI $\geq$ 25 kg/m$^2$, individuals with BMI $\geq$ 30 kg/m$^2$ are obese (19). In fact, NAFLD is associated with the metabolic syndrome, obesity and diabetes (20). These conditions all share insulin resistance as a diagnostic criterion. Insulin resistance is defined as a decreased biological

response to normal concentrations of circulating insulin. The role of insulin and the consequences of insulin resistance for (hepatic) metabolism will be discussed later.

According to diagnostic criteria for the metabolic syndrome defined by the National Cholesterol Education Program (NCEP) panel (21), a person suffers from the metabolic syndrome when he/she shows at least three of the criteria listed in table 1.2. The WHO stresses even more the importance of insulin resistance in the diagnosis of the metabolic syndrome (22), as mentioned in table 1.3.

Numerous clinical studies have shown that insulin resistance is a predisposing factor for NASH (20,23-27). The question that is still unanswered is whether hepatic steatosis is caused by insulin resistance, as suggested in the "two hit" hypothesis (13), or that hepatic steatosis predisposes to insulin resistance. Another possibility is that a common factor, such as the adipocyte-derived hormones leptin and adiponectin, contributes to development of both hepatic steatosis and insulin resistance. In the remaining part of this introduction, attention will be focussed on the first two possibilities. Considering the third possibility, recent studies show that people with low plasma leptin concentrations, *e.g.* subjects with congenital lipodystrophy, develop both NASH and insulin resistance (28). Leptin replacement therapies in lipodystrophic patients reverses their NASH (29). Leptin-deficient *ob/ob* mice develop hepatic steatosis, but not NASH, in combination with insulin resistance, hyperglycemia and hypertriglyceridemia (30). Low plasma adiponectin levels are associated with the development of insulin resistance (31) and administration of adiponectin to mice with alcohol-induced hepatic steatosis resulted in decreased liver TG concentrations (32). In *ob/ob* mice, adiponectin administration increased insulin sensitivity and reduced hepatic TG levels (32).

Table 1.1. Major causes or associations of nonalcoholic fatty livers (7).

| Cause | | Association |
|---|---|---|
| Primary | | Features of the metabolic syndrome |
| Secondary | Nutritional | Total parental nutrition |
| | | Rapid Weight loss |
| | | Startvation |
| | | Intestinal bypass surgery |
| | Drugs | Glucocorticoids |
| | | Estrogens |
| | | Tamoxifen |
| | | Amiodaron |
| | | Methotrexate |
| | | Aminosalicylate |
| | Toxins | |
| | Metabolic | Lipodystrophy |
| | | Dysbetalipoproteinemia |
| | | Acute fatty liver of pregnancy |
| | | Reye's syndrome |
| | Other | Inflammatory bowel disease |
| | | HIV infection |

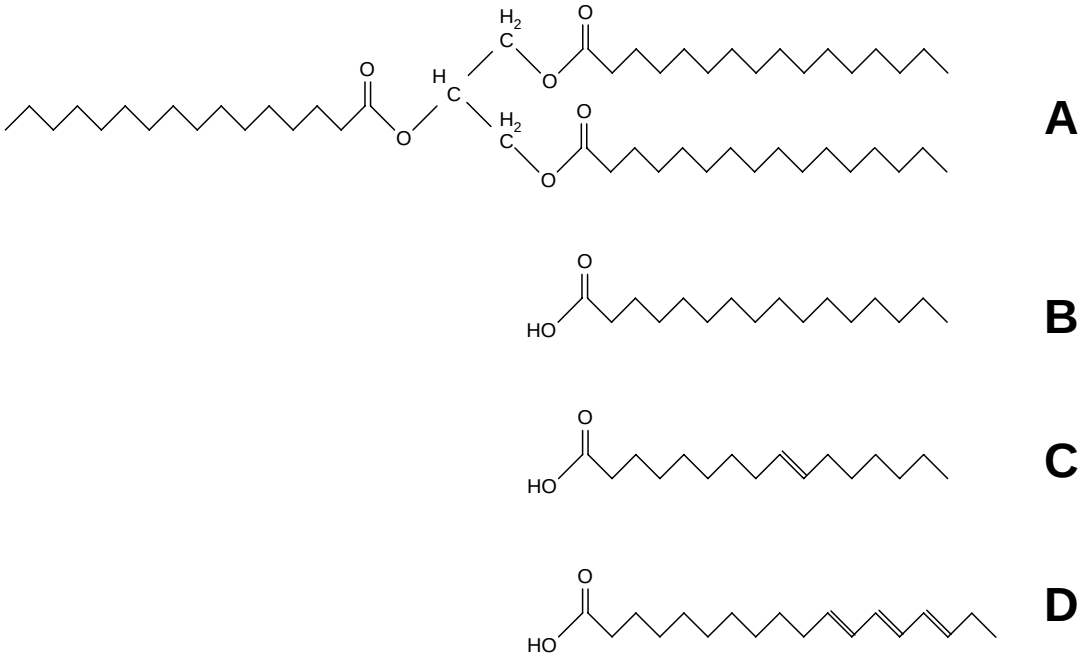


Figure 1.1. Structure of A, triglyceride (tripalmitic acid); B, saturated fatty acid (palmitic acid, C16:0); C, monounsaturated fatty acid (palmitoleic acid, C16:1w7); D, polyunsaturated fatty acid (α-linoleic acid, C18:3w3).

Table 1.2. NCEP diagnosis criteria for the metabolic syndrome (21).

| Risk factor | Abnormal level |
|---|---|
| Waist circumference | > 102 cm (men) or > 88 cm (women) |
| Fasting blood glucose | ≥ 6.1 mM |
| Serum triglycerides | ≥ 1.7 mM |
| Serum HDL cholesterol | < 1.0 mM (men) or < 1.3 mM (women) |
| Arterial blood pressure | ≥ 130/85 mm Hg |

Table 1.3 WHO diagnosis criteria for the metabolic syndrome (22).

| | | |
|---|---|---|
| | Insulin | in top 25% |
| Required | Fasting blood glucose | ≥ 6.1 mM |
| | 2-hour glucose | ≥ 7.8 mM |
| And ≥ 2 of: | Waist-to-hip circumference ratio | > 0.9 (men) or >0.85 (women) |
| | Body mass index | ≥ 30 mg/kg$^2$ |
| | Serum triglycerides | ≥ 1.7 mM |
| | Serum HDL cholesterol | < 0.9 mM (men) or < 1.0 mM (women) |
| | Arterial blood pressure | ≥ 140/90 mm Hg |

## Insulin: discovery, diabetes and intracellular actions

The hormone insulin was discovered by Best and Banting in 1921 (33) when they investigated the role of the pancreas in diabetes mellitus. Because the first known feature of this disease was the high urinary glucose concentration, it was named diabetes mellitus. “Diabetes” is derived from the Greek word for “pipe-line” to stress the fact that nutrients begin to pass through the system rather than being utilised. “Mellitus” is Latin for “honey” to stress the sweet taste of the urine produced in this condition. Later on, it was discovered that diabetic patients also have increased blood glucose levels.

Insulin is secreted by the B-cells located in the islets of Langerhans of the pancreas when blood glucose levels increase, for instance after a meal. Insulin has energy-saving properties: it enhances storage of glucose in the liver, inhibits hepatic glucose production (HGP) and stimulates uptake of glucose by the peripheral tissues, *i.e.*, muscle and adipose tissue. Insulin also influences whole-body lipid metabolism by inducing hepatic fatty acid and TG synthesis (*de novo* lipogenesis) and inhibiting peripheral breakdown of TG into fatty acids (lipolysis).

Two types of diabetes mellitus are generally distinguished. In diabetes mellitus type 1, high blood glucose levels are the result of the failure of the pancreas to produce sufficient amounts of insulin. Various auto-immune factors have been implicated herein (34) and genetic predisposition is thought to play a major role. Diabetes mellitus type 1 is usually diagnosed in childhood whereas diabetes mellitus type 2 has been associated with elderly but its prevalence in young people and even children is rapidly increasing. Diabetes mellitus type 2 is preceded by insulin resistance. As a result of insulin resistance, the pancreas starts to produce more insulin, a process that in the end will exhaust the B-cells and result in an inability of these cells to produce sufficient insulin. As a result, plain diabetes will develop over time.

Insulin actions are carried out via binding of the hormone to its receptor (a member of the tyrosine kinase receptor family) (figure 1.2). Upon binding, the receptor autophosphorylates and activates two distinct down-stream signaling pathways: the phosphatidylinositol-3-kinase (PI3K) pathway and the MAP kinase/ERK kinase (MEK) pathway. Protein tyrosine phosphatase 1B (PTP-1B) is an enzyme that dephosphorylates the insulin receptor and acts to terminate the signal. In mice, increased levels and activity of PTP-1B result in insulin resistance (35,36). Insulin-mediated effects on glucose and lipid metabolism, most relevant for the work described in this thesis, are thought to be predominantly carried out via the PI3K-pathway but the MEK pathway will also be discussed briefly.

Down-stream insulin receptor substrates (IRSs) are phosphorylated upon autophosphorylation of the insulin receptor. IRS1 and IRS2 are the two isoforms predominantly found in the liver. Recent studies with IRS1- and IRS2-specific knockout mice have shown that they control distinct metabolic pathways (37): IRS1 mainly controls the effects on glucose metabolism whereas IRS2 predominantly mediates the effects on lipid metabolism. In the MEK pathway, IRS phosphorylation results in phosphorylation of the SH2 domain-containing adaptor protein Grb2. As a result, this protein dimerizes with the guanine exchange factor “son-of-sevenless” (SOS) and the subsequent exchange of GTP for GDP activates Ras. Next, GTP-bound Ras binds Raf, the first kinase in the Raf-MAPK route, that will subsequently activate MEK. MEK activates the extracellular signal-related kinase (ERK) 1 and ERK2 that can activate various downstream targets involved in, for instance, gene expression and kinase activity (38).

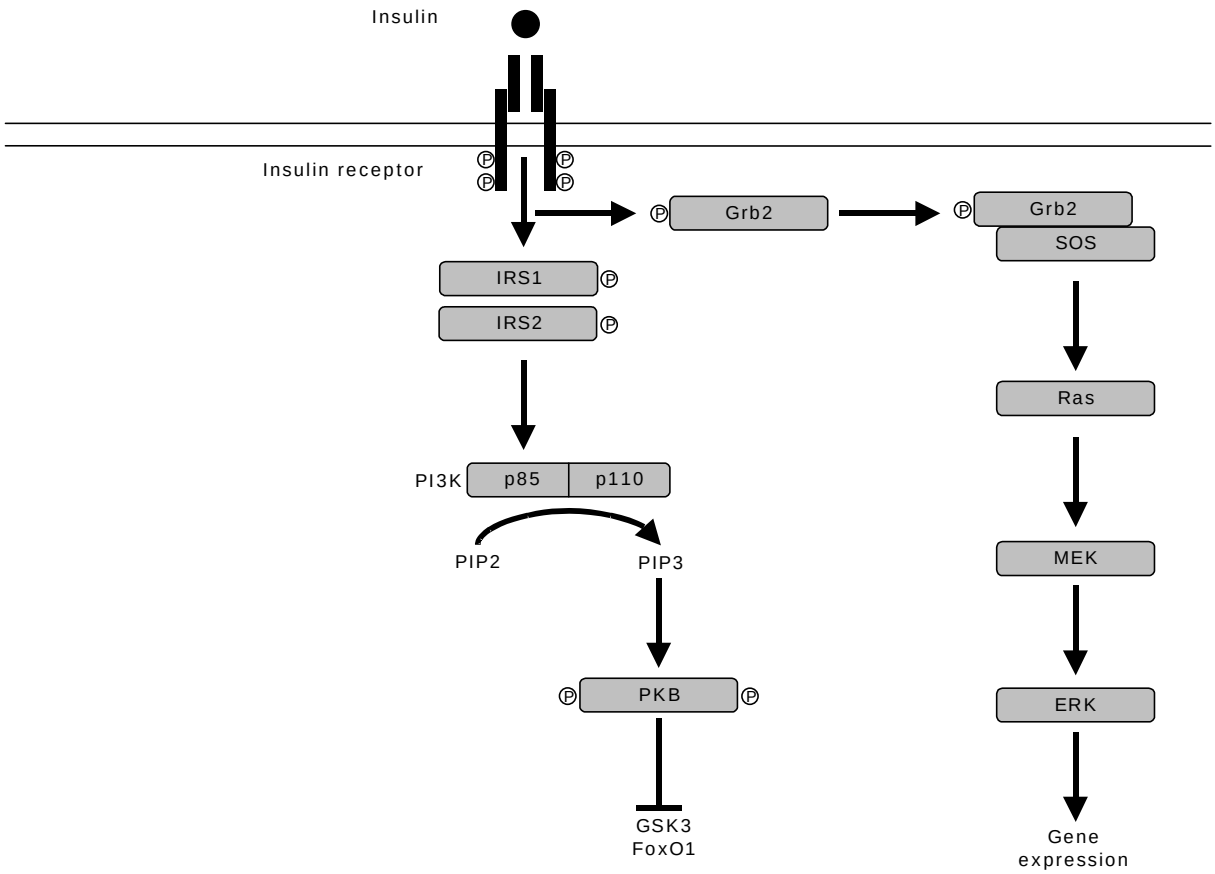


Figure 1.2. Schematic representation of the intracellular insulin signaling cascade. IRS, insulin receptor substrate; ERK, extracellular signal-related kinase; FoxO1, forkhead box "Other"-1; GSK3β, glycogen synthase kinase-3β; MEK, MAP kinase/ERK kinase; PI3K, phosphatidylinositol-4-kinase; PIP2, phosphatidylinositol-4,5-bisphosphate; PIP3, phosphatidylinositol-2,4,5-trisphosphate; PKB, protein kinase B; SOS, son-of-sevenless.

The PI3K pathway also starts after IRS phosphorylation. Phosphorylated IRS has an increased affinity for the p85 subunit of PI3K. Activated PI3K will start the production of the second messenger phosphatidylinositol 2,4,5-trisphosphate (PIP3) from the phospholipid PI4,5P2 (PIP2). This second messenger activates, amongst others, protein kinase B (PKB) via phosphorylation at two sites (Thr308 and Ser473). PKB is a key regulatory protein involved in many steps of insulin-mediated actions on hepatic glucose and lipid metabolism, as will be discussed in more detail in other paragraphs.

Although this topic will not further be discussed in detail, insulin also stimulates peripheral glucose uptake via PKB-mediated translocation of vesicles containing the glucose transporter-4 (GLUT4) to the membrane (39,40). Exactly how PKB influences this translocation is currently not known.

## The increasing world-wide prevalence of diabetes mellitus type 2

As mentioned, insulin resistance will normally result in diabetes mellitus type 2, a disease mainly found in adults in their forties or fifties until recently. Nowadays, its prevalence is steeply rising and the condition is increasingly present also in children and adolescents (41,42). In Japanese children, diabetes mellitus type 2 already accounts for 80% of childhood diabetes (43). Not only is childhood prevalence for diabetes mellitus type 2 increasing rapidly, the total number of people world-wide with this condition is thought to rise from 189 million (2003 situation) to 221 million in 2010 and to more than 300 million in 2025 (44-46). Remarkably, the 1995 to 2025 increase in diabetes is estimated to be stronger in developing countries than in developed countries (46). In developing countries, the increase will be 170%, from 84 to 228 million; in developed countries, this increase will be 42%, from 51 to 72 million. This marked difference can, in part, be explained by the "thrifty genotype hypothesis" (47). In ancient times, people in areas prone to famine, *e.g.*, the developing countries, developed a biological mechanism to store more fat to survive prolonged periods of food deprivation. Nowadays, these people, especially in countries like India and China, have more easy access to food and as a result, they accumulate excess fat more easily. When this is also accompanied by a reduction in physical activity (i.e, a sedentary lifestyle), these factors result in obesity, attraction of the metabolic syndrome and diabetes mellitus type 2 (47). The data from Ogden *et al*. (48) show that, in the US, the incidence of obesity is markedly increasing in children. In 1999-2000, the prevalence of overweight (defined as at or above the 95th percentile of the sex-specific BMI) was 15.5 % in 12- through 19-year-olds, 15.3% in the 6- through 11-year-olds, and 10.4% in the 2- through 5-year-olds. In 1988-1994, these percentages were 10.5%, 11.3%, and 7.2%, respectively.

## Hepatic glucose metabolism and the actions of insulin

In fed conditions, glucose from the intestine is transported via blood and taken up by tissues by a process regulated, in part, by insulin. Liver and muscle tissue can store excess glucose as glycogen, a highly branched, efficient storage form of glucose (49). The direct pathway from glucose to glycogen consists of two distinct steps (see figure 1.3 for an overview of the intrahepatic glucose fluxes). The first step involves conversion of glucose into glucose-6-phosphate (G6P), a process mediated by hexokinase. The liver-type hexokinase is called glucokinase (GK). The second step involves production of glycogen via uridine diphosphate (UDP)-glucose. Glycogen synthase (GS) is thought to be rate-controlling in the latter process. Although production of glycogen is an efficient way for the liver to store glucose, the glycogen storage capacity is limited. A certain amount of glucose is therefore also broken down in the glycolytic pathway into carbon-3 compounds, *i.e.*, pyruvate and lactate. This process is mediated by enzymes such as phosphofructo-1-kinase and pyruvate kinase (PK). As will be discussed later, the carbon-3 compounds can be the source of acetyl-CoA, that can be used for production of fatty acids (and subsequently TGs) in a process called *de novo* lipogenesis.

In fasted conditions, in contrast, the body largely depends on the glucose produced by the liver. The liver and, to a minor extent, the kidney are the sole organs capable of glucose production and secretion (50). First, the glycogen stores are used to yield glucose, a process that can be considered as a three-step process. The first step is the cleaving of a single glucose-1-phosphate from glycogen, a process controlled by glycogen phospatase (GP). The second step involves the action of a debranching enzyme that converts glucose-1-phosphate to G6P. The final step is the dephosphorylation of G6P to glucose, mediated by glucose-6-

phosphatase (G6Pase), an enzyme-complex only found in the liver (and kidneys), the reason why only the liver (and the kidney) can produce glucose. Apart from breakdown of glycogen, the liver can produce glucose from other substrates, such as the carbon-3 compounds, in a process called gluconeogenesis (GNG). When fasting exceeds 8 hours in humans, GNG progressively replaces breakdown of glycogen to preserve complete breakdown of this storage form of glucose (51). This gluconeogenic process is controlled by phosphoenolpyruvate carboxykinase (PEPCK) that catalyses conversion of pyruvate to oxaloacetate to phosphoenolpyruvate, by fructose-1,6-bisphosphatase (F1,6BP) that catalyses conversion of fructose-1,6,-bisphosphate to fructose-6-phosphate, and by a number of other enzymes. The final step in GNG is the conversion of G6P to glucose by G6Pase.

As mentioned, insulin lowers blood glucose via stimulation of glucose uptake by muscle and adipose tissue as well as by inhibition of HGP. In addition, insulin stimulates conversion of glucose into glycogen and into carbon-3 compounds that are subsequently converted acetyl-CoA, fatty acids, and TG. Studies demonstrate that, in humans, half maximal suppression of HGP occurs at insulin levels of 25 mU/ml, whereas half maximal stimulation of peripheral glucose uptake occurs at 50 mU/ml (52). Thus, HGP is more insulin sensitive than peripheral glucose clearance. Of particular interest are the studies with stable isotope techniques showing that, under basal conditions, HGP in type 2 diabetic individuals was unchanged or only modestly elevated (53-55). Under hyperinsulinemic or hyperglycemic conditions, however, insulin failed to suppress HGP, suggesting abnormal regulation of HGP in diabetes mellitus type 2 (56).

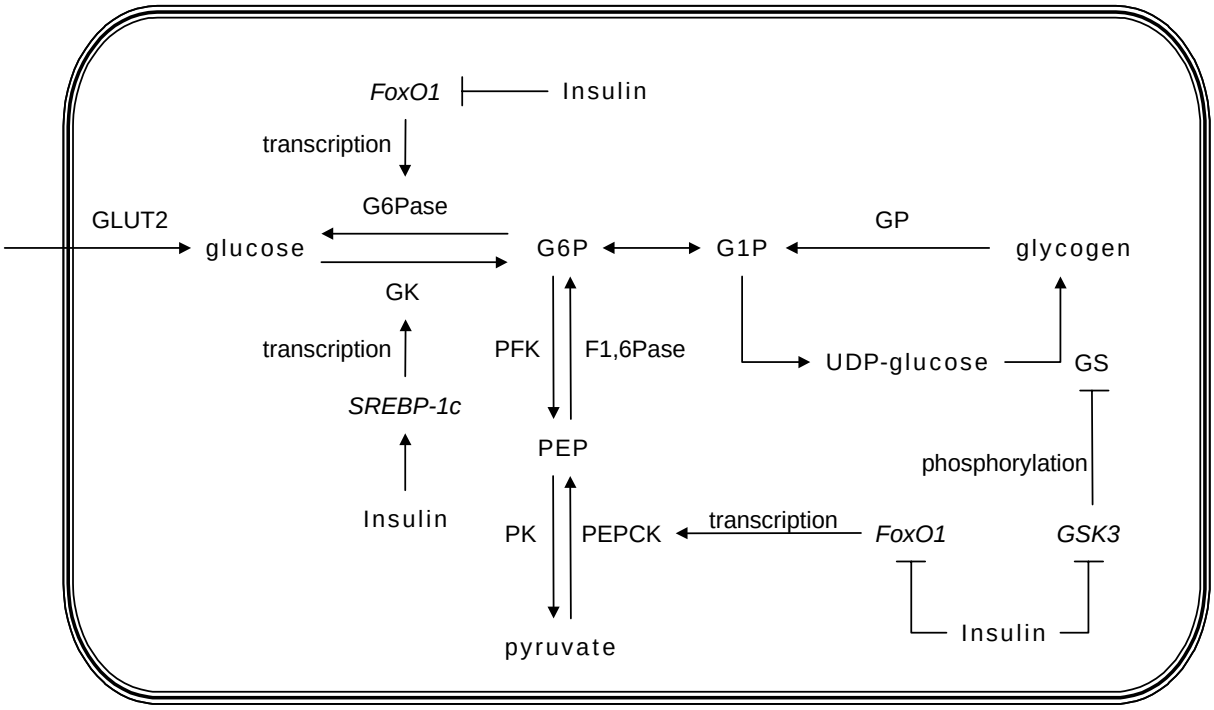


Figure 1.3. Schematic representation of the intrahepatic glucose fluxes and the regulation of these fluxes by insulin. F1,6BP, fructose-1,-bisphosphotase; FoxO1, forkhead box "Other"-1; G1P, glucose-1-phosphate; G6P, glucose-6-phosphate; G6Pase, glucose-6-phosphatase; GK, glucokinase; GLUT2, glucose transporter-2; GP, glycogen phosphorylase; GS, glycogen synthase; GSK3β, glycogen synthase kinase-3β; PEP, phosphoenolpyruvate; PEPCK, phosphoenolpyruvate carboxykinase; PFK, phosphofructo-1-kinase; PK, pyruvate kinase; SREBP-1c, sterol-regulatory element-binding protein-1c.

Via PI3K-induced PKB phosphorylation, insulin enhances phosphorylation of GS kinase-3β (GSK3β) (38), a protein whose activity is inhibited by phosphorylation. As a result, GS phosphorylation will be reduced and this enzyme will thus be more active. The final result is an increased storage of glucose in the form of glycogen. GK is also critically involved in insulin-mediated hepatic glucose metabolism. In insulin receptor-deficient mice, overexpression of GK improved glucose tolerance, emphasizing the importance of GK activity (57). Moreover, transcription of the GK gene is regulated by sterol-regulatory element-binding protein-1c (SREBP-1c) (58,59), a key transcription factor in the control of hepatic lipid metabolism (60) whose transcription and activation are regulated by insulin (61). SREBP-1c stimulates transcription of almost all genes involved in fatty acid and TG synthesis (60).

For long time, it was known that insulin suppresses GNG. Recently, the forkhead box "Other"-1 (FoxO1) has been identified as a transcription factor with an important role in mediating the effects of insulin on GNG (62). FoxO1 appears to be a negative modulator of insulin action, as it binds to insulin response sequences found in promotor regions of genes encoding G6Pase (63,64) and PEPCK (65). The actions of FoxO1 on gene transcription are mediated by PKB. PKB can phosphorylate FoxO1 at three sites (Thr24, Ser256, and Ser319 in human FoxO1), resulting in activation and nuclear exclusion of FoxO1 (66-72). Moreover, phosphorylation and cytoplasmic localization of FoxO1 promotes its degradation (73). In vivo evidence for the role of FoxO1 comes from the heterozygous FoxO1 knockout mouse (74,75) that showed reduced G6Pase gene expression and lower plasma insulin levels. Moreover, these heterozygous mice are, on a insulin receptor-knockout background, less insulin resistant than control mice.

In conclusion, via its effects on GS (via GSK3β), on GK (via SREBP-1c), and on GNG (via FoxO1), insulin stimulates hepatic glucose utilisation and inhibits HGP.

## Triglyceride-rich lipoproteins and free fatty acids

Chapter 8 of this thesis discusses hepatic lipid metabolism, very low density lipoprotein (VLDL) assembly and secretion, and the roles of the lipogenic transcription factors SREBP-1c, liver X receptor (LXR) and carbohydrate responsive element binding protein (ChREBP) herein. This introduction will therefore only briefly discuss these issues.

A surplus of (dietary) energy is incorporated into TG and stored in adipose tissue. In fasted conditions, the adipose TG store is used to deliver energy in the form of free fatty acids (FFA) and glycerol to liver and muscle to maintain whole-body energy homeostasis. To maintain this homeostasis, transport of lipids between various tissues (intestine, liver, adipose tissue) plays a crucial role. TGs are very hydrophobic and therefore need to be transported in association with lipoproteins together with cholesterol, phospholipids and proteins. The core of a lipoprotein contains TG and esterified cholesterol while the surface consists of phospholipids and free cholesterol. Embedded in the lipoprotein surface are apolipoproteins. These proteins are needed for stabilisation of the particle and solubility of the core lipids (76) Moreover, apolipoproteins act as ligands for specific receptors and are needed for the actions of enzymes (76).

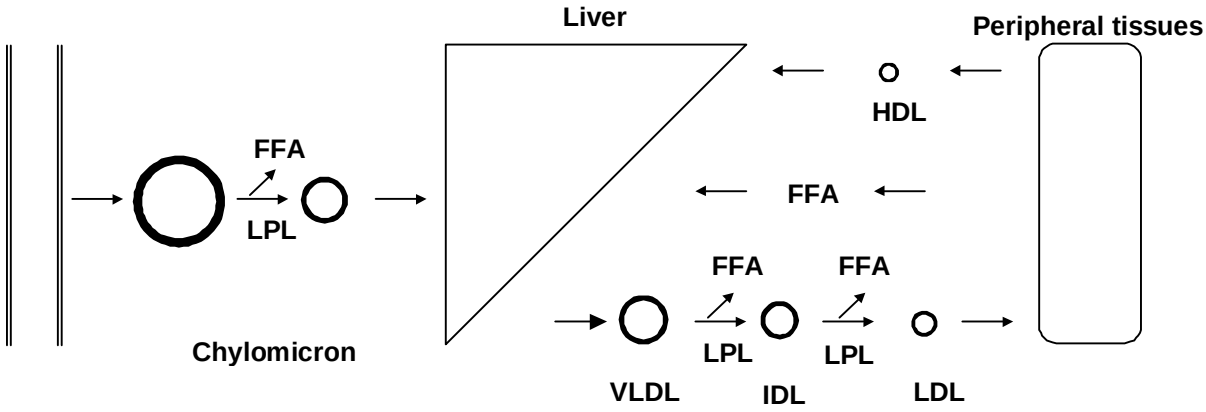


Figure 1.4. Schematic representation of lipoprotein and fatty acid fluxes. FFA, free fatty acid; HDL, high density lipoprotein; IDL, intermediate density lipoprotein; LDL, low density lipoprotein; LPL, lipoprotein lipase; VLDL, very low density lipoprotein.

Table 1.4. Characteristics of lipoproteins

| Lipoprotein | Density (g/ml) | Diameter (nm) | Apolipoproteins | Percentage lipids | | |
|---|---|---|---|---|---|---|
| | | | | TG | Cholesterol | PL |
| Chylomicron | 0.95 | 75 – 1200 | AI, AII, AIV, B48, CI, CII, CIII, E | 80 – 95 | 2 – 7 | 3 – 9 |
| VLDL | 0.95 – 1.006 | 30 – 80 | B100, CI, CII, CIII, E | 55 – 80 | 5 – 15 | 10 – 20 |
| IDL | 1.006 – 1.019 | 25 – 35 | B100, CI, CII, CIII, E | 20 – 50 | 20 – 40 | 15 – 25 |
| LDL | 1.019 – 1.063 | 18 – 25 | B100 | 5 – 15 | 40 – 50 | 20 – 25 |
| HDL | 1.063 – 1.21 | 5 – 12 | AI, AII, AIV, AV, CI, CII, CIII, E | 5 –10 | 12 – 25 | 20 – 30 |

HDL, high density lipoprotein; IDL, intermediate density lipoprotein; LDL, low density lipoprotein; PL, phospholipid; TG, triglyceride; VLDL, very low density lipoprotein.

Figure 1.4 shows a schematic overview of the lipoprotein fluxes within the body, table 1.4 summarizes the properties of the lipoproteins that constitute these fluxes. In the enterocytes, dietary TGs are incorporated into lipoproteins called chylomicrons. Apolipoprotein B (apoB) is the main protein of TG containing lipoproteins (chylomicrons and VLDL). In the surface of chylomicrons, a truncated form of apoB is present, consisting only of 48% of the N-terminal part of the protein and therefore called apoB48. Editing of the apoB100 into apoB48 is regulated by the apoB editing complex-1 (apobec1) (77). The TG content of these particles, when present in the circulation, is lipolysed by the action of lipoprotein lipase (LPL) secreted by muscle and adipose tissue. ApoCIII inhibits the actions of LPL and apoCII enhances these lipolytic actions. The released fatty acids can be taken up and are subsequently reesterified into TGs (*e.g.*, in adipocytes) or used as an energy source (*e.g.*, in muscle). When taken up by the liver, the fatty acids are re-esterified to form TG and first stored in an intracellular TG pool (78). Later on, the TGs stored in this pool can be released to be subsequently secreted in VLDL particles. As a result of lipolysis, chylomicrons are depleted of TGs, become smaller and are referred to as chylomicron remnants. Both chylomicrons and chylomicron remnants are cleared by the liver upon binding to the low density lipoprotein (LDL) receptor, the LDL receptor related protein (LRP) or hepatic lipase (HL) (79).

For transport from the liver to peripheral tissues, TGs need to be incorporated into VLDL particles. VLDL-TGs are lipolyzed by LPL in a similar way as chylomicron-TGs and the fatty acids are taken up by the peripheral tissues. Upon depletion of the TG content, the VLDL particle size decreases and the relative cholesterol concentration increases. The cholesterol-dense VLDL remnant particles are called intermediate density lipoprotein (IDL) or LDL particles, depending on their size and density. Insulin inhibits assembly and secretion of VLDL particles by the liver, as will be discussed later.

In fasted conditions, FFAs are released from the adipose stores after lipolysis of stored TG by two enzymes called triglyceride hydrolase (TGH) or adipose TG lipase (ATGL) and hormone sensitive lipase (HSL) (80) and carried by serum albumin to the liver. Insulin inhibits lipolysis in peripheral tissues. Thus, upon fasting, when insulin levels are low, the insulin-mediated inhibition of lipolysis is absent and FFAs are released into the circulation, taken up by the liver and muscle and used in the ß-oxidation process. Part of the FFA not directly used for oxidative purposes is stored in the liver, causing the well-established hepatic steatosis associated with fasting (81).

## Hepatic lipid metabolism and the actions of insulin

As discussed, dietary glucose taken up by the liver is stored as glycogen or broken down in the glycolytic pathway to yield carbon-3 compounds such as pyruvate. Pyruvate can be converted to citrate in the tricarboxylic acid (TCA) cycle and citrate can be converted to acetyl-CoA by ATP citrate lyase (ACL) (figure 1.5). Acetyl-CoA is the moiety from which fatty acids are synthesized. Two acetyl-CoA can be covalently linked to each other to form malonyl-CoA, a process controlled by acetyl-CoA carboxylase (ACC). Subsequently, via the actions of fatty acid synthase (FAS), malonyl-CoA condense to form fatty acids. Fatty acids can be incorporated into TG via the actions of acyl-CoA synthase (ACS) and glycerol-3-phosphate acyltransferase (GPAT). The expression of genes encoding ACL, ACC, FAS, ACS, and GPAT is regulated by both SREBP-1c (60) and ChREBP (82,83), whereas expression *Pk* of is regulated by ChREBP but not by SREBP-1c (84). Of notice, the SREBP-1c protein activity and gene transcription are regulated by insulin (61); the activity of ChREBP is regulated by glucose (83,85). More about these transcription factors can be found in chapter 8 of this thesis.

The liver is very well capable to synthesize fatty acids and TG from glucose and thus contributes to control of whole-body energy homeostasis. Insulin plays a key role herein, mainly via its effects on SREBP-1c expression (61). In the liver, insulin not only stimulates *de novo* lipogenesis but also inhibits VLDL assembly and secretion. How insulin influences VLDL assembly and secretion is not exactly known. Insulin might (i) decrease lipidation of the pre-VLDL particle via inhibition of microsomal TG transporting protein (MTTP) (86,87), (ii) stimulate degradation of the VLDL apolipoprotein apoB (88-90), and/or (iii) inhibit supply of substrates needed for VLDL assembly (78), *i.e.*, TG, cholesterol and phospholipids. More details about VLDL assembly and secretion and the role of insulin herein are discussed in chapter 8 of this thesis.

Comparable insulin-mediated, energy-conserving effects are found in peripheral tissues, especially in adipose tissues where insulin inhibits lipolysis. Of course, both hepatic and peripheral lipid-related effects of insulin are consistent with its role in fed conditions. In this condition, the liver does not need to add lipids to the total lipoprotein pool via secretion of VLDL and adipocytes do not need to deliver FFA to the periphery and the liver.

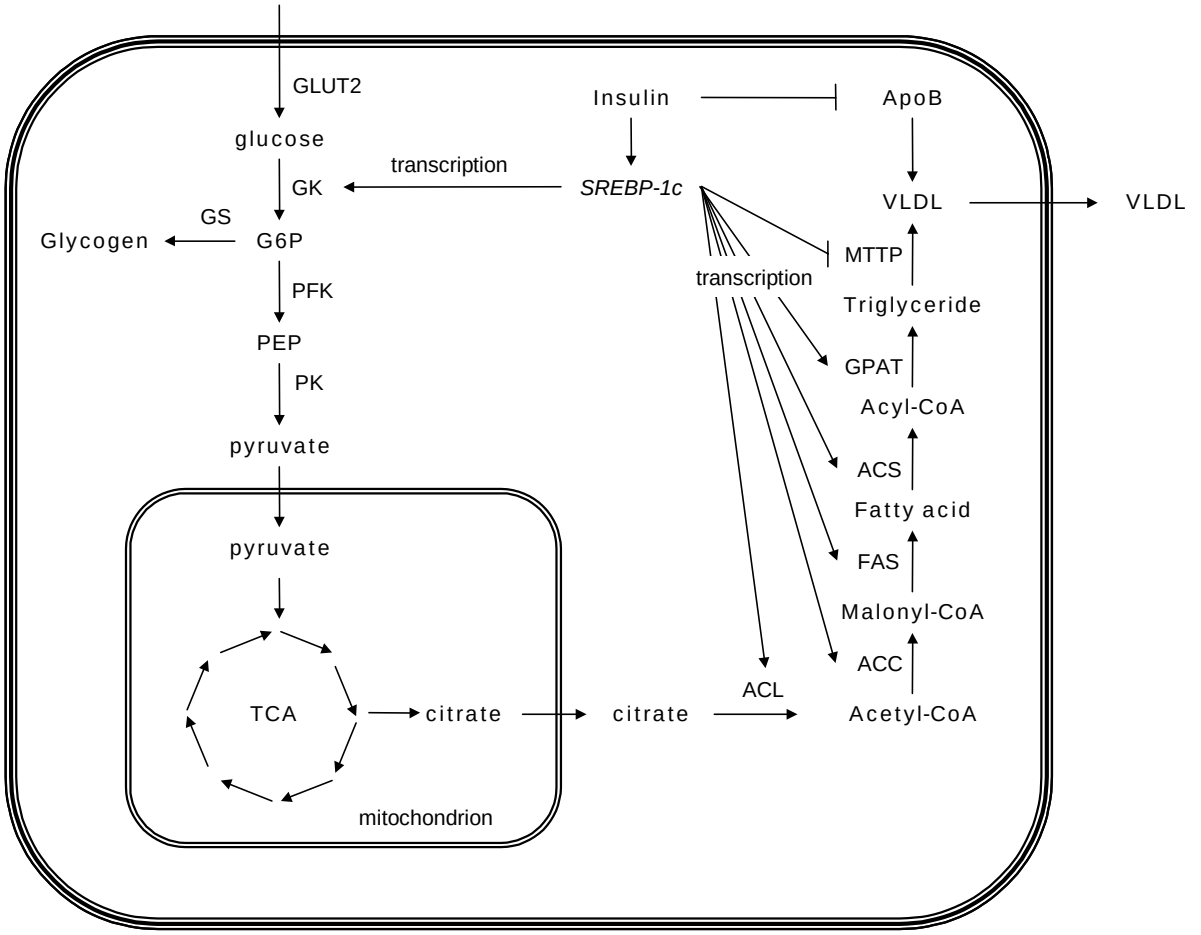


Figure 1.5. Schematic representation of the link between hepatic glucose and lipid metabolism and the role of insulin herein. ACC, acetyl-CoA carboxylase; ACL, ATP citrate lyase; ACS, acetyl-CoA synthase; apoB, apolipoprotein B; FAS, fatty acid synthase; G6P, glucose-6-phosphate; GLUT2, glucose transporter-2; GK, glucokinase; GS, glycogen synthase; GPAT, glycerol-phosphate acyltransferase; MTTP, microsomal triglyceride transport protein; PEP, phosphoenolpyruvate; PFK, phosphofructo-1-kinase; PK, pyruvate kinase; SREBP-1c, sterol-regulatory element-binding protein-1c; TCA, tricarboxylic acid cycle; VLDL, very low density lipoprotein.

## Hepatic steatosis and insulin resistance: beyond triglycerides

It is important to realize that TGs are inert molecules and therefore not cytotoxic themselves. Fatty acids, however, might display direct (adverse) cellular effects. Increased plasma FFA concentrations have for long been associated with enhanced hepatic glucose production and insulin resistance (reviewed by Boden (91)). Fatty acids are the substrates for hepatic β-oxidation, a process in which fatty acids are broken down to generate ketone bodies and energy for GNG (92). Interestingly, fatty acids stimulate transcription of genes encoding proteins involved in β-oxidation via binding to the nuclear peroxisome proliferator actived receptor-α (PPARα) (93). Thus, fatty acids might continously stimulate β-oxidation, resulting in elevated HGP, even under hyperinsulinemic conditions. The latter is a feature of hepatic insulin resistance. On the other hand, because insulin inhibits lipolysis of TG in adipose tissue, increased plasma FFA levels could also be the result of insulin resistance and not the cause of insulin resistance.

Various studies report other direct effects of fatty acids on insulin resistance. For instance, it was shown that PPARα induces transcription of TRB3 (94), a protein that prevents PKB phosphorylation and activation (95). In mice, TRB3 seems to promote hyperglycemia by increasing glucose production by the liver due to decreased PKB-mediated GSK-3β and FoxO1 phosphorylation.

Apart from their effects via PPARα, fatty acids are also source for other molecules suggested to interfere with insulin signaling, for instance ceramide and glycosphingolipids (figure 1.6). The major mammalian fatty acid palmitate is a precursor in ceramide synthesis. Ceramide is a precursor for numerous different glycosphingolipids (figure 1.6) (96). In skeletal muscle from obese insulin resistant individuals, the ceramide concentrations were 2-fold increased (97). Moreover, in vitro studies showed that excessive ceramide concentrations disturb insulin signaling via inhibitory effects on PKB phosphorylation (98). Ceramide is the precursor for glycosphingolipids (GSLs), thus the possibility exists that the latter molecules might also play an important role in the development of insulin resistance (99). Glycosphingolipids are important components of the protein-enriched membrane domains called rafts and caveolae (100) and insulin receptors are predominantly found in these membrane structures, at least in adipocytes (101). It is therefore speculated that the close contact interactions between the insulin receptor and glycosphingolipids result in reduced receptor integrity (99). As a consequence, the tissue in which the receptor is located is less insulin sensitive. Indeed, it was reported that addition of the glycosphingolipid GM3 to cultured adipocytes suppressed phosphorylation of the insulin receptor and IRS1, resulting in reduced glucose uptake (102). Compared to their wild-type littermates, mice that are deficient for GM3 synthase, an important enzyme in glycosphingolipid synthesis, showed decreased glycosphingolipid levels in combination with enhanced peripheral insulin signaling (103). In addition, the GM3-synthase deficient mice were protected from high-fat diet induced insulin resistance (103).

In conclusion, fatty acids themselves might induce insulin resistance via continuously enhanced GNG due to elevated β-oxidation, via PPARα-induced TRB3 transcription resulting in PKB blockade, via ceramide-mediated PKB inactivation, glycosphingolipids interfering with insulin receptor integrity, or combinations of these factors.

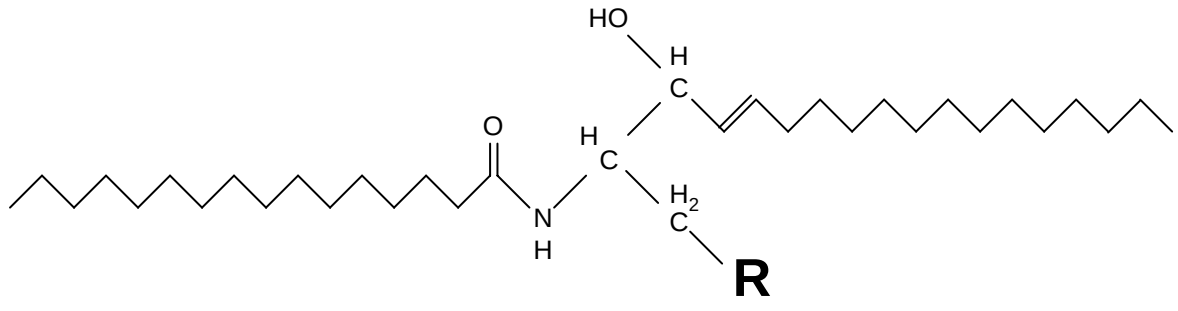


Figure 1.6. Basic structure of sphingolipids. For ceramide, R is H; for glycosphingolipids, R consists of series of glucose, galactose, N-acetyl galactosamine, and M-acetyl neuramic moieties.

## Animal models of hepatic steatosis

Several animal models have proven to be useful tools in metabolic studies, because whole-body metabolism is a complex network of various different factors that influence each other. Such interplay is necessary to ensure proper regulation of energy homeostasis needed to maintain life in under varying conditions.. For instance, one can argue that the main goal of whole-body glucose metabolism is to provide glucose to the brain, because this organ needs glucose to function. The brain is, however, not capable to synthesise its alternate energy sources, ketone bodies, by oxidation of amino acids or fatty acids without undergoing adverse structural and functional damage (104). Thus, the liver is the organ that produces glucose and ketone bodies, and secretes VLDL, depending on the overall metabolic condition of the body, simply to maintain whole-body energy homeostasis. Factors derived from peripheral tissues, such as leptin, adiponectin and fatty acids, and those derived from the liver, such as glucose, TGs and ketone bodies, all act together to help maintaining this homeostasis.

Knowing this, it is easy to imagine that, to study the effects of hepatic steatosis on insulin sensitivity, experiments with animals are preferred above those with isolated cells. Recently, Den Boer *et al.* (105) published an overview of the role of animal models of hepatic steatosis for research on insulin sensitivity. The authors concluded that complex interactions between endocrine, metabolic, and transcriptional pathways are involved in TG-induced hepatic insulin resistance. Thus, the liver seems be passively and actively involved in insulin resistance associated with hepatic steatosis. More recently, studies from Rossetti's group (106-108) emphasised the role of the brain in the regulation of the actions of insulin on the liver. The overall conclusion from these studies is that, in extreme conditions, the insulin-mediated control of HGP is controlled by the brain. So far, no studies were performed on the role of the brain in the other aspects of hepatic insulin sensitivity, *e.g.* control of VLDL production.

## Objectives and outline of this thesis

From the studies discussed in this introduction, it is clear that animal models of hepatic steatose are useful tools. We therefore performed *in vivo* experiments to study the effect of hepatic steatosis on insulin sensitivity in various animal models. In chapters 2, 4 and 5, the leptin-deficient *ob/ob* mice were used. These mice show enhanced *de novo* lipogenesis (30) that is considered a major cause of their hepatic steatosis. In chapter 2, we questioned whether the hyperglycemia seen in *ob/ob* mice was the result of reduced peripheral glucose clearance or enhanced HGP. Chapter 4 describes studies in which both hepatic and peripheral insulin sensitivity was investigated in more detail. For this, we used the "golden standard" to determine insulin sensitivity: the hyperinsulinemic euglycemic clamp technique. In the studies described in chapter 5 we used the *ob/ob* mice to study the effects of a novel inhibitor of the glycosphingolipid synthesis, the iminosugar derivative N-(5'-adamantane-1'-yl-methoxy)-pentyl-1-deoxynojirimycin (AMP-DNM). In these studies, insulin sensitivity was tested using the hyperinsulinemic euglycemic clamp technique described in chapter 4.

It was shown in previous studies that pharmacological LXR activation results in severe hepatic steatosis (109) and we used this model in the studies described in chapters 3 and 4. In chapter 3, we questioned whether LXR-induced hepatic steatosis resulted in affected VLDL-TG production. In chapter 4 we investigated whether hepatic and peripheral insulin sensitivity of glucose metabolism was affected due to this hepatic steatosis. In the studies described in chapter 6, we studied whether hepatic steatosis due to pharmacological inhibition of the rate-controlling enzyme in β-oxidation, carnitine palmitoyl transferase-1 (CPT1), affected insulin sensitivity of VLDL production. In the studies described in chapter 7, we questioned which lipogenic transcription factor (SREBP-1c, LXRα or ChREBP) was responsible for enhanced lipogenic gene expression upon pharmacological inhibition of glucose-6-phosphatase.

## References


1. Rao, RK, Sheth, P. Recent advances in alcoholic liver disease. I. Role of intestinal permeability and endotoxemia in alcoholic liver disease. Am J Physiol Gastrointest Liver Physiol 286: G881-G884, 2004
2. You, M, Crabb, DW. Recent advances in alcoholic liver disease. II. Minireview: molecular mechanisms of alcoholic fatty liver. Am J Physiol Gastrointest Liver Physiol 287: G1-G6, 2004
3. Hines, IN, Wheeler, MD. Recent advances in alcoholic liver disease. III. Role of the innate response in alcoholic hepatitis. Am J Physiol Gastrointest Liver Physiol 287: G310-G314, 2004
4. McClain, CJ, Song, Z, Barve, SS, Hill, DB, Deaciuc, I. Recent advances in alcoholic liver disease. IV. Dysregulated cytokine metabolism in alcoholic liver disease. Am J Physiol Gastrointest Liver Physiol 287: G497-G502, 2004
5. Ludwig, J, Viggiano, TR, McGill, DB, Oh, BJ. Nonalcholic steatohepatitis: Mayo Clin experiences with a hitherto unnamed disease. Mayo Clin Proc. 55: 434-438, 1980
6. Matteoni, CA, Younossi, ZM, Gramlich, T, Boparai, N, Liu, YC, McCullough, AJ. Nonalcoholic fatty liver disease: a spectrum of clinical and pathological severity. Gastroenterology 116: 1413-1419, 1999
7. Adams,LA, Angulo,P, Lindor,KD: Nonalcoholic fatty liver disease. CMAJ 172:899-905, 2005
8. Bugianesi, E, Leone, N, Vanni, E, Marchesini, G, Brunello, F, Carucci, P, Musso, A, De Paolis, P, Capussotti, L, Salizzoni, M, Rizzetto, M. Expanding the natural history of nonalcoholic steatohepatitis: from cryptogenic cirrhosis to hepatocellular carcinoma. Gastroenterology 123: 375-378, 2002
9. Day, CP. Natural history of NAFLD: remarkably benign in the absence of cirrhosis. Gastroenterology 129: 375-378, 2005
10. Adams, LA, Lymp, JF, St.Sauver, J, Sanderson, SO, Lindor, KD, Feldstein, A, Angulo, P. The natural history of nonalcoholic fatty liver disease: a population-based cohort study. Gastroenterology 129: 113-121, 2005
11. Cortez-Pinto, H, Camilo, ME. Non-alcoholic fatty liver disease/non-alcoholic steatohepatitis (NAFLD/NASH): diagnosis and clinical course. Best Pract Res Clin Gastroenterol 18: 1089-1104, 2004
12. Brunt, EM, Janney, CG, Di Bisceglie, AM, Neuschwander-Tetri, BA, Bacon, BR. Nonalcoholic steatohepatitis: a proposal for grading and staging the histological lesions. Am J Gastroenterol 94: 2467-2474, 1999
13. Day, CP, James, OF. Steatohepatitis: a tale of two "hits"? Gastroenterology 114: 842-845, 1998
14. Pessayre, D, Mansouri, A, Fromenty, B. Nonalcoholic steatosis and steatohepatitis. V. Mitochondrial dysfunction in steatohepatitis. Am J Physiol Gastrointest Liver Physiol 282: G193-G199, 2002
15. Jansen, PLM. Nonalcoholic steatohepatitis. Neth J Med 62:217-224, 2004
16. Clark, JM, Brancati, FL, Diehl, AM. The prevalence and etiology of elevated aminotransferase levels in the United States. Am J Gastroenterol 98: 960-967, 2003
17. Bellentani, S, Saccoccio, G, Masutti, F, Grocè, LS, Brandi, G, Sasso, F, Cristanini, G, Tiribelli, C. Prevalence of and risk factors for hepatic steatosis in northern Italy. Ann Intern Med 132: 112-117, 2000
18. Björntorp, P. Visceral obesity: a "civilization syndrome". Obes Res 1: 206-222, 1993
19. World Health Organization. WHO Consultation. Definition, diagnosis and classification of diabetes mellitus and its complications. Geneva, 31-33. 1999.
20. Marceau, P, Biron, S, Hould, F-S, Marceau, S, Simard, S, Thung, SN, Kral, JG. Liver pathology and the metabolic syndrome X in severe obesity. J Clin Endocrinol Metab 84: 1513-1517, 1999
21. Executive summary of the third report of the National Cholesterol Education Program (NCEP) Expert Panel on detection, evaluation and treatment of high blood cholesterol in adults (Adult Treatment Panel III). JAMA 285: 2486-2497, 2001
22. Alberti, KG, Zimmet, PZ. Definition, diagnosis and classification of diabetes mellitus and its complications. Part 1: diagnosis and classification of diabetes mellitus provisional report of a WHO consultation. Diabet Med 15: 539-553, 1998
23. Marchesini, G, Brizi, M, Morselli-Labata, AM, Bianchi, G, Bugianesi, E, McCullough, AJ, Forlani, G, Melchionda, N. Association of nonalcoholic fatty liver disease with insulin resistance. Am J Med 107: 450-455, 1999

24. Cortez-Pinto, H, Camilo, ME, Baptista, A, De Oliveira, AG, De Moura, MC. Non-alcoholic fatty liver: another feature of the metabolic syndrome? Clin Nutr 18:353-358, 1999
25. Sanyal, AJ, Campbell-Sargent, C, Mirshahi, F, Rizzo, WB, Contos, MJ, Sterling, RK, Luketic, VA, Shiffman, ML, Clore, JN. Nonalcoholic steatohepatitis: association of insulin resistance and mitochondrial abnormalities. Gastroenterology 120: 1183-1192, 2001
26. Marchesini, G, Brizi, M, Bianchi, G, Tomassetti, S, Bugianesi, E, Lenzi, M, McCullough, AJ, Natale, S, Forlani, G, Melchionda, N. Nonalcoholic fatty liver disease. A feature of the metabolic syndrome. Diabetes 50: 1844-1850, 2001
27. Seppälä-Lindroos, A, Vehkavaara, S, Häkkinen, A-M, Goto, T, Westerbacka, J, Sovijärvi, A, Halavaare, J, Yki-Järvinen, H. Fat accumulation in the liver is associated with defects in insulin suppression of glucose production and serum free fatty acids independent of obesity in normal men. J Clin Endocrinol Metab 87: 3023-3028, 2002
28. Garg, A, Misra, A. Hepatic steatosis, insulin resistance, and adiposetissue disorders. J Clin Endocrinol Metab 87: 3019-3022, 2002
29. Javor, ED, Ghany, MG, Cochran, EK, Arioglu Oral, E, DePaoli, AM, Premkumar, A, Kleiner, DE, Gorden, P. Leptin reverses nonalcoholic steatohepatitis in patients with severe lipodystrophy. Hepatology 41:753-760, 2005
30. Wiegman, CH, Bandsma, RHJ, Ouwens, M, van der Sluijs, FH, Havinga, R, Boer, T, Reijngoud, D-J, Romijn, JA, Kuipers, F. Hepatic VLDL production in ob/ob mice is not stimulated by massive de novo lipogenesis but is less sensitive to the suppressive effects of insulin. Diabetes 52: 1081-1089, 2003
31. Berg, AH, Combs, TP, Du, X, Brownlee, M, Scherer, PE. The adipocyte-secreted protein Acrp30 enhances hepatic insulin action. Nature Med 7: 947-953, 2001
32. Xu, A, Wang, Y, Keshaw, H, Xu, LY, Lam, KSL, Cooper, GJS. The fat-derived hormone adiponectin alleviates alcoholic and nonalcoholic fatty liver diseases in mice. J Clin Invest 112: 91-100, 2003
33. Banting, FG, Best, CH, Collip, JB, Campbell, WR, Fletcher, AA. Pancreatic extracts in the treatment of diabetes mellitus. CMAJ 22: 141-146, 1922
34. Dahlquist, G. Etiological aspects of insulin-dependent diabetes mellitus: an epidemiological perspective. Autoimmunity 15:61-65, 1993
35. Hashimoto, N, Zhang, WR, Goldstein, BJ. Insulin receptor and epidermal growth factor receptor dephosphorylation by three major rat liver protein-tyrosine phosphatases expressed in a recombinant bacterial system. Biochem J 284: 569-576, 1992
36. Chen, H, Wertheimer, SJ, Lin, CH, Katz, SL, Amrein, KE, Burn, P, Quon, MJ. Protein-tyrosine phosphatases PTP1B and Syp are modulators of insulin-stimulated translocation of GLUT4 in transfected rat adipose cells. J Biol Chem 272: 8026-8031, 1997
37. Taniguchi, CM, Ueki, K, Kahn, CR. Complementary roles of IRS-1 and IRS-2 in the hepatic regulation of metabolism. J Clin Invest 113: 718-727, 2005
38. Saltiel, AR, Kahn, CR. Insulin signalling and the regulation of glucose and lipid metabolism. Nature 414: 799-806, 2001
39. Whiteman, EL, Cho, H, Bimbaum, MJ. Role of Akt/protein kinase B in metabolism. Trends Endocrinol Metab 13: 444-451, 2002
40. Calera, MR, Martinez, C, Liu, H, El Jack, AK, Birnbaum, MJ, Pilch, PF: Insulin increases the association of Akt-2 with Glut4-containing vesicles. J Biol Chem 273: 7201-7204, 1998
41. Pinhas-Hamiel, O, Dolan, LM, Daniels, SR, Standiford, D, Khoury, PR, Zeitler, P. Increased incidence of non-insulin-dependent diabetes mellitus among adolescents. J Pediatr 128: 608-615, 1996
42. Sinha, R, Fisch, G, Teague, B, Tamborlane, WV, Banyas, B, Allen, K, Savoye, M, Rieger, V, Taksali, S, Barbetta, G, Sherwin, RS, Caprio, S. Prevalence of impaired glucose tolerance among children and adolescents with marked obesity. N Engl J Med 346: 802-810, 2002
43. Kitagawa, T, Owada, M, Urakami, T, Yamauchi, K. Increased incidence of non-insulin dependent diabetes mellitus among Japanese schoolchildren correlates with an increased intake of animal protein and fat. Clin Pediatr (Phila) 37: 111-115, 1998
44. Zimmet, P, Shaw, J, Alberti, GMM. Preventing type 2 diabetes and the dysmetabolic syndrome in the real world: a realistic view. Diabet Med 20: 693-702, 2003
45. Zimmet, P, Alberti, KGMM, Shaw, J. Global and societal implications of the diabetes epidemic. Nature 414: 782-787, 2001
46. King, H, Aubert, RE, Herman, WH: Global burden of diabetes, 1995-2025. Prevalence, numerical estimates, and projections. Diabetes Care 21. 1414-1431, 1998
47. Dowse, G, Zimmet, P. The thrifty genotype in non-insulin dependent diabetes. BMJ 306: 532-533, 1993
48. Ogden, CL, Flegal, KM, Carroll, MD, Johnson, CL. Prevalence and trends in overweight among US children and adolescents, 1999-2000. JAMA 288: 1728-1732, 2002
49. Bollen, M, Keppens, S, Stalmans, W. Specific features of glycogen metabolism in the liver. Biochem J 336: 19-31, 1998
50. Ekberg, K, Landau, BR, Wajngot, A, Chandramouli, V, Efendic, S, Brunengraber, H, Wahren, J. Contributions by kidney and liver to glucose production in the postabsorptive state and after 60 h of fasting. Diabetes 48: 292-298, 1999

51. Tirone, TA, Brunicardi, FC. Overview of glucose regulation. World J Surg 25: 461-467, 2001
52. Rizza, RA, Mandarino, LJ, Gerich, JE. Dose-response characteristics for effects of insulin on production and utilization of glucose in man. Am J Physiol Endocrinol Metab 240: E630-E639, 1981
53. Perrielo, G, De Feo, P, Torlone, E, Fanelli, C, Santeusanio, F, Brunetti, P, Bolli, GB. Nocturnal spikes of growth hormone secretion cause the dawn phenomenon in type 1 (insulin dependent) diabetes mellitus by decreasing hepatic (and extrahepatic) sensitivity to insulin in the absence of insulin waning. Diabetologia 33: 52-59, 1990
54. Anderwald, C, Bernroider, E, Krssak, M, Stingl, H, Brehm, A, Bischof, MG, Nowotny, P, Roden, M, Waldhausl, W. Effects of insulin treatment in type 2 diabetic patients on intracellular lipid content in liver and skeletal muscle. Diabetes 51: 3025-3032, 2002
55. Hother-Nielsen, O, Beck-Nielsen, H. Insulin resistance, but normal basal rates of glucose production in patients with newly diagnosed mild diabetes mellitus. Acta Endocrinol (Copenh) 124: 637-645, 1991
56. DeFronzo, RA. Lilly lecture 1987. The triumvirare: beta-cell, muscle, liver. A collusion responsible for NIDDM. Diabetes 37: 667-687, 1988
57. Jackerott, M, Baudry, A, Bucchini, D, Jami, J, Joshi, RL. Improved metabolic disorders of insulin receptor-deficient mice by transgenic overexpression of glucokinase in the liver. Diabetologia 45: 1292-1297, 2002
58. Shimomura, I, Bashmakov, Y, Ikemoto, S, Horton, JD, Brown, MS, Goldstein, JL. Insulin selectively increases SREBP-1c mRNA in the livers of rats with streptozocin-induced diabetes. Proc Natl Acad Sci USA 96: 13656-13661, 1999
59. Foretz, M, Guichard, C, Ferre, P, Foufelle, F. Sterol regulatory element binding protein -1c is a major mediator of insulin action on the hepatic expression of glucokinase and lipogenesis-related genes. Proc Natl Acad Sci USA 96: 12737-12742, 1999
60. Horton, JD, Goldstein, JL, Brown, MS. SREBPs: activators of the complete program of cholesterol and fatty acid synthesis in the liver. J Clin Invest 109: 1125-1131, 2002
61. Hegarty, BD, Bobard, A, Hainault, I, Ferré, P, Bossard, P, Foufelle, F. Distinct roles of insulin and liver X receptor in the induction and cleavage of sterol regulatory element-binding protein-1c. Proc Natl Acad Sci USA 102: 791-796, 2005
62. Barthel, A, Schmoll, D, Unterman, TG. FoxO proteins in insulin action and metabolism. Trends Endocrinol Metab 16: 183-189, 2005
63. Schmoll, D, Walker, KS, Alessi, DR, Grempler, R, Burchell, A, Guo, S, Walther, R, Unterman, TG. Regulation of glucose-6-phosphatase gene expression by protein kinase B alpha and the forkhead transcription factor FKHR. Evidence for insulin response unit-dependent and -independent effects of insulin on promoter activity. J Biol Chem 275: 36324-36333, 2000
64. Nakae, J, Kitamura, T, Silver, DL, Accili, D. The forkhead transcription factor Foxo1 (Fkhr) confers insulin sensitivity onto glucose-6-phosphatase expression. J Clin Invest 108: 1359-1367, 2001
65. Yeagley, D, Guo, S, Unterman, T, Quinn, PG. Gene- and activation-specific mechanisms for insulin inhibition of basal and glucocorticoid-induced insulin-like growth factor binding protein-1 and phosphoenolpyruvate carboxykinase transcription. Roles of forkhead and insulin response sequences. J Biol Chem 276: 33705-33710, 2001
66. Brunet, A, Bonni, A, Zigmond, MJ, Lin, MZ, Juo, P, Hu, LS, Anderson, MJ, Arden, KC, Blenis, J, Greenberg, ME. Akt promotes cell survival by phosphorylating and inhibiting a forkhead transcription factor. Cell 96: 857-868, 1999
67. Nakae, J, Park, BC, Accili, D. Insulin stimulates phosphorylation of the forkhead transcription factor FKHR on serine 253 through a Wortmannin-sensitive pathway. J Biol Chem 274: 15982-15985, 1999
68. Kops, GJ, de Ruiter, ND, de Vries-Smits, AM, Powell, DR, Bos, JL, Burgering, BM. Direct control of the forkhead transcription factor AFX by protein kinase B. Nature 398: 630-634, 1999
69. Guo, S, Rena, G, Cichy, S, He, X, Cohen, P, Unterman, T. Phosphorylation of serine 256 by protein kinase B disrupts transactivation by FKHR and mediates effects of insulin on insulin-like growth factor-binding protein-1 promoter activity through a conserved insulin response sequence. J Biol Chem 274: 17184-17192, 1999
70. Brunet, A, Park, J, Tran, H, Hu, LS, Hemmings, BA, Greenberg, ME. Protein kinase SGK mediates survival signals by phosphorylating the forkhead transcription factor FKHRL1 (FOXO3a). Mol Cell Biol 21: 952-965, 2001
71. Rena, G, Woods, YL, Prescott, AR, Peggie, M, Unterman, TG, Williams, MR, Cohen, P. Two novel phosphorylation sites on FKHR that are critical for its nuclear exclusion. EMBO J 21: 2263-2271, 2002
72. Biggs, WH, Meisenhelder, J, Hunter, T, Cavenee, WK, Arden, KC. Protein kinase B/Akt-mediated phosphorylation promotes nuclear exclusion of the winged transcription factor FKHR1. Proc Natl Acad Sci USA 96:7421-7426, 1999
73. Matsuzaki, H, Daitoku, H, Hatta, M, Tanaka, K, Fukamizu, A. Insulin-induced phosphorylation of FKHR (Foxo1) targets to proteasomal degradation. Proc Natl Acad Sci USA 100: 11285-11290, 2003
74. Hosaka, T, Biggs, WH, Tieu, D, Boyer, AD, Varki, NM, Cavenee, WK, Arden, KC. Disruption of forkhead transcription factor (FOXO) family members in mice reveals their functional diversification. Proc Natl Acad Sci USA 101: 2975-2980, 2004
75. Nakae, J, Biggs, WH, Kitamura, T, Cavenee, WK, Wright, CV, Arden, KC, Accili, D. Regulation of insulin action and pancreatic beta-cell function by mutated alleles of the gene encoding forkhead transcription factor Foxo1. Nature Gen 32: 245-253, 2002

76. Ginsberg, HN, Zhang, Y-L, Hernancez-Ono, A. Regulation of plasma triglycerides in insulin resistance and diabetes. Arch Med Res 36: 232-240, 2005
77. Anant, S, Davidson, NO. Molecular mechanisms of apolipoprotein B mRNA editing. Curr Opin Lipidol. 12: 159-165, 2001
78. Gibbons, GF, Wiggins, D, Brown, A-M, Hebbachi, A-M. Synthesis and function of hepatic very-low-density lipoprotein. Biochem Soc Trans. 32: 59-64, 2004
79. Cooper, AD. Hepatic uptake of chylomicron remnants. J Lipid Res. 38: 2173-2192, 1997
80. Gilham, D, Lehner, R. The physiological role of triacylglycerol hydrolase in lipid metabolism. Rev Endo Metab Disord 5: 303-309, 2004
81. Heijboer, AC, Donga, E, Voshol, PJ, Dang, Z-C, Havekes, LM, Romijn, JA, Corssmit, EPM. Sixteen hours of fasting differentially affects hepatic and muscle insulin sensitivity in mice. J Lipid Res. 46: 582-588, 2005
82. Ishii, S, Iizuka, K, Miller, BC, Uyeda, K. Carbohydrate response element binding protein directly promotes lipogenic enzyme gene transcription. Proc Natl Acad Sci USA 101: 15597-15602, 2004
83. Uyeda, K, Yamashita, H, Kawaguchi, T. Carbohydrate responsive element-binding protein (ChREBP): a key regulator of glucose metabolism and fat storage. Biochem Pharmacol. 63: 2075-2080, 2002
84. Kawaguchi, T, Takenoshita, M, Kabashima, T, Uyeda, K. Glucose and cAMP regulate the L-type pyruvate kinase gene by phosphorylation/dephosphorylation of the carbohydrate response element binding protein. Proc Natl Acad Sci USA 98: 13710-13715, 2001
85. Yamashita, H, Takenoshita, M, Sakurai, M, Bruick, RK, Henzel, WJ, Shillinglaw, W, Arnot, D, Uyeda, K. A glucose-responsive transcription factor that regulates carbohydrate metabolism in the liver. Proc Natl Acad Sci USA 98: 9116-9121, 2001
86. Hagan, DL, Kienzle, B, Jamil, H, Hariharan, N. Transcriptional regulation of human and hamster microsomal triglyceride transfer protein genes. Cell type-specific expression and response to metabolic regulators. J Biol Chem 269: 28737-28744, 1994
87. Wetterau, JR, Lin, MC, Jamil, H. Microsomal triglyceride transfer protein. Biochim Biophys Acta 1345: 136-150, 1997
88. Fisher, EA, Pan, M, Chen, X, Wu, X, Wang, H, Jamil, H, Sparks, JD, Williams, KJ. The triple threat to nascent apolipoprotein B. Evidence for multiple, distinct degradative pathways. J Biol Chem 276: 27855-27863, 2001
89. Au, CS, Wagner, A, Chong, T, Qiu, W, Sparks, JD, Adeli, K. Insulin regulates hepatic apolipoprotein B production independent of the mass or activity of Akt1/PKBα. Metabolism 53: 228-235, 2004
90. Brown, A-M, Gibbons, GF. Insulin inhibits the maturation phase of VLDL assembly via a phosphoinositide 3-kinase-mediated event. Arterioscler Thromb Vasc Biol 21: 1656-1661, 2001
91. Boden, G. Interaction between free fatty acids and glucose metabolism. Curr Opin Clin Nutr Metab Care 5: 545-549, 2002
92. Chu, CA, Sherck, SM, Igawa, K, Sindelar, DK, Neal, DW, Emshwiller, M, Cherrington, AD. Effects of free fatty acids on hepatic glycogenolysis and gluconeogenesis in conscious dogs. Am J Physiol Endocrinol Metab 282: E402-E411, 2002
93. Pineda Torra, I, Gervois, P, Staels, B. Peroxisome proliferator-activated receptor alpha in metabolic disease, inflammation, atherosclerosis and aging. Curr Opin Lipidol 10: 151-159, 1999
94. Koo, S-H, Satoh, H, Herzig, S, Lee, C-H, Hedrick, S, Kulkarni, R, Evans, RM, Olefsky, J, Montminy, M. PGC-1 promotes insulin resistance in liver through PPAR-α-dependent induction of TRB-3. Nature Med 10: 530-534, 2004
95. Du, K, Herzig, S, Kulkarni, R, Montminy, M. TRB3: A tribble homolog that inhibits Akt/PKB activation by insulin in liver. Science 300: 1574-1577, 2003
96. Sandhoff, K, Kolter, T. Biosynthesis and degradation of mammalian glycosphingolipids. Phil Trans R Soc Lond B 358: 847-861, 2003
97. Adams, JM, Pratipanawatr, T, Berria, R, Wang, E, DeFronzo, RA, Sullards, MC, Mandarino, LJ. Ceramide content is increased in skeletal muscle from obese insulin-resistant humans. Diabetes 53: 31, 2004
98. Stratford, S, Hoehn, KL, Liu, F, Summers, SA. Regulation of insulin action by ceramide: dual mechanisms linking ceramide accumulation to the inhibition of Akt/protein kinase B. J Biol Chem 279: 36608-36615, 2004
99. Aerts, JM, Ottenhoff, R, Grefhorst, A, Powlson, AS, van Eijk, M, van Dijk, TH, Kuipers, F, Aten, J, Groener, J, Strijland, A, Groen, AK, Boon, L, Serlie, MJ, Sauerwein, HP, Wennekes, T, Overkleeft, HS, Sethi, JK, O'Rahilly, S, Meijer, AJ. Pharmacological inhibition of glucopsylceramide synthase enhances insulin sensitivity: a novel therapeutic approach to insulin resistance. Submitted
100. Simons, K, Ikonen, E. Functional rafts in cell membranes. Nature 387: 569-572, 1997
101. Gustavsson, J, Parpal, S, Karlsson, M, Ramsing, C, Thorn, H, Borg, M, Lindroth, M, Peterson, KH, Magnusson, KE, Stralfors, P. Localization of the insulin receptor in caveolae of adipocyte plasma membrane. FASEB J 13: 1961-1971, 1999
102. Tagami, S, Inokuchi Ji, J, Kabayama, K, Yoshimura, H, Kitamura, F, Uemura, S, Ogawa, C, Ishii, A, Saito, M, Ohtsuka, Y, Igarashi, Y. Ganglioside GM3 participates in the pathological conditions of insulin resistance. J Biol Chem 277: 3085-3092, 2002

103. Yamashita, T, Hashiramoto, A, Haluzik, M, Mizukami, H, Beck, S, Norton, A, Kono, M, Tsuji, S, Daniotti, JL, Werth, N, Sandhoff, R, Sandhoff, K, Proia, RL. Enhanced insulin sensitivity in mice lacking ganglioside GM3. Proc Natl Acad Sci USA 100: 3445-3449, 2003
104. Auer, RN. Progress review: hypoglycemic brain damage. Stroke 17: 699-708, 1986
105. den Boer, M, Voshol, PJ, Kuipers, F, Havekes, LM, Romijn, JA. Hepatic steatosis: a mediator of the metabolic syndrome. Lessons from animal models. Arterioscler Thromb Vasc Biol 24: 644-649, 2004
106. Pocai, A, Lam, TKT, Gutierrez-Juarez, R, Obici, S, Schwartz, GJ, Bryan, J, Aguilar-Bryan, L, Rossetti, L. Hypothalamic $K_{ATP}$ channels control hepatic glucose production. Nature 434: 1026-1031, 2005
107. Buettner, R, Patel, R, Muse, ED, Bhanot, S, Monia, BP, McKay, R, Obici, S, Rossetti, L. Severe impairment in liver insulin signaling fails to alter hepatic insulin action in conscious mice. J Clin Invest 115: 1306-1313, 2005
108. Okamoto, H, Obici, S, Accili, D, Rossetti, L. Restoration of liver insulin signaling in Insr knockout mice fails to normalize hepatic insulin action. J Clin Invest 115: 1314-1322, 2005
109. Schultz, JR, Tu, H, Luk, A, Repa, JJ, Medina, JC, Li, L, Schwendner, S, Wang, S, Thoolen, M, Mangelsdorf, DJ, Lustig, KD, Shan, B. Role of LXR in control of lipogenesis. Genes Dev 14: 2831-2838, 2000

# Chapter 2

# Enhanced glucose cycling and suppressed de novo synthesis of glucose-6-phosphate result in a net unchanged hepatic glucose output in ob/ob mice

Robert H.J. Bandsma, Aldo Grefhorst, Theo H. van Dijk,
Fjodor H. van der Sluijs, Anke Hammer,
Dirk-Jan Reijngoud, Folkert Kuipers

Laboratory of Pediatrics, University Medical Center Groningen

**Diabetologia 2004: 47: 2022-2031**

## Summary

*Aims/hypothesis* Leptin-deficient *ob/ob* mice are hyperinsulinaemic and hyperglycaemic; however, the cause of hyperglycaemia remains largely unknown. *Methods* Glucose metabolism in vivo in 9-h fasted *ob/ob* mice and lean littermates was studied by infusing [U-$^{13}$C]-glucose, [2-$^{13}$C]-glycerol, [1-$^{2}$H]-galactose and paracetamol for 6 h, applying mass isotopomer distribution analysis on blood glucose and urinary paracetamol-glucuronide. *Results* When expressed on the basis of body weight, endogenous glucose production (109 ± 23 vs 152 ± 27 μmol·kg$^{-1}$·min$^{-1}$, obese versus lean mice, $p$<0.01) and *de novo* synthesis of glucose-6-phosphate (122 ± 13 vs 160 ± 6 μmol·kg$^{-1}$·min$^{-1}$, obese versus lean mice, $p$<0.001) were lower in *ob/ob* mice than in lean littermates. In contrast, glucose cycling was greatly increased in obese mice (56 ± 13 vs 26 ± 4 μmol·kg$^{-1}$·min$^{-1}$, obese versus lean mice, $p$<0.001). As a result, total hepatic glucose output remained unaffected (165 ± 31 vs 178 ± 28 μmol·kg$^{-1}$·min$^{-1}$, obese vs lean mice, NS). The metabolic clearance rate of glucose was significantly lower in obese mice (8 ± 2 vs 18 ± 2 ml·kg$^{-1}$·min$^{-1}$, obese versus lean mice, $p$<0.001). Hepatic mRNA levels of genes encoding for glucokinase and pyruvate kinase were markedly increased in *ob/ob* mice. *Conclusions/interpretation* Unaffected total hepatic glucose output in the presence of hyperinsulinaemia reflects hepatic insulin resistance in *ob/ob* mice, which is associated with markedly increased rates of glucose cycling. Hyperglycaemia in *ob/ob* mice primarily results from a decreased metabolic clearance rate of glucose.

## Introduction

Hyperinsulinaemia and fasting hyperglycaemia are hallmarks of type 2 diabetes. Insulin resistance of peripheral organs (muscle and adipocytes), as well as of the liver, may contribute to fasting hyperglycaemia. Peripheral insulin resistance reduces the ability of peripheral organs to clear glucose from the circulation. Hepatic insulin resistance develops in two stages. During the early stages in the development of type 2 diabetes, characterised by hyperinsulinaemia and normoglycaemia, hepatic glucose production is still normal under fasting conditions. However, during absorptive phases when insulin concentrations are elevated, hepatic glucose production remains inappropriately high. At later stages in the development of type 2 diabetes in humans, hepatic glucose production starts to increase even under fasting conditions (1).

Both gluconeogenesis and glycogenolysis may contribute to elevated hepatic glucose production. Furthermore, data indicates that cycling of glucose, the process of sequential glucose uptake and subsequent phosphorylation by glucokinase and dephosphorylation by glucose-6-phosphatase (G6Pase), occurs at increased rates in humans with type 2 diabetes (2,3). Little is known about the quantitative role of glucose cycling in the increased production of hepatic glucose in type 2 diabetes. Depending on the methodologies used for quantification of hepatic glucose fluxes, increased glucose cycling may affect the estimation of rates of gluconeogenesis and glycogenolysis.

Leptin-deficient *ob/ob* mice suffer from severe obesity and diabetes due to leptin deficiency, and provide a model for type 2 diabetes. These mice exhibit age-dependent hyperglycaemia and hyperinsulinaemia. Quantitative data on the perturbations of glucose metabolism in these mice in vivo are scarce. In vitro studies on perfused isolated livers of *ob/ob* mice have shown that glycogen turnover is increased (4). In addition, glucose cycling rates have been shown to be greatly increased in hepatocytes isolated from 24-h fasted *ob/ob* mice (5).

Novel methodologies using multiple stable isotopes in vivo now allow the determination of flux rates through the separate metabolic pathways involved in hepatic carbohydrate metabolism (6-8). In the current study, we used these methods to evaluate the quantitative role of gluconeogenesis, glycogenolysis and glucose cycling in hyperglycaemia in modestly fasted *ob/ob* mice.

## Experimental procedures

### *Animals*

Female *ob/ob* mice (n=7) and lean littermates (n=7), 8 weeks of age and on a C57Bl/6 genetic background, were purchased from Harlan (Zeist, The Netherlands). The mice were housed in a temperature-controlled (21 °C) room with a dark–light cycle of 12 h each. Experimental procedures were approved by the Ethics Committee for Animal Experiments of the State University Groningen. Mice were fitted with a permanent catheter in the right atrium via the right jugular vein, as described previously (9). Mice were allowed to recover from surgery for at least 4 days.

*Materials*

The following isotopes were used: [2-$^{13}$C]-glycerol (99% $^{13}$C atom percent excess), [1-$^{2}$H]-galactose (98% $^{2}$H atom percent excess) (Isotec, Miamisburg, Ohio, USA), [U-$^{13}$C]-glucose (99% $^{13}$C atom percent excess) (Cambridge Isotope Laboratories, Andover, Mass., USA). All chemicals used were reagent pro analysis grade. Blood spots and urine were collected on Schleicher and Schuell No. 2992 filter paper (Schleicher and Schuells, 's Hertogenbosch, The Netherlands). Infusates were freshly prepared and sterilised by the Hospital Pharmacy at the day before the experiment.

*Animal experiments*

Experiments were performed in awake, chronically catheterised mice, essentially as described previously (10). Mice were fasted for 9 h, after which they were placed in metabolic cages to allow frequent collection of blood spots and urine. Mice were infused with a sterile solution containing [U-$^{13}$C]-glucose (13.9 µmol/ml), [2-$^{13}$C]-glycerol (160 µmol/ml), [1-$^{2}$H]-galactose (33 µmol/ml) and paracetamol (1.0 mg/ml) at a rate of 0.6 ml/h. During the experiment, blood glucose was measured using EuroFlash test strips (LifeScan Benelux, Beerse, Belgium). Blood spots were collected on filter paper before the start of the infusion and hourly afterwards until 6 h after the start of the infusion. Blood spots were air-dried and stored at room temperature until analysis. Timed urine samples were collected on filter paper strips at hourly intervals. Strips were air-dried and stored at room temperature until analysis. At the end of the experiment, animals were anaesthetised with isoflurane, and a large blood sample was collected in heparin-containing tubes by heart puncture. The sample was centrifuged immediately and stored at –20 °C until analysis. The liver was quickly excised, weighed and immediately frozen in liquid nitrogen.

*Determination of metabolite concentrations*

Plasma was isolated from blood by centrifugation, and liver tissue was homogenised. Commercially available kits were use to determine plasma levels of ß-hydroxybutyrate, lactate (Roche Diagnostics, Mannheim, Germany) and NEFA (Wako Chemicals, Neuss, Germany). Plasma insulin levels were determined by RIA (RI-13K; Linco Research, St. Charles, Mo., USA). Total liver protein content was determined according to the method of Lowry *et al*. (11). Hepatic glycogen was determined by sonication after extraction with 1 mol/l KOH. The extract was incubated at 90 °C for 30 min, cooled and then adjusted to pH 4.5 by the addition of 3 mol/l acetic acid. Precipitated protein was removed by centrifugation. Glycogen was converted to glucose by treating the samples with amyloglucosidase. A glucose assay was then performed at pH 7.4 with ATP, $NADP^+$, hexokinase and G6P dehydrogenase.

Liver samples for the determination of G6P were treated by sonication in a 5% (w/v) $HClO_4$ solution. Precipitated protein was removed by rapid centrifugation at 20000 g for 1 min in a cold microcentrifuge, and the supernatant was neutralised to pH 7 by the addition of small amounts of a solution containing 2 mol/l KOH and 0.3 mol/l MOPS. Levels of G6P were determined fluorimetrically with $NADP^+$ and G6P dehydrogenase.

*Hepatic mRNA levels*

Total RNA was isolated from liver tissue using the Trizol method (Invitrogen, Paisley, UK). Using random primers, RNA was converted to cDNA with M-Mulv-RT (Roche Diagnostics) according to the manufacturer's protocol. The cDNA levels of the genes of interest were measured by RT-PCR using the ABI Prism 7700 Sequence Detection System (Applied Biosystems, Foster City, Calif., USA). An amount of cDNA equivalent to 20 ng of total RNA was amplified using the qPCR core kit (Eurogentec, Seraing, Belgium) according to the manufacturer's protocol with the appropriate forward and reverse primers (Invitrogen) and a

template-specific 3'-TAMRA, 5'-FAM-labelled Double Dye Oligonucleotide probe (Eurogentec). Calibration curves were run on serial dilutions of pooled cDNA solutions as used in the assay. The data were processed using the ABI Sequence Detector v.1.6.3 (Applied Biosystems). Quantified expression levels were within the linear part of the calibration curves. PCR results were normalised by *18S*-rRNA levels. The sequences of the primers and probes used in this study are listed in table 2.1.

Table 2.1. Sequences of the primers and probes used in PCR measurements

| Gene | Sense | Sequence | GeneBank no. |
|---|---|---|---|
| *β-actin* | Forward | ACCCACACTGTGCCCATCTAC | NM_007393 |
| | Reverse | GCTCGGTCAGGATCTTCATGA | |
| | Probe | AGGGCTATGCTCTCCCTCACGCCA | |
| *18S-rRNA* | Forward | CGGCTACCACATCCAAGGA | X00686 |
| | Reverse | CCAATTACAGGGCCTCGAAA | |
| | Probe | CGCGCAAATTACCCACTCCCGA | |
| *G6ph* | Forward | CTGCAAGGGAGAACTCAGCAA | NM_008061 |
| | Reverse | GAGGACCAAGGAAGCCACAAT | |
| | Probe | TGCTCCCATTCCGCTTCGCCT | |
| *G6Pt* | Forward | GAGGCCTTGTAGGAAGCATTG | NM_008063 |
| | Reverse | CCATCCCAGCCATCATGAGTA | |
| | Probe | CTCTGTATGGGAACCCTCGCCACG | |
| *Gk* | Forward | CCTGGGCTTCACCTTCTCCTT | NM_010292 |
| | Reverse | GAGGCCTTGAAGCCCTTGGT | |
| | Probe | CACGAAGACATAGACAAGGGCATCCTGCTC | |
| *Gp* | Forward | GAAGGAGGCAAACGGATCAAC | NM_133198 |
| | Reverse | TCACGATGTCCGAGTGGATCT | |
| | Probe | CCTCTGCATCGTGGGCTGCCA | |
| *Gs* | Forward | GCTCTCCAGACGATTCTTGCA | NM_145572 |
| | Reverse | GTGCGGTTCCTCTGAATGATC | |
| | Probe | CCTCTACGGGTTTTGTAAACAGTCACGCC | |
| *Pk* | Forward | CGTTTGTGCCACACAGATGCT | NM_013631 |
| | Reverse | CATTGGCCACATCGCTTGTCT | |
| | Probe | AGCATGATCACTAAGGCTCGACCAACTCGG | |
| *Pepck* | Forward | GTGTCATCCGCAAGCTGAAG | NM_011044 |
| | Reverse | CTTTCGATCCTGGCCACATC | |
| | Probe | CAACTGTTGGCTGGCTCTCACTGACCC | |

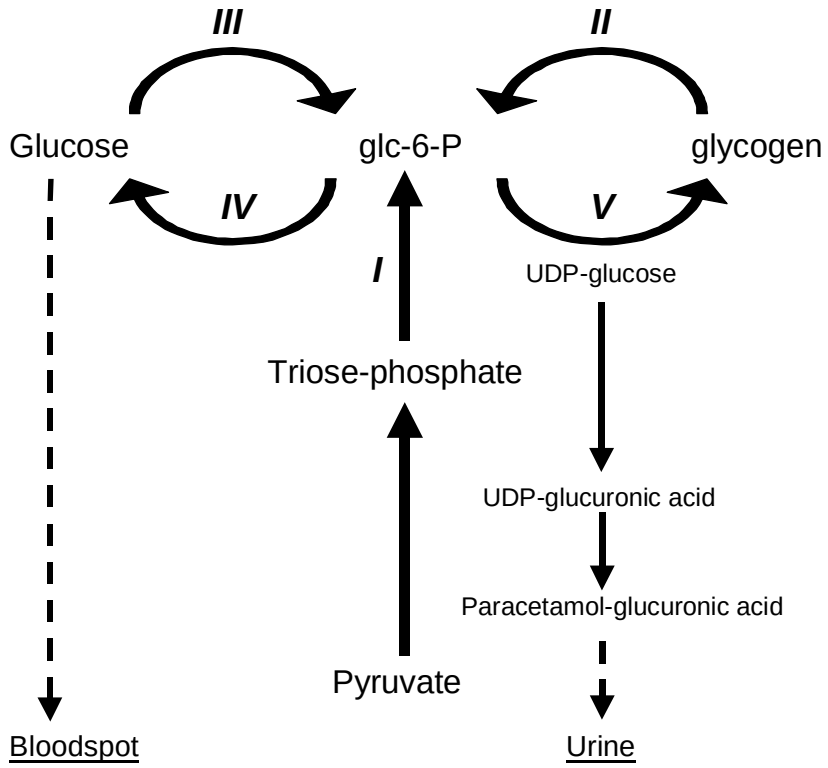


Figure 2.1. Schematic model of calculated hepatic carbohydrate fluxes. The major metabolic pathways and enzymatic reactions involved in hepatic carbohydrate metabolism that share G6P as a metabolite are shown, apart from glycolysis, which cannot be assessed in this model. These pathways are as follows: (i) *de novo* synthesis of G6P; (ii) glycogenolysis; (iii) glucokinase; (iv) glucose-6-phosphatase; and (v) glycogen synthesis. Gluconeogenesis is represented by (i) and (iv).

*Mass isotopomer distribution analysis*

Glucose and paracetamol-glucuronic acid (Par-GlcUA) were extracted from blood spot and urine filter paper strips respectively, derivatised, and measured by GC-MS, essentially as described previously (8,10). The fractional isotopomer distribution according to GC-MS ($m_0$–$m_6$) was corrected for the fractional distribution due to the natural abundance of $^{13}C$ by multiple linear regression, as described by Lee *et al.* (6) to obtain the excess mole fraction of mass isotopomers $M_0$–$M_6$ due to incorporation of infused labelled compounds, *i.e.* [2-$^{13}$C]-glycerol, [U-$^{13}$C]-glucose and [1-$^{2}$H]-galactose.

Figure 2.1 shows a graphical representation of the isotopic model applied in which the following metabolic pathways are considered: (i) *de novo* synthesis of G6P; (ii) glycogenolysis; (iii) glucokinase; (iv) glucose-6-phosphatase; and (v) glycogen synthesis. Gluconeogenesis is represented by the combination of the pathways (i) and (iv). Glycolysis is not considered in this model. Paracetamol, [2-$^{13}$C]-glycerol, [U-$^{13}$C]-glucose and [1-$^{2}$H]-galactose were used to calculate flux rates through the pathways mentioned above. Paracetamol, as its glycoconjugate Par-GlcUA, was used to sample UDP-glucose. Incorporation of [2-$^{13}$C]-glycerol into blood glucose and urinary Par-GlcUA was used to estimated the fractional contributions of *de novo* synthesis of G6P to blood glucose and UDP-glucose (via Par-GlcUA) respectively. These fractional contributions were subsequently converted into absolute rates of gluconeogenic flux into each of the compounds by

multiplying by the rate of appearance of blood glucose and UDP-glucose (via Par-GlcUA) respectively. The rates of appearance of blood glucose and UDP-glucose were calculated from the isotopic dilution of [U-$^{13}$C]-glucose and [1-$^{2}$H]-galactose in blood glucose and urinary Par-GlcUA respectively.

The whole-body blood glucose production rate [Ra(glc;whole body)], equal to blood glucose disposal [Rd(glc)] at isotopic steady-state, was calculated according to:

$$Ra(glc;whole\ body) = Rd(glc) = M_6(glc)_{infuse}/M_6(glc)_{blood} \times infusion(glc;M_6) \quad (1)$$

in which $M_6(glc)_{infuse}$ is the excess mole fraction of infused [U-$^{13}$C]-glucose, $M_6(glc)_{blood}$ is the excess mole fraction of blood [U-$^{13}$C]-glucose, and infusion(glc;$M_6$) is the infusion rate of uniformly labeled [U-$^{13}$C]-glucose.

Metabolic clearance rate of blood glucose [MCR(glc)] was calculated according to:

$$MCR(glc) = Rd(glc)/[glc] \quad (2)$$

where [glc] is the blood glucose concentration in mmol/l.

The rates of endogenous glucose production [Ra(glc;endo)] were calculated according to:

$$Ra(glc;endo) = Ra(glc;whole\ body) - infusion(glc;M_6) \quad (3)$$

The rates of whole-body production of UDP-glucose [Ra(UDPglc;whole body)] were calculated according to:

$$Ra(UDPglc;whole\ body) = M_1(gal)_{infuse}/M_1(Par\text{-}GlcUA) \times infusion\ (gal;M_1) \quad (4)$$

in which $M_1(gal)_{infuse}$ is the excess mole fraction of infused [1-$^{2}$H]-galactose, $M_1$(Par-GlcUA) is the excess mole fraction of urinary Par-[1-$^{2}$H]-GlcUA, and infusion(gal;$M_1$) is the infusion rate of [1-$^{2}$H]-galactose. Ra(UDPglc;whole body) was calculated assuming a constant and complete entry of infused galactose into the hepatic UDP-glucose pool. Furthermore, it was assumed that the fractional isotopomer distribution observed for Par-GlcUA reflects the fractional isotopomer distribution for UDP-glucose.

The rate of appearance of endogenously produced UDP-glucose [Ra(UDPglc;endo)] was calculated according to:

$$Ra(UDPglc;endo) = Ra(UDPglc;whole\ body) - infusion(gal;M_1) \quad (5)$$

In the isotopic model applied, stable isotopically labelled compounds, *i.e.* [1-$^{2}$H]-galactose and [U-$^{13}$C]-glucose, were used that did not lose their labeled atom(s) upon entering metabolism. As a consequence, these compounds can re-enter the circulation (recycling), acting as an additional infusion of labeled compounds of unknown magnitude, which add to the excess mole fractions observed. This results in an underestimation of the rates of appearance of these compounds (12). The contribution of recycling should therefore be added to the calculated rates of appearance of endogenous compounds to obtain the total rates of appearance of these compounds (12). To calculate the recycling of [U-$^{13}$C]-glucose and [1-$^{2}$H]-galactose, two exchange factors are introduced: the fractional contribution of blood glucose to UDP-glucose formation [c(glc)], and the fractional contribution of UDP-glucose to blood glucose [c(UDPglc)]. These two factors are calculated according to:

$$c(glc) = M_6(Par\text{-}GlcUA)/M_6(glc)_{blood} \quad (6)$$

in which $M_6$(Par-GlcUA) is the excess mole fraction of urinary Par-[U-$^{13}$C]-GlcUA; and

$$c(UDPglc) = M_1(glc)_{blood}/M_1(Par\text{-}GlcUA) \quad (7)$$

in which $M_1(glc)_{blood}$ is the excess mole fraction of blood [1-$^2$H]-glucose. The associated rates of recycling of blood glucose [R(r(glc))] and of UDP-glucose [R(r(UDPglc))] were calculated as follows:

$$R(r(glc)) = (c(glc)/(1 - c(glC))) \times Ra(glc;endo) \quad (8)$$
$$R(r(UDPglc)) = (c(UDPglc)/(1 - c(UDPglc))) \times Ra(UDPglc;endo) \quad (9)$$

Total rates of endogenous glucose production [total Ra(glc;endo)] and endogenous UDP-glucose [total Ra(UDPglc;endo)] are calculated according to:

$$total\ Ra(glc;endo) = Ra(glc;endo) + R(r(glc)) \quad (10)$$
$$total\ Ra(UDPglc;endo) = Ra(UDPglc;endo) + R(r(UDPglc)) \quad (11)$$

The fractional contribution of the *de novo* synthesis of G6P to the production of glucose [f(glc)] and UDP-glucose [f(UDPglc)] was calculated from the incorporation of [2-$^{13}$C]-glycerol into glucose and Par-GlcUA respectively, as described in detail elsewhere (7,8). The rates of the gluconeogenic fluxes into blood glucose [GNG(glc)] and into UDP-glucose [GNG(UDPglc)] were calculated according to:

$$GNG(glc) = f(glc) \times (total\ Ra(glc;endo) + infusion(glc;M_6)) \quad (12)$$
$$GNG(UDPglc) = f(UDPglc) \times (total\ Ra(UDPglc;endo) + infusion(gal;M_1) \quad (13)$$

The *de novo* synthesis of G6P [GNG(G6P)] is the sum of GNG(glc) and GNG(UDPglc), corrected for the exchange of label between blood glucose and UDP-glucose, calculated according to:

$$GNG(G6P) = GNG(glc) \times (1 - c(UDPglc)) + GNG(UDPglc) \times (1 - c(glc)) \quad (14)$$

The contribution of glycogenolysis to blood glucose formation [GLY(glc)] and UDP-glucose formation [GLY(UDPglc)] was calculated according to:

$$GLY(glc) = total\ Ra(glc;endo) – GNG(glc) \quad (15)$$

in which the contribution of glycogenolysis to the total rate of appearance of glucose in blood is equal to the part that is not derived from gluconeogenesis; and

$$GLY(UDPglc) = total\ Ra(UDPglc;endo) – GNG(UDPglc) – glc(UDPglc) \quad (16)$$

in which glc(UDPglc) represents the contribution of blood glucose to UDP-glucose, which was calculated according to:

$$glc(UDPglc) = c(glc) \times (total\ Ra(UDPglc;endo) + infusion(gal;M_1)) \quad (17)$$

In contrast to blood glucose, the total rate of appearance of UDP-glucose is determined by: (i) gluconeogenic flux from G6P; (ii) glycogenolysis; and (iii) the flux of blood glucose into the UDP-glucose pool. The flux of glycogen into UDP-glucose is a measure of glycogen/glucose-1-phosphate cycling (8).

The individual isotopic fluxes through the various enzymes involved in hepatic glucose metabolism were calculated based on a factorial model by adding the different contributions to the flux rates. For the enzymes glucokinase (Gk), glucose-6-phosphatase (G6pase), glycogen synthase (Gs) and glycogen phosphorylase (Gp) the flux rates were calculated according to:

$$Gk = glc(UDPglc) + R(r(glc)) \quad (18)$$

in which only two contributions to the flux through Gk are considered (*i.e.* the flux of blood glucose into UDP-glucose and glucose / G6P cycling), whereas glycolysis is not included

$$G6pase = \text{total } Ra(glc;endo) = GNG(glc) + GLY(glc) \quad (19)$$
$$Gs = Ra(UDPglc;\text{whole body}) \quad (20)$$
$$Gp = GLY(glc) + GLY(UDPglc) \quad (21)$$

in which two contributions to the flux through glycogen phosphorylase are considered (*i.e.* glycogenolysis resulting in blood glucose appearance and glycogen/G1P cycling).

*Statistical analysis*

All values are means ± SD. Levels of significance of difference of metabolite concentrations, gene expression and the values of the individual time points during isotope infusion experiments were determined using the non-parametric Mann–Whitney test for unpaired data. Levels of significance of differences between the averages of the values of the fluxes at individual time points between 3 and 6 h during the experiment were estimated using repeated measures ANOVA. A p-value of less than 0.05 was considered statistically significant.

## Results

Body and liver weights of obese mice were more than double those of lean mice (table 2.2). Consequently, normalisation of liver weight to body weight yielded no difference between obese and lean mice. Protein contents per gram of liver tissue were not significantly different between obese and lean mice. Hepatic glycogen content was mildly elevated in *ob/ob* mice, whereas G6P levels were not significantly different between the two groups. At the end of the experiment, plasma NEFA concentrations were almost two-fold higher in the *ob/ob* mice than in the lean mice. Plasma lactate and alanine concentrations were similar in the two groups, whereas plasma ß-hydroxybutyrate concentrations were elevated in *ob/ob* mice.

Figure 2.2 shows the blood glucose concentrations of the two groups of mice during the infusion experiment. Obese mice were clearly hyperglycaemic (8.8 ± 0.5 *vs.* 13.2 ± 1.9 mmol/l, lean versus obese mice, $p<0.05$) and hyperinsulinaemic. Insulin concentrations remained constant (45 ± 10 pmol/l at t=0 and 60 ± 45 pmol/l at t=6 h) during the experiment in lean mice, but decreased from 900 ± 480 pmol/l at t=0 to 435 ± 270 pmol/l at t=6 h in *ob/ob* mice.

Table 2.2. Hepatic and plasma parameters in *ob/ob* mice and lean littermates

| | Lean mice (n=7) | *Ob/ob* mice (n=7) |
|---|---|---|
| Liver | | |
| body weight (g) | 22.7 ± 1.2 | 49.7 ± 3.0 * |
| liver weight (g) | 1.1 ± 0.0 | 2.6 ± 0.4 * |
| relative liver weight (% body weight) | 4.7 ± 0.3 | 5.0 ± 0.8 |
| total liver protein (mg) | 156 ± 20 | 325 ± 63 * |
| liver protein content (mg/g liver) | 144 ± 18 | 127 ± 18 |
| G6P (nmol/g liver) | 118 ± 56 | 153 ± 34 |
| glycogen (µmol glucose/g liver) | 179 ± 16 | 207 ± 11 * |
| Plasma | | |
| glucose (mmol/l) | 8.8 ± 0.5 | 13.2 ± 1.9 * |
| insulin (pmol/l) | 45 ± 10 | 900 ± 480 * |
| NEFA (mmol/l) | 0.5 ± 0.1 | 0.9 ± 0.2 * |
| ß-hydroxybutyrate (mmol/l) | 0.5 ± 0.4 | 3.1 ± 1.4 * |
| alanine (µmol/l) | 133 ± 113 | 176 ± 33 |
| lactate (mmol/l) | 3.5 ± 1.0 | 3.5 ± 1.0 |

Figure 2.3 shows endogenous glucose production [Ra(glc;endo), equation (3)] and the metabolic clearance rate of glucose [MCR(glc), equation (2)]. At isotopic steady-state, *i.e.* between 3 h and 6 h after the start of the infusion of labelled compounds, endogenous glucose production was significantly decreased in *ob/ob* mice (152 ± 27 *vs.* 109 ± 23 $\mu mol \cdot kg^{-1} \cdot min^{-1}$, lean versus obese mice, $p<0.001$), as was the metabolic clearance rate of glucose (18 ± 2 *vs.* 8 ± 2 $ml \cdot kg^{-1} \cdot min^{-1}$, lean versus obese mice, $p<0.001$).

The rate of *de novo* synthesis of G6P [GNG(G6P), equation (14)] in obese mice was significantly lower than that in lean control mice (160 ± 6 *vs.* 122 ± 13 $\mu mol \cdot kg^{-1} \cdot min^{-1}$, lean versus obese mice, $p<0.001$) (figure 2.4a). In obese mice, the partitioning of newly synthesised G6P towards plasma glucose or glycogen was similar to that in lean control mice (figure 2.4b). In contrast, glucose cycling [R(r(glc)), equation (8)] was greatly enhanced in obese mice (56 ± 13 $\mu mol \cdot kg^{-1} \cdot min^{-1}$ *vs.* 26 ± 4 $\mu mol \cdot kg^{-1} \cdot min^{-1}$, obese versus lean mice, $p<0.001$) (figure 2.5a). Consequently, total endogenous glucose production, *i.e.* the sum of endogenous glucose production and glucose cycling, was not significantly different in obese and lean mice (178 ± 28 *vs.* 165 ± 31 $\mu mol \cdot kg^{-1} \cdot min^{-1}$, lean versus obese mice, NS) (figure 2.5b).

Figure 2.6 shows the calculated mean values obtained at steady-state for the individual fluxes through the various pathways of hepatic glucose metabolism. As anticipated, the calculated isotopic flux through glucokinase [Gk, equation (18)] was strongly increased in obese mice. The glucose-6-phosphatase flux [G6pase, equation (19)], equivalent to the total endogenous glucose production, was unchanged. The flux through glycogen phosphorylase [Gp, equation (21)] was not altered significantly, whereas the glycogen synthase flux [Gs, equation (20)] was significantly decreased in obese mice compared with lean littermates.

Table 2.3 provides a summary of the calculated flux rates, normalised to either body weight or amount of liver protein (liver is the major glucose-producing organ). Independent of the method of normalisation, the same conclusions can be drawn with respect to the changes in glucose metabolism in lean and *ob/ob* mice.

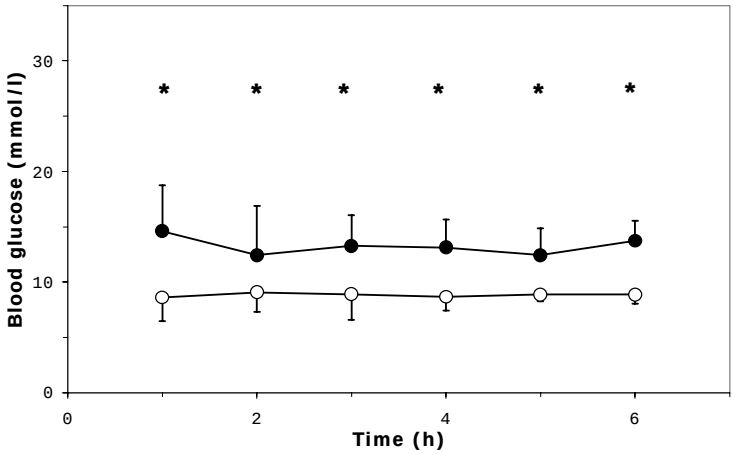


Figure 2.2. Plasma glucose concentrations during infusion experiments. Blood glucose levels in lean (empty circles, n=7) and *ob/ob* (filled circles, n=7) mice. Values shown are the means ± SD. * p<0.05 vs lean animals.

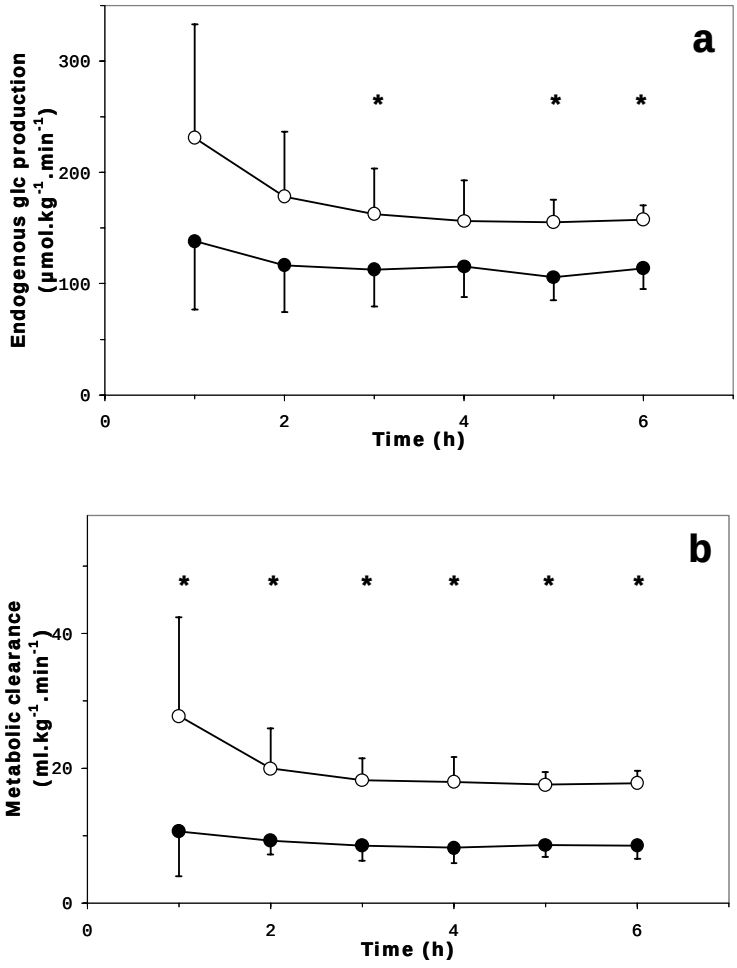


Figure 2.3. Endogenous glucose production (a) and metabolic clearance (b) during the infusion experiments in lean (empty circles, *n*=7) and *ob/ob* (filled circles, *n*=7) mice. Values shown are the means ± SD. * *p*<0.05 vs lean animals.

Levels of expression of relevant genes in the liver of lean and *ob/ob* mice are shown in figure 2.7. The expression of the genes encoding glucokinase and liver-type pyruvate kinase were strongly up-regulated in the liver of *ob/ob* mice. The mRNA levels of other key enzymes involved in carbohydrate metabolism (*i.e.* phosphoenolpyruvate carboxykinase, G6P hydrolase and G6P translocase) did not differ significantly between obese and lean mice. It has previously been shown that the expression of the genes encoding sterol regulatory element-binding protein-1c (*Srebp-1c*) and peroxisome proliferator-activated receptor-γ (*Pparγ*), transcription factors involved in control of hepatic glucose and fat metabolism, is significantly elevated in the liver of *ob/ob* mice compared with that of their lean littermates (13). Furthermore, mRNA levels of *Irs-1*, but particularly *Irs-2*, were observed to be strongly repressed in the liver of obese mice (13).

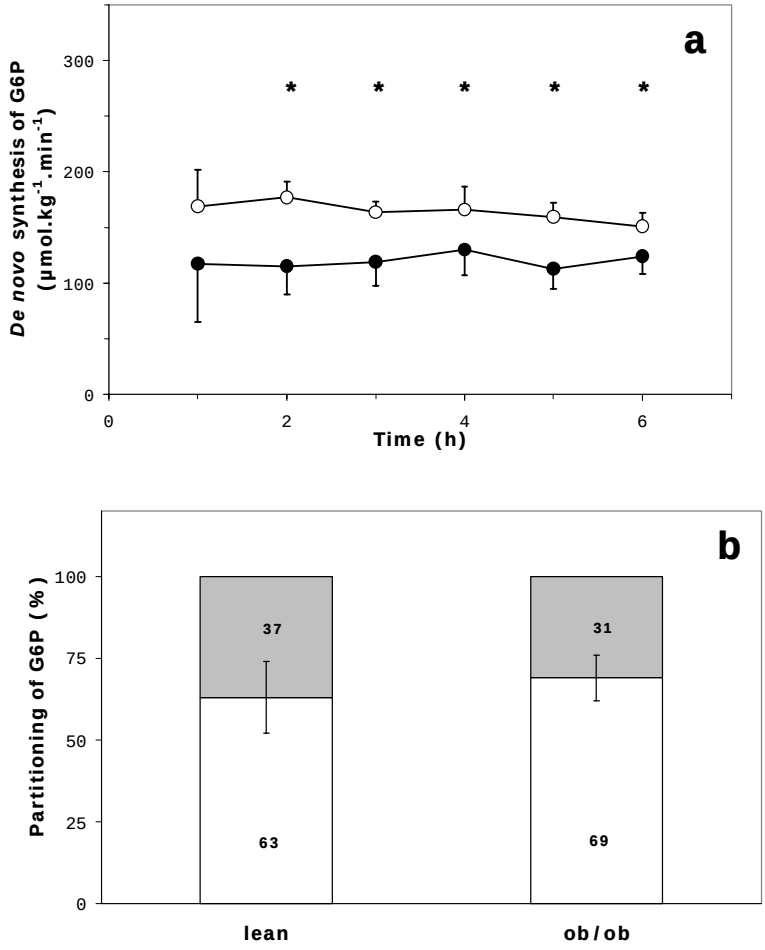


Figure 2.4. (a) The rate of *de novo* synthesis of G6P in lean (empty circles) and *ob/ob* (filled circles) mice. (b) The partitioning of the rates of *de novo* synthesis of G6P to UDP-glucose (shaded area) and to glucose (white area) during the last 3 h of the infusion experiment in lean and *ob/ob* mice. Values shown are the means ± SD ($n$=7 for each group). * $p$<0.05 *vs.* lean animals.

Table 2.3. Summary of the calculated values of the various flux rates, using the isotopic model shown in figure 2.1 normalised to either body weight or liver protein.

| | Normalised to body weight ($\mu mol \cdot kg^{-1} \cdot min^{-1}$) | | Normalised to liver protein ($\mu mol \cdot g\ protein^{-1} \cdot min^{-1}$) | |
|---|---|---|---|---|
| | lean | *Ob/ob* | lean | *Ob/ob* |
| *De novo* synthesis of G6P (Pepck) | 160 ± 6 | 122 ± 13 * | 23.6 ± 0.9 | 18.8 ± 2.0 * |
| Endogenous glucose production | 157 ± 27 | 109 ± 23 * | 23.1 ± 4.0 | 16.8 ± 3.5 * |
| Glucose cycling | 26 ± 4 | 56 ± 13 * | 3.8 ± 0.6 | 8.6 ± 2.0 * |
| Total endogenous glucose production (G6Pase) | 178 ± 28 | 165 ± 31 | 26.2 ± 4.1 | 25.4 ± 4.8 |
| Glucokinase | 73 ± 11 | 82 ± 18 * | 6.3 ± 1.6 | 12.6 ± 2.8 * |
| Glycogen synthase | 100 ± 35 | 67 ± 16 * | 14.7 ± 5.2 | 10.3 ± 2.5 * |
| Glycogen phosphorylase | 40 ± 18 | 50 ± 15 | 5.9 ± 2.7 | 7.7 ± 2.3 |

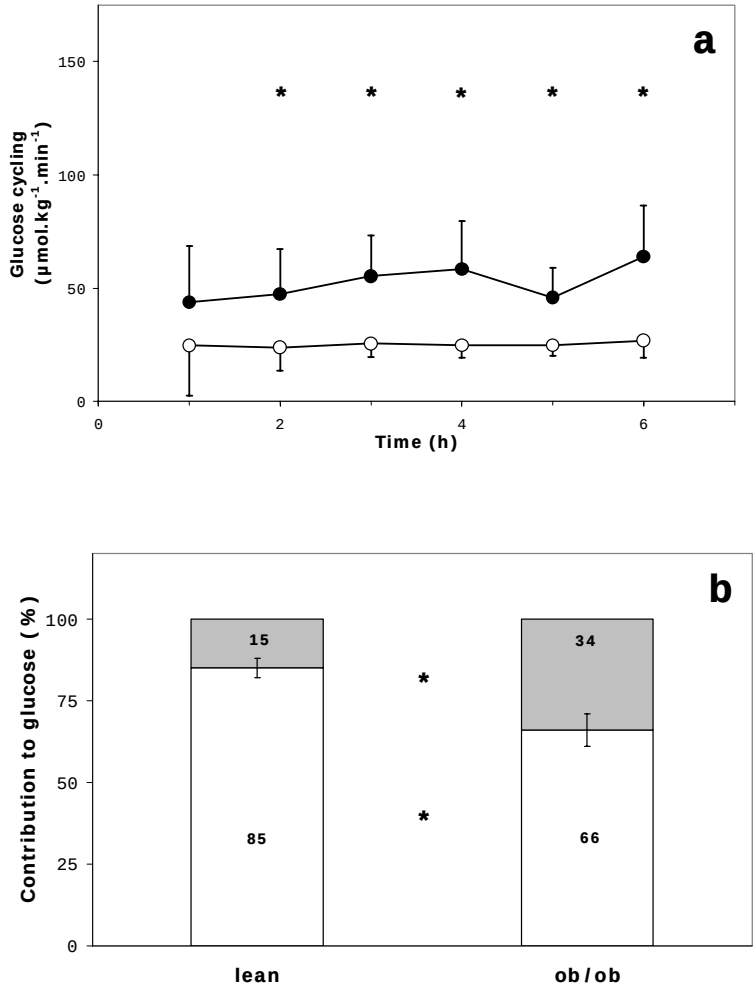


Figure 2.5. (a) Rate of cycling between glucose and G6P during the infusion experiment in lean (empty circles) and *ob/ob* (filled circles) mice. (b) The contributions of endogenous glucose production (white area) and glucose cycling (shaded area) to the total endogenous glucose production in lean and *ob/ob* mice during the last 3 h of the infusion experiment. Values shown are the means ± SD ($n$=7 for each group). * $p$<0.05 vs lean animals.

## Discussion

The leptin-deficient *ob/ob* mouse is a commonly used mouse model of type 2 diabetes, but quantitative *in vivo* data on the disturbances that underlie hyperglycaemia in this model are sparse. In this study, we determined flux rates through various pathways relevant in hepatic carbohydrate metabolism in lean and *ob/ob* mice. When expressed per unit of body weight or liver protein, hepatic glucose metabolism activity was, in general, suppressed in obese mice compared with that in their lean littermates. However, glucose cycling was an exception to this, and was observed to be greatly increased in obese mice. Interestingly, the newly produced G6P was not preferentially directed towards plasma glucose in *ob/ob* mice, but instead was partitioned to glycogen stores to a similar extent as that observed in lean mice. Furthermore, the expression of genes of key enzymes involved in glucose metabolism were similar in livers of *ob/ob* and lean mice, apart from the expression of glucokinase and liver-type pyruvate kinase which was increased in the liver of *ob/ob* mice.

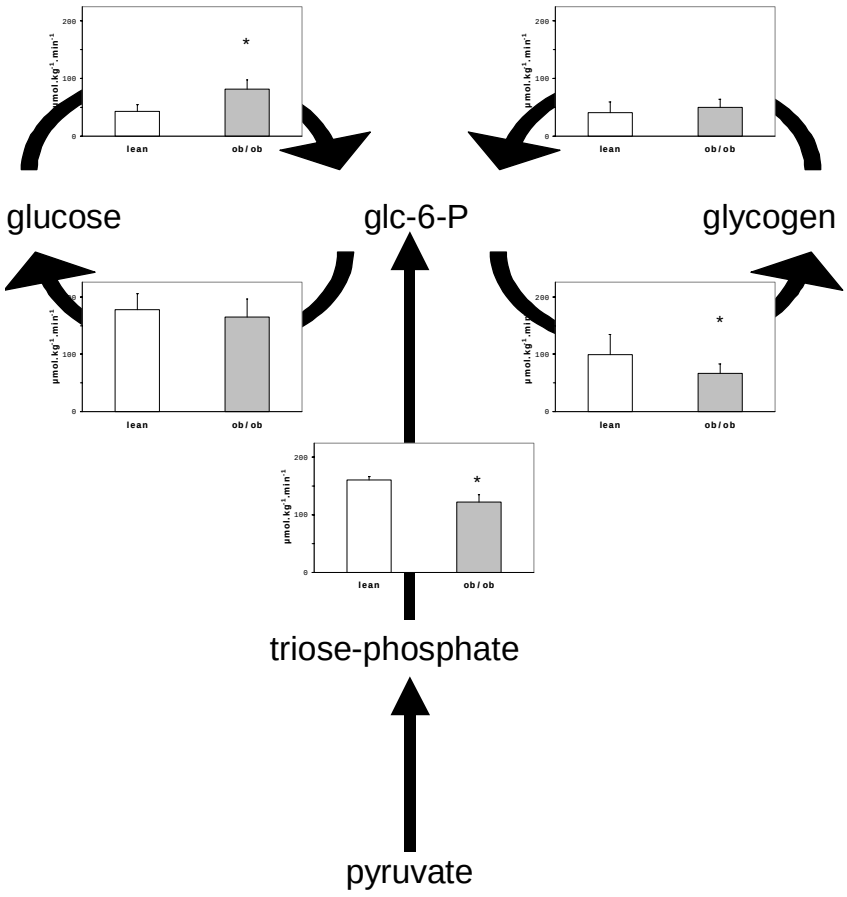


Figure 2.6. Separate fluxes through the relevant metabolic pathways involved in hepatic carbohydrate metabolism during the last 3 h of the infusion experiment in lean and *ob/ob* mice. Values shown are the means ± SD ($n$=7 for each group). * $p$<0.05 vs lean animals.

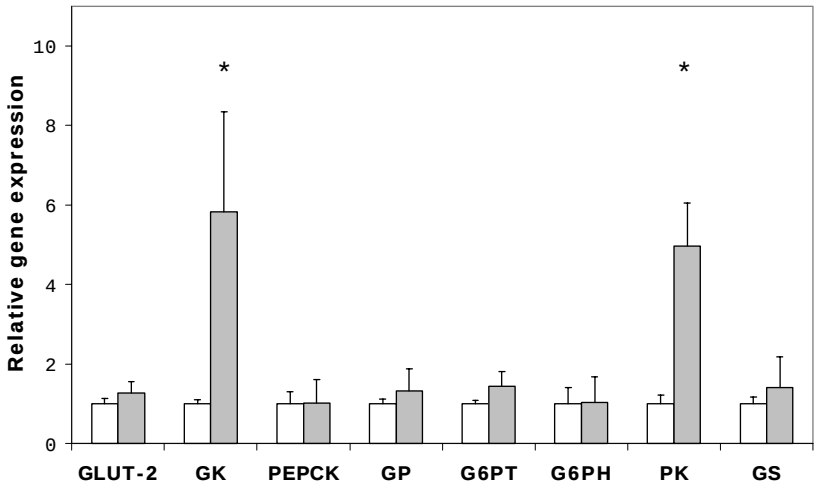


Figure 2.7. Gene expression of enzymes involved in glucose metabolism at the end of the infusion experiment in lean (*n*=3) and *ob/ob* (*n*=3) mice. Levels of cDNA were measured by RT-PCR as described in the Materials and methods section. Data are expressed relative to *18S-rRNA* and the results of the lean animals are set equal to 1. Expression of genes was normalised to 18S-rRNA, since the level of *ß-actin* mRNA in livers of obese mice was increased by ~30% when normalised by liver weight. In contrast, 18S-rRNA levels were similar in livers of obese and lean mice. * $p<0.05$ vs lean animals. *G6ph*, G6P hydrolase; *G6pt*, G6P translocase; *Gk*, glucokinase; *Gp*, glycogen phosphorylase; *Gs*, glycogen synthase; *Pepck*, phosphoenolpyruvate carboxykinase; *Pk*, pyruvate kinase.

Before discussing the results, some methodological issues have to be addressed. In this study, a multiple isotope infusion protocol was used to calculate the relevant fluxes of glucose metabolism (7). The validity of the isotope model, with the application of glycoconjugates, and the mass isotopomer distribution analysis (MIDA) approach has been substantiated in various studies, although some controversy still remains (14,15). Since the contribution of glycolysis to intracellular G6P metabolism has not been included in this model, the calculated flux rate through glucokinase represents a minimal estimate. We have validated the application of MIDA in 9-h fasted C57Bl/6 mice in a separate study (10). In 24-h fasted mice, no stable isotopic steady-state could be obtained (10). In the current study, we compared hepatic glucose metabolism in groups of mice with strongly different body compositions. Our data show that, with respect to hepatic glucose metabolism, normalisation to body weight appeared to be appropriate, since the same conclusions could be drawn regardless of whether the data was normalised to body weight or liver protein.

Irrespective of hyperinsulinaemia and hyperglycaemia, total glucose output (glucose-6-phosphatase flux) was not affected, while endogenous glucose production was only modestly inhibited in *ob/ob* mice. This points to hepatic insulin resistance. Previously reported values of endogenous glucose production in C57Bl/6 mice are almost identical to those reported in this study in lean littermates of *ob/ob* mice (16,17). Furthermore, endogenous glucose production in C57Bl/6 mice could be suppressed almost completely during hyperinsulinaemic clamp at normal or increased glucose concentrations (16-18). The impaired suppression of endogenous glucose production was mainly due to the blunted response of *de novo* synthesis of G6P to the combined hyperinsulinaemia and hyperglycaemia in *ob/ob* mice. This indicates that, in the absence of leptin, insulin appears to be largely ineffective in suppressing hepatic *de novo* synthesis of G6P by an as yet unknown mechanism.

In the liver of *ob/ob* mice, the decreased contribution of endogenous glucose production to total glucose output appeared to be compensated by enhanced glucose cycling. Glucose cycling was increased by a factor of ~2.5 in the liver of *ob/ob* mice, due to an enhanced flux through glucokinase. A previous study reported a high rate of glucose cycling in hepatocytes isolated from the liver of *ob/ob* mice fasted for 24 h (5). Similarly, in an earlier publication, glucokinase activity was found to remain elevated in the liver of *ob/ob* mice throughout a 48-h fast (19). Collectively, these observations indicate that, independent of the duration of fasting, the liver of *ob/ob* mice maintains a high capacity to phosphorylate glucose.

Besides hepatic insulin resistance, peripheral organs were also found to be insulin resistant in *ob/ob* mice. Metabolic clearance of plasma glucose was decreased by a factor of ~2 at blood glucose concentrations that were almost double that in lean mice. This indicates that net glucose uptake by peripheral tissue was similar in *ob/ob* and lean mice, irrespective of the elevated insulin concentrations in the obese group. Thus, hyperglycaemia in *ob/ob* mice is due to peripheral insulin resistance. This finding is in agreement with an earlier study using different means to investigate peripheral insulin resistance in *ob/ob* mice, which reported that uptake of 2-deoxyglucose was severely inhibited in isolated skeletal muscle of obese mice compared with that in lean mice (20).

As discussed, we observed 'normal' rates of total glucose output and high rates of glucose cycling. In accordance with these observations, 'normal' mRNA levels of the gluconeogenic enzymes G6P hydrolase and phosphoenolpyruvate carboxykinase were observed, while mRNA levels of glucokinase and liver-type pyruvate kinase were significantly increased in the liver of obese mice compared to those in liver of lean littermates. Significant increases in mRNA levels of *Srebp-1c* and its target genes in lipogenesis, *i.e. Fas* and *Acc1*, in livers of fasted *ob/ob* mice have previously been reported (13,21). This indicates an enhanced glycolytic flux into lipogenesis. It should be realised that the glycolytic flux as part of the glucokinase flux cannot be assessed in the isotopic model applied. Recent data indicate that hyperglycaemia could directly induce increased expression of the genes encoding *Srebp-1c* and pyruvate kinase in an insulin-independent way (22).

In humans with type 2 diabetes, there is evidence for enhanced gluconeogenesis and glycogenolysis after an overnight fast, particularly in patients with severe fasting hyperglycaemia (1,23-28). Although liver was insulin resistant in *ob/ob* mice, this did not result in enhanced hepatic glucose production. In the present study, only a moderate fasting hyperglycaemia was observed in *ob/ob* mice at 8 weeks of age. Apparently, in these mice the disease had not yet progressed to a more severe stage with (very) high fasting blood glucose concentrations. Furthermore, in most studies on (often obese) diabetic subjects, the data was normalised to lean body mass instead of body weight, which might have led to seemingly elevated values for gluconeogenic and glycogenolytic fluxes in these individuals compared with those in non-diabetic subjects. Until now, only very few studies have considered the role of glucose cycling in hepatic glucose production. There are indications that hepatic cycling of glucose is elevated in humans with type 2 diabetes (2,3).

In conclusion, this study demonstrates that in *ob/ob* mice, *de novo* synthesis of G6P is diminished while glucose cycling is increased, resulting in an unaffected total glucose output by the liver. However, these observations were made where there was a background of hyperglycaemia and hyperinsulinaemia. This points to a co-existence of hepatic and peripheral insulin resistance, with peripheral insulin resistance as the cause of hyperglycaemia.

## Acknowledgements

This work was supported by the Dutch Diabetes Foundation (grant 96.604). R.H.J. Bandsma is supported by the Dutch Organisation for Scientific Research (NWO). We thank T. Boer, P. Modderman and T. Jager for excellent technical assistance.

## References

1. DeFronzo RA, Bonadonna RC, Ferrannini E (1992) Pathogenesis of NIDDM. A balanced overview. Diabetes Care 15:318–368
2. Efendic S, Wajngot A, Vranic M (1985) Increased activity of the glucose cycle in the liver: early characteristic of Type 2 diabetes. Proc Natl Acad Sci USA 82:2965–2969
3. Rooney DP, Neely RDG, Beatty O *et al*. (1993) Contribution of glucose/glucose-6-phosphate cycle activity to insulin resistance in Type 2 (non-insulin-dependent) diabetes mellitus. Diabetologia 36:106–112
4. Shull KH, Mayer J (1956) The turnover of liver glycogen in obese hyperglycemic mice. J Biol Chem 218:885–896
5. Lahtela JT, Wals PA, Katz J (1990) Glucose metabolism and recycling by hepatocytes of *OB/OB* and *ob/ob* mice. Am J Physiol 259:E389–E396
6. Lee WN, Byerley LO, Bergner EA, Edmond J (1991) Mass isotopomer analysis: theoretical and practical considerations. Biol Mass Spectrom 20:451–458
7. Hellerstein MK, Neese RA, Linfoot P, Christiansen M, Turner S, Letscher A (1997) Hepatic gluconeogenic fluxes and glycogen turnover during fasting in humans. A stable isotope study. J Clin Invest 100:1305–1319
8. Van Dijk TH, Van der Sluijs FH, Wiegman CH *et al*. (2001) Acute inhibition of hepatic glucose-6-phosphatase does not affect gluconeogenesis but directs gluconeogenic
flux toward glycogen in fasted rats. A pharmacological study with the chlorogenic acid derivative S4048. J Biol Chem 276:25727–25735
9. Kuipers F, Havinga R, Bosschieter H, Toorop GP, Hindriks FR, Vonk RJ (1985) Enterohepatic circulation in the rat. Gastroenterology 88:403–411
10. Van Dijk TH, Boer TS, Havinga R, Stellaard F, Kuipers F, Reijngoud DJ (2004) Quantification of hepatic carbohydrate metabolism in conscious mice using serial blood and urine spots. Anal Biochem 322:1–13
11. Lowry OH, Rosebrough NJ, Farr AL, Randall RL (1951) Protein measurement with the Folin phenol reagent. J Biol Chem 193:265–275
12. Rognstad R (1994) Isotopic estimation of the hepatic glucose balance in vivo. J Theor Biol 168:161–173
13.Wiegman CH, Bandsma RHJ, Ouwens M *et al*. (2003) Hepatic VLDL production in *ob/ob* mice is not stimulated by massive *de novo* lipogenesis but is less sensitive to the suppressive effects of insulin. Diabetes 52:1081–1089
14. Landau BR, Wahren J, Chandramouli V, Schumann WC, Ekberg K, Kalhan SC (1996) Contributions of gluconeogenesis to glucose production in the fasted state. J Clin Invest 98:378–385
15. Landau BR, Wahren J, Ekberg K, Previs SF, Yang D, Brunengraber H (1998) Limitations in estimating gluconeogenesis and Cori cycling from mass isotopomer distributions using [U-13C6]glucose. Am J Physiol 274:E954–E961
16. Massillon D, Chen W, Hawkins M, Liu R, Barzilai N, Rossetti L (1995) Quantification of hepatic glucose fluxes and pathways of hepatic glycogen synthesis in conscious mice. Am J Physiol 269:E1037–E1043
17. Ren J-M, Marshall BA, Mueckler MM, McCaleb M, Amatruda JM, Shulman G (1995) Overexpression of Glut4 protein in muscle increases basal and insulin-stimulated whole body glucose disposal in conscious mice. J Clin Invest 95:429–432
18. Grefhorst A, van Dijk TH, Hammer A, van der Sluijs FH, Havinga R, Havekes LM, Romijn JA, Groot PH, Reijngoud DJ, Kuipers F (2005) Differential effects of pharmacological liver X receptor activation on hepatic and peripheral insulin sensitivity in lean and *ob/ob* mice. Am J Physiol Endocrinol Metab, in press
19. Hron WT, Sobocinski KA, Menahan LA (1984) Enzyme activities of hepatic glucose utilization in the fed and genetically obese mouse at 4-5 months of age. Horm Metab Res 16:S32–S36
20. Cuendet GS, Loten EG, Jeanrenaud B, Renold AE (1976) Decreased basal, non insulin-stimulated glucose uptake and metabolism by skeletal soleus muscle isolated from obesehyperglycemic (*ob/ob*) mice. J Clin Invest 58:1078–1088
21. Shimomura I, Bashmakov Y, Horton JD (1999) Increased levels of nuclear SREBP-1c associated with fatty livers in two mouse models of diabetes mellitus. J Biol Chem 274:30028–30032
22. Matsuzaka T, Shimano H, Yahagi N *et al*. (2004) Insulin independent induction of sterol regulatory element-binding protein-1c expression in the livers of streptozotocin-treated mice. Diabetes 53:560–569
23. Gastaldelli A, Baldi S, Pettiti M *et al*. (2000) Influence of obesity and Type 2 diabetes on gluconeogenesis and glucose output in humans: a quantitative study. Diabetes 49:1367–1373

24. Magnusson I, Rothman DL, Katz LD, Shulman RG, Shulman GI (1992) Increased rate of gluconeogenesis in type II diabetes mellitus. A13C nuclear magnetic resonance study. J Clin Invest 90:1323–1327
25. Boden G, Chen X, Capulong E, Mozzoli M (2001) Effects of free fatty acids on gluconeogenesis and autoregulation of glucose production in Type 2 diabetes. Diabetes 50:810–816
26. Tayek JA, Katz J (1996) Glucose production, recycling, and gluconeogenesis in normals and diabetics: a mass isotopomer [U-13C]glucose study. Am J Physiol 270:E709–E717
27. Consoli A, Nurjhan N, Capani F, Gerich J (1989) Predominant role of gluconeogenesis in increased hepatic glucose production in NIDDM. Diabetes 38:550–557
28. Consoli A, Nurjhan N (1990) Contribution of gluconeogenesis to overall glucose output in diabetic and non diabetic men. Ann Med 22:191–195

# Chapter 3

# Stimulation of lipogenesis by pharmacological activation of the liver X receptor leads to production of large, triglyceride-rich very low density lipoprotein particles

Aldo Grefhorst[1*], Baukje M. Elzinga[1*], Peter J. Voshol[2,3], Torsten Plösch[1], Tineke Kok[1], Vincent W. Bloks[1], Fjodor H. van der Sluijs[1], Louis M. Havekes[2,4,], Johannes A. Romijn[3], Henkjan J. Verkade[1], Folkert Kuipers[1]

[1]Laboratory of Pediatrics, University Medical Center Groningen
[2]TNO Prevention and Health, Leiden
[3]Department of Endocrinology and Diabetes, Leiden University Medical Center
[4]Department of Internal Medicine, Leiden University Medical Center
[*]These authors contributed equally to this work

**J. Biol. Chem. 2002: 277: 34182-34190**

## Abstract

The oxysterol-activated liver X receptor (LXR) provides a link between sterol and fatty acid metabolism; activation of LXR induces transcription of lipogenic genes. This study shows that induction of the lipogenic genes *Srebp-1c*, *Fas*, and *Acc1* upon administration of the synthetic LXR agonist T0901317 to C57BL/6J mice (10 mg/kg/day, 4 days) is associated with massive hepatic steatosis along the entire liver lobule and a 2.5-fold increase in very low density lipoprotein-triglyceride (VLDL-TG) secretion. The increased VLDL-TG secretion was fully accounted for by formation of larger (129 ± 9 nm versus 94 ± 12 nm, a 2.5-fold increase of particle volume) TG-rich particles. Stimulation of VLDL-TG secretion did not lead to elevated plasma TG levels in C57BL/6J mice, indicating efficient particle metabolism and clearance. However, T0901317 treatment did lead to severe hypertriglyceridemia in mouse models of defective TG-rich lipoprotein clearance, *i.e.* APOE*3-Leiden transgenic mice (3.2-fold increase) and apoE -/- LDLr -/- double knockouts (12-fold increase). Incubation of rat hepatoma McA-RH7777 cells with T0901317 also resulted in intracellular TG accumulation and enhanced TG secretion. We conclude that, in addition to raising high density lipoprotein cholesterol concentrations, pharmacological LXR activation in mice leads to development of hepatic steatosis and secretion of atherogenic, large TG-rich VLDL particles.

## Introduction

The nuclear liver X receptor α (LXRα; NR1H3) and LXRβ (NR1H2) are involved in the control of cholesterol and fatty acid metabolism. LXRα is expressed mainly in the liver whereas LXRβ is ubiquitously expressed (1,2). Activated LXRs heterodimerize with the retinoid X receptor (NR2B1) and bind to a LXR response element, consisting of two hexameric nucleotide direct repeats separated by four nucleotides, to induce gene transcription (1,2). Oxysterols constitute the physiological ligands for LXR. The most potent LXR-activating oxysterols are 22(R)-hydroxycholesterol, 24(S)-hydroxycholesterol, and 24(S),25-epoxycholesterol (3). Activation of LXR in macrophages results in increased expression of genes encoding ATP-binding cassette (ABC) cholesterol transporters ABCA1 (4-7) and ABCG1 (8,9) and apolipoprotein E (apoE) (9). ABCA1, ABCG1, and apoE are involved in cholesterol efflux from macrophages toward high density lipoproteins (HDL), which is considered the critical first step of reverse cholesterol transport. In the liver, LXR is involved in transcriptional control of *Cyp7A1*, encoding a critical enzyme in the conversion of cholesterol into bile acids (3, 10), as well as in transcriptional control of ABCG5/ABCG8 (11,12), ABC transporters implicated in biliary cholesterol excretion. Induction of intestinal *Abca1*, *Abcg5*, and *Abcg8* expression upon LXR activation is thought to reduce the efficiency of cholesterol absorption and hence to accelerate fecal cholesterol disposal (4). The physiological role of LXR in the control of cholesterol metabolism and the possibility of pharmacological interventions aimed at prevention of atherosclerosis via this regulatory system have recently been reviewed extensively (13-17).

In addition to cholesterol transport genes, LXR has been reported to control genes that encode proteins involved in *de novo* lipogenesis. Induced transcription has been reported for the gene encoding the sterol-regulatory element-binding protein-1c (SREBP-1c) (18-20), the transcription factor that regulates expression of various lipogenic genes, including those encoding acetyl-CoA carboxylase (ACC) and fatty acid synthase (21). Apart from indirect actions through SREBP-1c, LXR also directly influences transcription of *Fas* (22) and of genes encoding lipoprotein lipase (23), cholesterol ester transfer protein (24), and stearoyl-CoA desaturase-1 (25).

Recently, the availability of synthetic LXR agonists, *e.g.* T0901317, has provided more insight into metabolic consequences of LXR activation. Oral administration of T0901317 to C57BL/6 mice increased HDL cholesterol concentrations in plasma, probably related to induction of the *Abca1* and *Abcg1* expression (18). In addition to this potentially beneficial effect, treatment with LXR agonists also led to a marked increase in hepatic triglyceride (TG) content (18). In Lxrα/Lxrβ double knockout mice, hepatic steatosis did not occur upon treatment with high doses of the agonist (18). In wild type mice, but not in *Lxrα* knockout mice, hepatic TG accumulation was also observed upon feeding a high cholesterol diet (10). Hepatic steatosis is thought to be a result of increased fatty acid synthesis caused by induction of lipogenic genes. *De novo* lipogenesis, in turn, is thought to contribute to regulation of hepatic very low density lipoprotein (VLDL) production (26), but data on VLDL production upon LXR activation are not available. In this study, we examined the effects of T0901317 treatment on VLDL-TG production rates in relation to steady state plasma TG levels in mice. Our results demonstrate that administration of the synthetic LXR agonist resulted in an increased hepatic production rate of VLDL-TG, caused by formation of large TG-rich particles. In wild type mice, increased VLDL-TG production was compensated for by efficient metabolism and clearance, and no effects on fasting TG levels were seen. However, in mice with impaired particle clearance (apoE -/- LDLr -/- double knockouts, APOE*3-Leiden transgenics) treatment with the LXR agonist resulted in a marked hypertriglyceridemia.

## Experimental procedures

*Animals*

Male C57BL/6J mice (Harlan, Horst, The Netherlands), were housed in a light- and temperature-controlled facility. The animals were fed a commercially available lab chow (RMH-B, Hope Farms BV, Woerden, The Netherlands), containing 6.2% fat and ~0.01% cholesterol (w/w), and water ad libitum. Male transgenic mice expressing the human APOE*3-Leiden gene (27,28) and apoE -/- LDLr -/- double knockout mice (29) were bred at the animal facility of the Gaubius Laboratory (Leiden, The Netherlands) and were fed the same standard diet. The mice received humane care, and experimental procedures were in accordance with local guidelines for use of experimental animals.

*Plasma and liver tissue sampling*

C57BL/6J mice received 10 mg/kg LXR agonist T0901317 (kindly donated by Organon Laboratories, Lanarkshire, United Kingdom) or its solvent by gavage daily for 4 days. T0901317 was dissolved in Me2SO and Chremophor (both from Sigma) in 5% mannitol/water, to a final concentration of 2.5 mg/ml. On the morning of the fifth day, a large blood sample was collected by cardiac puncture and centrifuged. The obtained plasma was stored at  20 °C until analyzed. The liver was quickly removed, weighed, and frozen in separate portions for RNA isolation and lipid analysis. Parts of the liver were frozen in isopentane and used for microscopic examination.

ApoE -/- LDLr -/- double knockout mice and APOE*3-Leiden transgenic mice were treated for 4 days with T0901317 (10 mg/kg/day) or its solvent as described. Before onset of treatment (day 0) and on day 2 of treatment, a small EDTA blood sample was collected by tail bleeding and plasma was obtained for measurement of triglyceride concentrations. On day 4 of treatment, a large blood sample was obtained by cardiac puncture.

*In vivo VLDL triglyceride production rate*

C57BL/6J wild type mice received T0901317 or the solvent only exactly as described. On the fifth day, after a fasting period of 10 h, mice received an injection of 12.5 mg of Triton WR-1339 in 100 µl of phosphate-buffered saline via the penile vein. Tail blood samples were taken under light halothane anesthesia before and 1, 2, and 3 h after the injection of Triton WR-1339. At 4 h after Triton WR-1339, a large blood sample was collected by cardiac puncture. The collected blood samples were used for triglyceride measurements. VLDL triglyceride production rate was calculated from the slope of the triglyceride concentration versus time curve (30). The large blood sample was used for isolation of VLDL.

*Hepatic RNA isolation and measurement of mRNA levels by real-time PCR (Taqman)*

Total RNA was isolated from ~30 mg of liver tissue with the TRIzol method (Invitrogen, Paisley, United Kingdom). RNA was converted to single stranded cDNA by a reverse transcription procedure with Moloney murine leukemia virus-RT (Roche Diagnostics, Mannheim, Germany) according to the protocol of the manufacturer using random primers. cDNA levels were measured by real-time PCR using the ABI Prism 7700 sequence detection system (Applied Biosystems, Foster City, CA).

For the PCR amplification studies, an amount of cDNA corresponding to 20 ng of total RNA was amplified using the qPCR core kit (Eurogentec, Seraing, Belgium) essentially according to the protocol of the manufacturer and optimized for amplification of the particular gene using the appropriate forward and reverse primers (Invitrogen) and a template-specific 3'-TAMRA (6-carboxytetramethylrhodamine)/5'-FAM (6-carboxyfluorescein)-labeled double dye oligonucleotide probe (Eurogentec). In the same experiments, calibration curves were run

on serial dilutions of pooled 8× concentrated cDNA solution as used in the assay, resulting in series containing 4, 2, 1, 0.5, 0.25, 0.125, 0.062, and 0.031 × cDNA present in the assay incubation. The data obtained were processed using the software program ABI Sequence Detector (version 1.6.3; System Applied Biosystems, Foster City, CA). All quantified expression levels were within the linear part of the calibration curves and were calculated by using these curves. PCR results were normalized to β-Actin mRNA levels. The sequences of the primers and probes used in this study are listed in table 3.1.

*Hepatic lipid and protein analyses*

Livers were homogenized and hepatic concentrations of triglycerides, free cholesterol and total cholesterol were measured using commercial kits (Roche Diagnostics and Wako Chemicals, Neuss, Germany) after lipid extraction according to Bligh and Dyer (31) and redissolving the lipids in 2% Triton X-100 in water. Phospholipid content of the liver was determined according to Böttcher *et al.* (32) after lipid extraction. Protein concentrations in livers were determined according to Lowry *et al.* (33) using bovine serum albumin as standard (Pierce). Fatty acid composition was determined by gas chromatography after methylation as described previously (34).

*Histology*

Liver histology was examined on frozen liver sections after Oil-Red-O staining for neutral lipids by standard procedures.

*Plasma lipid analyses*

Plasma triglycerides, phospholipids, free fatty acids, HDL cholesterol, free cholesterol, and total cholesterol were determined using commercially available kits (Roche Diagnostics and Wako Chemicals). Lipoproteins of C57BL/6J mice, apoE -/- LDLr -/- double knockout mice and APOE*3-Leiden transgenic mice were separated using fast protein liquid chromatography (FPLC) on a Superose 6B 10/30 column (Amersham Biosciences). The contents of apoB100, apoB48, and apoA-I in the fractions were visualized by Western blotting. Proteins in the fractions were separated by SDS-PAGE using 4-15% gradient gels (Ready Gels, Bio-Rad) and transferred to nitrocellulose membranes (Hyperbound, Amersham Biosciences, Roosendaal, The Netherlands). The membranes were incubated with sheep anti-human apoB (Roche Diagnostics) or rabbit anti-human apoA-I (Calbiochem, San Diego, CA), followed by incubation with donkey anti-sheep IgG horseradish peroxidase or donkey anti-rabbit IgG horseradish peroxidase and visualized by ECL detection (all three from Amersham Biosciences, Uppsala, Sweden) according to the instructions from the manufacturer.

*VLDL isolation and analyses*

Plasma VLDL/IDL ($d < 1.019$ g/ml) was isolated by density gradient ultracentrifugation. For this, 300 µl of plasma was adjusted to 800 µl with a NaCl/KBr solution with a density of 1.019 g/ml, containing 1 mM EDTA and NaN3, and centrifuged at 120,000 rpm in a Optima TM LX tabletop ultracentrifuge (Beckman Instruments, Inc., Palo Alto, CA). VLDL was isolated by tube slicing, and the volume was recorded by weight. ApoB100 and apoB48 were determined by Western blotting, using antibodies against human apoB raised in sheep. Triglyceride and cholesterol content were determined as described for plasma. Phospholipids were determined using a commercial kit (Wako Chemicals). Fatty acid composition was determined as described previously (34).

Table 3.1. Primers and probes used for Real Time PCR analysis of hepatic gene expression.

| Gene | | Sequences (5' to 3') | GenBank™ accession no. |
|---|---|---|---|
| *β-Actin* | forward | AGCCATGTACGTAGCCATCCA | NM_007393 (mouse) |
| | reverse | TCTCCGGAGTCCATCACAATG | NM_031144 (rat) |
| | probe | TGTCCCTGTATGCCTCTGGTCGTACCAC | |
| *Srebp-1c* | forward | GGAGCCATGGATTGCACATT | AF286470 (mouse) |
| | reverse | CCTGTCTCACCCCCAGCATA | Ref. (50) (rat) |
| | probe | CAGCTCATCAACAACCAAGACAGTGACTTCC | |
| *Srebp-1a* | forward | GAGGCGGCTCTGGAACAGA | Ref. (50) |
| | reverse | TGTCTTCGATGTCGTTCAAAACC | |
| | probe | TGTGTCCAGTTCGCACATCTCGGC | |
| *Acc1* | forward | GCCATTGGTATTGGGGCTTAC | AF374170 (mouse) |
| | reverse | CCCGACCAAGGACTTTGTTG | NM_022193 (rat) |
| | probe | CTCAACCTGGATGGTTCTTTGTCCCAGC | |
| *Fas* | forward | GGCATCATTGGGCACTCCTT | AF127033 (mouse) |
| | reverse | GCTGCAAGCACAGCCTCTCT | NM_017332 (rat) |
| | probe | CCATCTGCATAGCCACAGGCAACCTC | |
| *Apob* | forward | GCCCATTGTGGACAAGTTGATC | AW012827 |
| | reverse | CCAGGACTTGGAGGTCTTGGA | |
| | probe | AAGCCAGGGCCTATCTCCGCATCC | |
| *Apobec-1* | forward | TCGTCCGAACACCAGATGCT | NM_031159 |
| | reverse | GGTGTCGGCTCAGAAACTCTGT | |
| | probe | CCTGGTTCCTGTCCTGGAGTCCCTG | |
| *Mttp* | forward | CAAGCTCACGTACTCCACTGAAG | NM_008642 |
| | reverse | TCATCATCACCATCAGGATTCCT | |
| | probe | ACCGCAAGACAGCGTGGGCTACA | |
| *Apoe* | forward | CCTGAACCGCTTCTGGGATT | NM_009696 |
| | reverse | GCTCTTCCTGGACCTGGTCA | |
| | probe | AAAGCGTCTGCACCCAGCGCAGG | |
| *Hl* | forward | ACTGCAGGAGTGTGGCTTCAAC | NM_008280 |
| | reverse | TGGGACTGTCGGGACTTCAG | |
| | probe | CAAGCCATCCACCGACCACCCG | |
| *Lpl* | forward | AAGGTCAGAGCCAAGAGAAGCA | NM_008509 |
| | reverse | CCAGAAAAGTGAATCTTGACTTGGT | |
| | probe | CCTGAAGACTCGCTCTCAGATGCCCTACA | |
| *Pltp* | forward | TCAGTCTGCGCTGGAGTCTCT | NM_011125 |
| | reverse | AAGGCATCACTCCGATTTGC | |
| | probe | TCCCACTGCAGGCCCCACTGAA | |
| *Vldlr* | forward | CCACAGCAGTATCAGAAGTCAGTGT | NM_013703 |
| | reverse | CACCTACTGCTGCCATCACTAAGA | |
| | probe | CAGCTGCCTGGGCCATCCTTCC | |
| *Ldlr* | forward | GCATCAGCTTGGACAAGGTGT | X64414 |
| | reverse | GGGAACAGCCACCATTGTTG | |
| | probe | CACTCCTTGATGGGCTCATCCGACC | |
| *Lxrα* | forward | GCTCTGCTCATTGCCATCAG | AF085745 |
| | reverse | TGTTGCAGCCTCTCTACTTGGA | |
| | probe | TCTGCAGACCGGCCCAACGTG | |

*VLDL size determination*

VLDL size and volume distribution profiles were analyzed by dynamic scattering using a Nicomp model 370 submicron particle analyzer (Nicomp Particle Sizing Systems, Santa Barbara, CA). Particle diameters were calculated from the volume distribution patterns provided by the analyzer.

*Cell culture experiments*

McA-RH7777 (rat hepatoma) cells were plated in 35-mm six-well plastic dishes (Costar Corp., Cambridge, MA) in 2 ml of Dulbecco's modified Eagle's medium containing 10% fetal calf serum, 10% natural horse serum, penicillin/streptomycin, and geneticin. At a confluence of ~30%, the medium was removed and cells were washed with Hanks' balanced salt solution (HBSS) and subsequently incubated with Dulbecco's modified Eagle's medium + 10% fetal calf serum + 10% natural horse serum containing either 0 or 10 μM T0901317 and the above mentioned antibiotics. After 24 h, the medium was removed and half of the wells were incubated with the same medium for another 41 h. The other half of the wells were incubated with the same medium to which was added 25 μM [$^3$H]glycerol (4.4 μCi/well) for 41 h. The medium was then collected, centrifuged to remove debris, and stored at 4 °C until further analysis. Cells were washed with ice-cold HBSS and either used for RNA isolation or scraped into 2 ml of HBSS for lipid extraction ([$^3$H]glycerol- labeled cells).

*Lipid analyses of cells and medium*

Lipids secreted by McA-RH7777 cells into medium and cellular lipids were extracted as described previously (35). [$^3$H]TG was separated from the other lipids by thin layer chromatography with hexane/diethyl ether/acetic acid (80/20/1 v/v/v) as developing solvent. After iodine staining, the spots containing [$^3$H]TG (as a measure for VLDL-TG secretion) were scraped into vials and assayed for radioactivity by scintillation counting. Part of the extracted lipids was dissolved in chloroform containing 2% Triton X-100. The chloroform was replaced by the same volume of water after evaporation of the chloroform, the lipids were resuspended, and total cellular TG concentration was determined using the commercially available triglyceride assay kit (Roche Diagnostics).

*Western blotting of apoB in medium*

Secreted apoB in medium of McA-RH7777 cells was concentrated with fumed silica according to the methods described by Vance *et al.* (36). ApoB was separated by SDS-PAGE using 4-15% gradient gels as described.

*Protein measurements of cells*

Protein concentrations of cell suspensions were determined according to Lowry *et al*. (33) using bovine serum albumin as standard (Pierce).

*mRNA expression levels in cells*

Total RNA from McA-RH7777 cells was isolated by using the SV Total RNA Isolation System (Promega RNA, Madison, WI) according to the instructions from the manufacturer. RNA was processed for real-time PCR as described under "Hepatic RNA isolation and measurement of mRNA levels by real-time PCR (Taqman)."

*Statistics*

All values represent mean ± standard deviation for the number of animals, wells, or experiments indicated. Statistical analysis of two groups was assessed by Mann-Whitney U test. Level of significance was set at $p < 0.05$. Analyses were performed using SPSS for Windows software (SPSS, Chicago, IL).

Table 3.2. Comparison of hepatic lipid parameters of mice treated with T0901317 or its solvent. Male C57BL/6J mice were treated with 10 mg/kg of the synthetic LXR agonist T0901317, or its solvent (control) during four days. Livers were weighed and concentrations of lipids were measured as described under "Experimental Procedures". Each value represents the mean ± S.D.; n=10. *, $p < 0.05$.

| | control | T0901317 |
|---|---|---|
| liver weight (% of body weight) | 4.6 ± 0.6 | 6.6 ± 0.3 * |
| protein (mg/g liver) | 225 ± 17 | 225 ± 17 |
| triglycerides (nmol/mg liver) | 6.92 ± 2.65 | 57.74 ± 16.61 * |
| free cholesterol (nmol/mg liver) | 4.21 ± 0.50 | 3.83 ± 0.71 * |
| cholesterylester (nmol/mg liver) | 1.44 ± 0.52 | 0.98 ± 0.40 * |
| phospholipids (nmol/mg liver) | 35.74 ± 3.48 | 36.43 ± 3.63 |

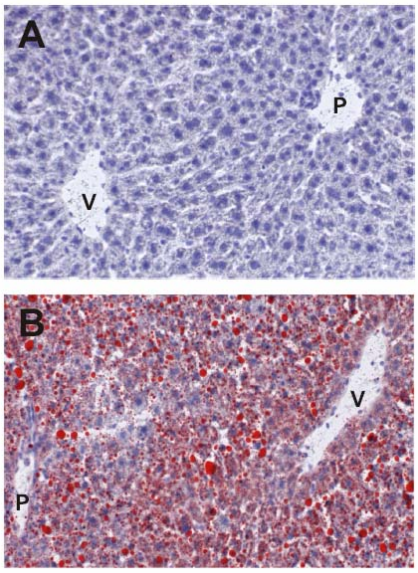


Figure 3.1. Uniform Oil-Red-O (ORO) staining for neutral fat in livers of T0901317-treated mice. No staining was observed in liver sections from male C57BL/6J mice receiving the solvent (A). Massive staining was found in liver sections from mice treated four days with 10 mg/kg of the LXR agonist T0901317 (B). V, central vein; P, portal vein. Original magnification 50x.

## Results

*Effects of T0901317 on hepatic and plasma lipids in C57BL/6J Mice*

Livers from mice that had received T0901317 were clearly heavier than those in the control group (table 3.2). The hepatic TG content in treated mice was ~10 times higher than in controls. There were no differences in protein, phospholipid, and free cholesterol contents, whereas the cholesteryl ester content was slightly decreased after treatment (table 3.2). Oil-Red-O staining for neutral lipids on frozen liver sections showed massive lipid accumulation in periportal (zone 1) as well as in perivenous (zone 3) hepatocytes in mice receiving T0901317 (figure 3.1). The hepatic fatty acid composition was changed upon treatment: the relative amount of oleate (C18:1) was sharply increased (figure 3.2), whereas the relative amounts of palmitate (C16:0), linoleate (C18:2), and arachidonate (C20:4) were markedly decreased upon LXR activation.

Hepatic expression of *Lxrα* was slightly reduced upon treatment with the agonist (figure 3.3A), but expression of genes involved in de novo lipogenesis was clearly increased (figure 3.3B). Expression of *Srebp-1c* was more than doubled after LXR activation, whereas mRNA levels of *Acc1* and *Fas* were 3.5-4.5 times higher than in controls. *Acc1* encodes the cytosolic isoform of ACC. No induction of mRNA levels of *Srebp-1a* was observed.

The plasma concentrations of free cholesterol, cholesteryl esters, phospholipids, and free fatty acids (FFA) were significantly elevated in the treated group as compared with controls (table 3.3). As expected, HDL cholesterol was increased by ~60%, but the TG concentration was not affected by LXR activation in these experiments. Upon FPLC separation of plasma lipoproteins, distribution of TG appeared to be unaffected after LXR activation (figure 3.4A). Cholesterol contents of fractions 25-29 were higher in the group treated with T0901317 (figure 3.4B). Figure 3.4C shows that apoA-I was present in these earlier fractions after LXR activation, indicating that the "shoulder" in the cholesterol profile could be attributed to the presence of large HDL particles.

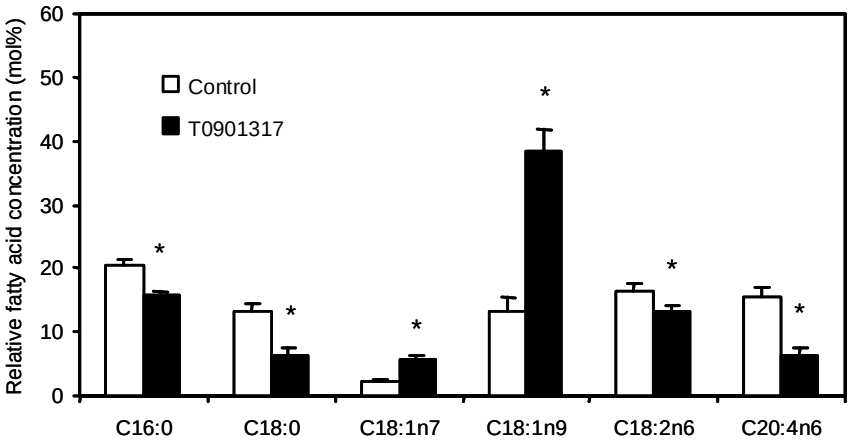


Figure 3.2. Changes in relative hepatic concentrations of major fatty acid species upon LXR activation. Fatty acid composition was determined in ~15 mg liver tissue by gas chromatography after methylation, with heptadecanoic acid (C17:0) as internal standard. Open bars: livers from male C57BL/6J mice receiving the solvent (control). Closed bars: livers from mice treated four days with 10 mg/kg of the LXR agonist T0901317. Values represent the mean percentage ± S.D.; n=10; *, $p < 0.05$.

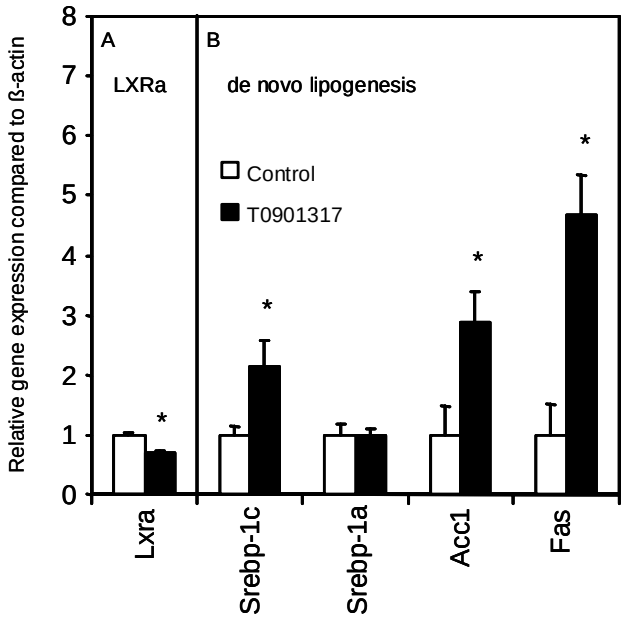


Figure 3.3. Changes in relative hepatic gene expression upon LXR activation, determined by Real Time PCR. RNA was isolated from ~30 mg liver tissue of male C57BL/6J mice and converted to cDNA. Levels of cDNA were measured by Real Time PCR as described in "Experimental Procedures". Results were normalized to *β-Actin* mRNA levels. (A) Expression of the gene encoding LXRα. (B) Expressions of genes encoding proteins involved in *de novo* lipogenesis. Open bars, mice receiving the solvent (control), arbitrarily defined as 1. Closed bars, mice treated four days with 10 mg/kg of the LXR agonist T0901317. *Lxra*, liver X receptor α; *Srebp-1c*: sterol-regulatory element-binding protein-1c; *Acc1*, acetylCoA carboxylase-1; *Fas*, fatty acid synthase.Values represent the mean ± S.D.; n=4; *, $p < 0.05$.

### *LXR activation leads to stimulation of VLDL-TG secretion through formation of larger particles*

Figure 3.5 shows the plasma TG concentration versus time curve after injection of Triton WR-1339 in control and T0901317-treated mice. The VLDL-TG production rates were calculated from these curves. Upon LXR activation, the production rate was 2.56 times higher than control values: 201.9 ± 36.4 versus 78.8 ± 18.7 μmol/kg/h (figure 3.5, inset). The concentrations of free cholesterol, cholesteryl esters, phospholipids, and TG in nascent VLDL particles isolated from plasma obtained at 4 h after Triton WR-1339 injection are summarized in table 3.4. The mol% of surface lipids (free cholesterol and phospholipids) was reduced relative to that of core lipids (TG and cholesteryl esters), leading to an increase of the core:surface ratio by 14.4%. Accordingly, direct measurement of particle sizes revealed that after LXR activation the mean diameter of the VLDL particles was increased by 48% (129 ± 9 versus 94 ± 12 nm, $p < 0.001$). The diameter was used to calculate the particle volume. The increase in mean particle volume (factor 2.54) was virtually identical to the increase in VLDL-TG production (factor 2.56), indicating that the latter increase was caused by the production of larger particles rather than by the production of more particles. In accordance with this notion, no differences in apoB contents were found in isolated VLDL fractions by Western blotting (figure 3.6).

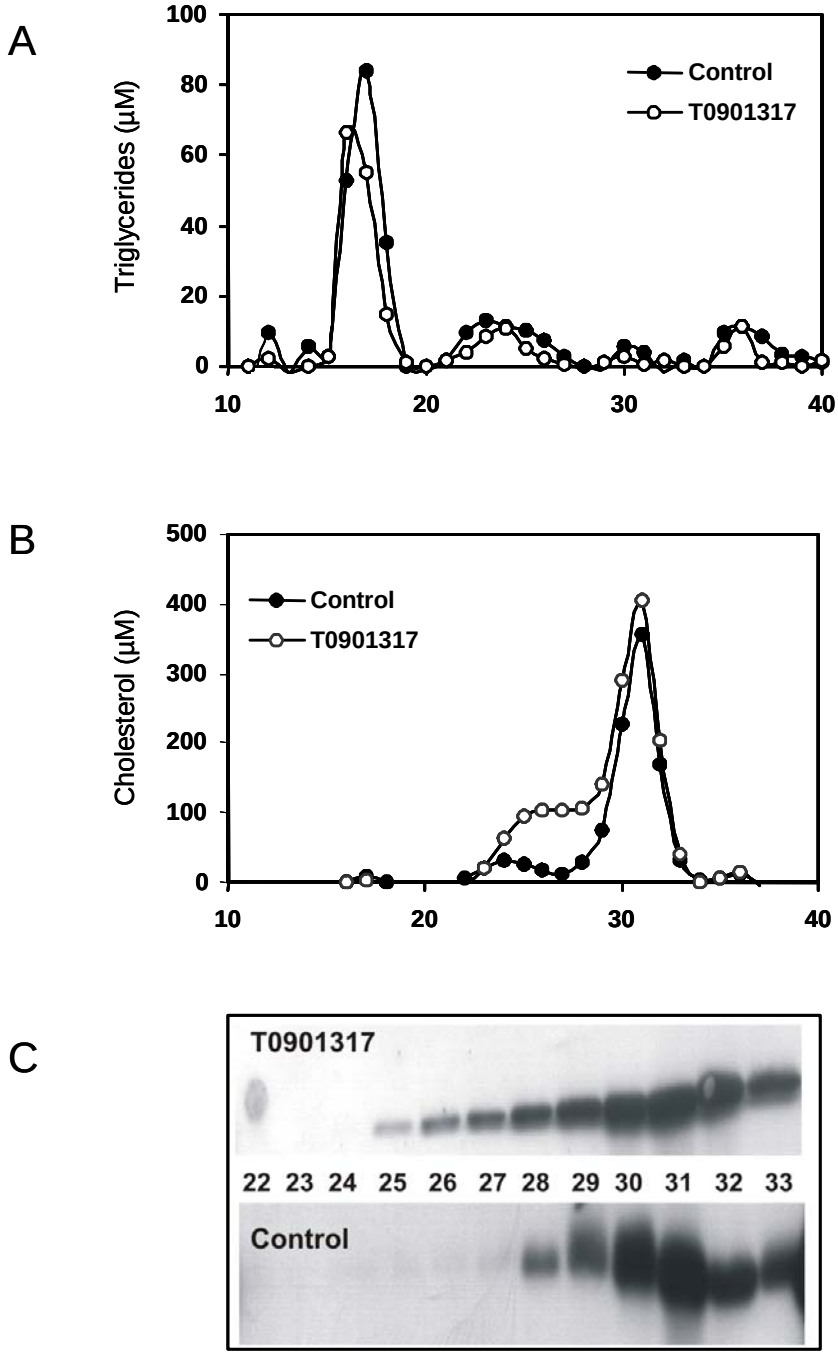


Figure 3.4. Effect of LXR activation on distribution of triglycerides and cholesterol in plasma lipoprotein fractions. Lipoproteins were separated using FPLC (fast protein liquid chromatography) on a Pharmacia Superose 6B 10/30 column. Plasma of 10 male C57BL/6J mice per group was pooled, and 0.2 ml was applied to the column and eluted with phosphate-buffered saline at a flow of 0.5 ml/min. Triglycerides and cholesterol were measured as described under "Experimental Procedures". (A) Profiles of triglycerides. (B) Profiles of cholesterol. (○) Mice receiving the solvent (control). (●) Mice treated four days with 10 mg/kg of the LXR agonist T0901317. (C) SDS-polyacrylamide gel electrophoresis followed by Western blotting of ApoA-I in the indicated FPLC fractions. Top panel, mice treated four days with 10 mg/kg of the LXR agonist T0901317; Bottom panel, mice receiving the solvent (control).

Table 3.3. Comparison of plasma lipid parameters of mice treated with T0901317 or its solvent. Male C57BL/6J mice were treated with 10 mg/kg of the synthetic LXR agonist T0901317 or its solvent (control) during four days. Blood was collected by cardiac puncture, and plasma obtained by centrifugation. Concentrations of lipids were measured as described under "Experimental Procedures". Each value represents the mean ± S.D.; n=10. *, $p < 0.05$.

| | control | T0901317 |
|---|---|---|
| free cholesterol (mM) | 0.60 ± 0.07 | 0.87 ± 0.05 * |
| cholesterylester (mM) | 1.36 ± 0.31 | 2.27 ± 0.21 * |
| HDL cholesterol (mM) | 1.35 ± 0.27 | 2.15 ± 0.14 * |
| phospholipids (mM) | 2.55 ± 0.41 | 3.94 ± 0.21 * |
| triglycerides (mM) | 0.46 ± 0.16 | 0.49 ± 0.21 |
| free fatty acids (mM) | 0.34 ± 0.07 | 0.47 ± 0.08 * |

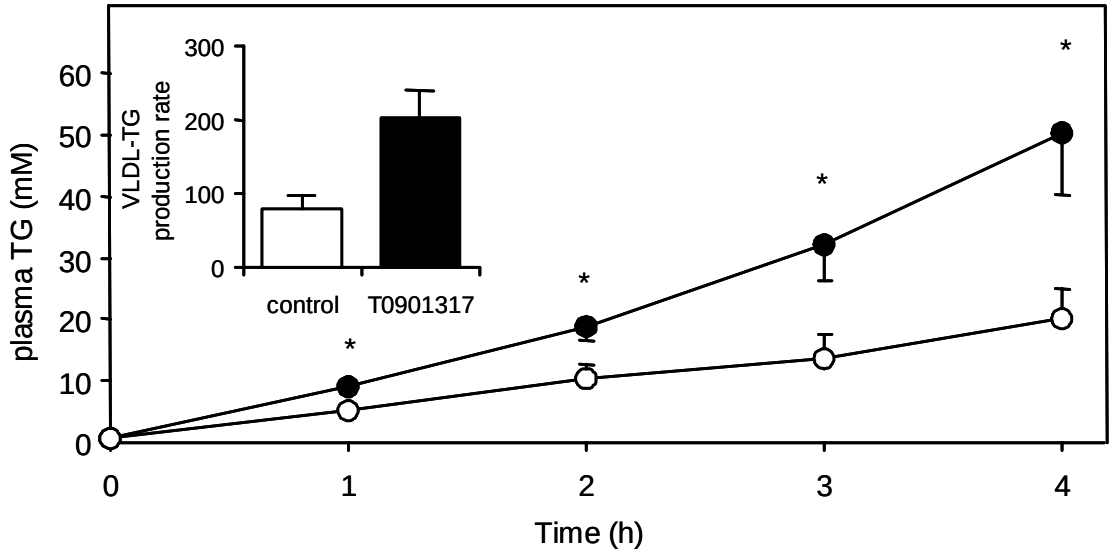


Figure 3.5. Plasma triglyceride concentrations in T0901317-treated and control mice after injection of Triton WR-1339. Male C57BL/6J mice received at t=0 an injection of 12 mg Triton WR-1339 in 100 µl PBS via the penile vein. Triglyceride concentration was measured in the plasma samples collected at indicated time points as described under "Experimental Procedures". (○) Plasma from mice receiving the solvent (control). (●) Plasma from mice treated four days with 10 mg/kg of the LXR agonist T0901317. The inset shows the VLDL-TG production rate in µmol/kg/hr, calculated from the plasma TG *vs.* time curve. Open bar, mice receiving the solvent (control). Closed bar, mice treated four days with 10 mg/kg of the LXR agonist T0901317; Values represent the mean ± S.D.; n=6 (T0901317), n=7 (control); *, $p < 0.05$.

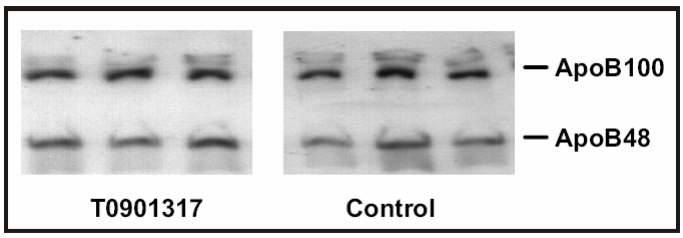


Figure 3.6. Apolipoprotein B contents in nascent VLDL particles of control and T0901317-treated mice. Plasma was obtained by cardiac puncture at 4 hours after injection of Triton WR1339. 300 µl plasma was adjusted to 800 µl with a NaCl/KBr solution (d = 1.019 g/ml), containing 1 mM EDTA and $NaN_3$, and centrifuged at 120.000 rpm. VLDL was isolated by tube slicing and this fraction was applied to SDS-polyacrylamide gel electrophoresis followed by Western blotting. Each lane represents VLDL from an individual mouse. Left panel, mice receiving the solvent (control). Right panel, mice treated four days with 10 mg/kg of the LXR agonist T0901317.

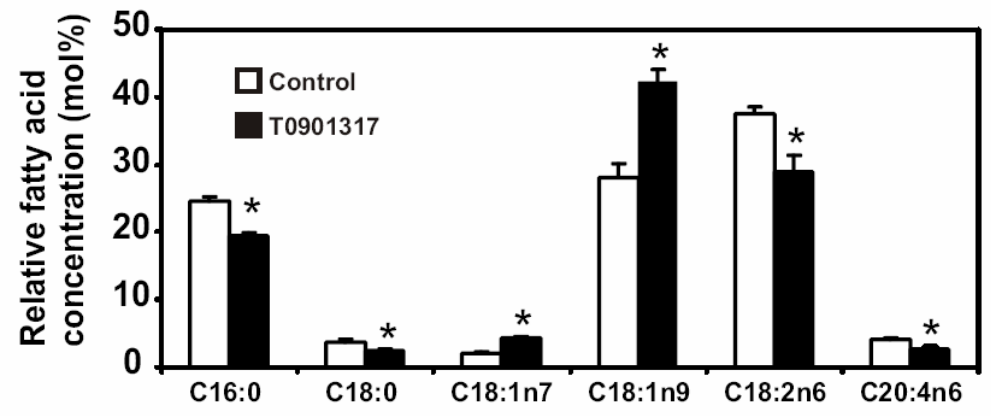


Figure 3.7. Changes in relative concentrations of major fatty acid species in VLDL fractions upon LXR activation. VLDL fractions were isolated from plasma obtained by cardiac puncture at 4 hours after injection of Triton WR1339. Fatty acids were determined by gas chromatography after methylation, with heptadecanoic acid (C17:0) as internal standard. Open bars: VLDL from mice receiving the solvent (control). Closed bars: VLDL from mice treated four days with 10 mg/kg of the LXR agonist T0901317. Values represent the mean percentage ± S.D.; n=10; *, $p < 0.05$.

The fatty acid composition of the VLDL fraction was changed upon treatment, resulting in changes similar as seen for the hepatic fatty acids (figure 3.7). The relative amount of VLDL-associated oleate (C18:1) was increased, and relative amounts of palmitate (C16:0), linoleate (C18:2), and arachidonate (C20:4) were decreased upon LXR activation.

To gain further insight into the molecular background of LXR-induced stimulation of VLDL-TG secretion, the expression of genes involved in the control of this process was investigated. Figure 3.8A shows that expression of the *Apob* gene was slightly but significantly reduced upon LXR activation. No changes in expression of *Mttp* and *Apoe* were noted. Likewise, expression of *Apobec-1*, encoding the apoB mRNA-editing protein, was not affected. In contrast, a marked induction of *Lpl* and *Pltp* mRNA levels was found (figure 3.8B), the latter encoding the phospholipid transfer protein. Expression of *Ldlr*, encoding the low density lipoprotein receptor involved in the clearance of TG-rich lipoproteins, was slightly induced.

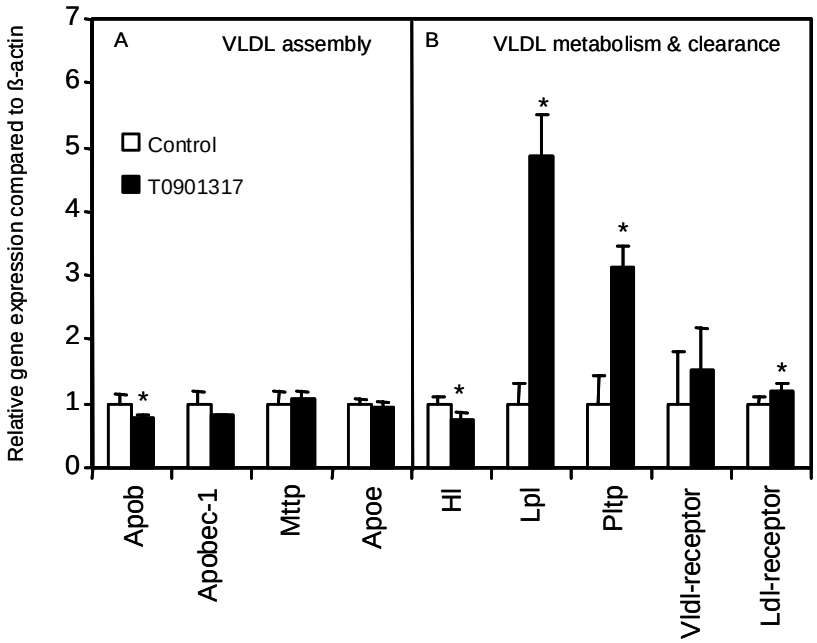


Figure 3.8. Changes in relative hepatic gene expression upon LXR activation, determined by Real Time PCR. RNA was isolated from ~30 mg liver tissue of male C57BL/6J mice and converted to cDNA. Levels of cDNA were measured by Real Time PCR as described in "Experimental Procedures". Results were normalized to *β-Actin* mRNA levels. (A) Expressions of the genes encoding proteins involved in VLDL assembly and secretion. (B) Expressions of genes encoding proteins involved in VLDL metabolism and clearance. Open bars, mice receiving the solvent (control), arbitrarily defined as 1. Closed bars, mice treated four days with 10 mg/kg of the LXR agonist T0901317. *Apob*, apolipoprotein B; *Apobec-1*, apolipoprotein B editing complex-1; *Mttp*, microsomal triglyceride transfer protein; *Apoe*, apolipoprotein E; *Hl*, hepatic lipase; *Lpl*, lipoprotein lipase; *Pltp*, phospholipid transfer protein. Values represent the mean ± S.D.; n=4; *, $p < 0.05$.

Table 3.4. Comparison of composition and size of nascent VLDL particles of mice treated with T0901317 or its solvent. Male C57BL/6J mice were treated with 10 mg/kg of the synthetic LXR agonist T0901317 or its solvent (control) during four days. Mice were injected with Triton WR-1339 on the fifth day. At 4 hours after injection, blood was collected by cardiac puncture and VLDL was isolated from plasma by density gradient ultracentrifugation. Concentrations of lipids were measured as described under "Experimental Procedures" and particle diameter using a particle sizer. Particle volume was calculated using the equation Volume = $4/3 \cdot \pi \cdot (½\text{diameter})^3$. Each value represents the mean ± S.D.; n=7 (control); n=6 (T0901317); *, $p < 0.05$.

| | control | T0901317 |
|---|---|---|
| free cholesterol (mM) | 1.50 ± 0.31 | 2.01 ± 0.31 * |
| cholesterylester (mM) | 0.63 ± 0.10 | 1.34 ± 0.19 * |
| phospholipids (mM) | 2.95 ± 0.62 | 4.47 ± 0.45 * |
| triglycerides (mM) | 28.53 ± 5.86 | 47.10 ± 8.66 * |
| core:surface lipids | 6.55 ± 0.35 | 7.49 ± 1.10 |
| diameter (nm) | 94 ± 12 | 129 ± 9 * |
| volume ($10^5$ $nm^3$ ) | 4.5 ± 1.7 | 11.3 ± 2.3 * |

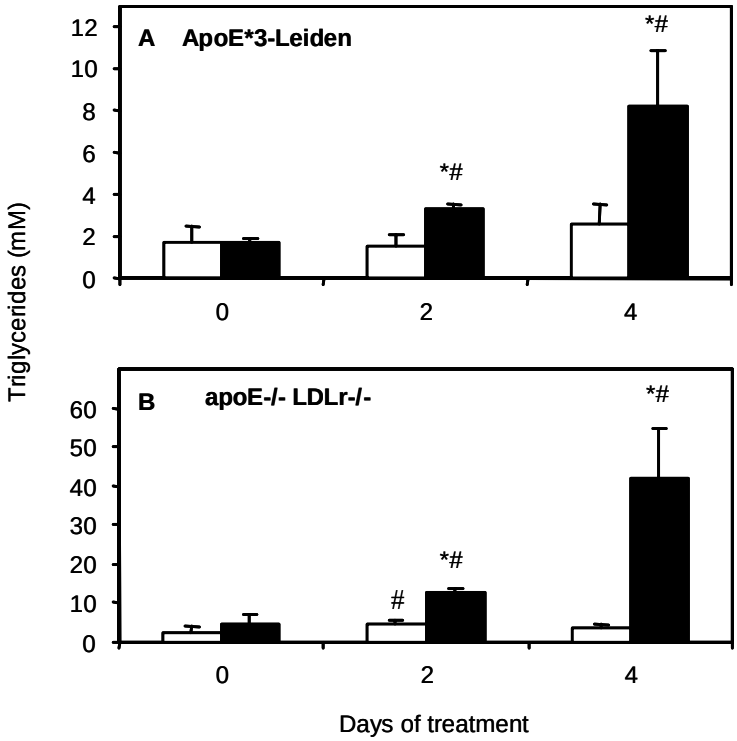


Figure 3.9. Plasma triglyceride concentrations in apoE-/- LDLr-/- mice and APOE*3-Leiden transgenic mice upon LXR activation. Male apoE-/- LDLr-/- mice and APOE*3-Leiden transgenic mice were treated for 4 days with T0901317 or its solvent. Before onset of treatment (day 0) and on the second day of treatment, a small EDTA-bloodsample was collected by tail bleeding. On the fourth day, blood was obtained by cardiac puncture. Triglyceride concentration was measured in plasma as described under "Experimental Procedures". (A) Plasma triglyceride concentrations in APOE*3-Leiden transgenic mice. (B) Plasma triglyceride concentrations in apoE -/- LDLr-/- double knockout mice. Open bars: mice receiving the solvent (control). Closed bars: mice treated with 10 mg/kg of the LXR agonist T0901317; Values represent the mean ± S.D.; n=4 (ApoE*3-Leiden); n=3 (apoE-/- LDLr-/- double knockouts); *, $p < 0.05$ for treated *vs.* control; #, $p < 0.05$ compared to concentration at t=0.

### *LXR Activation leads to hypertriglyceridemia in apoE-/- LDLr- /- double knockout and APOE*3-Leiden transgenic mice*

Increased VLDL-TG production in C57BL/6J mice was not accompanied by elevated fasting TG levels (table 3.3), possibly as a result of efficient particle metabolism and clearance. To test this option, effects of LXR activation on plasma TG levels were also studied in mouse models with defective particle clearance, *i.e.* apoE -/- LDLr -/- double knockout and APOE*3-Leiden transgenic mice. Figure 3.9 shows that, in both apoE -/- LDLr -/- mice and in APOE*3-Leiden transgenic mice, treatment with T0901317 resulted in a very strong, progressive increase in plasma TG concentrations. As expected, TG was almost exclusively present in VLDL-sized lipoprotein fractions in T0901317-treated apoE -/- LDLr -/- double knockouts and in APOE*3-Leiden transgenics upon FPLC separation of plasma lipoproteins (data not shown).

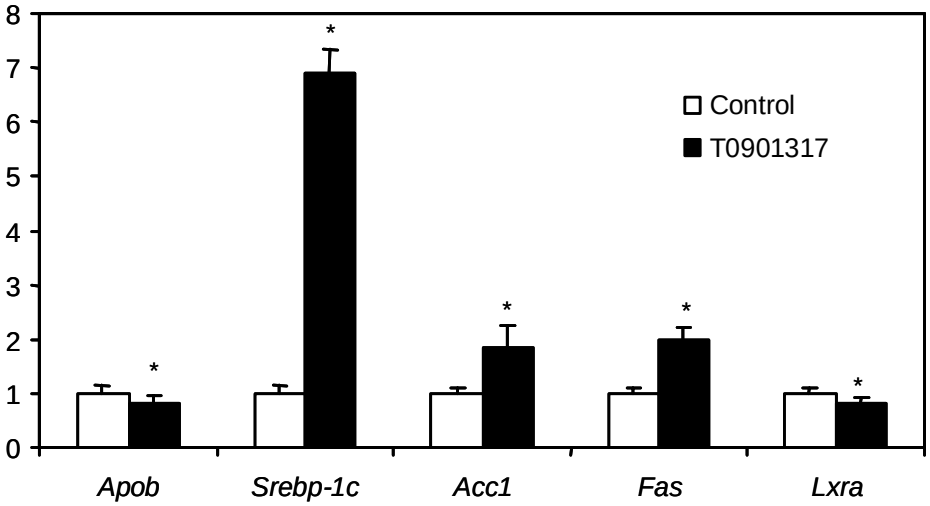


Figure 3.10. Changes in relative hepatic gene expression, determined by Real Time PCR, upon LXR activation in McA-RH7777 cells. RNA was isolated from McA-RH7777 cells exposed to T0901317-containing medium or control medium and converted to cDNA. Levels of cDNA were measured by Real Time PCR as described in "Experimental Procedures". Results were normalized to *β-Actin* mRNA levels. Open bars: cells without T0901317 (control), arbitrarily defined as 1. Closed bars: cells incubated with 10 μM of the LXR agonist T0901317 during 65 hour. *Apob*, apolipoprotein B; *Srebp-1c*, sterol-regulatory element-binding protein-1c; *Acc1*, acetylCoA carboxylase-1; *Fas*, fatty acid synthase; *Lxra*, liver X receptor α. Values represent the mean ± S.D.; n=6; *, $p < 0.05$.

*Effects of LXR Activation on VLDL-TG Production in Cultured Liver Cells*

To determine whether LXR effects on VLDL production can be achieved via direct actions on liver cells, the rat hepatoma cell line McA-RH7777 was exposed to the LXR agonist T0901317 for 65 h. Figure 3.10 shows the effects of LXR activation on mRNA expression of genes involved in VLDL assembly and fatty acid synthesis. After incubation with T0901317, a 7-fold increase in *Srebp-1c* mRNA levels was observed as well as a 2-fold increase in both *Acc1* and *Fas* mRNA levels. Similar to the in vivo situation, a 20% decrease in *Apob* and a slight decrease in *Lxrα* mRNA levels were observed after exposure of the cells to the LXR agonist.

After 24 h of incubation with T0901317 alone, the medium was replaced by medium also containing [$^3$H]glycerol. After another 41-h incubation, lipids were isolated from cells and media to determine the amount and secretion of newly synthesized VLDL-TG. Incubation with T0901317 resulted in a 2.6-fold induction of VLDL-TG secretion and a 3.4-fold induction of TG synthesis (figure 3.11A). Intracellular total TG mass was also increased upon incubation with T0901317 (1.4-fold compared with control situation). The amount of apoB isolated from medium after incubation with T0901317 was compared with that in the control medium. No significant differences in apoB100 or apoB48 were detected (figure 3.11B).

## Discussion

Pharmacological activation of LXR leading to accelerated reverse cholesterol transport has been advocated as a potential novel treatment or prevention of atherosclerosis (17). This study shows that the beneficial raise of HDL levels is accompanied by potentially adverse effects on triglyceride metabolism. In mice, an increased VLDL-TG production was seen upon LXR activation by the LXR agonist T0901317, caused by the formation of large, TG-rich particles. Large VLDL particles, also known as $VLDL_1$ particles, are considered pro-atherogenic and are metabolized to small dense low density lipoprotein. Increased production of $VLDL_1$ is a hallmark of diabetes type 2-related hyperlipidemia (37).

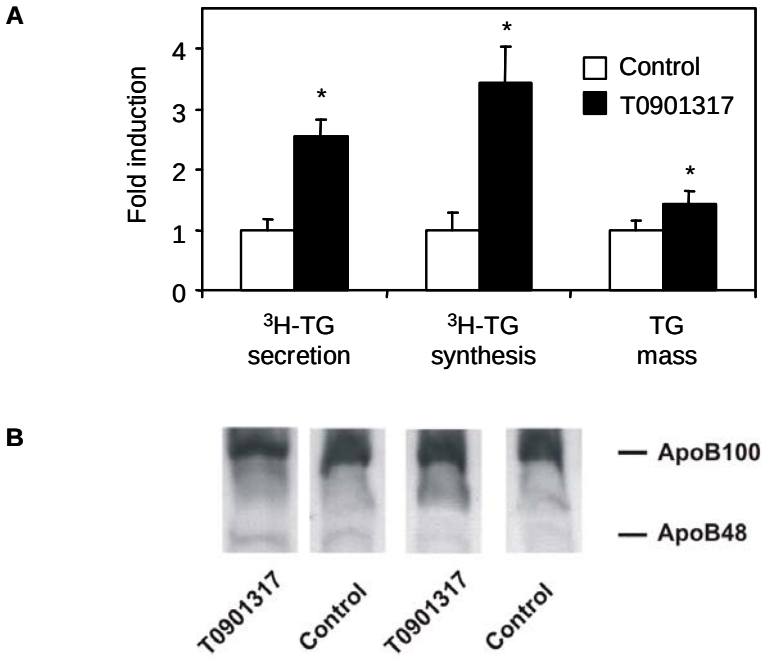


Figure 3.11. Triglyceride synthesis and VLDL-triglyceride secretion in the rat hepatoma cell line McA-RH7777. McA-RH7777 cells were incubated with or without 10 μM T0901317 for 24 h. After 24 h the medium was removed and replaced by medium containing $^3$H-glycerol with or without 10 μM T0901317. After 41 h medium was collected and cells were harvested. Lipids were extracted from medium and cell suspensions and $^3$H-TG was separated from other lipids by TLC. $^3$H-TG spots were assayed for radioactivity by scintillation counting. The intracellular TG mass was enzymatically determined as described under "Experimental Procedures". Secreted ApoB in the medium was concentrated with fumed silica and separated from other proteins on a 4-15% gradient gel by SDS PAGE followed by Western blotting. (A) Fold induction of $^3$H-TG secretion, $^3$H-TG synthesis and intracellular TG mass after a 65-h incubation with 10 μM T0901317 (closed bars) compared to the control situation (open bars). Values represent mean fold induction from three independent experiments ± S.D., * significantly different from control, $p < 0.05$. (B) Secreted apoB100 and apoB48 after a 65-h-incubation with or without 10 μM T0901317. The ApoB blot is representative for the results from three independent experiments.

The development of a severe hepatic steatosis, also reported previously (18), is likely related to increased *de novo* lipogenesis in combination with an increased FFA flux toward the liver. Slight quantitative differences in T0901317-induced gene expression patterns between our and other studies (18,22,25) are probably the result of differences in treatment protocols. For instance, Liang *et al.* (25) supplied T0901317 via the food during 12 h, which may have resulted in a more constant exposure of the liver to the agonist. Livers were removed immediately after this 12-h period. In our study mice received T0901317 daily for 4 days, and livers were taken out ~20 h after the last administration. Second, effects of the agonist may be transient because Joseph *et al.* (22) showed that hepatic expression of *Fas* and *Scd-1* was higher after 3 days of LXR activation than after 7 days.

The accumulated neutral lipids were distributed uniformly across the liver lobule, in contrast to most models of steatosis, *e.g.* the *ob/ob* mice (38), in which fat accumulates mainly in perivenous (zone 3) hepatocytes. After LXR activation, TG accumulated both in perivenous (zone 3) hepatocytes, which may reflect increased de novo lipogenesis (39), and in periportal (zone 1) hepatocytes. The fatty acid profile showed a specific increase in 18:1 fatty acids, in accordance with increased expression of *Scd-1* after LXR activation (25). The fatty acid composition of VLDL was comparable with that of liver homogenates, indicating that TG containing specific fatty acids are not preferentially recruited for VLDL assembly.

The increase of HDL cholesterol was mainly the result of the presence of larger particles in the circulation. Elevated HDL levels are probably caused by increased cholesterol efflux from peripheral and/or liver cells caused by induction of ABCA1 and ABCG1. The HDL elevating action of the LXR agonist may be, in part, counteracted by the LXR-induced expression of *Pltp*, because overexpression of *Pltp* is shown to reduce HDL in mice (40). However, induction of *Pltp* expression might also contribute to the presence of large HDL particles, as PLTP is a main factor in the regulation of the size and composition of HDL. PLTP has been proposed to catalyze conversion of two HDL particles to yield one larger HDL particle and a small lipid-poor apoA-I particle, pre-β-HDL (41,42). These latter particles are efficient acceptors of cholesterol from peripheral cells.

The induced VLDL-TG production rate upon LXR activation was found to be the result exclusively of formation of larger particles. The increase in VLDL-TG production exactly matched the increased mean VLDL particle volume. The apoB content of isolated VLDL fractions was not affected upon treatment, strengthening our conclusion that LXR activation leads to formation of larger instead of more VLDL particles. The increased TG production by the liver did not lead to a raise in plasma TG levels in CL57BL/6J mice, but defective clearance in apoE -/- LDLr -/- double knockout and APOE*3-Leiden transgenic mice clearly unmasked the hypertriglyceridemic actions of LXR activation. Plasma TG levels markedly and progressively increased upon treatment with the agonist in these mice. Interestingly, Schultz *et al.* (18) showed that treatment of wild type C57BL/6 mice with T0901317 during 7 days did lead to elevated plasma TG levels. The discrepancy with our results may be caused by a difference in duration of treatment. Possibly, net effects of T0901317-treatment on plasma lipid levels are determined by time-dependent effects on gene expression levels and their metabolic consequences.

It is tempting to speculate that LXR-stimulated de novo lipogenesis is the primary cause of the raised VLDL-TG secretion. The increased VLDL-TG production together with the induced transcription of hepatic *Lpl* might account for the elevated plasma FFA levels observed upon treatment (table 3.2). Lipoprotein lipase hydrolyzes TG and thereby catalyzes the conversion of VLDL into IDL, and subsequently of IDL into low density lipoprotein. Both conversions result in the release of FFAs into the bloodstream (43) and these FFAs will to large extent be taken up again by the liver. Increased supply of FFAs to liver cells stimulates VLDL-TG production (44); part of the observed stimulation of VLDL-TG production may

therefore occur via this indirect mechanism. To investigate whether LXR activation stimulates the VLDL-TG secretion by liver cells directly, we performed a limited series of experiments with McA-RH7777 cells kept under fixed FA concentrations. In these in vitro studies, we also found a gene expression profile consistent with increased *de novo* lipogenesis and stimulated cellular TG secretion, again without changes in apoB production. Administration of T0901317 to C57BL/6 mice also results in induction of *Srebp-1* and *Scd-1* mRNA levels in intestine and kidney (18). A recent study from Mak *et al.* (45) showed that incubation of murine macrophages with T0901317 resulted in increased *Srebp-1* and *Fas* mRNA levels. Nevertheless, actions of the LXR agonist in hepatocytes may be responsible for the observed increased VLDL-TG production rate in vivo because these cells are primarily involved in this process. It should be stressed that increased hepatic *de novo* lipogenesis is not always associated with increased VLDL-TG secretion. For instance, the strong induction of *de novo* lipogenesis upon inhibition of glucose-6-phosphatase activity in rats is not associated with increased VLDL production (46). Apparently, different regulatory factors dominate under different metabolic conditions.

Genes encoding proteins involved in assembly and secretion of VLDL, *i.e.*, *Apoe* and *Mttp*, were not affected upon treatment. The production of larger VLDL particles might be accounted for by an intracellular action of PLTP. Jiang *et al.* (47) reported that PLTP-deficient mice show a decreased secretion of apoB-containing particles. Because this decreased apoB production rate was observed both *in vivo* and in hepatocytes *in vitro*, it was concluded that PLTP must also be active within the cells. This suggestion is supported by the fact that mice overexpressing the human PLTP show increased VLDL-TG production (48). However, neither of these studies provided information about the size of the particles produced in the presence or absence of PLTP. Alternatively, induction of *Cyp7A1* expression and activity may contribute to increased VLDL-TG production, as mice overexpressing the human *Cyp7A1* gene also show this feature (49). Thus, various mechanisms may be responsible for the production of larger VLDL particles after LXR activation, but the exact mode of action is currently not known.

In conclusion, pharmacological activation of LXR is associated with development of hepatic steatosis and strongly affects the VLDL production process in mice, leading to formation of large, TG-rich particles. This combination of hepatic fat accumulation and overproduction of large VLDL strikingly resembles that observed in human diabetic states.

## Acknowledgements

This work was supported by Grants 903-39-291 (to A. G.) and 902-23-244 (to B. M. E.) from the Netherlands Organization for Scientific Research. We thank Rick Havinga and Juul F. W. Baller for skilful technical assistance.

## References

1. Willy, P. J., Umesono, K., Ong, E. S., Evans, R. M., Heyman, R. A., and Mangelsdorf, D. J. (1995) Genes Dev. 9, 1033-1045
2. Teboul, M., Enmark, E., Li, Q., Gustafsson, J.-A., Pelto-Huikko, M., and Gustafsson, J.-Å. (1995) Proc. Natl. Acad. Sci. U. S. A. 92, 2096-2100
3. Lehmann, J. M., Kliewer, S. A., Moore, L. B., Smith-Oliver, T. A., Oliver, B. B., Su, J.-L., Sundseth, S. S., Winegar, D. A., Blanchard, D. E., Spencer, T. A., and Willson, T. M. (1997) J. Biol. Chem. 272, 3137-3140
4. Repa, J. J., Turley, S. D., Lobaccaro, J.-M. A., Medina, J., Li, L., Lustig, K., Shan, B., Heyman, R. A., Dietschy, J. M., and Mangelsdorf, D. J. (2000) Science 289, 1524-1529
5. Costet, P., Luo, Y., Wang, N., and Tall, A. R. (2000) J. Biol. Chem. 275, 28240-28245
6. Venkateswaran, A., Lafitte, B. A., Joseph, S. B., Mak, P. A., Wilpitz, D. C., Edwards, P. A., and Tontonoz, P. (2000) Proc. Natl. Acad. Sci. U. S. A. 97, 12097-12102
7. Schwartz, K., Lawn, R. M., and Wade, D. P. (2000) Biochem. Biophys. Res. Commun. 274, 794-802
8. Venkateswaran, A., Repa, J. J., Lobaccaro, J.-M. A., Bronson, A., Mangelsdorf, D. J., and Edwards, P. A. (2000) J. Biol. Chem. 275, 14700-14707
9. Laffitte, B. A., Repa, J. J., Joseph, S. B., Wilpitz, D. C., Kast, H. R., Mangelsdorf, D. J., and Tontonoz, P. (2001) Proc. Natl. Acad. Sci. U. S. A. 98, 507-512
10. Peet, D. J., Turley, S. D., Ma, W., Janowski, B. A., Lobaccaro, J.-M. A., Hammer, R. E., and Mangelsdorf, D. J. (1998) Cell 93, 693-704
11. Berge, K. E., Tian, H., Graf, G. A., Yu, L., Grishin, N. V., Schultz, J., Kwiterovich, P., Shan, B., Barnes, R., and Hobbs, H. H. (2000) Science 290, 1771-1775
12. Repa, J. J., Berge, K. E., Pomajzl, C., Richardson, J. A., Hobbs, H., and Mangelsdorf, D. J. (2002) J. Biol. Chem. 277, 18793-18800
13. Song, C., and Liao, S. (2001) Steroids 66, 673-681
14. Xie, W., and Evans, R. M. (2001) J. Biol. Chem. 276, 37739-37742
15. Edwards, P. A., Kast, H. R., and Anisfeld, A. M. (2002) J. Lipid Res. 43, 2-12
16. Fayard, E., Schoonjans, K., and Auwerx, J. (2001) Curr. Opin. Lipidol. 12, 113-120
17. Lu, T. T., Repa, J. J., and Mangelsdorf, D. J. (2001) J. Biol. Chem. 276, 37735-37738
18. Schultz, J. R., Tu, H., Luk, A., Repa, J. J., Medina, J. C., Li, L., Schwender, S., Wang, S., Thoolen, M., Mangelsdorf, D. J., Lustig, K. D., and Shan, B. (2000) Genes Dev. 14, 2831-2838
19. Repa, J. J., Liang, G., Ou, J., Bashmakov, Y., Lobaccaro, J.-M. A., Shimomura, I., Shan, B., Brown, M. S., Goldstein, J. L., and Mangelsdorf, D. J. (2000) Genes Dev. 14, 2819-2830
20. Yoshikawa, T., Shimano, H., Amemiya-Kudo, M., Yahagi, N., Hasty, A. H., Matsuzaka, T., Okazaki, H., Tamura, Y., Iizuka, Y., Ohashi, K., Osuga, J.-I., Harada, K., Gotoda, T., Kimura, S., Ishibashi, S., and Yamada, N. (2001) Mol. Cell. Biol. 21, 2991-3000
21. Horton, J. D., Shimomura, I., Brown, M. S., Hammer, R. E., Goldstein, J. L., and Shimano, H. (1998) J. Clin. Invest. 101, 2331-2339
22. Joseph, S. B., Lafitte, B. A., Patel, P. H., Watson, M. A., Matsukuma, K. E., Walczak, R., Collins, J. L., Osborne, T. F., and Tontonoz, P. (2002) J. Biol. Chem. 277, 11019-11025
23. Zhang, Y., Repa, J. J., Gauthier, K., and Mangelsdorf, D. J. (2001) J. Biol. Chem. 276, 43018-43024
24. Luo, Y., and Tall, A. R. (2000) J. Clin. Invest. 105, 513-520
25. Liang, G., Yang, J., Horton, J. D., Hammer, R. E., Goldstein, J. L., and Brown, M. S. (2002) J. Biol. Chem. 277, 9520-9528
26. Parks, E. J., Krauss, R. M. C. M. P., Neese, R. A., and Hellerstein, M. K. (1999) J. Clin. Invest. 104, 1087-1096
27. van den Maagdenberg, A. M. J. M., Hofker, M. H., Krimpenfort, P. J. A., de Bruijn, I. H., van Vlijmen, B. J. M., van der Boom, H., Havekes, L. M., and Frants, R. R. (1993) J. Biol. Chem. 268, 10540-10545
28. van Vlijmen, B. J. M., Willems van Dijk, K., van't Hof, H. B., van Gorp, P. J. J., van der Zee, A., van der Boom, H., Breuer, M. L., Hofker, M. H., and Havekes, L. M. (1996) J. Biol. Chem. 271, 30595-30602
29. Teusink, B., Mensenkamp, A. R., van der Boom, H., Kuipers, F., Willems van Dijk, K., and Havekes, L. M. (2001) J. Biol. Chem. 276, 40693-40697
30. Mensenkamp, A. R., Jong, M. C., van Goor, H., van Luyn, M. J. A., Bloks, V., Havinga, R., Voshol, P. J., Hofker, M. H., Willems van Dijk, K., Havekes, L. M., and Kuipers, F. (1999) J. Biol. Chem. 274, 35711-35718
31. Bligh, E. G., and Dyer, W. J. (1959) Can. J. Biochem. Physiol. 37, 911-917
32. Böttcher, C. F. J., van Gent, C. M., and Pries, C. (1961) Anal. Chim. Acta 24, 203-204
33. Lowry, O. H., Rosenbrough, N. J., Farr, A. L., and Randall, R. J. (1951) J. Biol. Chem. 193, 265-275
34. Lepage, G., and Roy, C. C. (1986) J. Lipid Res. 27, 114-120

35. Fisher, E. A., Zhou, M., Mitchell, D. M., Wu, X., Omura, S., Wang, H., Goldberg, A. L., and Ginsberg, H. N. (1997) J. Biol. Chem. 272, 20427-20434
36. Vance, D. E., Weinstein, D. B., and Steinberg, D. (1984) Biochim. Biophys. Acta 792, 39-47
37. Malmström, R., Packard, C. J., Caslake, M., Bedford, D., Stewart, P., Yki-Järvinen, H., Shepherd, J., and Taskinen, M.-R. (1997) Diabetologia 40, 454-462
38. Lin, H. Z., Yang, S. Q., Chuckaree, C., Kuhajda, F., Ronnet, G., and Diehl, A. M. (2000) Nat. Med. 6, 998-1003
39. Guzman, M., and Castro, J. (1989) Biochem. J. 264, 107-113
40. van Haperen, R., van Tol, A., Vermeulen, P., Jauhiainen, M., van Gent, T., van den Berg, P., Ehnholm, J., Grosveld, F., van der Kamp, A., and de Crom, R. (2000) Arterioscler. Thromb. Vasc. Biol. 20, 1082-1088
41. Huuskonen, J., Olkkonen, V. M., Jauhiainen, M., and Ehnholm, C. (2001) Atherosclerosis 155, 269-281
42. Rye, K.-A., Clay, M. A., and Barter, P. J. (1999) Atherosclerosis 145, 227-238
43. Eckel, R. H. (1989) N. Engl. J. Med. 320, 1060-1068
44. Lewis, G. F. (1997) Curr. Opin. Lipidol. 8, 146-153
45. Mak, P. A., Laffitte, B. A., Desrumaux, C., Joseph, S. B., Curtiss, L. K., Mangelsdorf, D. J., Tontonoz, P., and Edwards, P. A. (2002) J. Biol. Chem. 277, in press
46. Bandsma, R. H. J., Wiegman, C. H., Herling, A. W., Burger, H.-J., ter Harmsel, A., Meijer, A. J., Romijn, J. A., Reijngoud, D.-J., and Kuipers, F. (2001) Diabetes 50, 2591-2597
47. Jiang, X.-C., Qin, S., Qiao, C., Kawano, K., Lin, M., Skold, A., Xiao, X., and Tall, A. R. (2001) Nat. Med. 7, 847-852
48. Lie, J., van Gent, T., van Haperen, R., Scheek, L., Lankhuizen, I., de Crom, R., and van Tol, A. (2002) Eur. J. Clin. Invest., in press
49. Miyake, J. H., Doung, X.-D. T., Strauss, W., Moore, G. L., Castellani, L. W., Curtiss, L. K., Taylor, J. M., and Davis, R. A. (2001) J. Biol. Chem. 276, 23304-23311
50. Shimomura, I., Shimano, H., Horton, J. D., Goldstein, J. L., and Brown, M. S. (1997) J. Clin. Invest. 99, 838-845

# Chapter 4

# Differential effects of pharmacological liver X receptor activation on hepatic and peripheral insulin sensitivity in lean and ob/ob mice

Aldo Grefhorst[1], Theo H. van Dijk[1], Anke Hammer[1],
Fjodor H. van der Sluijs[1],Rick Havinga[1], Louis M. Havekes[2,3],
Johannes A. Romijn[4], Pieter H. Groot[5],
Dirk-Jan Reijngoud[1], Folkert Kuipers[1]

[1]Laboratory of Pediatrics, University Medical Center Groningen
[2]TNO Prevention and Health, Leiden
[3]Departments of General Internal Medicine and Cardiology, Leiden University Medical Center
[4]Department of Endocrinology and Diabetes, Leiden University Medical Center
[5]Atherosclerosis Department, GlaxoSmithKline, Stevenage, United Kingdom

**Am. J. Physiol. Endocrinol. Metab. 2005: 289: E829 - E838**

## Abstract

Liver X receptor (LXR) agonists have been proposed to act as anti-diabetic drugs. However, pharmacological LXR activation leads to severe hepatic steatosis, a condition usually associated with insulin resistance and type 2 diabetes mellitus. To address this apparent contradiction, lean and *ob/ob* mice were treated with the LXR agonist GW-3965 for 10 days. Insulin sensitivity was assessed by hyperinsulinemic-euglycemic clamp studies. Hepatic glucose production (HGP) and metabolic clearance rate (MCR) of glucose were determined with stable isotope techniques. Blood glucose and hepatic and whole body insulin sensitivity remained unaffected upon treatment in lean mice, despite increased hepatic triglyceride contents (61.7 ± 7.2 *vs.* 12.1 ± 2.0 nmol/mg liver, $P < 0.05$). In *ob/ob* mice, LXR activation resulted in lower blood glucose levels and significantly improved whole body insulin sensitivity. GW-3965 treatment did not affect HGP under normo- and hyperinsulinemic conditions, despite increased hepatic triglyceride contents (221 ± 13 *vs.* 176 ± 19 nmol/mg liver, $P < 0.05$). Clamped MCR increased upon GW-3965 treatment (18.2 ± 1.0 *vs.* 14.3 ± 1.4 $ml \cdot kg^{-1} \cdot min^{-1}$, $P = 0.05$). LXR activation increased white adipose tissue mRNA levels of *Glut4*, *Acc1* and *Fas* in *ob/ob* mice only. In conclusion, LXR-induced blood glucose lowering in *ob/ob* mice was attributable to increased peripheral glucose uptake and metabolism, physiologically reflected in a slightly improved insulin sensitivity. Remarkably, steatosis associated with LXR activation did not affect hepatic insulin sensitivity.

## Introduction

Nuclear receptors act as cellular sensors of endogenous and exogenous compounds. When activated by their ligands, these receptors modulate transcription of their target genes to allow the cell to adapt adequately to changing conditions. The liver X receptor (LXR; NR1H3) has been identified as an oxysterol-activated nuclear receptor (26,40,47). After ligand binding, LXR forms a heterodimer with the retinoid X receptor (RXR; NR2B1). This complex binds to LXR response elements in promoter regions of genes, resulting in adaptation of gene transcription by attracting coactivator or corepressor complexes (13). LXR is well known to induce transcription of genes encoding proteins involved in reverse cholesterol transport, *i.e.*, ATP-binding cassette transporter (ABC) A1 (10,34,36,38,44), ABCG1 (24,45), ABCG5, ABCG8 (4,35,48), and Cyp7A1 (15,26,33). Pharmacological LXR activation increases high-density lipoprotein (HDL) cholesterol levels and stimulates fecal cholesterol excretion in mice (30,34,38,44). Treatment with agonists such as T-0901317 or GW-3965 attenuated development of atherosclerosis in apolipoprotein E-deficient (Apoe –/–) and low-density lipoprotein (LDL) receptor-deficient (Ldlr –/–) mice (11,41). Thus synthetic LXR agonists were considered as potential anti-atherosclerotic agents. Application of LXR agonists, however, was found to be associated with a number of undesirable side effects. LXR also controls expression of various genes involved in lipogenesis and triglyceride (TG) metabolism, and severe hepatic steatosis developed in mice upon LXR agonist treatment (14,37). We have previously shown that pharmacological activation of LXR is associated with production of large, TG-rich very low density lipoprotein (VLDL) particles, leading to hypertriglyceridemia in a mouse model with a humanized lipid profile (14).

Hepatic steatosis is associated with hepatic insulin resistance and type 2 diabetes mellitus (2,22). Counterintuitively, despite induction of hepatic steatosis, treatment with the LXR agonist GW-3965 improved the response to a glucose tolerance test in C57BL/6J mice on a high-fat diet (23) but not in chow-fed mice. Cao *et al.* (8) showed that LXR activation reduced blood glucose levels in diabetic rodents, which was associated with decreased hepatic expression of the gene encoding phosphoenolpyruvate carboxykinase (PEPCK), supposedly rate controlling in gluconeogenesis (GNG). Moreover, treatment of *db/db* mice with T-0901317 markedly lowered hepatic *Pepck* gene expression in combination with more severe hepatic TG accumulation (9), suggesting that suppressed hepatic *Pepck* expression might result in a shift from GNG toward lipogenesis.

So far, no quantitative data have been reported concerning the effects of LXR activation on hepatic and peripheral insulin sensitivity and on hepatic glucose metabolism. Moreover, the commonly used animal model for type 2 diabetes mellitus, the obese, leptin-deficient *ob/ob* mouse, has not been used to evaluate the anti-diabetic effects of LXR activation. Therefore, we quantified the effects of LXR activation by GW-3965 on whole body and hepatic insulin sensitivity in lean and obese (*ob/ob*) mice.

## Materials and methods

### *Animals*

Male lean and obese (*ob/ob*) C57BL/6J mice (Harlan, Horst, The Netherlands) were housed in a light- and temperature-controlled facility and were fed commercially available laboratory chow (RMH-B; Hope Farms, Woerden, The Netherlands) containing 6.2% fat and 0.01% cholesterol (wt/wt). For 10 days, the animals were fed the same diet with or without the synthetic LXR agonist GW-3965 (0.03% wt/wt; kindly provided by GlaxoSmithKline Pharmaceuticals, Stevenage, UK). On the 11th day, mice were subjected to one of the experiments described below. Experimental procedures were approved by the Ethics Committee for Animal Experiments of the State University Groningen.

### *Plasma and tissue sampling and analyses*

Lean and *ob/ob* mice were killed under isoflurane anesthesia on the 11th day of treatment. A large blood sample was collected by cardiac puncture and centrifuged. Plasma was stored at -20°C until analyzed. The liver was quickly removed, weighed, and frozen in separate portions for RNA isolation and lipid analyses. Abdominal white adipose tissue (WAT) and backlimb muscle tissue were collected and frozen for RNA isolation.

Plasma TGs, phospholipids, nonesterified fatty acid (NEFA), HDL cholesterol, free cholesterol, and total cholesterol were determined using commercially available kits (Roche Diagnostics, Mannheim, Germany, and Wako Chemicals, Neuss, Germany). Plasma insulin concentrations were determined using RIA RI-13K (Linco Research, St. Charles, MO). Hepatic concentrations of TGs, free cholesterol, and total cholesterol were measured using commercial kits (Roche Diagnostics and Wako Chemicals) after lipid extraction according to Bligh and Dyer (6). Phospholipid content of the liver was determined according to Böttcher *et al*. (7) after lipid extraction. Protein concentrations in livers were determined according to Lowry *et al*. (28) using BSA (Pierce, Rockford, IL) as standard. Hepatic glycogen and glucose 6-phosphate (G6P) levels were determined as described before (17,19). Fatty acid composition was determined by gas chromatography after methylation, as described previously (27).

### *Hyperinsulinemic euglycemic clamps*

Lean and *ob/ob* mice were equipped with a permanent catheter in the right atrium via the jugular vein (21). The two-way entrance of the catheter was attached to the skull with acrylic glue. The mice were allowed a resting period of at least 5 days during which the treatment period was completed. Before the start of the experiment (9 h), food was withdrawn, but mice still had free access to water. They were kept in metabolic cages during the experiment, allowing frequent collection of blood spots from the mice without anesthesia (42).

The mice were infused for 6 h with two solutions. The first one (insulin solution) was a 1% BSA solution containing 40 μg/ml somatostatin (UCB, Breda, The Netherlands). This solution contained insulin (Actrapid; Novo Nordisk, Bagsvaerd, Denmark), leading to an insulin infusion rate of 10 $mU \cdot kg^{-1} \cdot min^{-1}$. To prevent high total infusion rates leading to possible higher morbidity, this solution contained 200 mg/ml glucose, from which 2% was [U-$^{13}$C]glucose (99% $^{13}$C atom %excess; Cambridge Isotope Laboratories, Andover, MA). The solution was infused at a constant flow rate of 0.135 ml/h. The second infusate (glucose solution) was a 30% glucose solution, from which 3% was [U-$^{13}$C]glucose. Its infusion rate was adjusted according to measured blood glucose levels to maintain euglycemic conditions. Just before the start of the experiment, a small blood sample was obtained by tail bleeding. Blood glucose levels were measured with a Lifescan EuroFlash glucose meter (Lifescan Benelux, Beerse, Belgium) in a small tail blood sample that was taken every 15 min. For gas

chromatography/mass spectrometry (GC-MS) measurements, a blood spot was obtained by tail bleeding every hour. After the clamp, animals were killed by cardiac puncture under anesthesia. Blood samples were centrifuged, and the obtained plasma was stored at –20°C until analyzed.

*Hepatic carbohydrate flux measurements*

After 10 days of treatment, hepatic carbohydrate fluxes were determined using infusion of stable isotopes, as previously described by van Dijk *et al.* (42). The mice were allowed a resting period after surgery of at least 5 days during which the treatment period was completed. Before the start of infusion (9 h), food was withdrawn, but mice still had free access to water. They were infused at a rate of 0.3 ml/h (lean mice) or 0.6 ml/h (*ob/ob* mice) with a solution containing 13.9 μmol/ml [U-$^{13}$C]glucose, 160 μmol/ml [2-$^{13}$C]glycerol, 33 μmol/ml [1-$^{2}$H]galactose, and 1.0 mg/ml paracetamol. Blood and urine spots were collected at hourly intervals on filter papers.

*Measurement of mass isotopomer distribution by GC-MS*

Analytical procedures for extraction of glucose from blood spots filter paper (hyperinsulinemic-euglycemic clamp and hepatic carbohydrate flux experiment) and paracetamol-glucuronide from urine filter paper (hepatic carbohydrate flux experiment), derivatization of the extracted compounds, and GC-MS measurements of derivatives were essentially, according to van Dijk and colleagues (42,43).

*Mass isotopomer distribution analysis for hepatic carbohydrate fluxes*

The measured fractional isotopomer distribution by GC-MS ($m_0$-$m_6$) was corrected for the fractional distribution resulting from natural abundance of $^{13}$C by multiple linear regression as described by Lee *et al.* (25) to obtain the excess mole fraction of mass isotopomers $M_0$-$M_6$ due to incorporation of infused labeled compounds. For the determination of the hepatic carbohydrate fluxes, this distribution was used in mass isotopomer distribution analysis algorithms of isotope incorporation and dilution according to Hellerstein *et al.* (16) and as described by van Dijk and colleagues (42, 43).

*Calculation of endogenous glucose production and metabolic clearance rate under clamped conditions*

Two solutions with [U-$^{13}$C]glucose were infused with different rates. Therefore, the total rate of appearance of glucose into plasma [Ra(Glc;whole body)] was calculated as follows:

$$Ra(glc;\text{whole body}) = (M_6(glc)_{glucose} \times infusion(glc;M_6)_{glucose} + M_6(glc)_{insulin} \times infusion(glc;M_6)_{insulin})/M_6(glc)_{blood} \quad (1)$$

in which $M_6(Glc)_{glucose}$ and $M_6(Glc)_{insulin}$ are the excess mole fractions of infused [U-$^{13}$C]glucose in the glucose and insulin solution, respectively, and $infusion(Glc;M_6)_{glucose}$ and $infusion(Glc;M6)_{insulin}$ are the infusion rates of [U-$^{13}$C]glucose of the glucose and insulin solution, respectively. $M_6(Glc)$blood is the excess mole fraction of infused [U-$^{13}$C]glucose in blood.

The rate of endogenous plasma glucose [Ra(Glc;endo)] was calculated as follows:

$$Ra(glc;endo) = Ra(glc;\text{whole body}) - infusion(glc;M_6)_{glucose} - infusion(glc;M_6)_{insulin} \quad (2)$$

Table 4.1.Primers and probes used for realtime-PCR analysis.

| Gene | | Sequences (5' to 3') | GenBank™ accession no. |
|---|---|---|---|
| *β-Actin* | Forward | AGCCATGTACGTAGCCATCCA | NM_007393 |
| | Reverse | TCTCCGGAGTCCATCACAATG | |
| | Probe | TGTCCCTGTATGCCTCTGGTCGTACCAC | |
| *18S rRNA* | Forward | CGGCTACCACATCCAAGGA | X00686 |
| | Reverse | CCAATTACAGGGCCTCGAAA | |
| | Probe | CGCGCAAATTACCCACTCCCGA | |
| *Srebp-1c* | Forward | GGAGCCATGGATTGCACATT | AF286470 |
| | Reverse | CCTGTCTCACCCCCAGCATA | |
| | Probe | CAGCTCATCAACAACCAAGACAGTGACTTCC | |
| *Fas* | Forward | GGCATCATTGGGCACTCCTT | NM_007988 |
| | Reverse | GCTGCAAGCACAGCCTCTCT | |
| | Probe | CCATCTGCATAGCCACAGGCAACCTC | |
| *Acc1* | Forward | GCCATTGGTATTGGGGCTTAC | XM_109883/ |
| | Reverse | CCCGACCAAGGACTTTGTTG | |
| | Probe | CTCAACCTGGATGGTTCTTTGTCCCAGC | |
| *Acc2* | Forward | CATACACAGAGCTGGTGTTGGACT | NM_133904 |
| | Reverse | CACCATGCCCACCTCGTTAC | |
| | Probe | CAGGAAGCCGGTTCATCTCCACCAG | |
| *Lxrα* | Forward | GCTCTGCTCATTGCCATCAG | AF085745 |
| | Reverse | TGTTGCAGCCTCTCTACTTGGA | |
| | Probe | TCTGCAGACCGGCCCAACGTG | |
| *Gk* | Forward | CCTGGGCTTCACCTTCTCCTT | NM_010292 |
| | Reverse | GAGGCCTTGAAGCCCTTGGT | |
| | Probe | CACGAAGACATAGACAAGGGCATCCTGCTC | |
| *G6pt* | Forward | GAGGCCTTGTAGGAAGCATTG | NM_008063 |
| | Reverse | CCATCCCAGCCATCATGAGTA | |
| | Probe | CTCTGTATGGGAACCCTCGCCACG | |
| *G6ph* | Forward | CTGCAAGGGAGAACTCAGCAA | NM_008061 |
| | Reverse | GAGGACCAAGGAAGCCACAAT | |
| | Probe | TCGTTCCCATTCCGCTTCGCCT | |
| *Gp* | Forward | GAAGGAGGCAAACGGATCAAC | NM_133198 |
| | Reverse | TCACGATGTCCGAGTGGATCT | |
| | Probe | CCTCTGCATCGTGGGCTGCCA | |
| *Gs* | Forward | GCTCTCCAGACGATTCTTGCA | AA537291 |
| | Reverse | GTGCGGTTCCTCTGAATGATC | |
| | Probe | CCTCTACGGGTTTTGTAAACAGTCACGCC | |
| *Pepck* | Forward | GTGTCATCCGCAAGCTGAAG | NM_011044 |
| | Reverse | CTTTCGATCCTGGCCACATC | |
| | Probe | CAACTGTTGGCTGGCTCTCACTGACCC | |
| *Pk* | Forward | CGTTTGTGCCACACAGATGCT | NM_013631 |
| | Reverse | CATTGGCCACATCGCTTGTCT | |
| | Probe | AGCATGATCACTAAGGCTCGACCAACTCGG | |
| *Glut4* | Forward | CTCATGGGCCTAGCCAATG | NM_009204 |
| | Reverse | GGGCGATTTCTCCCACATAC | |
| | Probe | CATTGGCGCCTACTCAGGGCTAACATC | |
| *Hk1* | Forward | CACCGGCAGATTGAGGAAAC | NM_010438 |
| | Reverse | CTCAGCCCCATTTCCATCTCT | |
| | Probe | TCCCACTTCCGCCTCAGCAAGC | |
| *Hk2* | Forward | GGAACCCAGCTGTTTGACCA | NM_013820 |
| | Reverse | CAGGGGAACGAGAAGGTGAAA | |
| | Probe | TGCCTGGCCAACTTCATGGACAAGC | |

The metabolic clearance rate of glucose (MCR) was calculated according to:

$$MCR = Ra(glc;whole\ body)/[glc] \quad (3)$$

where [Glc] is the blood glucose concentration (mM).

*RNA isolation and measurement of mRNA levels by real-time PCR (Taqman)*

mRNA expression levels in liver, WAT, and skeletal muscle were measured by real-time PCR, as described previously (14). PCR results were normalized to *β-actin* (hepatic tissue) or *18S* (WAT, skeletal muscle) mRNA levels. The sequences of the primers and probes used are listed in table 4.1.

*Statistics*

All values represent means ± SE for the number of animals or experiments indicated. Statistical analysis of two groups was assessed by Mann-Whitney U-test (plasma and hepatic parameters) or ANOVA for repeated measurement (flux and clamp experiment). Level of significance was set at $P < 0.05$. Analyses were performed using SPSS for Windows software (SPSS, Chicago, IL).

## Results

*LXR activation increased hepatic TG content in both lean and ob/ob mice*

Feeding the synthetic LXR agonist GW-3965 (0.03% wt/wt) for 10 days did not affect body weights of either lean or *ob/ob* mice (table 4.2). Lean mice developed increased liver weights and a fivefold increase in hepatic TG content upon GW-3965 treatment (table 4.2). Although *ob/ob* mice already showed severe hepatic steatosis on the control diet, LXR activation resulted in a further 25% increase in hepatic TG content. LXR activation resulted in a clearly altered hepatic fatty acid composition in lean mice (figure 4.1). GW-3965 treatment significantly reduced the relative amount of hepatic saturated fatty acids and polyunsaturated fatty acids from 37.8 ± 0.7 to 28.7 ± 0.6% and from 42.3 ± 2.8 to 27.5 ± 1.4%, respectively. In contrast, the relative amount of monounsaturated fatty acids significantly increased from 19.9 ± 3.4 to 43.8 ± 1.9% upon LXR activation. In *ob/ob* mice, LXR activation did not significantly affect hepatic fatty acid composition. Glycogen and G6P levels were higher in *ob/ob* mice than in lean mice. GW-3965 treatment did not affect glycogen and G6P levels of lean mice. In *ob/ob* mice, in contrast, LXR activation reduced glycogen to levels comparable to those of lean mice, whereas G6P levels remained unchanged (table 4.2).

LXR activation resulted in elevated plasma cholesterol levels in lean mice (table 4.2), mainly because of increased HDL cholesterol levels. Plasma TG and NEFA levels were not affected by the agonist in lean mice. Blood glucose levels were not affected by the treatment in lean mice (figure 4.2), but insulin levels were somewhat increased in the treated mice (table 4.2). In *ob/ob* mice, LXR activation had no significant effect on plasma lipid levels, but the treatment resulted in reduced lower blood glucose (figure 4.2) and plasma insulin levels (table 4.2).

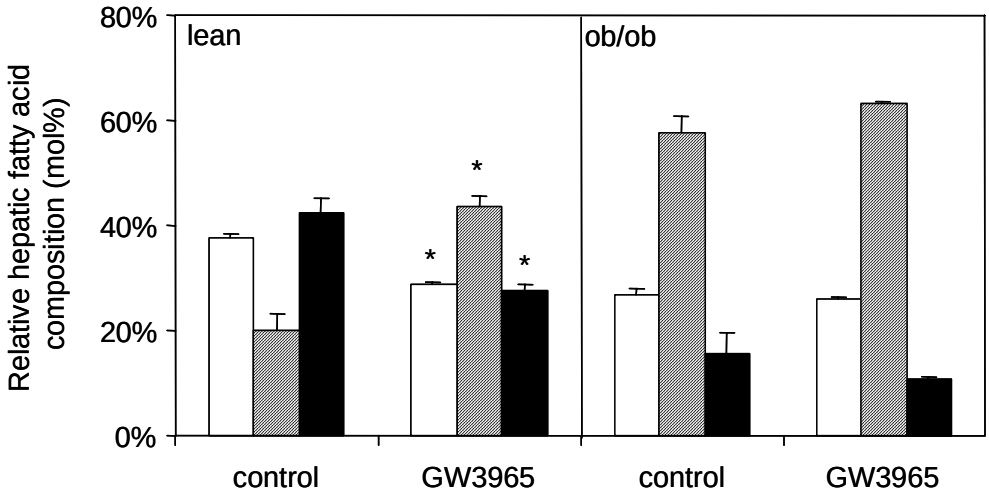


Figure 4.1. Hepatic fatty acid composition in lean and *ob/ob* mice fed a diet with or without the synthetic LXR agonist GW3965 for 10 days. Relative amounts of saturated (SAFA, white bars), monounsaturated (MUFA, striped bars) and polyunsaturated (PUFA, black bars) fatty acids; n=6; *, $p<0.05$ treated *vs.* untreated.

Table 4.2. Hepatic and plasma parameters in lean and *ob/ob* mice fed a diet with or without the synthetic LXR agonist GW3965 for 10 days. Values are means ± S.E.M.; n = 6; *, $p<0.05$ treated *vs.* untreated; †, $p<0.05$ *ob/ob vs.* lean untreated. G6P, glucose-6-phosphate.

| | Lean | | *ob/ob* | |
|---|---|---|---|---|
| | Control | GW3965 | Control | GW3965 |
| Body weight (gram) | 25.5 ± 1.0 | 25.0 ± 0.5 | 47.0 ± 1.3 † | 47.4 ± 0.7 † |
| Liver weight (% of bodyweight) | 5.3 ± 0.1 | 6.3 ± 0.1 * | 8.5 ± 0.4 † | 8.4 ± 0.2 † |
| Liver proteins (mg/g liver) | 229.5 ± 4.2 | 223.6 ± 9.5 | 292.4 ± 14.5 † | 296.9 ± 18.9 † |
| Liver triglycerides (nmol/mg liver) | 12.1 ± 2.0 | 61.7 ± 7.2 * | 176.2 ± 18.8 † | 220.8 ± 13.2 *† |
| Liver glycogen (nmol/mg liver) | 166 ± 9 | 152 ± 17 | 309 ± 23 † | 209 ± 18 * |
| Liver G6P (nmol/g liver) | 645 ± 30 | 692 ± 35 | 762 ± 22 † | 929 ± 67 † |
| Plasma triglycerides (mM) | 0.79 ± 0.06 | 1.10 ± 0.30 | 0.96 ± 0.11 | 0.59 ± 0.08 † |
| Plasma free cholesterol (mM) | 0.80 ± 0.03 | 1.21 ± 0.04 * | 1.12 ± 0.09 | 1.17 ± 0.06 † |
| Plasma cholesterylester (mM) | 1.88 ± 0.07 | 2.73 ± 0.05 * | 4.64 ± 0.34 † | 5.18 ± 0.25 † |
| Plasma HDL cholesterol (mM) | 1.76 ± 0.44 | 2.88 ± 0.13 | 2.90 ± 0.33 | 3.51 ± 0.26 † |
| Plasma NEFA (mM) | 0.22 ± 0.02 | 0.21 ± 0.03 | 0.58 ± 0.03 † | 0.51 ± 0.05 † |
| Plasma insulin (ng/ml) | 0.25 ± 0.06 | 0.48 ± 0.06 * | 1.26 ± 0.49 † | 0.47 ± 0.22 |

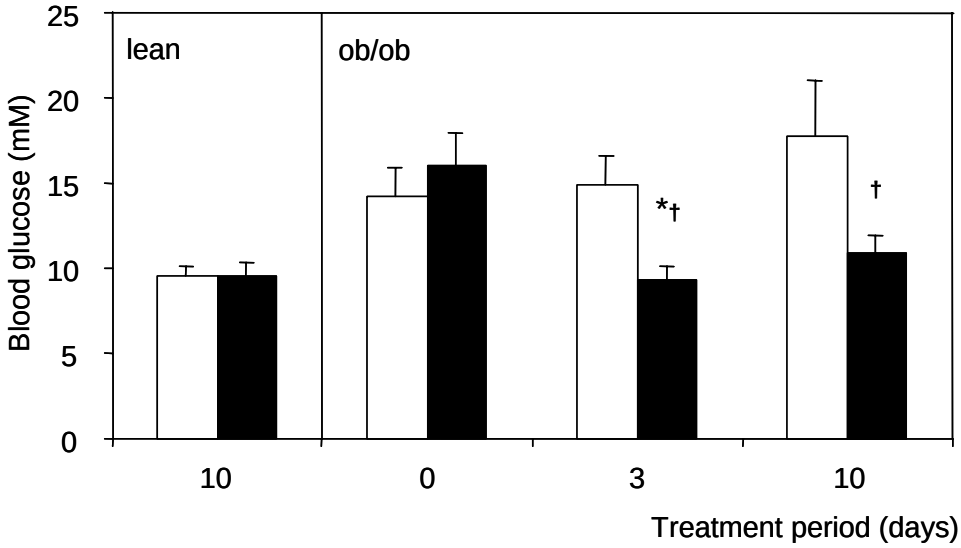


Figure 4.2. Blood glucose levels (mM) in lean and *ob/ob* mice before and after 3 or 10 days diet with or without the synthetic LXR agonist GW3965. N=6; *, $p<0.05$ treated *vs.* untreated; †, $p<0.05$ *vs.* before treatment.

*Improved insulin sensitivity in ob/ob mice upon LXR activation*

To test whether insulin sensitivity was influenced by LXR activation, we performed hyperinsulinemic-euglycemic clamp studies in conscious mice for 6 h. The total glucose infusion rate (GIR) was adjusted such that euglycemic conditions were maintained throughout the infusion period (figure 4.3A). In all four groups of mice, GIR reached constant values after 3 h of infusion (figure 4.3B). In lean mice, GIR did not differ significantly between the treated and nontreated group. Calculated for the last 3 h of the experiment, GIR was 593 ± 13 and 564 ± 14 $\mu mol \cdot kg^{-1} \cdot min^{-1}$ for untreated and treated lean mice, respectively. In untreated *ob/ob* mice, GIR was markedly lower than in lean mice, *i.e.*, 95 ± 5 $\mu mol \cdot kg^{-1} \cdot min^{-1}$. After the 10-day treatment period, insulin sensitivity was improved significantly, as is evident from the 50% increase in GIR to a value of 141 ± 5 $\mu mol \cdot kg^{-1} \cdot min^{-1}$.

*Hyperinsulinemia reduced hepatic glucose production irrespective of GW-3965 treatment.*

LXR agonist treatment (10 days) did not affect any of the measurable fluxes in lean mice, but resulted in a tendency toward increased GNG and significantly increased fluxes through glycogen phosphorylase (GP), glucose-6-phosphatase (G6Pase), and glucokinase (GK) in *ob/ob* mice (table 4.3). The *ob/ob* mice showed slightly higher glucose cycling rates upon LXR activation (table 4.3), confirming recent findings from our laboratory (3). Most importantly, endogenous glucose production [Ra(Glc;endo), hepatic glucose production (HGP)] did not differ between untreated and treated lean and *ob/ob* mice (table 4.3).

In lean mice, steady-state HGP during the last 3 h of the clamp was strongly reduced and not affected by administration of the agonist: 11 ± 18 *vs.* 23 ± 15 $\mu mol \cdot kg^{-1} \cdot min^{-1}$, untreated *vs.* treated (figure 4.3A). Thus HGP was almost completely inhibited in both groups, *i.e.*, by 94 and 86%, respectively. Steady-state HGP under clamped conditions was higher in *ob/ob* mice compared with lean mice, indicating hepatic insulin resistance, without significant differences between untreated and treated *ob/ob* mice, *i.e.*, 79 ± 7 *vs.* 64 ± 16 $\mu mol \cdot kg^{-1} \cdot min^{-1}$, respectively (figure 4.4A). The insulin-mediated suppression of HGP was similar in untreated and GW-3965-treated *ob/ob* mice, *i.e.*, 48 and 61% respectively.

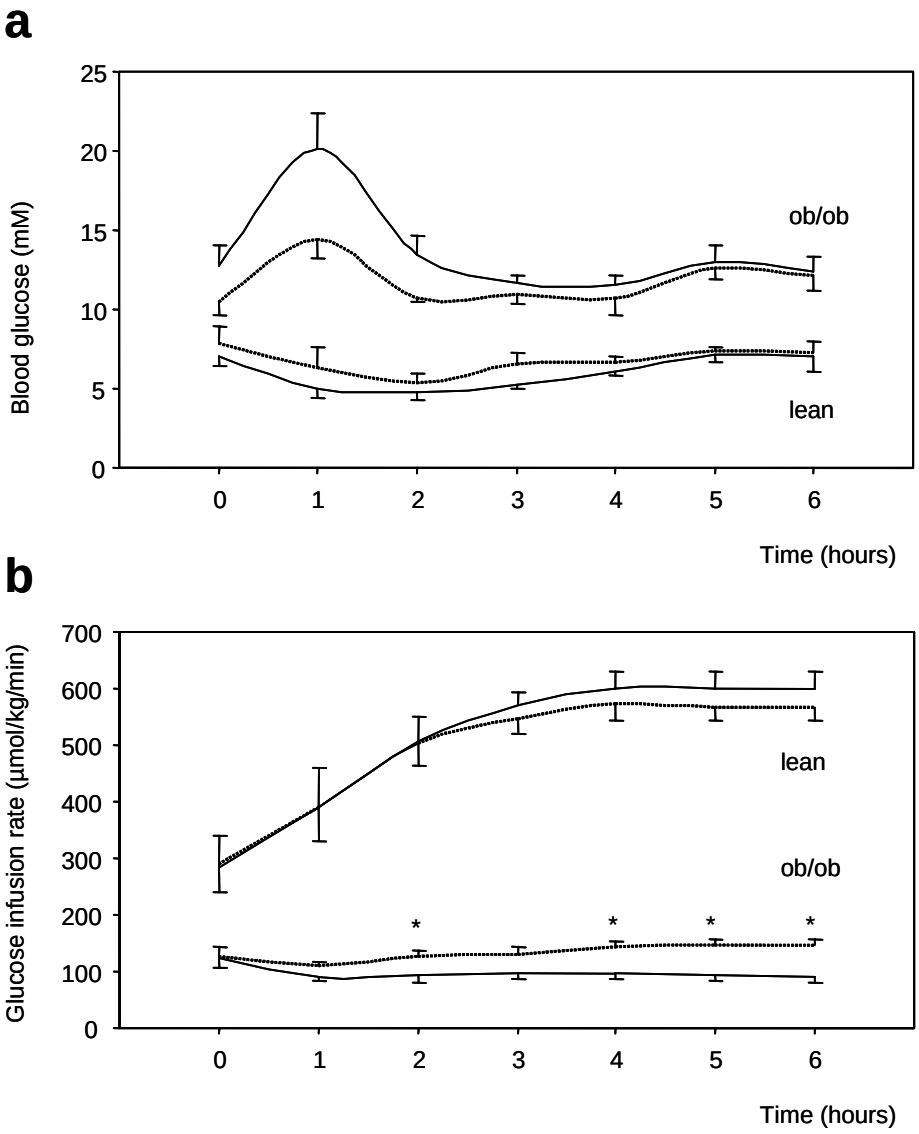


Figure 4.3. Blood glucose level and glucose infusion rate during hyperinsulinemic euglycemic clamps in lean and *ob/ob* mice fed a diet with (dotted line) or without (solid line) the synthetic LXR agonist GW3965 for 10 days. a) Blood glucose levels (mM); b) glucose infusion rates (µmol/kg/min) during clamping; n=6, n=5 (treated *ob/ob* mice); *, $p<0.05$ treated *vs.* untreated.

Table 4.3. Hepatic carbohydrate fluxes in lean and *ob/ob* mice fed a diet with or without the synthetic LXR agonist GW3965 for 10 days. Values are means ± S.E.M.; n=5; *, $p<0.05$ treated *vs.* untreated; †, $p<0.05$ *ob/ob vs.* lean untreated.

| | Lean | | *ob/ob* | |
|---|---|---|---|---|
| | Control | GW3965 | Control | GW3965 |
| Total gluconeogenic flux (µmol/kg/min) | 144 ± 8 | 131 ± 6 | 143 ± 10 | 185 ± 4 |
| Glycogen synthase flux (µmol/kg/min) | 111 ± 7 | 96 ± 7 | 56 ± 7 † | 70 ± 12 † |
| Glycogen phosphorylase flux (µmol/kg/min) | 97 ± 7 | 84 ± 8 | 85 ± 7 | 114 ± 3 * |
| Glucose-6-phosphatase flux (µmol/kg/min) | 228 ± 16 | 191 ± 10 | 232 ± 12 | 289 ± 14 *† |
| Glucokinase flux (µmol/kg/min) | 82 ± 10 | 60 ± 7 | 101 ± 17 | 148 ± 17 *† |
| Hepatic glucose production (µmol/kg/min) | 173 ± 9 | 152 ± 8 | 153 ± 9 | 169 ± 2 |
| Cycling glucose – glucose-6-phospate (%) | 23 ± 2 | 20 ± 2 | 34 ± 4 | 40 ± 4 |

*Slightly improved metabolic clearance of glucose under clamped conditions in GW-3965-treated ob/ob mice*

From the data available, it is possible to calculate the MCR under both basal and clamped conditions (figure 4.4B). In lean mice, basal MCR was not affected by LXR activation. During the clamp, values of MCR increased 5.5-fold and 5.7-fold in untreated and treated C57BL/6J mice, respectively. In contrast, MCR did not change upon hyperinsulinemia in untreated *ob/ob* mice, but clamping increased MCR by 80% in treated *ob/ob* mice. Thus clamped MCR values were 18.2 ± 1.0 and 14.3 ± 1.4 $ml \cdot kg^{-1} \cdot min^{-1}$ (P = 0.05) in treated and untreated *ob/ob* mice, respectively.

*Effects of LXR activation on hepatic gene expression in lean and ob/ob mice*

As expected, hepatic mRNA levels of genes encoding sterol-regulatory element-binding protein-1c (SREBP-1c) and fatty acid synthetase (FAS) increased upon LXR activation in the lean mice (table 4.4). Expression of *Fas* was higher in *ob/ob* mice than in lean mice but was not affected by LXR activation. Expression of *Lxrα*, the major LXR isoform, was not affected by LXR activation.

From the genes encoding relevant enzymes in hepatic carbohydrate metabolism, only expression of *Gk*, encoding for glucokinase, was significantly increased by 54% upon GW-3965 treatment in the lean mice (table 4.4). Data suggest a tendency toward lower expression of *Pepck* and higher expression of the pyruvate kinase gene (*Pk*) in treated lean mice. Compared with lean mice, *ob/ob* mice showed significantly higher expression of *Gk* and *G6pt*. The latter gene encodes for G6P translocase, which is part of the G6Pase complex that controls the flux of G6P toward glucose. Upon LXR activation, expression of the genes encoding for both subunits of the G6Pase complex, *G6pt* and *G6ph*, was markedly reduced in *ob/ob* mice.

*Normalization of Glut4, Acc1, and Fas WAT mRNA levels in ob/ob mice upon LXR activation*

Because previous studies reported effects of LXR agonists on adipose and muscle mRNA expression profiles (23,39), we determined WAT in skeletal muscle mRNA levels of several genes encoding proteins involved in glucose or lipogenesis (figure 4.5). LXR activation resulted in a threefold increase of *Srebp-1c* in adipose tissue of the lean mice, but *Fas* and *Acc1* (encoding for acetyl-CoA carboxylase-1) mRNA levels were not affected. Expression of these lipogenic genes was lower in untreated *ob/ob* mice compared with untreated lean mice. Yet, LXR activation resulted in a fourfold increased expression of *Srebp-1c*, whereas *Fas* and *Acc1* expression were increased 2.6- and 2.3-fold, respectively. Untreated *ob/ob* mice showed lower adipose mRNA levels of *Glut4* than untreated lean mice, but *Glut4* expression normalized upon LXR activation in *ob/ob* mice. Expression of the genes encoding for hexokinase-1 (*Hk1*) and hexokinase-2 (*Hk2*) was not different between the two strains and not affected by LXR activation. In muscle tissue, LXR activation led a 8.6- and 3.5-fold increase of *Srebp-1c* mRNA levels in lean and *ob/ob* mice, respectively. Neither *Fas*, *Acc2* (the isoform of ACC predominantly expressed in muscle; see Ref. 1), nor *Glut4* muscle mRNA levels in lean and *ob/ob* mice were affected upon LXR activation. In *ob/ob* mice only, LXR activation slightly reduced muscle mRNA levels of *Hk1* and *Hk2*. WAT and muscle *Lxrα* expression was not affected upon GW-3965 activation in either lean or *ob/ob* mice.

Table 4.4. Hepatic gene expression in lean and *ob/ob* mice fed a diet with or without the synthetic LXR agonist GW3965 for 10 days. Values are means ± S.E.M.; results normalized to *β-Actin* mRNA levels; data from untreated lean mice defined as 1; n=4 (lean), n=6 (*ob/ob*); *, p<0.05 treated *vs.* untreated; †, p<0.05 *ob/ob vs.* lean untreated. *Srebp-1c*, sterol-regulatory element-binding protein-1c; *Fas*, fatty acid synthetase; *Lxrα*, liver x receptor α; *Gk*, glucokinase; *G6ph*, glucose-6-phosphate hydrolase; *G6pt*, glucose-6-phosphate translocase; *Gs*, glycogen synthase; *Gp*, glycogen phosphorylase; *Pepck*, phospho*enol*pyruvate carboxykinase; *Pk*, pyruvate kinase.

| | Lean | | *ob/ob* | |
|---|---|---|---|---|
| | Control | GW3965 | Control | GW3965 |
| *Srebp-1c* | 1.00 ± 0.18 | 2.61 ± 0.53 * | 1.27 ± 0.20 | 1.84 ± 0.18 † |
| *Fas* | 1.00 ± 0.16 | 3.76 ± 1.27 * | 3.15 ± 0.31 † | 2.96 ± 0.38 † |
| *Lxrα* | 1.00 ± 0.15 | 0.71 ± 0.05 | 1.46 ± 0.17 | 1.52 ± 0.25 |
| *Gk* | 1.00 ± 0.12 | 1.54 ± 0.18 * | 2.21 ± 0.07 † | 2.45 ± 0.24 † |
| *G6ph* | 1.00 ± 0.20 | 1.05 ± 0.41 | 1.07 ± 0.15 | 0.41 ± 0.08 * † |
| *G6pt* | 1.00 ± 0.21 | 1.08 ± 0.11 | 1.56 ± 0.08 † | 0.86 ± 0.09 * |
| *Gs* | 1.00 ± 0.19 | 0.94 ± 0.19 | 1.11 ± 0.15 | 0.99 ± 0.12 |
| *Gp* | 1.00 ± 0.14 | 1.26 ± 0.36 | 1.11 ± 0.11 | 0.74 ± 0.11 |
| *Pepck* | 1.00 ± 0.16 | 0.78 ± 0.23 | 0.96 ± 0.12 | 0.71 ± 0.07 |
| *Pk* | 1.00 ± 0.15 | 1.35 ± 0.20 | 1.02 ± 0.24 | 0.60 ± 0.08 † |

## Discussion

This study documents that pharmacological LXR activation improves glucose metabolism in *ob/ob* mice by increased peripheral glucose uptake and slightly increased peripheral insulin sensitivity. Remarkably, HGP and hepatic insulin sensitivity remained unaffected although LXR activation increased hepatic TG content dramatically. These observations indicate tissue-specific effects of LXR activation on fat and glucose metabolism. Treatment with the LXR agonist resulted in reduced blood glucose concentrations in *ob/ob* mice but had no effect whatsoever in lean mice (figure 4.2), in accordance with previous studies (8,9,23). Laffitte *et al.* (23) showed that obese, but not lean, C57BL/6 mice had improved glucose tolerance after 1 week of GW-3965 treatment. The LXR agonist T-0901317 lowered blood glucose in male *db/db* mice and male Zucker diabetic fatty rats but not in their nondiabetic controls (8,9).

Previous studies (8,9,23) suggested that reduced GNG might, at least in part, account for the anti-diabetic effect of LXR agonists. However, this conclusion was based merely on the finding of reduced *Pepck* mRNA levels. To assess the actual effects of LXR activation on GNG flux and HGP, we quantified hepatic carbohydrate fluxes using stable isotope techniques (42,43). From these data (table 4.3) it is evident that neither GNG nor HGP was affected upon LXR activation in lean or *ob/ob* mice. We found reduced blood glucose levels in *ob/ob* mice upon GW-3965 treatment, but our data clearly indicate that this effect of LXR activation is not the result of reduced GNG. We found hepatic *Pepck* expression to be slightly reduced in both strains of mice upon GW-3965 treatment. Previous reports (8,23) showed more drastic effects on *Pepck* expression. The type of agonist (T-0901317 *vs.* GW-3965),

mode and dose of administration, and the diabetic animal model could account for the differences in this respect between these studies and our results. For *Gk* expression, we found a 54% increase in lean mice and no change in *ob/ob* mice upon LXR activation, whereas others found a more than threefold induction in 12-h fasted female C57BL/6J mice (23). Changes in *Gk* mRNA levels could, at least in part, be the result of *Srebp-1c* induction (20). Nonetheless, our study demonstrates that changes in hepatic gene expression do not fully translate into changes in the metabolic fluxes. The slight reduction of *Pepck* gene expression was not reflected in the GNG flux (table 4.3). Recently, is was pointed out that only severe reductions (–90%) or drastic increases (+300%) of *Pepck* expression are associated with changes in GNG in mice (29). Consequently, relatively small alterations in *Pepck* mRNA levels per se do not predict changes in gluconeogenic flux.

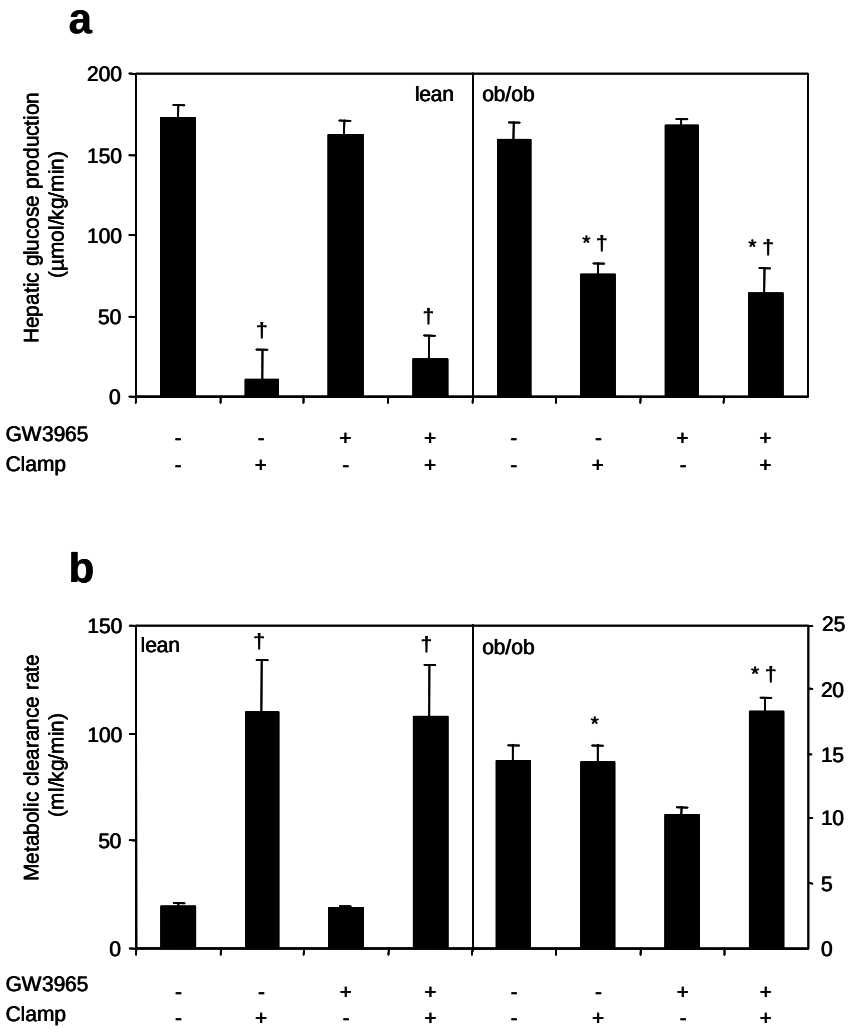


Figure 4.4. Hepatic glucose production and metabolic clearance rate under basal (stable isotope infusion) and clamped conditions in lean and *ob/ob* mice fed a diet with or without the synthetic LXR agonist GW3965 for 10 days. a) Hepatic glucose production (µmol/kg/min); b) metabolic clearance rate (ml/kg/min); n=6, n=5 (clamped treated *ob/ob* and basal lean); *, $p<0.05$ *ob/ob vs.* lean untreated; †, $p<0.05$ clamped *vs.* basal, same mice and treatment.

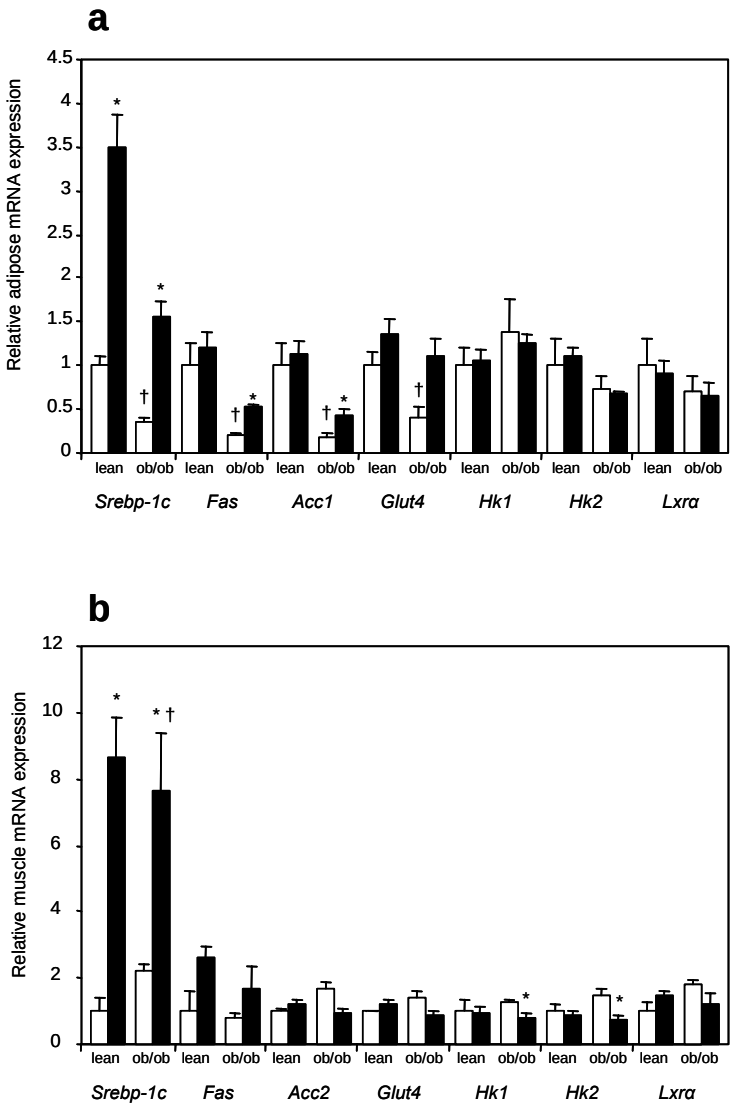


Figure 4.5. White adipose tissue (WAT) and skeletal muscle gene expression in mice fed a diet with (black bars) or without (white bars) the synthetic LXR agonist GW3965 for 10 days. a) WAT mRNA levels; b) skeletal muscle mRNA levels; results normalized to *18S* mRNA levels; data from untreated lean mice defined as 1; n=3 (untreated), n=5 (treated); *, $p<0.05$ treated *vs.* untreated; †, $p<0.05$ *ob/ob vs.* lean untreated. *Srebp-1c*, sterol-regulatory element-binding protein-1c, *Fas*, fatty acid synthetase; *Acc1*, acetyl-CoA carboxylase-1; *Glut4*, glucosetransporter-4; *Hk*, hexokinase; *Lxrα*, liver X receptor α.

Cao *et al.* (8) suggested that LXR activation improves insulin sensitivity. In contrast, we found a slight increase of plasma insulin levels in lean mice upon LXR activation (table 4.2), which might suggest worsening of insulin sensitivity. The best possible technique to determine insulin sensitivity *in vivo* is the hyperinsulinemic-euglycemic clamp. Hence, to determine whether insulin sensitivity was actually affected, we used this technique in conscious, unrestrained mice to mimic the normal, physiological situation. Insulin-mediated glucose uptake did not differ between treated and untreated lean mice (figure 4.4A), indicating that LXR activation did not affect whole body insulin sensitivity. In addition, insulin-mediated suppression of HGP in lean mice was not affected by treatment with the LXR agonist (figure 4.4B), indicative for unaffected hepatic insulin sensitivity. In *ob/ob* mice,

LXR activation resulted in a 50% increase of the GIR required to maintain euglycemia (figure 4.3, A and B). HGP was not significantly affected (figure 4.4A), indicating that the agonist had no measurable effect on hepatic insulin sensitivity. Yet, MCR was slightly increased upon clamping (figure 4.4B), indicating a positive, albeit only marginal, effect of the agonist on peripheral insulin sensitivity. Overall, insulin sensitivity of the treated *ob/ob* mice was still poor, since the effects on GIR, insulin-mediated suppression of HGP, and stimulation of MCR by no means yielded values for these parameters observed in lean C57BL/6J mice.

LXR activation induced a considerable increase in hepatic TG content. Steatosis is usually associated with hepatic insulin resistance, which means that the liver is less sensitive to the suppressive effects of insulin on hepatic glucose and VLDL-TG production. There are multiple endocrine, metabolic, and transcriptionally active factors involved in the interaction between hepatic TG metabolism and hepatic insulin sensitivity. The hierarchy between these different factors in modulating hepatic insulin sensitivity is at present unclear (12). In the present study, however, we report the striking observation that LXR-induced hepatic steatosis lacks the association with insulin resistance, at least with respect to insulin-mediated suppression of HGP. This might be a result of potential counteracting antidiabetic effects of the LXR agonist. In previous reports, it was already noticed that beneficial effects of LXR agonists on carbohydrate metabolism were only present in diabetic animal models (8,9,23). In these animals, insulin resistance associated with hepatic steatosis probably failed to overrule the effects of LXR on glucose homeostasis. Changes in hepatic fatty acid profile upon LXR activation may contribute in this respect (figure 4.1). LXR activation enhances transcription of the gene encoding stearoyl-CoA desaturase-1, *Scd1*, an enzyme involved in the conversion of saturated fatty acid into monounsaturated fatty acids (31). An increase in dietary monounsaturated fatty acids resulted in improved insulin sensitivity in healthy men and women (46), but had no effect on insulin secretion. Therefore, hepatic steatosis in which TG contain relatively more monounsaturated fatty acids, as observed in GW-3965-treated lean mice, might be "healthier" than steatosis with predominantly saturated fatty acids containing TG.

The LXR agonist increased expression of lipogenic genes *Acc1* and *Fas* in WAT of *ob/ob* mice, but not in lean mice (figure 4,5A). A similar pattern was found for *Glut4*. Being aware of the discrepancy between mRNA expression and real enzyme activity and hence fluxes of substrates, it is tempting to speculate that LXR activation leads to increased uptake of glucose by adipocytes in *ob/ob* mice. The observation that GW-3965 treatment did not affect expression of *Acc2*, *Fas*, and *Glut4* in muscle tissue of lean and *ob/ob* mice (figure 4.5B) suggests that LXR activation specifically improved glucose uptake by adipocytes and not of muscle tissue, suggestive for a fat-specific mechanism for improved peripheral insulin sensitivity. After uptake in adipocytes, glucose is metabolized into acetyl-CoA, which serves as substrate for lipogenesis. Juvet *et al.* (18) already reported that LXR agonists increased the lipid content of 3T3-L1 adipocytes in culture. Therefore, in the long turn, LXR activation may lead to a further increase in adipose tissue mass in the already obese *ob/ob* mice. The fact that GW-3965 treatment failed to increase *Acc1*, *Fas*, and *Glut4* expression in WAT of lean mice might be attributable to circulating leptin. Orci *et al.* (32) reported that adenovirus-induced hyperleptinemia led to transformation of adipocytes to fat-oxidizing cells in wild-type Zucker diabetic fatty rats. Moreover, WAT lipogenic gene expression was decreased in these rats. In our study, normal plasma leptin levels in the lean mice were apparently still able to suppress lipogenic gene expression, but the *ob/ob* mice lack this capability. As a result, the WAT lipogenic mRNA levels were increased in *ob/ob* mice but not in lean mice.

This study unequivocally demonstrates that antidiabetic effects of LXR agonists in *ob/ob* mice are exclusively the result of increased glucose uptake by peripheral tissues, *i.e.*, probably by WAT. Moreover, LXR activation had no effect whatsoever on hepatic carbohydrate metabolism in lean or *ob/ob* mice. In adipose tissue, glucose might be more rapidly used as substrate for *de novo* lipogenesis. Because effects of general LXR activation on (peripheral) insulin sensitivity are limited in *ob/ob* mice and coincide with undesirable side effects as hepatic steatosis and hypertriglyceridemia, potential application of LXR modulators in diabetes treatment will require the development of gene- and/or organ-specific compounds.

## Acknowledgements

This work was supported by Grant 903-39-291 from the Netherlands Organisation for Scientific Research. We thank Theo Boer, Klaas Bijsterveld, Maaike H. Oosterveer, and Renze Boverhof for skillful technical assistance.

## References

1. Abu-Elheiga L, Matzuk MM, Abo-Hashema KAH, and Wakil SJ. Continuous fatty acid oxidation and reduced fat storage in mice lacking acetyl-coa carboxylase 2. Science 291: 2613–2616, 2001.
2. Angulo P. Nonalcoholic fatty liver disease. N Engl J Med 346: 1221–1231, 2002.
3. Bandsma RHJ, Grefhorst A, van Dijk TH, van der Sluijs FH, Hammer A, Reijngoud DJ, and Kuipers F. Enhanced glucose cycling and suppressed de novo synthesis of glucose-6-phosphate result in a net unchanged hepatic glucose output in *ob/ob* mice. Diabetologia 47: 2022–2031, 2004.
4. Berge KE, Tian H, Graf GA, Yu L, Grishin NV, Schultz J, Kwiterovich P, Shan B, Barnes R, and Hobbs HH. Accumulation of dietary cholesterol in sitosterolemia caused by mutations in adjacent ABC transporters. Science 290: 1771–1775, 2000.
6. Bligh EG and Dyer WJ. A rapid method of total lipid extraction and purification. Can J Biochem Physiol 37: 911–917, 1959.
7. Böttcher CFJ, van Gent CM, and Pries C. A rapid and sensitive sub-micro-phosphorus determination. Anal Chim Acta 24: 203–204, 1961.
8. Cao G, Liang Y, Broderick CL, Oldham BA, Beyer TP, Schmidt RJ, Zhang Y, Stayrook KR, Suen C, Otto KA, Miller AR, Dai J, Foxworthy P, Gao H, Ryan TP, Jiang XC, Burris TP, Eacho PI, and Etgen GJ. Antidiabetic action of a liver X receptor agonist mediated by inhibition of hepatic gluconeogenesis. J Biol Chem 278: 1131–1136, 2003.
9. Chisholm JW, Hong J, Mills SA, and Lawn RM. The LXR ligand T0901317 induces severe lipogenesis in the db/db diabetic mouse. J Lipid Res 44: 2039–2048, 2003.
10. Costet P, Luo Y, Wang N, and Tall AR. Sterol-dependent transactivation of the ABC1 promoter by the liver X receptor/retinoid X receptor. J Biol Chem 275: 28240–28245, 2000.
11. Davis RA and Hui TY. 2000 George Lyman Duff Memorial Lecture. Atherosclerosis is a liver disease of the heart. Arterioscler Thromb Vasc Biol 21: 887–898, 2001.
12. Den Boer M, Voshol PJ, Kuipers F, Havekes LM, and Romijn JA. Hepatic steatosis: a mediator of the metabolic syndrome. Lessons from animal models. Arterioscler Thromb Vasc Biol 24: 644–649, 2004.
13. Glass CK. Differential recognition of target genes by nuclear receptor monomers, dimers, and heterodimers. Endocr Rev 15: 391–407, 1994.
14. Grefhorst A, Elzinga BM, Voshol PJ, Plösch T, Kok T, Bloks VW, van der Sluijs FH, Havekes LM, Romijn JA, Verkade HJ, and Kuipers F. Stimulation of lipogenesis by pharmacological activation of the liver X receptor leads to production of large, triglyceride-rich very low density lipoprotein particles. J Biol Chem 277: 34182–34190, 2002.
15. Gupta S, Pandak WM, and Hylemon PB. LXRalpha is the dominant regulator of CYP7A1 transcription. Biochem Biophys Res Commun 293: 338–343, 2002.
16. Hellerstein MK, Neese RA, Linfoot P, Christiansen M, Turner S, and Letscher A. Hepatic gluconeogenic fluxes and glycogen turnover during fasting in humans. A stable isotope study. J Clin Invest 100: 1305–1319, 1997.
17. Hohorst HJ. D-Glucose-6-phosphat und D-fructose-6-phosphat. In: Methoden der Enzymatischen Analyse, edited by Bergmeyer HU. Weinheim, Germany: Verlag Chemie, 1970, p. 1200–1204.

18. Juvet LK, Andresen SM, Schuster GU, Dalen KT, Tobin KAR, Hollung K, Haugen F, Jacinto S, Ulven SM, Bamberg K, Gustafsson J, and Nebb HI. On the role of liver X receptors in lipid accumulation in adipocytes. Mol Endocrinol 17: 172–182, 2003.
19. Keppler D and Decker K. Glykogen. Bestimmung mit amyloglucosidase. In: Methden der Enzymatischen Analyse, edited by Bergmeyer HU. Weinheim, Germany: Verlag Chemie, 1970, p. 1089–1094.
20. Kim SY, Kim H, Kim TH, Im SS, Park SK, Lee IK, Kim KS, and Ahn YH. SREBP-1c mediates the insulin-dependent hepatic glucokinase expression. J Biol Chem 279: 30823–30829, 2004.
21. Kuipers F, Havinga R, Bosschieter H, Toorop GP, Hindriks FR, and Vonk RJ. Enterohepatic circulation in the rat. Gastroenterology 88: 403–411, 1985.
22. Kumar KS and Malet PF. Nonalcoholic steatohepatitis. Mayo Clin Proc 75: 733–739, 2000.
23. Laffitte BA, Chao LS, Li J, Walczak R, Hummasti S, Joseph SB, Castrillo A, Wilpitz DC, Mangelsdorf DJ, Collins JL, Saez E, and Tontonoz P. Activation of liver X receptor improves glucose tolerance through coordinate regulation of glucose metabolism in liver and adipose tissue. Proc Natl Acad Sci USA 100: 5419–5424, 2003.
24. Laffitte BA, Repa JJ, Joseph SB, Wilpitz DC, Kast HR, Mangelsdorf DJ, and Tontonoz P. LXRs control lipid-inducible expression of the apolipoprotein E gene in macrophages and adipocytes. Proc Natl Acad Sci USA 98: 507–512, 2001.
25. Lee WN, Byerley LO, Bergner EA, and Edmond J. Mass isotopomer analysis: theoretical and practical considerations. Biol Mass Spectrom 20: 451–458, 1991.
26. Lehmann JM, Kliewer SA, Moore LB, Smith-Oliver TA, Oliver BB, Su JL, Sundseth SS, Winegar DA, Blanchard DE, Spencer TA, and Willson TM. Activation of the nuclear receptor LXR by oxysterols defines a new hormone response pathway. J Biol Chem 272: 3137–3140, 1997.
27. Lepage G and Roy CC. Direct transesterification of all classes of lipids in a one-step reaction. J Lipid Res 27: 114–120, 1986.
28. Lowry OH, Rosenbrough NJ, Farr AL, and Randall RJ. Protein measurement with Folin-phenol reagent. J Biol Chem 193: 265–275, 1951.
29. Magnuson MA, She P, and Shiota M. Gene-altered mice and metabolic flux control. J Biol Chem 278: 32485–32488, 2003.
30. Millatt LJ, Bocher V, Fruchart JC, and Staels B. Liver X receptors and the control of cholesterol homeostasis: potential therapeutic targets for the treatment of atherosclerosis. Biochim Biophys Acta 1631: 107–118, 2003.
31. Miyazaki M and Ntambi JM. Role of stearoyl-coenzyme A desaturase in lipid metabolism. Prostaglandins Leukot Essent Fatty Acids 68: 113–121, 2003.
32. Orci L, Cook WS, Ravazzola M, Wang M, Park BH, Montesano R, and Unger RH. Rapid transformation of white adipocytes into fat-oxidizing machines. Proc Natl Acad Sci USA 101: 2058–2063, 2004.
33. Peet DJ, Turley SD, Ma W, Janowski BA, Lobaccaro JMA, Hammer RE, and Mangelsdorf DJ. Cholesterol and bile acid metabolism are impaired in mice lacking the nuclear oxysterol receptor LXR. Cell 93: 693–704, 1998.
34. Plösch T, Kok T, Bloks VW, Smit MJ, Havinga R, Chimini G, Groen AK, and Kuipers F. Increased hepatobiliary and fecal cholesterol excretion upon activation of the liver X receptor is independent of ABCA1. J Biol Chem 277: 33870–33877, 2002.
35. Repa JJ, Berge KE, Pomajzl C, Richardson JA, Hobbs H, and Mangelsdorf DJ. Regulation of ATP-binding cassette sterol transporters, ABCG5 and ABCG8 by the liver X receptors alpha and beta. J Biol Chem 272: 18793-18800, 2002.
36. Repa JJ, Turley SD, Lobaccaro JMA, Medina J, Li L, Lustig K, Shan B, Heyman RA, Dietschy JM, and Mangelsdorf DJ. Regulation of absorption and ABC1-mediated efflux of cholesterol by RXR heterodimers. Science 289: 1524–1529, 2000.
37. Schultz JR, Tu H, Luk A, Repa JJ, Medina JC, Li L, Schwendner S, Wang S, Thoolen M, Mangelsdorf DJ, Lustig KD, and Shan B. Role of LXR in control of lipogenesis. Genes Dev 14: 2831–2838, 2000.
38. Schwartz K, Lawn RM, and Wade DP. ABC1 gene expression and ApoA-I-mediated cholesterol efflux are regulated by LXR. Biochem Biophys Res Commun 274: 794–802, 2000.
39. Stulnig TM, Steffensen KR, Gao H, Reimers M, Dahlman-Wright K, Schuster GU, and Gustafsson J. Novel roles of liver X receptors exposed by gene expression profiling in liver and adipose tissue. Mol Pharmacol 62: 1299–1305, 2002.
40. Teboul M, Enmark E, Li Q, Wikström AC, Pelto-Huikko M, and Gustafsson J. OR-1, a member of the nuclear superfamily that interacts with the 9-cis-retinoic acid receptor. Proc Natl Acad Sci USA 92: 2096–2100, 1995.
41. Terasaka N, Hiroshima A, Koieyama T, Ubukata N, Morikawa Y, Nakai D, and Inaba T. T-0901317, a synthetic liver X receptor ligand, inhibits development of atherosclerosis in LDL receptor-deficient mice. FEBS Lett 536: 6–11, 2003.
42. Van Dijk TH, Boer TS, Havinga R, Stellaard F, Kuipers F, and Reijngoud DJ. Quantification of hepatic carbohydrate metabolism in conscious mice using serial blood and urine spots. Anal Biochem 322: 1–13, 2003.
43. Van Dijk TH, van der Sluijs FH, Wiegman CH, Baller JFW, Gustafson LA, Burger HJ, Herling AW, Kuipers F, Meijer AJ, and Reijngoud DJ. Acute inhibition of hepatic glucose-6-phosphate does not affect gluconeogenesis but directs gluconeogenic flux toward glycogen in fasted rats. J Biol Chem 276: 25727–25735, 2001.
44. Venkateswaran A, Laffitte BA, Joseph SB, Mak PA, Wilpitz DC, Edwards PA, and Tontonoz P. Control of cellular cholesterol efflux by the nuclear oxysterol receptor LXR. Proc Natl Acad Sci USA 97: 12097–12102, 2000.

45. Venkateswaran A, Repa JJ, Lobaccaro JMA, Bronson A, Mangelsdorf DJ, and Edwards PA. Human white/murine ABC8 mRNA levels are highly induced in lipid-loaded macrophages. A transcriptional role for specific oxysterols. J Biol Chem 275: 14700–14707, 2000.
46. Vessby B, Uusitupa M, Hermansen K, Riccardi G, Rivellese AA, Tapsell LC, Nälsén C, Berglund L, Louheranta A, Rasmussen BM, Calvert GD, Maffetone A, Pedersen E, Gustafsson IB, and Storlien LH. Substituting dietary saturated for monounsaturated fat impairs insulin sensitivity in healthy men and women: the KANWU study. Diabetologia 44: 312–319, 2001.
47. Willy PJ, Umesono K, Ong ES, Evans RM, Heyman RA, and Mangelsdorf DJ. LXR, a nuclear receptor that defines a distinct retinoid response pathway. Genes Dev 9: 1033–1045, 1995.
48. Yu L, York J, von Bergmann K, Lutjohann D, Cohen JC, and Hobbs HH. Stimulation of cholesterol excretion by LXR agonist requires ATP-binding cassette transporters G5 and G8. J Biol Chem 278: 15565–15570, 2003.

# Chapter 5

# Pharmacological inhibition of glucosylceramide synthase enhances insulin sensitivity: a novel therapeutic approach to insulin resistance

J.M. Aerts[1], R. Ottenhoff[1,2], A. Grefhorst[3], A.S. Powlson[4], M. van Eijk[1], R.G. Boot[1],T.H. van Dijk[3], F. Kuipers[3], P.F. Dubbelhuis[1], J. Aten[5], J. Groener[1], A. Strijland[1], A.K. Groen[6], L. Boon[2], M.J. Serlie[7], H.P. Sauerwein[7], T. Wennekes[8],H.S. Overkleeft[8], J.K. Sethi[4], S. O'Rahilly[4], A.J. Meijer[1]

[1]Department of Medical Biochemistry, Academic Medical Center, University of Amsterdam
[2]Macrozyme, Amsterdam
[3]Laboratory of Pediatrics, University Medical Center Groningen
[4]Department of Clinical Biochemistry, University of Cambridge, Cambridge, United Kingdom
[5]Department of Pathology, Academic Medical Center, University of Amsterdam
[6]Department of Experimental Hepatology, Academic Medical Center, University of Amsterdam
[7]Department of Endocrinology and Metabolism, Academic Medical Center, University of Amsterdam
[8]Leiden Institute of Chemistry, Leiden University

**Submitted**

## Abstract

A growing body of evidence implicates ceramide and/or its glycosphingolipid metabolites in the pathogenesis of insulin resistance. We have developed a highly specific small molecule inhibitor of glucosylceramide synthase, an enzyme which catalyses a necessary step in the conversion of ceramide to glycosphingolipids. In cultured adipocytes the iminosugar derivative N-(5'-adamantane-1'-ylmethoxy)-pentyl-1-deoxynojirimycin (AMP-DNM), enhanced insulin-stimulated glucose uptake and reversed TNF-alpha induced abnormalities in insulin signal transduction. When administered to mice, AMP-DNM significantly reduced glycosphingolipid but not ceramide concentrations in various tissues. Treatment of *ob/ob* mice with AMP-DNM for 7 days normalised their elevated tissue glucosylceramide levels, markedly lowered circulating glucose levels, improved oral glucose tolerance, improved insulin sensitivity in muscle and liver, reduced hepatic fat deposition and increased cell surface expression of GLUT4 on adipocytes. These findings provide evidence that metabolites of ceramide, rather than ceramide itself, may be involved in mediating the link between obesity and insulin resistance and that interference with glycosphingolipid biosynthesis might present a novel approach to the therapy of states of impaired insulin action such as type 2 diabetes.

## Introduction

Impaired responsiveness to insulin is reflected by increased glucose synthesis by the liver and reduced glucose uptake by skeletal muscle and adipose tissue (1-3). In insulin-resistant individuals the translocation of the glucose transporter GLUT4 to the plasma membrane of myocytes and adipocytes is impaired. Obesity is strongly associated with insulin resistance but the underlying pathogenic mechanism is still an enigma. The strong correlation between insulin resistance and intramyocellular lipid levels suggests that excessive exposure to lipids or their metabolites, so called lipotoxicity, may play a crucial role (1-7). The rapid induction of insulin resistance in rodents by infusions with palmitate, and in cultured cells by supplying this fatty acid, has directed attention to the sphingolipid ceramide as a potential mediator of insulin resistance (1,4-7). Palmitate is a critical precursor in the synthesis of ceramide and its enhanced supply inevitably increases sphingolipid formation in tissues (8,9). Increased ceramide concentrations (two-fold) were indeed recently reported for skeletal muscle from obese insulin-resistant individuals4. The well-established induction of insulin resistance by the cytokine TNFα may also be attributed to its ability to promote sphingolipid biosynthesis, as has been demonstrated at both mRNA and cellular lipid levels (10-12). In addition, investigations with cultured cells have linked excessive ceramide concentrations to disturbed insulin signalling (6,13-15). Manipulation of ceramide levels in cultured cells was consistently found to affect the insulin signalling pathway downstream at the level of AKT, but conflicting reports exist regarding effects on the insulin receptor, IRS-1 and associated PI 3-kinase activity (6,13-15). Surprisingly, in most studies it has been overlooked that metabolites of ceramide, such as glycosphingolipids, might also play an important role in the development of insulin resistance. Glycosphingolipids are found in specific (detergent-resistant) membrane microdomains in close physical proximity to the insulin receptor, as well as other tyrosine kinase receptors such as the epidermal growth factor (EGF) receptor (5). A regulatory role for glycosphingolipids in hormone sensitivity was first proposed by Bremer and coworkers who showed that EGF-mediated signalling is inhibited by GM3, the simplest ganglioside (16). More recently, Tagami *et al*. reported that addition of GM3 to cultured adipocytes also suppresses phosphorylation of the insulin receptor and its down-stream substrate IRS-1, resulting in reduced glucose uptake (17).

Other observations further substantiate the role of the gangliosides GM3 in responsiveness to insulin. Mutant mice lacking GM3 show an enhanced phosphorylation of the skeletal muscle insulin receptor after ligand binding and are protected from high-fat diet induced insulin resistance (18). Conversely, GM3 levels are elevated in the muscle of certain obese, insulin resistant mouse and rat models (17). Inokuchi and coworkers employed the ceramide-analogue 1-phenyl-2-decanoylamino-3-morpholinopropanol (PDMP), an inhibitor of glucosylceramide synthase, to reduce glycosphingolipids in cultured adipocytes. They noted that PDMP counteracted the inhibitory effects of TNF-alpha on IR and IRS-1 phosphorylation (17). Very recently it was reported by the same researchers that high GM3 levels diminished IR accumulation in detergent-resistant membrane microdomains and insulin-dependent IR internalization (19). Again glycosphingolipid depletion by incubation of cells with PDMP prevented these abnormalities. However, the observations made with PDMP are difficult to interpret since this compound not only inhibits conversion of ceramide to glucosylceramide but also its transacylation to 1-O-acylceramide and consequently increases cellular levels of ceramide (20). Based on the present information it may be therefore conceived that not ceramide itself but rather its glycosphingolipid metabolites are instrumental in the development of insulin resistance. To discriminate between these possibilities we examined in obese mice the effect of reduction of glycosphingolipids by N-(5'-adamantane-1'-yl-methoxy)-pentyl-1-deoxynojirimycin (AMP-DNM), a specific inhibitor

of glucosylceramide synthase (21). Here we show that pharmacological lowering of glycosphingolipids, without significant reduction of ceramide, dramatically reverses insulin resistance in *in vitro* and *in vivo* models.

## Materials and methods

### *Mice*

Experimental procedures were all approved by the appropriate Ethics Committee for Animal Experiments. C57Bl/6J and *ob/ob* mice (C57Bl/6J background) were obtained from Harlan (Horst, The Netherlands) and housed in a light- and temperature controlled facility. The animals were fed a commercially available lab chow (RMH-B, Hope Farms BV, Woerden, The Netherlands) containing about 6% fat and ~0.01% cholesterol (w/w). The iminosugar AMP-DNM was mixed in the food for most experiments. In indicated experiments animals were used to which the compound had been administered by oral gavage two times daily.

### *Plasma and tissue sampling*

Animals were sacrificed under isoflurane anaesthesia. A large blood sample was collected by cardiac puncture. Tissues were quickly removed and frozen for further analysis.

### *Cells*

Human adipocytes and appropriate cell culture medium were obtained from Zen-Bio Inc. (Chapel Hill, USA). 3T3-L1 pre-adipocytes were obtained from the ATCC (Manassas, USA). They were propagated and differentiated as previously described (22). Primary adipocytes were prepared from epididymal fat pads as described earlier (23).

### *Iminosugar*

AMP-DNM (N-(5'-adamantane-1'-yl-methoxy)-pentyl-1-deoxynojirimycin) was synthesized as described previously (24). Plasma levels of AMP-DNM were determined by mass spectrometry following high pressure liquid chromatography (Xendo, Groningen, The Netherlands).

### *Analysis of lipids and measurement of enzyme activities*

Lipids were extracted according to Folch *et al* (25). Ceramide and glucosylceramide collected from the chloroform phase were determined by HPLC analysis of orthophtaldehyde-conjugated lipids according to a procedure described previously with some modifications (26). The chloroform layer was thoroughly dried and deacylation of lipids was performed in 0.5 ml 0.1 M NaOH in methanol in a microwave oven (CEM microwave Solids/Moisture System SAM-155). After deacylation 0.5 ml methanol and 2 ml chloroform were added and phase separation was performed. The chloroform layer was dried under N2 and the deacylated lipids were taken up in 250 µl methanol. Deacylated glycolipids were derivatised on line for 30 min with Ophtalaldehyde. Analysis was performed using an HPLC system (Waters Associates, Milford, MA) and a Hypersil BDS C18 3µ, 150 x 4.6 mm reverse phase column (Alltech). Chromotographic profiles were analysed using Waters Millenium software. All samples were run in duplicate and in every run a reference sample was included.

Ganglioside composition was determined by HPTLC analysis of the acidic glycolipid fraction obtained after Folch extraction using chloroform/methanol/water (65:25:4) as solvent. Gangliosides were visualized by spraying resorcinol reagent followed by heating at 105 °C for 10 min and quantified by densitometry. Total sphingolipids biosynthesis by cultured cells was quantified by exposing cells to [$^3$H]serine or [$^3$H]palmitate as described previously (9).

Palmitate was administered as 1:1 complex with bovine serum albumin. Activity of glucosylceramide synthase and glucocerebrosidase in living cells was determined using as substrates fluorescently labelled NBD-ceramide and NBD-glucosylceramide, respectively (27). Briefly, NBD-ceramide or NBD-glucosylceramide was complexed to fatty acid-free bovine serum albumin in a molar ratio of 1:1. Cells were incubated with 150 μM lipid and harvested at different time points. Lipids were extracted, separated by thin layer chromatography and NBD-ceramide and NBD-glucosylceramide were quantified (27).

IC50 values of AMP-DNM for various enzyme activities were determined by exposing cells or enzyme preparations to an appropriate range of iminosugar concentrations. IC50 values for glucosylceramide synthase and glucocerebrosidase activities were measured using living cells with NBD-ceramide and NBD-glucosylceramide as respective substrates. Lactase, maltase and sucrase were determined with homogenates of freshly isolated rat intestine using assay conditions described earlier (28). Debranching enzyme (alpha-1,6-glucosidase) was measured with an erythrocyte preparation as enzyme source as described previously (29).

*2-[$^3$H]deoxyglucose uptake*

Cultured adipocytes were deprived of serum for 1 h prior to exposure to 0.1 mM 2-[$^3$H]deoxyglucose (0.4 mCi/ml). 2-[$^3$H]deoxyglucose uptake measurements were made in triplicate under conditions when hexose uptake was linear (29). Non-specific absorption of 2-[$^3$H]deoxyglucose, as determined by cell-associated counts in the presence of 5 μM cytochalasin B, was always less than 10% of the total uptake.

*Analysis of insulin signalling in 3T3L1 adipocytes*

Fully differentiated 3T3-L1 adipocytes were serum deprived, by incubation in DMEM + 1% BSA, and simultaneously pre-treated with or without AMP-DNM (50 μM) and/or TNF alpha (0.6 nM) for 24hrs. Following insulin stimulation (5 min with 100 nM) cells were washed with ice-cold PBS, and lysed in modified RIPA buffer (50 mM Tris-HCL pH 7.4, 1% NP-40, 0.25% sodium deoxycholate, 150 mM sodium chloride, 1mM EDTA, 50 mM β-glycerol-2-phosphate, 5 μM AEBSF, 1 μg/ml aprotinin, 1 μg/ml leupeptin, 1 μg/ml pepstatin A, 1 mM sodium pervanadate, 1 mM sodium fluoride, 50 nM okadaic acid). Cell lysates were clarified by centrifugation (13,000 rpm for 10 min) and the supernatant collected. Protein concentrations were determined using the BioRad DC protein assay kit. Equal amounts of whole cell lysates were separated by SDS-PAGE and immunoblots performed in parallel using anti-phosphotyrosine antibody (4G10), anti-IRS-1- Upstate Biotech. US), anti-IR (K. Siddle), anti-pSer473 AKT, Anti-AKT (Cell Signalling Technology Inc., US), appropriate HRP-linked secondary Ab (DAKO, US) and an enzymelinked chemiluminescent kit (Amersham, UK).

*Measurement of whole-body insulin sensitivity*

Whole-body insulin sensitivity of *ob/ob* mice was determined using hyperinsulinemic euglycaemic clamps as described previously (31,32). Male *ob/ob* mice were treated for 7 days with a diet with or without MZ21 (25 mg/kg BW). At the start of the diet, mice were equipped with a permanent catheter in the right atrium via the jugular vein. Nine hours before the start of the clamp experiment, food was withdrawn but mice still had free access to water. Mice were kept in metabolic cages during the experiment, allowing frequent collection of bloodspots from the tail under conscious and unrestrained conditions. The mice were infused for six hours with two solutions. The first infusate contained 220 mU/ml insulin (Actrapid, Novo Nordisk., Bagsvaerd, Denmark), 40 μg/ml somatostatin (UCB, Breda, The Netherlands), 10 mg/ml BSA (Sigma, St. Louis, MO). To prevent high infusion rates leading

to higher morbidity, this solution contained, when given to treated mice, 100 mg/ml glucose, from which 3% was [U-$^{13}$C]-glucose (99% $^{13}$C APE) (Cambridge Isotope Laboratories Inc., Andover, MA). The solution was infused at a rate of 0.3 ml/h. The second infusate was a 30% (treated mice) or 15% (untreated mice) glucose solution, from which 3% was [U-$^{13}$C]-glucose. Its infusion rate was adjusted according to measured blood glucose levels to maintain euglycemic conditions. Blood glucose levels were measured with a Lifescan EuroFlash glucose meter (Lifescan Benelux, Beerse, Belgium) in a small tail blood sample that was drawn every 15 minutes. Just before the start of the experiment, a small blood sample was obtained by tail bleeding. Blood samples were centrifuged and the obtained plasma was stored at -20°C until analysed. Every hour, a bloodspot was obtained by tail bleeding. After the clamp, animals were sacrificed by cardiac puncture under anaesthesia. Plasma was obtained by centrifugation. The liver was removed, weighed and frozen in liquid $N_2$ until further analysis.

*Calculation of endogenous glucose production and metabolic clearance rate under clamped conditions*

Analytical procedures for extraction of glucose from bloodspots from filterpaper, derivatization glucose to its aldonitril pentaacetate derivative and GC-MS were essential according to Van Dijk *et al.* (31,32). The measured fractional isotopomer distribution by GCMS ($m_0$-$m_6$) was corrected for the fractional distribution due to natural abundance of $^{13}$C, by multiple linear regression to obtain the excess mole fraction of mass isotopomers $M_0$-$M_6$ due to isotope dilution of infused labelled glucose. Two solutions with [U-$^{13}$C]-glucose were infused with different rates. Therefore, the total rate of appearance of glucose into plasma (Ra(glc;whole body)) was calculated as follows:

$$Ra(glc;whole\ body) = (M_6(glc)g_{lucose} \times infusion(glc;M_6)_{glucose} + M_6(glc)_{insulin} \times infusion(glc;M_6)_{insulin})/M_6(glc)_{blood}$$

in which $M_6(glc)_{glucose}$ and $M_6(glc)_{insulin}$ are the excess mole fractions of infused [U-$^{13}$C]-glucose in the glucose and insulin solution, respectively, and $infusion(glc;M_6)_{glucose}$ and $infusion(glc;M_6)_{insulin}$ are the infusion rates of [U-$^{13}$C]-glucose of the glucose and insulin solution, respectively. The rate of endogenous plasma glucose (Ra(glc;endo)) was calculated as follows:

$$Ra(glc;endo) = Ra(glc;whole\ body) - infusion(glc;M_6)_{glucose} - infusion(glc;M_6)_{insulin}.$$

The metabolic clearance rate of glucose (MCR) was calculated according to:

$$MCR = Ra(glc;whole\ body)/[glc],$$

where [glc] is the blood glucose concentration (mM).

*Glucose tolerance test*

The tolerance test was performed in fasted mice (13–15 h) with oral gavage of glucose (2 g of glucose per kg of body weight). Blood glucose values were measured immediately before and 10, 20, 30, 60, 90 and 120 min after glucose injection. AUCs (areas under the curve) were determined for individual mice.

*Cell surface expression of GM3 and GLUT4*

Flow cytometry using monoclonal anti-GM3 antibody (Seikagu, Japan) or monoclonal anti-GLUT4 antibody (Abcam, USA) and FITC-or Alexa 488-conjugated rabbit anti-mouse secondary antibody were employed according to the procedure described earlier (17).

*Statistical testing*

Values presented in figures represent mean +/- SEM. Statistical analysis of two groups was assessed by Student's t-test (one-tailed) or ANOVA for repeated measurement (clamp experiment). Level of significance was set at $p < 0.05$.

## Results

*Modulation of glycosphingolipids with AMP-DNM*

N- (5'-adamantane-1'-yl-methoxy)-pentyl-1-deoxynojirimycin (AMP-DNM) is a very potent inhibitor of glucosylceramide synthase activity in all cell types tested. As measured using fluorescently labelled C6-NBD-ceramide as substrate, exposure of cells to AMP-DNM results in swift and marked inhibition of synthesis of glucosylceramide. As determined in this manner, IC50 values in cultured macrophages, myoblasts, melanoma cells, HepG2 cells and skin fibroblasts are about 150, 220, 200, 150 and 220 nM, respectively. Cellular levels of glucosylceramide and its metabolites lactosylceramide and gangliosides are gradually reduced by AMP-DNM, reaching equilibrium within 36 hours. Ceramide levels however remain constant upon exposure to AMP-DNM. Figure 5.1 shows an illustrative response in lipid levels of cultured macrophages and melanoma cells after exposure to 200 nM AMP-DNM.

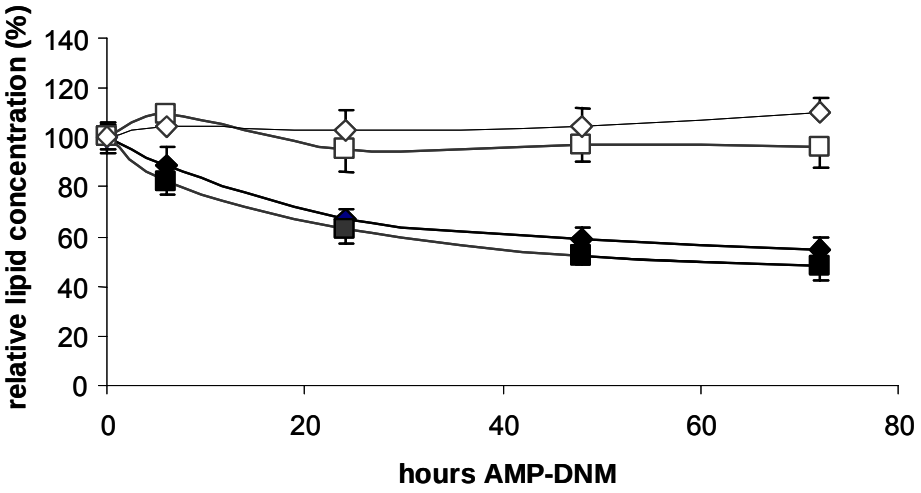


Figure 5.1. Effect of AMP-DNM on ceramide and glucosylceramide concentrations in cultured cells. Macrophages derived from peripheral blood monocytes and melanoma cells were cultured in the absence or presence of 250 nM AMP-DNM. At different time points, cells were harvested and ceramide and glucosylceramide content were determined. Lipid levels are expressed as percentage of those of cells not exposed to AMP-DNM. Macrophages: glucosylceramide (closed squares), ceramide (open squares); melanoma cells: glucosylceramide (closed diamonds), ceramide (open diamonds). Error bars indicate standard deviation.

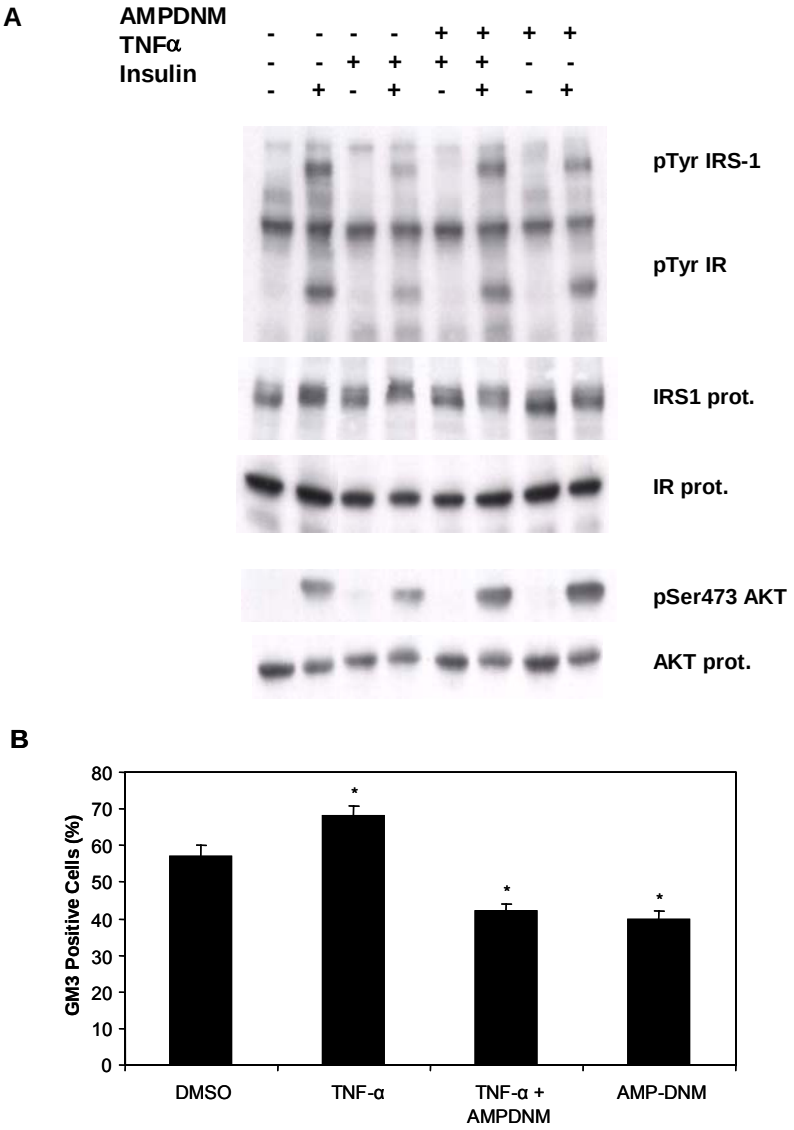


Figure 5.2. AMP-DNM reverses TNF-alpha induced insulin resistance (A) and surface expression of GM3 (B) in 3T3-L1 adipocytes. Serum starved 3T3-L1 adipocytes were treated with either vehicle control, AMP-DNM (50 μM) and/or TNF-alpha (0.6 nM) for 24hrs prior to stimulation with or without insulin (100nM for 5 min.) (A) Immunoblots of whole cell lysates were performed in parallel as described in materials and methods. Representative blots are shown from one of 3 independent experiments. (B) Cell surface expression of GM3 was determined on basal adipocytes (not stimulated with insulin) by FACS analysis. Values represent mean (± SE) % of viable cells that stained positive for GM3. * indicates statistical significance ($p<0.05$) and was observed in four independent experiments.

Table 5.1. 2-[$^3$H]deoxyglucose uptake by cultured human adipocytes in the presence and absence of insulin.

| | Uptake in cpm/μg protein | | |
|---|---|---|---|
| | $10^{-7}$ M insulin | $10^{-8}$ M insulin | No insulin |
| 0 μM AMP-DNM | 27.6 ± 3.0 | 23.4 ± 2.9 | 24.3 ± 2.8 |
| 10 μM AMP-DNM | 50.7 ± 4.5 | 46.4 ± 6.8 | 29.7 ± 3.1 |

*Reduction of glycosphingolipids in normal mice by AMP-DNM*

Normal, six week old C57Bl/6J mice (n=4) were treated with or without AMP-DNM at a dose of 25 mg/kg body weight/day for 14 days. The plasma concentration of AMP-DNM was 108 ± 6 nM and remained stable during the period of treatment. Exposure to AMP-DNM was well tolerated by the animals as reflected by unchanged body weight gain. After two weeks treatment, liver ceramide and glucosylceramide concentrations were analysed by HPLC following microwave-mediated deacylation. The hepatic ceramide content of C57Bl/6J mice was not changed by the AMP-DNM diet, being 0.24 ± 0.02 and 0.26 ± 0.05 μmol/liver of treated and untreated animals. In sharp contrast, liver glucosylceramide (85 ± 15 nmol/liver) was reduced by 41 ± 5 % by the AMP-DNM diet. Analysis by HPTLC showed that the ganglioside GM2 was concomitantly reduced by ~30%. Similar effects on sphingolipids were observed in muscle tissue of treated animals (not shown). The pronounced reduction by AMP-DNM of glycosphingolipids levels in mouse tissues without concomitant change in ceramide concentrations is comparable to the observed effect of the iminosugar in cultured cells.

*Effect of AMP-DNM on insulin sensitivity of cultured adipocytes*

In order to study the effect of AMP-DNM on insulin sensitivity in normal cells, we examined basal and insulin-stimulated glucose uptake in cultured human adipocytes. Basal uptake of 2-[$^{3}$H]deoxyglucose glucose was not significantly affected by AMP-DNM treatment. However uptake of 2-[$^{3}$H]deoxyglucose in the presence of $10^{-7}$ M insulin was increased by 84 ± 12 % after 16 h exposure to 10 μM AMP-DNM (table 5.1). Glucosylceramide levels in the treated cells were reduced to 63 ± 8 % of basal but ceramide levels were unaffected (not shown). In order to study the effects of AMP-DNM on insulin signalling in an insulin-resistant cellular model we examined 3T3-L1 adipocytes exposed to TNF-alpha. As expected TNF-alpha impaired insulin receptor autophosphorylation, IRS-1 tyrosine phosphorylation and the serine phosphorylation of AKT at residue 473. All of these abnormalities were significantly ameliorated by the simultaneous exposure to AMP-DNM (figure 5.2a). TNF-alpha increased cell surface levels of GM3 gangliosides and this was blocked by AMP-DNM (figure 5.2b).

*Ceramide and glycosphingolipids in ob/ob mice before and after treatment with AMP-DNM*

In *ob/ob* mice, the hepatic concentration of glucosylceramide was higher (115 ± 16 nmol/liver) compared to wild types animals (85 ± 15 nmol/liver; p=0.045). Increased concentrations of gangliosides were also noted upon HPTLC separation of lipids and charring densitometry. The ganglioside GM2 content was 36 ± 12 % increased, a finding consistent with previous studies in other tissues of *ob/ob* mice (17). The ceramide content of liver of *ob/ob* mice was also higher than that in wild type animals (3.15 ± 0.72 and 0.24 ± 0.02 μmol/liver, respectively). In muscle tissue of *ob/ob* mice glucosylceramide was again elevated compared to wild type mice (2.5 ± 0.5 *vs.* 1.5 ± 0.4 nmol/mg protein, p=0.031), however ceramide concentrations were similar (1.2 ± 0.4 and 1.4 ± 0.6 nmol/mg protein respectively, n.s.).

Two weeks treatment with AMP-DNM did not result in any significant changes in ceramide levels in muscle or liver from *ob/ob* mice (figure 5.3). In sharp contrast, glucosylceramide content of muscle and liver from *ob/ob* mice decreased by 45 ± 23 % and 45 ± 11% with AMP-DNM, reaching values similar to those in wild-type animals (figure 5.3).

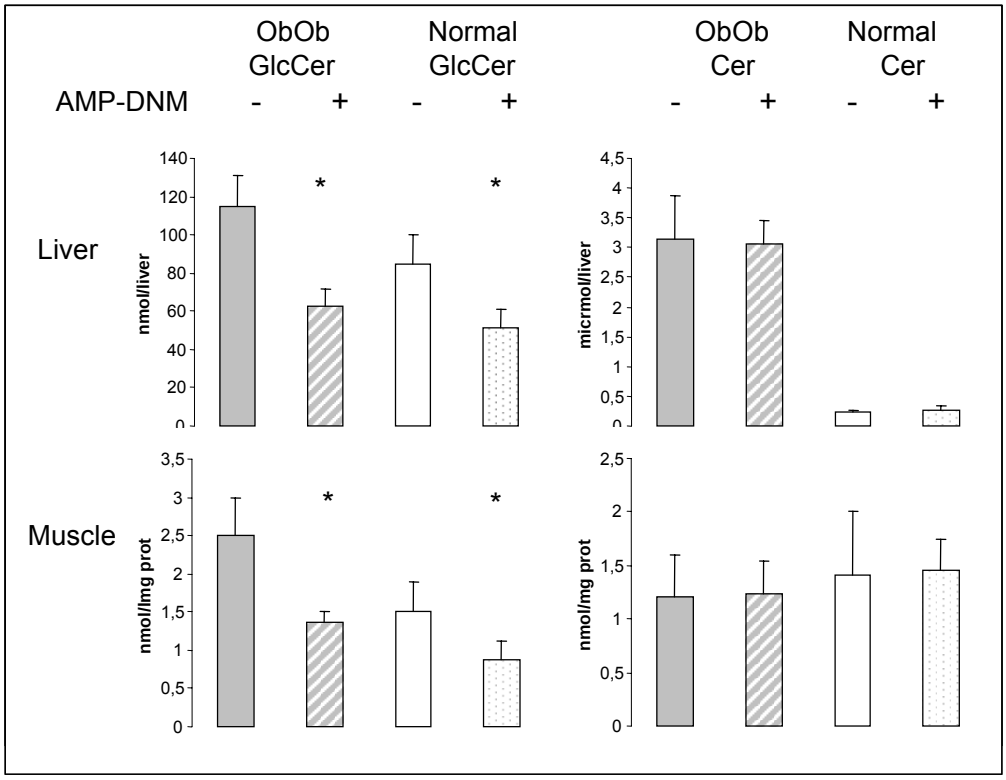


Figure 5.3. Ceramide and glucosylceramide levels in liver and muscle of normal and ob/ob mice treated with AMP-DNM. Animals were fed for two weeks with or without 25 mg AMP-DNM/kg. Liver (upper panel) and muscle tissue (lower panel) was collected and analysed on ceramide and glucosylceramide content. *, $P < 0.05$ by Student's t test.

*Beneficial effects of AMP-DNM on metabolism in ob/ob mice*

Prominent effects of AMP-DNM on glucose homeostasis were noted when six week old C57Bl/6J mice (n=4) were treated at a dose of 25 mg/kg body weight/day. AMP-DNM had no significant effect on body weight or food intake (figure 5.4a). Concomitantly, *ob/ob* mice treated with AMP-DNM showed a dramatic reduction in blood glucose levels (p=0.008) (figure 5.4b). Hyperinsulinemic euglycemic clamp studies demonstrated that this was associated with a marked improvement in whole body insulin sensitivity (p=0.003) (figure 5.4c). This was due in part to a significant (~26%) decrease in hepatic glucose production (Ra) (p=0.035) as well as a significant (~29%) increase in glucose disposal (Rd) (p=0.0028) (figure 5.4d).

The beneficial effect of AMP-DNM was also revealed by glucose tolerance tests. Animals fed with 25 mg/kg AMP-DNM for 8 days showed a better response to oral glucose administration as compared to untreated mice. The AUCs of blood glucose levels were significantly lower (p=0.023) in AMP-DNM treated mice (see insert figure 5.5).

Hepatic fat accumulation was apparent in untreated *ob/ob* mice and this was visibly reduced by AMP-DNM therapy. This was confirmed by direct measurement of triglyceride levels in livers of AMP-DNM fed *ob/ob* mice which significantly decreased from 107 ± 13 to 80 ± 11 nmol/mg liver (p = 0.035).

Adipocytes were isolated from epididymal fat pads of *ob/ob* mice treated with or without 25 mg AMP-DNM/kg for 2 weeks. GLUT 4 cell surface expression was examined using FACS analysis. Cell surface levels of GLUT4 protein were on average 3.2 fold increased in adipocytes from AMP-DNM treated mice as compared to those of controls (not shown).

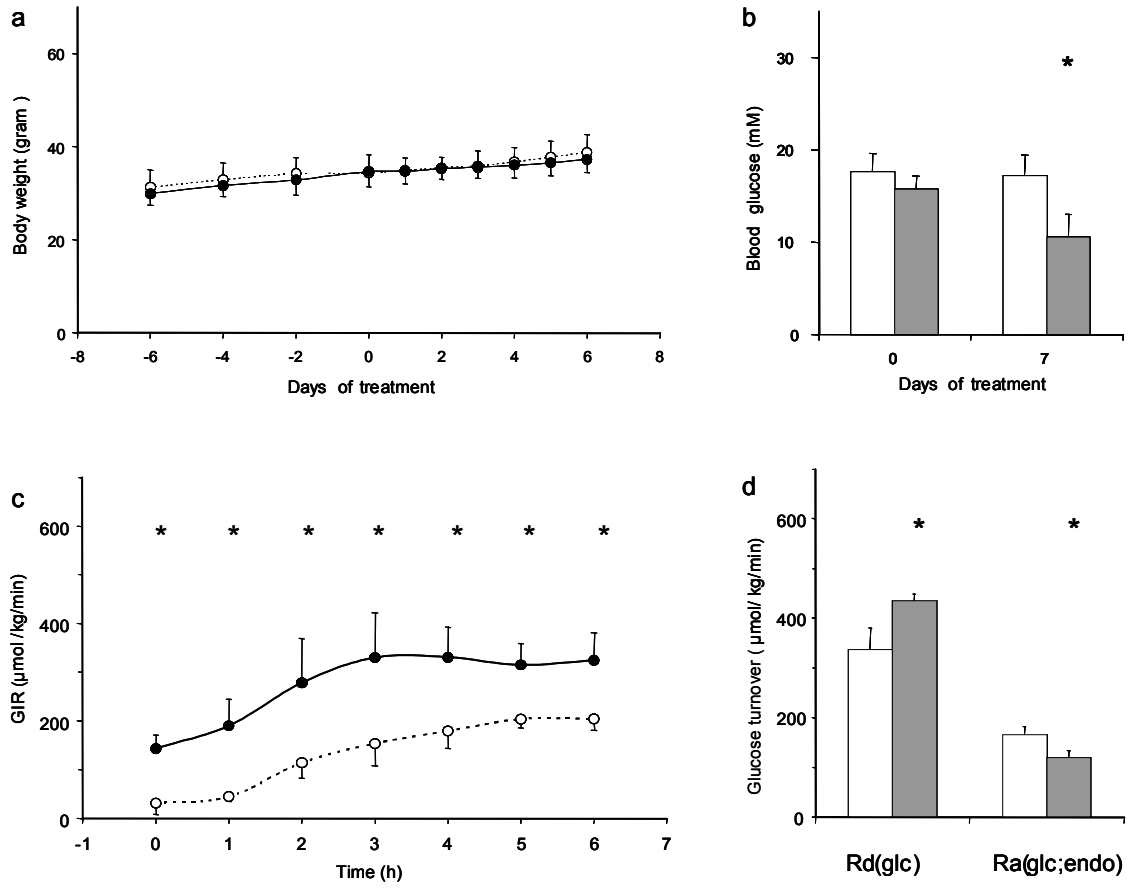


Figure 5.4. Beneficial effects of iminosugar feeding on glucose metabolism in *ob/ob* mice. *Ob/ob* mice were fed either with control chow (open circles and white bars) or with chow providing a dose of 25 mg AMP-DNM per kg bodyweight/day (closed circles and grey bars). Body weight (panel a), blood glucose level (panel b), were determined at indicated time points. During the clamp, glucose infusion rate (GIR) was monitored (panel c), the rate of glucose disposal (Rd(glc) and the rate of endogenous hepatic glucose production (Ra(glc;endo)) were calculated (panel d). Data presented are means +/- SD. Significant differences between both groups (*) are indicated. Statistical significance of differences were determined using Student's t test, except in calculations over time where ANOVA with repeated measurements was used; $p < 0.05$ was considered as statistically significant.

## Discussion

In these studies we have demonstrated that AMP-DNM, a potent inhibitor of glucosylceramide synthase, enhances insulin stimulated glucose uptake in normal adipocytes studies *ex vivo* and reverses the insulin signalling defect produced by exposure of adipocytes to TNF-alpha. More importantly, AMP-DNM has dramatic beneficial effects on the insulin resistance and hyperglycaemia seen in *ob/ob* mice, via a mechanism that does not require a reduction in food intake or loss of body weight.

A key question that arises relates to the specificity of AMP-DNM as an inhibitor of glucosylceramide synthase. At a concentration <1 µM, AMP-DNM causes no significant inhibition of activity of the lysosomal enzymes glucocerebrosidase and acid α-glucosidase or the ER trimming α-glucosidases. The cytosolic debranching enzyme and glycogen synthase are also unaffected at such concentrations (data not shown). AMP-DNM was originally developed as an inhibitor of a non-lysosomal glucosylceramidase (24). The molecular identity of the latter enzyme and its physiological function has still not been established. The enzyme

activity is already inhibited by AMP-DNM in the picomolar range (IC50 ~1 nM). Cultured adipocytes or *ob/ob* mice exposed to low nanomolar concentrations of AMP-DNM that completely inhibit the non-lysosomal glucosylceramidase activity but do not effectively reduce glucosylceramide synthase activity, do not show improved responsiveness to insulin. It therefore can be concluded that inhibition of the non-lysosomal glucosylceramidase by AMP-DNM is not sufficient, and possibly even not needed, to increase insulin sensitivity. Iminosugars can also significantly inhibit intestinal glycosidases, thus reducing the rate of digestion and absorption of oligo- and polysaccharides. This may additionally contribute to the beneficial effects of AMP-DNM on glucose homeostasis in *ob/ob* mice. However, AMP-DNM is only a low affinity inhibitor of sucrase and maltase, with of IC50 values for these enzymes of 4.5 μM and 18 μM, respectively (personal observations). Therefore it appears highly unlikely that at the dose used AMP-DNM would have significant impact on intestinal glycosidases. Finally, it is unlikely that AMP-DNM had significant non-specific toxic effects as food intake remained unchanged in treated *ob/ob* mice and no abnormalities were noted upon histological examination of liver, kidney and brain of *ob/ob* or wild-type mice fed for up to 4 weeks with 25 mg/kg body weight/day AMP-DNM. Only modest (30-50%) increases of liver glycogen were observed during the first week of feeding of *ob/ob* mice with AMP-DNM diet. Subsequently, glycogen levels remained stable in the normal range of C57Bl/6J animals, suggesting that there was no marked inhibition of debranching enzyme.

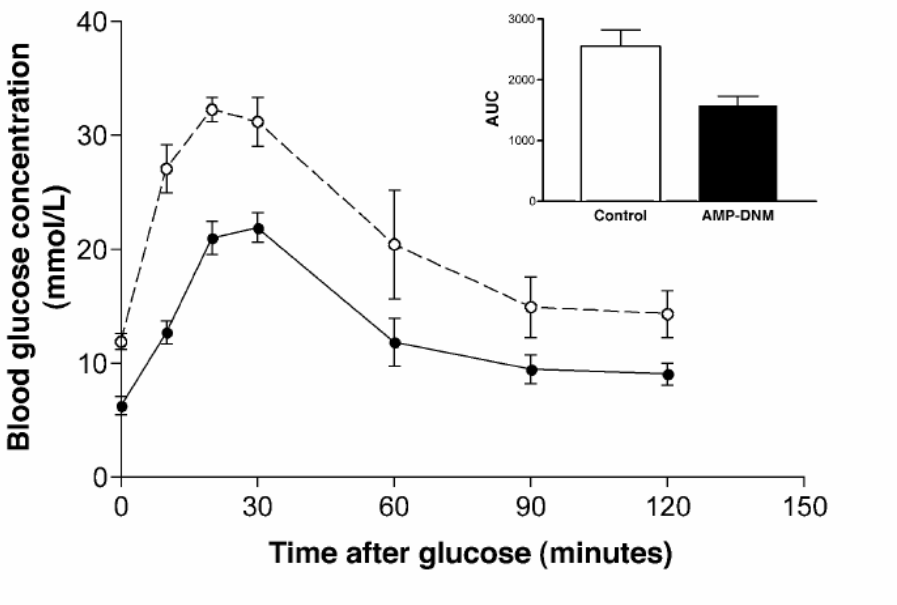


Figure 5.5. Improved glucose tolerance in AMP-DNM treated ob/ob mice. Glucose tolerance tests of male *ob/ob* mice, 8 weeks old, treated for 8 days with or without 25 mg AMP-DNM/ kg (*n* =6 each) administered by gavage two times daily. Animals were starved for 16 h prior to test. Values are expressed +/- SD. *P* =0.023 by ANOVA.

Our studies with this pharmacological inhibitor may help to clarify the relationship between obesity, ceramides and insulin resistance and suggest a molecular mechanism for "lipotoxic" insulin resistance. Firstly, we confirmed previous observations that liver tissue from insulin resistant *ob/ob* mice had elevated levels of ceramide, glucosylceramide and gangliosides and demonstrated that muscle tissue from these animals had increased glucosylceramide but normal ceramide concentrations. We then demonstrated that AMP-DNM had dramatic beneficial effects on insulin sensitivity without any change in ceramide levels but with a marked reduction in tissue levels of glucosylceramide. These observations strongly suggest that it is unlikely to be the elevation in ceramide itself that mediates the insulin resistance seen in *ob/ob* mice, but that downstream metabolites of ceramide are more likely to be critically involved. This explanation is consistent with recent observations by other researchers implicating GM3 gangliosides in the pathogenesis of insulin resistance.

Our studies in cultured adipocytes provide some potential clues to the mechanism whereby AMP-DNM enhances insulin sensitivity. Thus, in normal human adipocytes, AMP-DNM has no effect in basal glucose uptake but significantly enhances insulin stimulated glucose uptake, suggesting an effect in insulin signalling. This is supported by the studies of TNF-alpha treated murine adipocytes in which AMP-DNM reversed the adverse effects of TNF-alpha on several steps in the insulin signal transduction pathway. This effect was demonstrable at a proximal step, *i.e.* insulin receptor autophosphorylation, of interest because of the previously reported localisation of GM3 gangliosides in plasma membrane subdomains containing the insulin receptor and the effect of genetic depletion of GM3 on insulin receptor autophosphorylation.

The pharmacological manipulation of the cellular levels of ceramide and its metabolites seems, at first sight, to be an intrinsically problematic therapeutic avenue since these sphingolipids are implicated in many crucial cellular processes. Ceramide analogues like PDMP that inhibit glycosphingolipid biosynthesis and concomitantly cause an increase in ceramide are known to exert cytotoxic effects. However, our finding that pharmacological manipulation of glycosphingolipid levels with AMP-DNM reverses insulin resistance without causing changes in ceramide concentrations may hold promise for the treatment of insulin resistance. One hydrophobic iminosugar, N-butyldeoxynojirimycin is already registered for the treatment of type 1 Gaucher patients suffering from a deficiency in lysosomal degradation of glucosylceramide (33). Although this compound inhibits glucosylceramide synthase, compared to AMP-DNM, it is neither a potent nor a selective inhibitor. The IC50 value of N-butyldeoxynojirimycin for glucosylceramide formation is close to 100 μM when measured with a fluorescent ceramide-analogue in living cells (21). The relatively poor bioavailability of the compound in mice requires oral administration of large quantities (>5 g/kg body weight/day) to reach a plasma concentration consistent with the IC50 value. At such high dosages intestinal glycosidases are likely to be inhibited given the measured IC50 values of 0.5 μM and 9 μM for sucrase and maltase, respectively. Intestinal complaints are a relatively common side-effects reported by Gaucher patients receiving N-butyldeoxynojirimycin. Interestingly, a more hydrophilic iminosugar, N-hydroxyethyldeoxynojirimycin (Miglitol), is already registered as an oral agent for treating diabetes (34). The ancient use of iminosugar-rich mulberry leaves in the Far East to control hyperglycaemia stimulated the development of this drug (35). The presumed mode of action of Miglitol is inhibition of intestinal glycosidase activities, thereby buffering monosaccharide assimilation (34). We have established that Miglitol does not inhibit glucosylceramide synthase in intact cells or homogenates (personal observations). However, since Miglitol is well absorbed it is possible that some proportion of the compound is metabolized to some structure that is capable of inhibiting glucosylceramide synthase.

In summary, our investigations indicate that the beneficial effects of hydrophobic iminosugars like AMP-DNM on hyperglycaemia are largely mediated by reduction of excessive glycosphingolipids in tissues. These findings support the notion that glycosphingolipids may play a critical role in the mediation of lipotoxic insulin resistance and should encourage the further evaluation of this class of iminosugar-based compounds for the treatment of human insulin resistance and diabetes.

## Acknowledgements

We gratefully acknowledge the technical assistance by Edward van Wezel, Sijmen Kuiper, Yuri van Geertruy, Cindy van Roomen, Wilma Donker, Karen Ghauharalli, Peter Simons, Jos Out and Judith Weerts and the support of the Wellcome Trust (SOR AP) and the BBSRC UK (JS).

## References

1. Unger, R.H. Minireview: weapons of lean body mass destruction: the role of ectopic lipids in the metabolic syndrome. *Endocrinology* **144**, 5159-5165 (2003).

2. Turcotte, L.P., Swenberger, J.R., Zavitz Tucker, M. & Yee, A.J. Increased fatty acid uptake and altered fatty acid metabolism in insulin-resistant muscle of obese Zucker rats. *Diabetes* **50**, 1389-1396 (2001).

3. Hegarty, B.D., Furler, S.M., Ye, J., Cooney, G.J. & Kraegen, E.W. The role of intramuscular lipid in insulin resistance. *Acta Physiol Scand*.**178**, 373-83 (2003).

4. Adams, J.M. 2nd *et al*. Ceramide content is increased in skeletal muscle from obese insulin-resistant humans. *Diabetes* **53**, 25-31 (2004).

5. Allende, M.L. & Proia, R.L. Lubricating cell signalling pathways with gangliosides. *Curr. Opin. Struct. Biol.* **12**, 587-592 (2002).

6. Boden, G. & Shulman, G.I. Free fatty acids in obesity and type 2 diabetes: defining their role in the development of insulin resistance and beta-cell dysfunction. *Eur. J. Clin. Invest.* **32** Suppl 3, 14-23 (2002).

7. McGarry, J.D. Banting lecture 2001: dysregulation of fatty acid metabolism in the etiology of type 2 diabetes. *Diabetes* **51**, 7-18 (2002).

8. Kolter, T., Proia, R.L. & Sandhoff, K. Combinatorial ganglioside biosynthesis. *J. Biol. Chem.* **277**, 25859-25862 (2002).

9. Menaldino, D.S. *et al*. Sphingoid bases and de novo ceramide synthesis: enzymes involved, pharmacology and mechanisms of action. *Pharmacol. Res.* **47**, 373-381 (2003).

10. Stricklett, P.K., Hughes, A.K., Ergonul, Z. & Kohan, D.E. Molecular basis for up-regulation by inflammatory cytokines of Shiga toxin 1 cytotoxicity and globotriaosylceramide expression. *J. Infect. Dis.* **186**, 976-982 (2002).

11. Peraldi, P. & Spiegelman, B. TNF-alpha and insulin resistance: summary and future prospects. *Mol. Cell. Biochem.* **182**, 169-175 (1998).

12. Peraldi, P., Hotamisligil, G.S., Buurman, W.A., White, M.F. & Spiegelman, B.M. Tumor necrosis factor (TNF)-alpha inhibits insulin signaling through stimulation of the p55 TNF receptor and activation of sphingomyelinase. *J. Biol. Chem.* **271**, 13018-13022 (1996).

13. Miura, A. *et al*. Inhibitory effect of ceramide on insulin-induced protein kinase Czeta translocation in rat adipocytes. *Metabolism* **52**, 19-24 (2003).

14. Stratford, S., Hoehn, K.L., Liu, F. & Summers, S.A. Regulation of insulin action by ceramide: Dual mechanisms linking ceramide accumulation to the inhibition of Akt/protein kinase B. *J. Biol. Chem.* **279**, 26608-36615 (2004).

15. Powell, D.J., Turban, S., Gray, A., Hajduch, E. & Hundal, H.S. Intracellular ceramide synthesis and PKCzeta activation play an essential role in palmitate-induced insulin resistance in rat L6 skeletal muscle cells. *Biochem. J.* **382**, 619-629 (2004).

16. Rebbaa, A., Hurh, J., Yamamoto, H., Kersey, D.S. & Bremer, *E.G.* Ganglioside GM3 inhibition of EGF receptor mediated signal transduction. *Glycobiol.***6**, 399-406 (1996).

17. Tagami, S. *et al*. Ganglioside GM3 participates in the pathological conditions of insulin resistance. *J. Biol. Chem*. **277**, 3085-3092 (2002).

18. Yamashita, T. *et al*. Enhanced insulin sensitivity in mice lacking ganglioside GM3. *Proc. Natl. Acad. Sci. U. S. A.* **100**, 3445-3449 (2003).

19. Kabayama, K. *et al*. TNF alpha-induced insulin resistance in adipocytes as a membrane microdomain disorder: involvement of ganglioside GM3. *Glycobiol***. 15**, 21-29 (2004).
20. Shayman, J.A., Abe, A. & Hiraoka, M. A turn in the road: How studies on the pharmacology of glucosylceramide synthase inhibitors led to the identification of a lysosomal phospholipase A2 with ceramide transacylase activity. *Glycoconj. J*. **20**, 25-32 (2004).
21. Aerts, J.M., Hollak, C., Boot, R. & Groener, A. Biochemistry of glycosphingolipid storage disorders: implications for therapeutic intervention. *Philos. Trans. R. Soc. Lond. B Biol. Sci*. **358**, 905-914 (2003).
22. Nugent, C, Prins, J.B., Whitehead, J.P., Savage, D., Wentworth, J.M., Chatterjee, V.K. & O'Rahilly, S. Potentiation of glucose uptake in 3T3-L1 adipocytes by PPAR gamma agonists is maintained in cells expressing a PPAR gamma dominant-negative mutant: evidence for selectivity in the downstream responses to PPAR gamma activation. *Mol Endocrinol.* **15**, 1729-1738 (2001).
23. Rodbell M. Metabolism of isolated fat cells. I. Effects of hormones on glucose metabolism and lipolysis. *J. Biol. Chem*. **239**, 375-80 (1964).
24. Overkleeft, H.S. *et al*. Generation of specific deoxynojirimycin-type inhibitors of the nonlysosomal glucosylceramidase. *J. Biol. Chem*. **273**, 26522-26527 (1998).
25. Folch J., Lees, M. & Sloane Stanley, G.H. A simple method for the isolation and purification of total lipids from animal tissues**.** *J.Biol.Chem.* **226**, 497- 509 (1957).
26. Taketomi, T., Hara, A., Uemura, K. & Sugiyama, E. Rapid method of preparation of glysoglycosphingolipids and their confirmation by delayed extraction matrix-assisted laser desorption ionization time-of-flight mass spectrometry. *J. Biochem. (Tokyo)* **120**, 573-579 (1996).
27. van Weely, S. *et al.* Clinical phenotype of Gaucher disease in relation to properties of mutant glucocerebrosidase in cultured fibroblasts. *Biochim.Biophys.Acta* **1096**, 301-311 (1991)
28. Andersson, U., Butters, T.D., Dwek, R.A. & Platt F.M. N-butyldeoxygalactonojirimycin: a more selective inhibitor of glycosphingolipid biosynthesis than N-butyldeoxynojirimycin, in vitro and in vivo. *Biochem Pharmacol.* **59**, 821-829 (2000).
29. Andersson, U., Reinkensmeier, G., Butters, T.D., Dwek, R.A. & Platt F.M Inhibition of glycogen breakdown by iminosugars in vitro and in vivo. *Biochem Pharmacol*. **67**, 697-705 (2004).
30. Ebina, Y., Edery, M., Ellis, L., Standring, D., Beaudoin, J., Roth, R., & Rutter, W. J. Expression of a functional human insulin receptor from a cloned cDNA in Chinese hamster ovary cells. *Proc. Natl. Acad. Sci. U. S. A.* **82**, 8014-801829 (1985).
31. van Dijk, T.H. *et al*. Quantification of hepatic carbohydrate metabolism in conscious mice using serial blood and urine spots. *Anal. Biochem*. **322**,1-13 (2003).
32. van Dijk, T.H. *et al*. Acute inhibition of hepatic glucose-6-phosphatase does not affect gluconeogenesis but directs gluconeogenic flux toward glycogen in fasted rats. A pharmacological study with the chlorogenic acid derivative S4048. *J. Biol. Chem*. **276**, 25727-25735 (2001).
33. Cox, T. *et al*. Novel oral treatment of Gaucher's disease with N-butyldeoxynojirimycin (OGT918) to decrease substrate biosynthesis. *Lancet* **355**, 1481-1485 (2000).
34. Scott, L.J. & Spencer, C.M. Miglitol: a review of its therapeutic potential in type 2 diabetes mellitus. *Drugs* **59**, 521-549 (2000).
35. Nojima, H. *et al*. Antihyperglycemic effects of N-containing sugars from Xanthocercis zambesiaca, Morus bombycis, Aglaonema treubii, and Castanospermum australe in streptozotocin-diabetic mice. *J. Nat. Prod.* **61**, 397-400 (1998).

# Chapter 6

# Acute hepatic steatosis in mice by blocking ß-oxidation does not reduce insulin sensitivity of very low density lipoprotein production

Aldo Grefhorst[1], Jildou Hoekstra[1], Terry G.J. Derks[1], D. Margriet Ouwens[2], Julius F.W. Baller[1], Rick Havinga[1], Louis M. Havekes[3,4], Johannes A. Romijn[5], Folkert Kuipers[1]

[1]Laboratory of Pediatrics, University Medical Center Groningen
[2]Department of Molecular Cell Biology, Leiden University Medical Center
[3]TNO Prevention and Health, Leiden
[4]Departments of General Internal Medicine and Cardiology, Leiden University Medical Center
[5]Department of Endocrinology and Diabetes, Leiden University Medical Center

**Am. J. Physiol. Liver Gastrointest. Physiol. 2005: 289: G592-G598**

## Abstract

Accumulation of triglycerides (TG) in the liver is generally associated with hepatic insulin resistance. We questioned whether acute hepatic steatosis induced by pharmacological blockade of β-oxidation affects hepatic insulin sensitivity, *i.e.*, insulin-mediated suppression of VLDL production and insulin-induced activation of phosphatidylinositol 3-kinase (PI3-kinase) and PKB. Tetradecylglycidic acid (TDGA), an inhibitor of carnitine palmitoyl transferase-1 (CPT1), was used for this purpose. Male C57BL/6J mice received 30 mg/kg TDGA or its solvent intraperitoneally and were subsequently fasted for 12 h. CPT1 inhibition resulted in severe microvesicular hepatic steatosis (19.9 ± 8.3 *vs.* 112.4 ± 25.2 nmol TG/mg liver, control *vs.* treated, $P < 0.05$) with elevated plasma nonesterified fatty acid (0.68 ± 0.25 *vs.* 1.21 ± 0.41 mM, $P < 0.05$) and plasma TG (0.39 ± 0.16 *vs.* 0.60 ± 0.10 mM, $P < 0.05$) concentrations. VLDL-TG production rate was not affected on CPT1 inhibition (74.9 ± 15.2 *vs.* 79.1 ± 12.8 μmol $TG \cdot kg^{-1} \cdot min^{-1}$, control *vs.* treated) although treated mice secreted larger VLDL particles (59.3 ± 3.6 *vs.* 66.6 ± 4.5 nm diameter, $P < 0.05$). Infusion of insulin under euglycemic conditions suppressed VLDL production rate in control and treated mice by 43 and 54%, respectively, with formation of smaller VLDL particles (51.2 ± 2.5 and 53.2 ± 2.8 nm diameter). Insulin-induced insulin receptor substrate (IRS)1- and IRS2-associated PI3-kinase activity and PKB-phosphorylation were not affected on TDGA treatment. In conclusion, acute hepatic steatosis caused by pharmacological inhibition of β-oxidation is not associated with reduced hepatic insulin sensitivity, indicating that hepatocellular fat content per se is not causally related to insulin resistance.

## Introduction

The liver is a key player in the control of whole body energy metabolism by its ability to synthesize, oxidize, store, and distribute the major sources of energy, *i.e.*, glucose and fatty acids. In fed conditions, when excess glucose is available from the intestine, plasma insulin levels are high, and glucose is stored in the liver as glycogen or enters the glycolytic pathway. High insulin suppresses hepatic glucose production (HGP), increases hepatic glucose uptake, and stimulates de novo lipogenesis (11). In addition, insulin suppresses the secretion of VLDL particles by the liver (36). The actions of insulin on the liver, initiated by binding of insulin to its receptor, involve signaling pathways that transduce its effects on gene transcription, protein metabolism, and, finally, fluxes of substrates. Of relevance for this work is insulin signaling through the phosphatidylinositol 3-kinase (PI3-kinase) pathway. On insulin binding, the insulin receptor substrate (IRS) is phosphorylated, and, subsequently, PI3-kinase is activated. PI3-kinase-mediated phosphatidylinositol 3,4,5-trisphophate (PIP3) generation and PIP3-mediated phosphorylation of PKB at Ser473 and Thr308 are key processes in the insulin signaling cascade (34). Both PI3-kinase and PKB are involved in execution of the effects of insulin on hepatic glucose metabolism (34). It has been reported that insulin affects VLDL production via accelerated degradation of apolipoprotein B (apoB) (10), a process mediated by PI3-kinase (7) but thought to be independent of PKB (2).

When insulin levels are low, *e.g.*, during fasting, glucose is mobilized from hepatic glycogen stores and hepatic gluconeogenesis is facilitated. β-Oxidation of fatty acids is considered the primary source of the energy and reducing equivalents (ATP, NADH) needed for gluconeogenesis. β-Oxidation disorders in humans and mice are associated with hypoglycemia and reduced ketogenesis as well as with hepatic triglyceride (TG) accumulation (hepatic steatosis) on fasting (33). For instance, mice deficient for the major regulator of β-oxidation, peroxisome proliferator-activated receptor-α, showed massively increased hepatic TG levels on fasting (3,17). Hepatic steatosis is generally associated with reduced hepatic insulin sensitivity (1,9,24,35), and various animal models have been used to study the effects of hepatic steatosis on insulin sensitivity with regard to glucose and fatty acid homeostasis (9). For instance, the hepatic steatosis in leptin-deficient *ob/ob* mice is associated of reduced insulin sensitivity of both HGP (16a) and VLDL secretion (44). Moreover, mice that lack the peripheral fatty acid transporter (CD36–/– mice) showed massive hepatic TG accumulation with decreased sensitivity of HGP to insulin (15).

During the β-oxidation process, fatty acyl-CoAs are broken down into shorter chains by a series of dehydrogenases. Long-chain fatty acids are unable to freely pass the mitochondrial membrane and their transfer across the outer mitochondrial membrane is mediated by carnitine palmitoyltransferase-1 (CPT1). CPT1 facilitates coupling of carnitine to fatty acyl-CoA (32,41). The acylcarnitine thus generated can be transferred across the outer membrane by CPT1. Acylcarnitines pass the inner mitochondrial membrane with the help of carnitine acylcarnitine translocase. Finally, inside the mitochondria, carnitine is removed from the acylchain by CPT2. CPT1 activity has been shown to be rate controlling for a major part of hepatic β-oxidation (32). Tetradecylglycidic acid (TDGA) is an inhibitor of CPT1 (22,38,39) and can be used to evaluate the immediate effects of impaired β-oxidation. We used TDGA to address the question of whether hepatic steatosis due to impaired β-oxidation is associated with impaired hepatic insulin sensitivity, *i.e.*, insulin-mediated suppression of VLDL secretion and insulin-stimulated PKB phosphorylation and PI3-kinase activity.

## Material and methods

### *Animals and chemicals*

Male C57BL/6J mice (Harlan, Horst, The Netherlands) were housed in a light- and temperature-controlled facility and were fed a commercially available lab chow (cat. no. RMH-B; Hope Farms, Woerden, The Netherlands). All experiments were approved by the Animal Experiments Ethical Committee of the University of Groningen.

TDGA was a kind gift from Dr. P. J. Voshol (TNO, Leiden, The Netherlands) and was suspended in a concentration of 2.0 mg/ml in a vehicle consisting of 90 mg/ml BSA in saline (45).

### *Collection of basal plasma and liver samples*

Mice received either 30 mg/kg TDGA or its solvent by intraperitoneal injection. Food was removed, but the mice still had access to water. Blood glucose levels were measured with a Lifescan EuroFlash glucose meter (Lifescan Benelux, Beerse, Belgium) in a small tail blood sample taken every hour. After 12 h, mice were killed under isoflurane anesthesia. A large blood sample was collected by cardiac puncture and centrifuged. Plasma was stored at –20°C until analyzed. The liver was quickly removed, weighed, and frozen in separate portions for RNA isolation and lipid analyzes. Plasma TG, phospholipid, nonesterified fatty acids (NEFAs), and cholesterol were determined using commercially available kits (Roche Diagnostics, Mannheim, Germany, and Wako Chemicals, Neuss, Germany).

Hepatic TG and cholesterol concentrations were measured using commercial kits (Roche Diagnostics and Wako Chemicals) after lipid extraction according to Bligh and Dyer (5). After lipid extraction, phospholipid content of the liver was determined according to Böttcher *et al*. (6). Protein concentrations in livers were determined according to Lowry *et al.* (26) by using BSA (Pierce, Rockford, IL) as standard. Hepatic glycogen and glucose-6-phosphate levels were determined as described previously (18,20). Fatty acid composition was determined by gas chromatography after methylation as described previously (25). Liver histology was examined on 4-µm-thick frozen liver sections after Oil-Red-O staining for neutral lipids by standard procedures. mRNA expression levels in liver was measured by real-time RT-PCR as described previously (16). PCR results were normalized to *β-actin* and *18S* mRNA levels. The sequences of the primers and probes used were listed previously (16,31).

### *In vivo VLDL-TG production rate*

Mice received either 30 mg/kg TDGA or its solvent as described and were subsequently fasted for 9 h. After fasting, mice received an orbital injection of 12.5 mg Triton WR-1339 in 100 µl PBS. Tail blood samples were taken under light isoflurane anesthesia before and every 30 min after Triton injection. A large blood sample was collected by cardiac puncture, 90 min after Triton injection. The collected blood samples were used for TG measurements.

To determine the VLDL-TG production rate under hyperinsulinemic conditions, mice were equipped with a permanent catheter in the right atrium via the jugular vein (23). The two-way entrance of the catheter was attached to the skull with acrylic glue. The mice were allowed a resting period of at least 5 days. Mice then received either 30 mg/kg TDGA or its solvent as described and were subsequently fasted. Mice were kept in metabolic cages during the experiment and the preliminary fasting period, allowing frequent collection of small tail blood samples under conscious and unrestrained conditions (40). After 9 h of fasting, the mice were infused for 3 h with two solutions. The first was a 1% BSA solution containing 40 µg/ml somatostatin (UCB, Breda, The Netherlands). This solution contained insulin (Actrapid; Novo Nordisk, Bagsvaerd, Denmark), leading to an insulin infusion rate of 20 $mU \cdot kg^{-1} \cdot min^{-1}$. To prevent too high total infusion rates, this solution contained 200 mg/ml glucose. The solution

was infused at a constant flow rate of 0.135 ml/h. The second infusate was a 30% glucose solution and its infusion rate was adjusted according to measured blood glucose levels to maintain euglycemic conditions. Blood glucose levels were measured in a small tail blood sample taken every 15 min. After 90 min of infusion, mice received an injection of 12.5 mg Triton WR-1339 in 100 µl PBS via the orbita under light isoflurane anesthesia. Orbital blood samples were taken under light isoflurane anesthesia before and every 30 min after Triton WR-1339 injection. A large blood sample was collected by cardiac puncture 90 min after Triton WR-1339 injection. The collected blood samples were used for TG measurements. VLDL-TG production rate was calculated from the slope of the TG concentration *vs.* time curve (27). The large blood sample was used for isolation of VLDL.

*VLDL isolation and analyses*

Plasma VLDL/intermediate-density lipoprotein (IDL) (density < 1.006 g/ml) was isolated by density gradient ultracentrifugation. Hereto, 300 µl plasma was adjusted to 1,000 µl with a NaCl/KBr solution of density = 1.006 g/ml and centrifuged at 120,000 rpm in a Optima LX tabletop ultracentrifuge (Beckman Instruments, Palo Alto, CA). VLDL was isolated by tube slicing, and the volume was recorded by weight. ApoB100 and apoB48 were determined by Western blot analysis, using antibodies against human apoB raised in rabbit. TG and cholesterol content were determined as described for plasma. Phospholipid content was determined using a commercially available kit (Wako Chemicals), and fatty acid composition as described previously (25).

VLDL size and volume distribution profiles were analyzed by dynamic scattering using a Nicomp model 370 submicron particle analyzer (Nicomp Particle Sizing Systems, Santa Barbara, CA). Particle diameters were calculated from the volume distribution patterns provided by the analyzer.

*Hepatic insulin signaling pathways*

Mice received either 30 mg/kg TDGA or its solvent as described. After 9 h of fasting, the mice were anesthetized and equipped with an infusion line in the vena cava inferior. During 30 min, mice were infused with saline or a 1% BSA solution containing 13.3 µg/ml somatostatin and 100 mg/ml glucose. The latter solution contained insulin resulting in an insulin infusion rate of 10 $mU \cdot kg^{-1} \cdot min^{-1}$. The solutions were infused at a flow rate of 0.405 ml/h. After 30 min of infusion, the liver was quickly removed and frozen in liquid nitrogen.

Hepatic lysates were made in buffer [in mM: 30 Tris·Cl, pH 7.4, 2.5 EDTA, pH 8.0, 150 NaCl, 0.5 $Na_3VO_4$, 5 NaF, 5 $MgCl_2$, and 1.3 M glycerol and protease inhibitors (Complete; Roche Diagnostics)] and cleared by centrifugation. Protein content was determined using BCA-kit (Pierce), and equal amounts of protein were used to determine PKB-Ser473 and PKB-Thr308 phosphorylation by Western blotting, using antibodies against PKB-Ser473P and PKB-Thr308P raised in rabbit (Cell Signaling, Beverly, MA). For PI3-kinase activity, the lysates were immunoprecipitated overnight with antibodies against IRS1 (29) or IRS2 (37) raised in rabbits. Following extensive washing, PI3-kinase activity was determined as described previously (29). The incorporated radioactivity was quantified using a phosphorimager.

*Statistics*

All values represent means ± SD for the number of animals indicated. Statistical analysis was assessed by the Mann-Whitney U-test. The level of significance was set at $P < 0.05$. Analyses were performed using SPSS for Windows software (SPSS, Chicago, IL).

## Results

*Severe hepatic steatosis on treatment with CPT1 inhibitor TDGA*

To determine the acute effects of β-oxidation inhibition during fasting, *i.e.*, when the body strongly depends on fatty acid oxidation for its energy, we treated male C57BL/6J mice with the CPT1 inhibitor TDGA and fasted them for 12 h. From 3 h fasting onward, the blood glucose levels in TDGA-treated mice were statistically significantly lower than in the control mice (figure 6.1). Plasma NEFAs, TG, and free cholesterol levels were increased on TDGA treatment (table 6.1). Relative liver weight was increased by 18% on treatment, probably related to a marked increase in TG content (table 6.1). In contrast, liver glucose-6-phosphate levels were lower in the treated mice. Oil-Red-O staining for neutral lipids on frozen liver sections showed massive microvesicular lipid accumulation in periportal (zone 1) as well as in perivenous (zone 3) hepatocytes in mice receiving TDGA (figure 6.2). TDGA treatment lead to significant changes in the hepatic fatty acid composition (figure 6.3). Relative amounts of saturated fatty acids (SAFAs) and polyunsaturated fatty acids (PUFAs) decreased in favor of monounsaturated fatty acids (MUFAs).

*Insulin sensitivity of VLDL production is not affected by treatment with CPT1 inhibitor TDGA*

Figure 6.4 shows the plasma TG concentration *vs.* time curve after injection of Triton WR-1339 in control and TDGA-treated mice, with and without infusion of insulin. From these curves, the VLDL-TG production rates were calculated. TDGA treatment did not affect VLDL-TG production rate and insulin suppressed the production rate in control and treated mice by 43 and 54%, respectively. The concentrations of cholesterol, phospholipids, and TG in nascent VLDL particles isolated from plasma obtained at 90 min after Triton WR-1339 injection are summarized in table 6.2. Under basal conditions, the VLDL TG-to-phospholipid ratio tended to increase on TDGA treatment, indicative of the presence of larger particles (12). On insulin infusion, this ratio was decreased in both control and treated mice, suggesting that insulin-mediated suppression of VLDL-TG secretion was, at least partly, due to the secretion of smaller particles. Accordingly, direct measurement of particle sizes revealed that the mean diameter of the VLDL particles under basal conditions was increased on TDGA treatment (67 ± 5 *vs.* 59 ± 4 nm, $P < 0.05$). The diameters were smaller in both control and treated mice on insulin infusion (51 ± 3 and 53 ± 3 nm, control and treated, respectively). In accordance with these data, apoB100 and apoB48 contents in isolated VLDL fractions were increased on insulin infusion, but no significant difference was seen between control and TDGA treatment, as determined by Western blot analysis (figure 6.5). The fatty acid composition of the VLDL fraction was changed on treatment, resulting in changes similar to those seen for the hepatic fatty acids, *i.e.*, increased MUFAs and decreased SAFAs and PUFAs (figure 6.6). The hepatic expression of genes encoding enzymes involved in VLDL secretion was investigated with real-time RT-PCR (figure 6.7). Expression of Apob and Mttp, the latter encoding microsomal TG transfer protein, was slightly increased on TDGA treatment. Expression of lipoprotein lipase (*Lpl*) was slightly reduced in livers of TDGA-treated mice.

Table 6.1. Plasma and hepatic parameters after 12 h of fasting in mice treated with or without CPT1 inhibitor TDGA. Values are means ± SD; n = 6 mice. CPT1, carnitine palmytoyl transferase-1; TDGA, tetradecylglycidic acid. *$P$ < 0.05, TDGA *vs.* control.

| | Control | TDGA |
|---|---|---|
| Plasma triglycerides (mM) | 0.39 ± 0.16 | 0.60 ± 0.10 * |
| Plasma free cholesterol (mM) | 0.61 ± 0.35 | 0.86 ± 0.36 |
| Plasma cholesterylester (mM) | 1.06 ± 0.54 | 1.07 ± 0.53 |
| Plasma NEFA (mM) | 0.68 ± 0.26 | 1.21 ± 0.41 * |
| Liver weight (% of bodyweight) | 4.26 ± 0.66 | 5.03 ± 0.39 * |
| Liver proteins (mg/g liver) | 228 ± 44 | 211 ± 39 |
| Liver triglycerides (nmol/mg liver) | 19.9 ± 8.3 | 112.4 ± 25.2 * |
| Liver cholesterol (nmol/mg liver) | 9.91 ± 1.32 | 11.13 ± 2.92 * |
| Liver phospholipids (nmol/mg liver) | 52.65 ± 11.50 | 49.81 ± 4.61 |
| Liver glucose-6-phosphate (nmol/g liver) | 50.6 ± 15.6 | 25.7 ± 2.6 * |

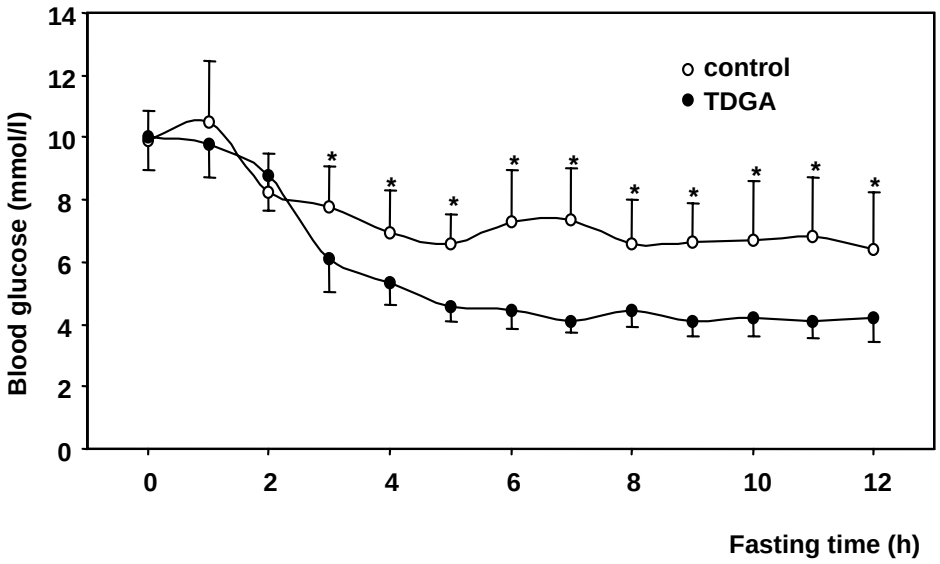


Figure 6.1. Blood glucose levels during fasting period in mice treated with or without carnitine palmytoyl transferase-1 (CPT1)-inhibitor tetradecylglycidic acid (TDGA; 30 mg/kg body wt) (n = 6 mice; *$P$ < 0.05, TDGA *vs.* control).

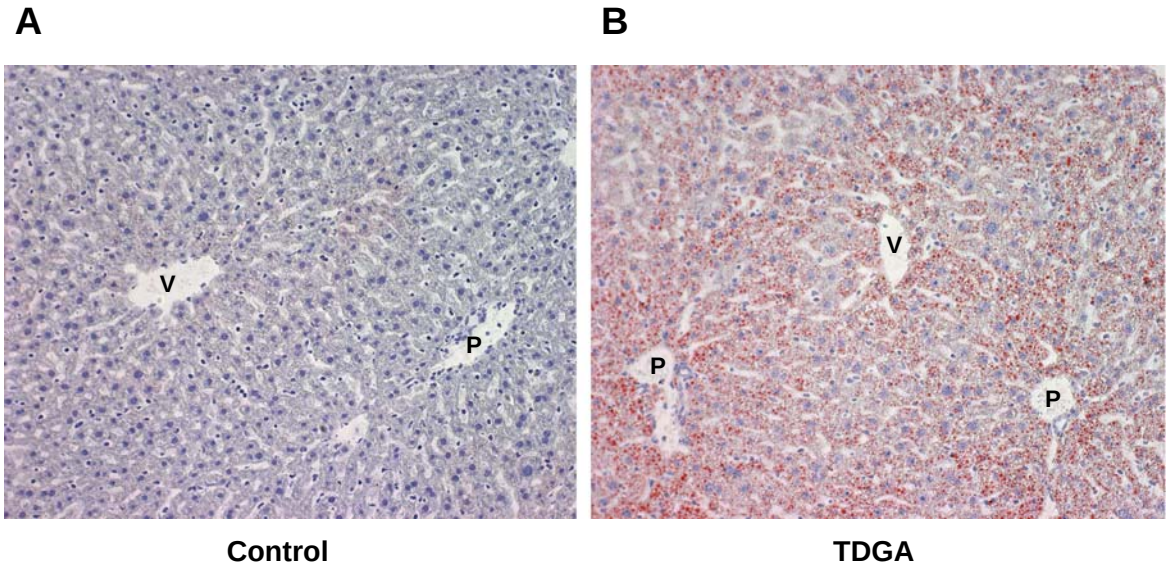


Figure 6.2. Oil-Red-O staining for neutral lipids in livers of mice treated with or without CPT1-inhibitor TDGA. V, central vein; P, portal vein.

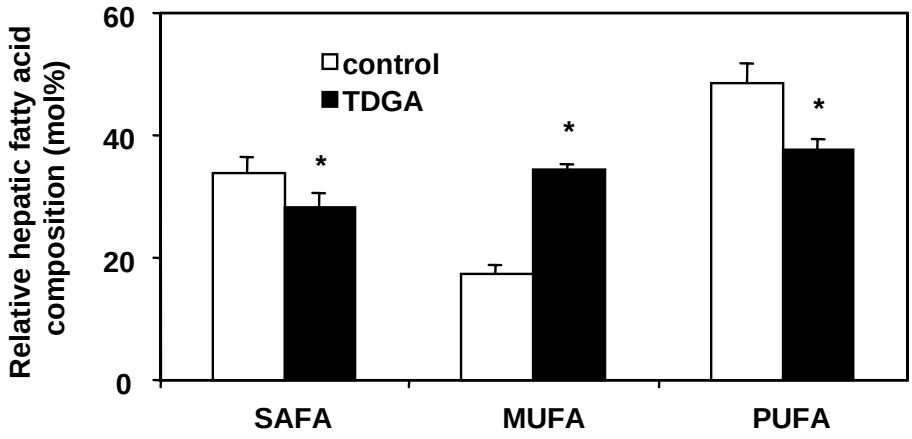


Figure 3. Relative fatty acid profile of livers from mice treated with or without CPT1-inhibitor TDGA. SAFA, saturated fatty acids; MUFA, monounsaturated fatty acids; PUFA, polyunsaturated fatty acids. N = 6 mice; * $P < 0.05$, TDGA *vs.* control.

*Hepatic insulin signaling is not affected on treatment with CPT1 inhibitor TDGA*

To determine whether hepatic steatosis on TDGA treatment affected hepatic insulin signaling, we determined PI3-kinase activity and PKB-phosphorylation, both supposedly major steps in hepatic insulin signaling. Hereto, TDGA-treated and control mice were subjected to 30-min infusion with either saline or insulin. Both IRS1- and IRS2-associated insulin-induced increase of PI3-kinase activity did not differ between control and treated mice (figure 6.8). Moreover, insulin-induced phosphorylation of PKB, the key mediator of hepatic insulin signaling, was not affected by TDGA; insulin-induced PKB phosphorylation on Ser473 and Thr308 did not differ between control and TDGA-treated mice (figure 6.9).

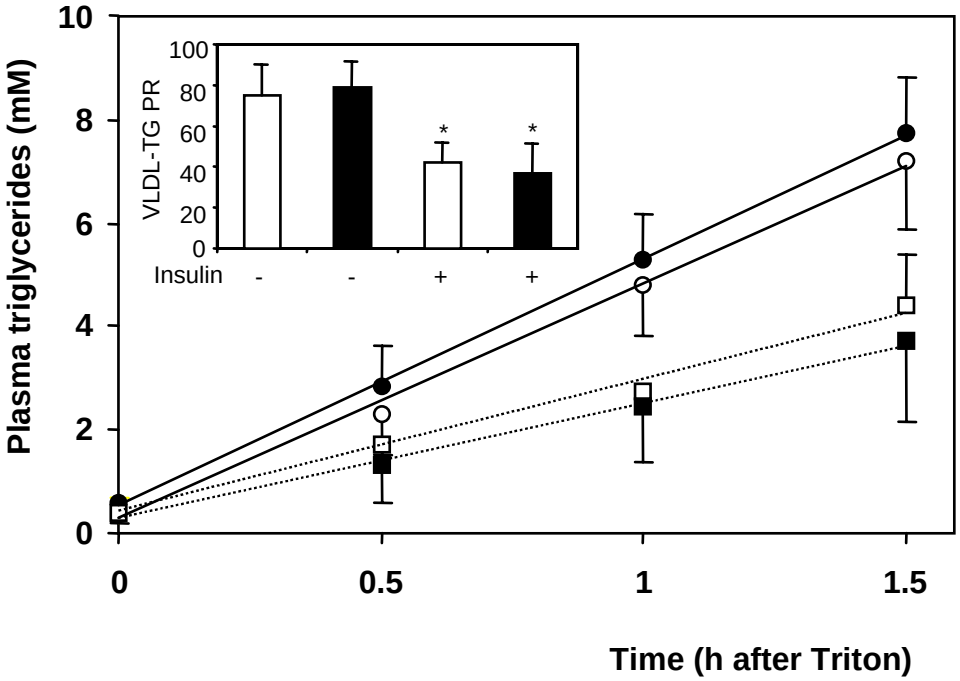


Figure 6.4. Plasma triglyceride (TG) concentrations and VLDL-TG production rates of mice treated with or without CPT1-inhibitor TDGA, under basal and hyperinsulinemic conditions. *Inset*: VLDL-TG production rate in $\mu mol \cdot kg^{-1} \cdot h^{-1}$ calculated from the plasma TG *vs.* time curves (n = 6 mice; *P < 0.05, TDGA *vs.* control). Open bars, control mice; closed bars, TDGAtreated mice; open circles, control mice, basal conditions; closed circles, TDGA-treated mice, basal conditions; open squares, control mice, hyperinsulinemic conditions; closed squares, TDGA-treated mice, hyperinsulinemic conditions.

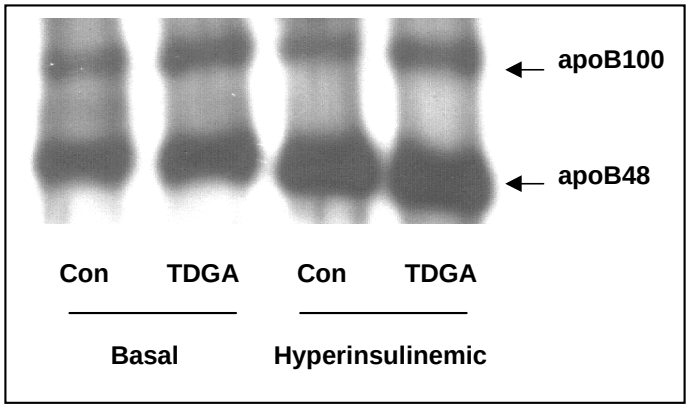


Figure 6.5. Representative apolipoprotein B (apoB) Western blots of VLDL fractions of mice treated with or without (Con) CPT1 inhibitor TDGA, under basal and hyperinsulinemic conditions.

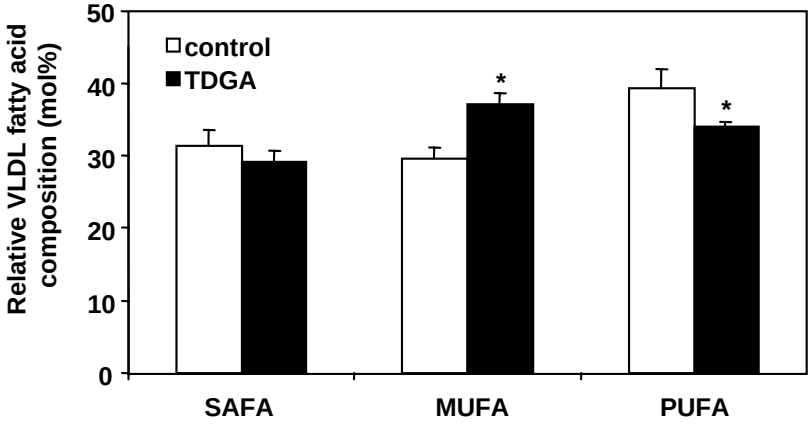


Figure 6.6. Relative fatty acid profile of VLDL fractions from mice treated with or without (control) CPT1 inhibitor TDGA (n = 6 mice; * P < 0.05, TDGA *vs.* control).

Table 6.2. Composition and size of nascent VLDL particles of mice treated with or without CPT1 inhibitor TDGA under basal and hyperinsulinemic conditions. Values are means ± SD; n = 6 mice; * P < 0.05 TDGA *vs.* control; † P < 0.05 hyperinsulinemic *vs.* basal.

| | Basal | | Hyperinsulinemic | |
|---|---|---|---|---|
| | Control | TDGA | Control | TDGA |
| Triglycerides (%) | 76.8 ± 1.6 | 79.1 ± 1.6 * | 67.9 ± 1.6 † | 66.8 ± 3.8 † |
| Phospholipids (%) | 12.2 ± 0.7 | 11.7 ± 0.8 | 15.8 ± 0.9 † | 16.2 ± 1.6 † |
| Cholesterol (%) | 10.9 ± 0.9 | 9.2 ± 1.1 * | 16.4 ± 1.5 † | 17.0 ± 2.3 † |
| TG:PL ratio | 6.3 ± 0.5 | 6.8 ± 0.6 | 4.3 ± 0.3 † | 4.2 ± 0.7 † |
| Particle size (nm) | 59.3 ± 3.6 | 66.6 ± 4.5 * | 51.2 ± 2.5 † | 53.2 ± 2.8 † |

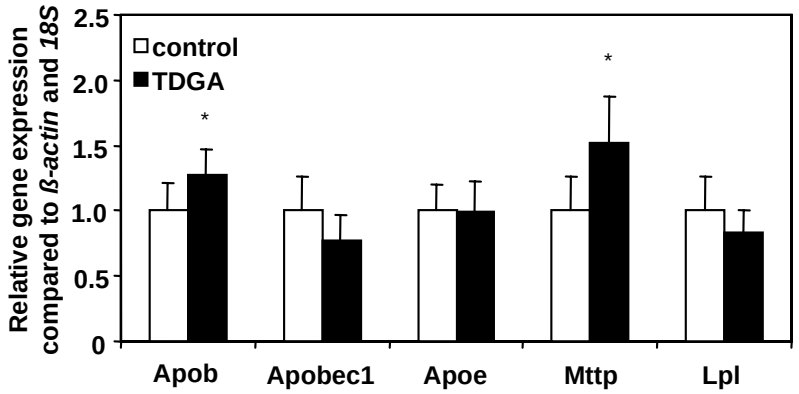


Figure 6.7. Changes in hepatic gene expression patterns on TDGA treatment. Results were normalized to *β-actin* and *18S* mRNA levels, data from control mice defined as 1. *Apob*, apolipoprotein B; *Apobec1*, apolipoprotein B editing complex-1; *Apoe*, apolipoprotein E, *Mttp*, microsomal triglyceride transfer protein, *Lpl*, lipoprotein lipase. N = 6 mice; * P < 0.05.

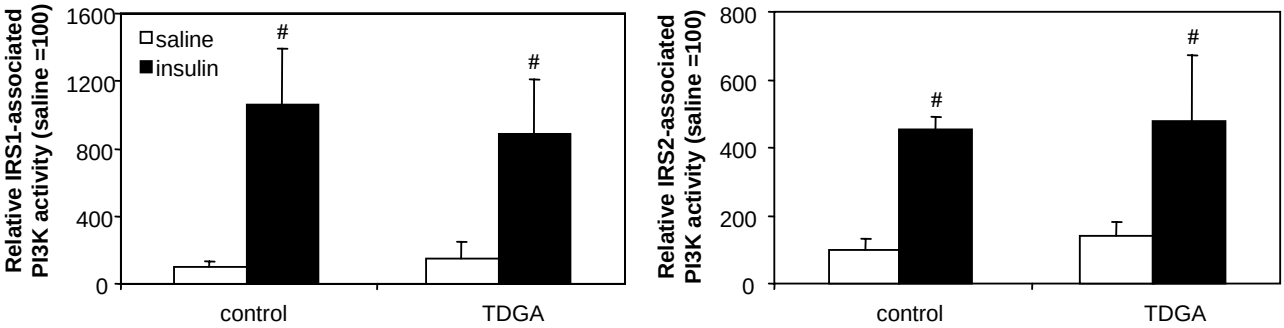


Figure 6.8. Hepatic phosphatidylinositol 3-kinase (PI3-kinase) activity in mice treated with or without CPT1-inhibitor TDGA on infusion of saline or insulin. Liver lysates were precipitated with antibodies against Insulin receptor substrate (IRS)1 (*left*) or IRS2 (*right*). The PI3-kinase activity in acquired pellets was determined by incorporation of 32P-ATP into PIP3. The amount of incorporated radioactivity was quantified using a phosphorimager. Hepatic PI3-kinase activity in control mice on saline infusion is set as value 100; n = 6 mice; # $P < 0.05$, insulin infusion *vs.* saline infusion.

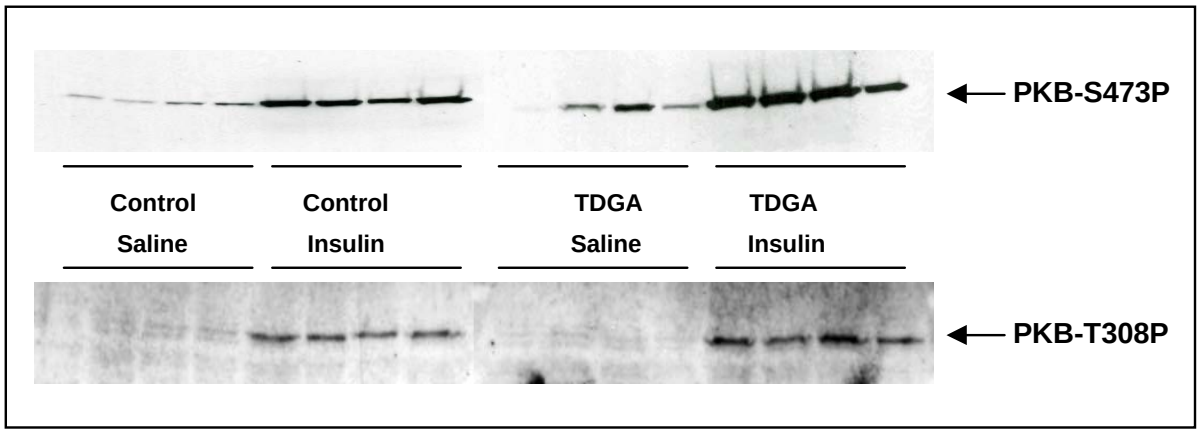


Figure 6.9. Hepatic PKB-phosphorylation in mice treated with or without CPT1-inhibitor TDGA on infusion of saline or insulin. Liver lysates were applied to SDS-PAGE followed by Western blot analysis. Antibody staining for PKBphosphorylation at Ser473 (*top*) and Thr308 (*bottom*). Each lane represents an individual mouse that received infusion of saline or insulin.

## Discussion

This study demonstrates that pharmacological inhibition of CPT1 by TDGA leads to severe hepatic steatosis without affecting insulin sensitivity of hepatic VLDL production. Moreover, the PI3-kinase insulin signaling cascade was not affected in the TDGA-induced fatty livers. Therefore, this study provides evidence that hepatic fat accumulation per se does not lead to insulin resistance in mice and underscores the fact that not all forms of hepatic steatosis are associated with insulin resistance.

In humans, various inherited β-oxidation disorders are associated with increased hepatic TG levels, hypoglycemia, and low plasma ketone body levels on fasting (33). The TDGA-treated mice showed marked hypoglycemia during fasting. From 3 h of fasting on, blood glucose levels were lower in TDGA-treated than controls and showed a steady state. Therefore, we performed all subsequent experiments within 9 to 12 h of fasting.

Two types of hepatic steatosis are usually discerned, *i.e.*, macrovesicular and microvesicular steatosis. The latter type is particularly found in subjects with β-oxidation disorders (8,13); TDGA treatment was also associated with microvesicular hepatic steatosis in mice (figure 6.2). Despite the overabundance of fat in the liver and slightly increased hepatic *Apob* and *Mttp* gene expression (figure 6.7), basal VLDL-TG production rate was not affected on TDGA treatment (figure 6.4). Because this unaffected VLDL-TG production rate was accompanied by a 54% increase of plasma TG levels (table 6.1), clearance of TG-rich lipoproteins was, by definition, affected in TDGA-treated mice. Slightly reduced hepatic *Lpl* expression (figure 6.7) might contribute to reduced VLDL lipolysis. Moreover, the increased NEFA levels on TDGA treatment (table 6.1) might also reduce the capacity of LPL to lipolyse VLDL-TG (30). The unaffected VLDL-TG production rate on TDGA treatment may, at first sight, seems surprising because VLDL production is one means for the liver to get rid of large amounts of TG that accumulate during fasting. A stimulatory effect on VLDL-TG production was found in mice with hepatic steatosis due to increased de novo lipogenesis on liver X receptor agonist treatment (16). On the other hand, *ob/ob* mice show severe hepatic steatosis and increased de novo lipogenesis, but do not have increased VLDL-TG production under basal conditions (44). Furthermore, hepatic steatosis associated with inhibition of glucose-6-phosphatase activity was also without effect on VLDL production (4). These observations suggest that increased hepatic TG content per se does not stimulate hepatic VLDL production. Various factors, apart from the accumulation of TG, might contribute to changes in VLDL production. TGs are not the sole components of VLDL; hepatic cholesterol and phospholipid availability or synthesis might also influence the secretion and assembly of VLDL. In our TDGA-treated mice, hepatic cholesterol levels were slightly higher but phospholipid content was not affected. It has been suggested that de novo synthesis of cholesterol (19) and phospholipid (42), rather than their concentrations, are determinants of VLDL production. Although we have no direct measurements of these parameters, in a microarray experiment employing TDGA, we found significantly reduced hepatic gene expression of *Pemt*, encoding phosphatidylethanolamine N-methyltransferase, a key player in phospholipid synthesis (F. R. van der Leij, personal communication). Interestingly, PEMT is thought to play an important role in providing phospholipid needed for the surface of VLDL (28).

Another explanation for the unaffected VLDL-TG production might be duration of TG accumulation. It is reported that fatty acids taken up by the hepatocyte are not directly used for VLDL production (14) but are esterified and stored in a cytoplasmic pool. Utilization of TGs from this pool for VLDL assembly requires hydrolysis followed by reesterification. Thus an TG accumulation over a short period of time, as shown in this study, might not immediately lead to increased VLDL-TG production.

Hepatic steatosis is commonly associated with decreased insulin sensitivity (1,24,35). Hepatic insulin sensitivity was tested in a number of ways. First, we checked whether insulin would be able to effectively suppress the secretion of VLDL by the liver. Unexpectedly, insulin suppressed VLDL-TG production rate equally well in control and TDGA-treated mice (figure 6.4). This is in contrast to the situation in *ob/ob* mice, a commonly used model of insulin resistance. Wiegman *et al.* (44) showed that insulin failed to effectively suppress VLDL-TG production in ob/ob mice. Exactly how insulin suppresses VLDL production is not entirely clear. It has been suggested that insulin stimulates intracellular degradation of the major VLDL apolipoprotein apoB (7) through a mechanism involving PI3-kinase but not PKB (2,7,10). Therefore, we determined PI3-kinase activity and PKB phosphorylation in the steatotic livers of TDGA-treated mice. Indeed, Western blot analyses revealed that TDGA treatment did not affect insulin-induced hepatic PKB-phosphorylation at Ser473 nor at Thr308 (figure 6.9). Moreover, IRS1- nor IRS2-associated insulin-stimulated PI3-kinase

activities in the liver were affected on TDGA treatment (figure 6.8). Both results strongly suggest that hepatic insulin signaling is not affected in the rapidly developed fatty liver of TDGA-treated mice. From these data, and from figure 6.4, it cannot be concluded whether insulin-mediated suppression of VLDL production is independent from PKB, as suggested recently (2). In the study from Au *et al.* (2), however, it was concluded that PKB was not involved in insulin-mediated inhibition of apoB degradation. Other subclasses of PKB and/or PKC might be responsible for the effects of insulin on VLDL production. A recent report showed that PKC-Θ knockout mice are protected from fat-induced insulin resistance (21), suggesting that PKC-Θ is an important component in (skeletal muscle) insulin signaling.

An aspect that might be involved in the lack of association between hepatic steatosis and insulin resistance relates to the difference in the hepatic fatty acid profile between control and treated mice (figure 6.3). An increase in dietary MUFAs resulted in improved insulin sensitivity in healthy men and women (43), but had no effect on insulin secretion. Therefore, hepatic insulin sensitivity might be better preserved in fatty livers that contain relatively more MUFAs, as observed in TDGA-treated mice, than fatty livers with predominantly SAFA-containing TG.

In conclusion, CPT1 inhibition with TDGA led to the expected microvesicular hepatic steatosis in C57BL/6J mice. However, this was not associated with reduced hepatic insulin sensitivity because the hepatic insulin signaling cascade was not affected and the inhibitory effects of insulin on VLDL production *in vivo* were not blunted. Therefore, in combination with other data (4,16a,44), these observations support the notion that hepatocellular fat content per se is not causally related to induction of insulin resistance in mice.

## References

1. Angulo P. Nonalcoholic fatty liver disease. N Engl J Med 346: 1221–1231, 2002.
2. Au CS, Wagner A, Chong T, Qiu W, Sparks JD, and Adeli K. Insulin regulates hepatic apolipoprotein B production independent of the mass or activity of Akt1/PKB-α. Metabolism 53: 228–235, 2004.
3. Bandsma RHJ, van Dijk TH, ter Harmsel A, Kok T, Reijngoud DJ, Staels B, and Kuipers F. Hepatic de novo synthesis of glucose-6-phosphate is not affected in PPAR− -deficient mice but is preferentiallydirected towards hepatic glycogen stores after a short-term fast. J Biol Chem 279: 8930–8937, 2004.
4. Bandsma RHJ, Wiegman CH, Herling AW, Burger HJ, ter Harmsel A, Meijer AJ, Romijn JA, Reijngoud DJ, and Kuipers F. Acute inhibition of glucose-6-phosphate translocator activity leads to increased de novo lipogenesis and development of hepatic steatosis without affecting VLDL production in rats. Diabetes 50: 2591–2597, 2001.
5. Bligh EG and Dyer WJ. A rapid method of total lipid extraction and purification. Can J Biochem Physiol 37: 911–917, 1959.
6. Böttcher CFJ, van Gent CM, and Pries C. A rapid and sensitive sub-micro-phosphorus determination. Anal Chim Acta 24: 203–204, 1961.
7. Brown AM and Gibbons GF. Insulin inhibits the maturation phase of VLDL assembly via a phosphoinositide 3-kinase-mediated event. Arterioscler Thromb Vasc Biol 21: 1656–1661, 2001.
8. Burt AD, Mutton A, and Day CP. Diagnosis and interpretation of steatosis and steatohepatitis. Semin Diagn Pathol 15: 246–258, 1998.
9. Den Boer M, Voshol PJ, Kuipers F, Havekes LM, and Romijn JA. Hepatic steatosis: a mediator of the metabolic syndrome. Lessons from animal models. Arterioscler Thromb Vasc Biol 24: 644–649, 2004.
10. Fisher EA, Pan M, Chen X, Wu X, Wang H, Jamil H, Sparks JD, and Williams KJ. The triple threat to nascent apolipoprotein B. Evidence for multiple, distinct degradative pathways. J Biol Chem 276: 27855–27863, 2001.
11. Foufelle F and Ferre` P. New perspectives in the regulation of hepatic glycolytic and lipogenic genes by insulin and glucose: a role for the transcription factor sterol regulatory element binding protein-1c. Biochem J 366: 377–391, 2002.
12. Fraser R. Size and lipid composition of chylomicrons of different Svedberg units of flotation. J Lipid Res 11: 60–65, 1970.
13. Fromenty B and Pessayre D. Inhibition of mitochondrial beta-oxidation as a mechanism of hepatotoxicity. Pharmacol Ther 67: 101–154, 1995.

14. Gibbons GF, Bartlett SM, Sparks CE, and Sparks JD. Extracellular fatty acids are not utilized directly for the synthesis of very-low-density lipoprotein in primary cultures of rat hepatocytes. Biochem J 287: 749–753, 1992.
15. Goudriaan JR, Dahlmans VEH, Teusink B, Ouwens DM, Febbraio M, Maassen JA, Romijn JA, Havekes LM, and Voshol PJ. CD36 deficiency increases insulin sensitivity in muscle, but induces insulin resistance in the liver in mice. J Lipid Res 44: 2270–2277, 2003.
16. Grefhorst A, Elzinga BM, Voshol PJ, Plösch T, Kok T, Bloks VW, van der Sluijs FH, Havekes LM, Romijn JA, Verkade HJ, and Kuipers F. Stimulation of lipogenesis by pharmacological activation of the liver X receptor leads to production of large, triglyceride-rich very low density lipopoprotein particles. J Biol Chem 277: 34182–34190, 2002.
16a.Grefhorst A, van Dijk TH, Hammer A, van der Sluijs FH, Havinga R, Havekes LM, Romijn JA, Groot PH, Reijngoud D-J, and Kuipers F. Differential effects of pharmacological liver X receptor activation on hepatic and peripheral insulin sensitivity in lean and ob/ob mice. Am J Physiol Endocrinol Metab. In press.
17. Guerre-Millo M, Rouault C, Poulain P, Andre´ J, Poitout V, Peters JM, Gonzalez FJ, Fruchart JC, Reach G, and Staels B. PPAR-α-null mice are protected from high-fat diet-induced insulin resistance. Diabetes 50: 2809–2814, 2001.
18. Hohorst HJ. D-Glucose-6-phosphat und D-fructose-6-phosphat. In: Methoden der Enzymatischen Analyse, edited by Bergmeyer HU. Weinheim, Germany: Verlag Chemie, 1970.
19. Isusi E, Aspichueta P, Liza M, Hernández ML, Díaz C, Hernández G, Martínez MJ, and Ochoa B. Short- and long-term effects of atorvastatin, lovastatin and simvastatin on the cellular metabolism of cholesteryl esters and VLDL secretion in rat hepatocytes. Atherosclerosis 153: 283–294, 2000.
20. Keppler D and Decker Glykogen K. Bestimmung mit Amyloglucosidase. In: Methoden der Enzymatischen Analyse, edited by Bergmeyer HU. Weinheim, Germany: Verlag Chemie, 1970.
21. Kim JK, Fillmore JJ, Sunshine MJ, Albrecht B, Higashimori T, Kim DW, Liu ZX, Soos TJ, Cline GW, O'Brien WR, Littman DR, and Shulman GI. PKC- Θ knockout mice are protected from fat-induced insulin resistance. J Clin Invest 114: 823–827, 2004.
22. Kiorpes TC, Hoerr D, Ho W, Weaner LE, Inman MG, and Tutwiler GF. Identification of 2-tetradecylglycidyl coenzyme A as the active form of methyl 2-tetradecylglycidate (methyl palmoxirate) and its characterization as an irreversible, active site-directed inhibitor of carnitine palmitoyltransferase A in isolated rat liver mitochondria. J Biol Chem 259: 9750–9755, 1984.
23. Kuipers F, Havinga R, Bosschieter H, Toorop GP, Hindriks FR, and Vonk RJ. Enterohepatic circulation in the rat. Gastroenterology 88: 403–411, 1985.
24. Kumar KS and Malet PF. Nonalcoholic steatohepatitis. Mayo Clin Proc 75: 733–739, 2000.
25. Lepage G and Roy CC. Direct transesterification of all classes of lipids in a one-step reaction. J Lipid Res 27: 114–120, 1986.
26. Lowry OH, Rosenbrough NJ, Farr AL, and Randall RJ. Protein measurement with Folin reagent. J Biol Chem 193: 265–275, 1951.
27. Mensenkamp AR, Jong MC, van Goor H, van Luyn MJA, Bloks V, Havinga R, Voshol PJ, Hofker MH, Willems van Dijk K, Havekes LM, and Kuipers F. Apolipoprotein E participates in the regulation of very low density lipoprotein-triglyceride secretion by the liver. J Biol Chem 274: 35711–35718, 1999.
28. Noga AA, Zhao Y, and Vance DE. An unexpected requirement for phosphatidylethanolamine N-methyltransferase in the secretion of very low density lipoproteins. J Biol Chem 277: 42358–42365, 2002.
29. Ouwens DM, van der Zon GCM, Pronk GJ, Bos JL, Mo¨ller W, Cheatham B, Kahn CR, and Maassen JA. A mutant insulin receptor induces formation of a Shc-growth factor receptor bound protein 2 (Grb2) complex and p21ras-GTP without detectable interaction of insulin receptor substrate 1 (IRS1) with Grb2. Evidence for IRS1-independent p21ras-GTP formation. J Biol Chem 269: 33116–33122, 1994.
30. Peterson J, Bihain BE, Bengtsson-Olivecrona G, Deckelbaum RJ, Carpentier YA, and Olivecrona T. Fatty acid control of lipoprotein lipase: a link between energy metabolism and lipid transport. Proc Natl Acad Sci USA 87: 909–913, 1990.
31. Plösch T, Kok T, Bloks VW, Smit MJ, Havinga R, Chimini G, Groen AK, and Kuipers F. Increased hepatobiliary and fecal cholesterol excretion upon activation of the liver X receptor is independent of ABCA1. J Biol Chem 277: 33870–33877, 2002.
32. Ramsay RR, Gandour RD, and van der Leij FR. Molecular enzymology of carnitine transfer and transport. Biochim Biophys Acta 1546: 21–43, 2001.
33. Rinaldo P, Matern D, and Bennett MJ. Fatty acid oxidation disorders. Annu Rev Physiol 64: 477–502, 2002.
34. Saltiel AR and Kahn CR. Insulin signalling and the regulation of glucose and lipid metabolism. Nature 414: 799–806, 2001.
35. Seppälä-Lindroos A, Vehkavaara S, Häkkinen AM, Goto T, Westerbacka J, Sovijärvi A, Halavaare J, and Yki-Järvinen H. Fat accumulation in the liver is associated with defects in insulin suppression of glucose production and serum free fatty acids independent of obesity in normal men. J Clin Endocrinol Metab 87: 3023–3028, 2002.
36. Sparks JD and Sparks CE. Insulin modulation of hepatic synthesis and secretion of apolipoprotein B by rat hepatocytes. J Biol Chem 265: 8854–8862, 1990.

37. Telting D, van der Zon GC, Dorrestijn J, and Maassen JA. IRS-1 tyrosine phosphorylation reflects insulin-induced metabolic and mitogenic repsonses in 3T3–L1 pre-adipoctes. Arch Physiol Biochem 109: 52–56, 2001.
38. Tutwiler GF, Ho W, and Mohrbacher RJ. 2-Tetradecylglycidic acid. Methods Enzymol 72: 393–397, 1981.
39. Tutwiler GF and Ryzlak MT. Inhibition of mitochondrial carnitine palmitoyl transferase by 2-tetradecylglycidic acid (McN-3802). Life Sci 26: 393–397, 1980.
40. Van Dijk TH, Boer TS, Havinga R, Stellaard F, Kuipers F, and Reijngoud DJ. Quantification of hepatic carbohydrate metabolism in conscious mice using serial blood and urine spots. Anal Biochem 322: 1–13, 2003.
41. Vaz FM and Wanders RJA. Carnitine biosynthesis in mammals. Biochem J 361: 417–429, 2002.
42. Verkade HJ, Fast DG, Rusin˜ol AE, Scraba DG, and Vance DE. Impaired biosynthesis of phosphatidylcholine causes a decrease in the number of very low density lipoprotein particles in the Golgi but not in the endoplasmic reticulum of rat liver. J Biol Chem 268: 24990–24996, 1993.
43. Vessby B, Uusitupa M, Hermansen K, Riccardi G, Rivellese AA, Tapsell LC, Na¨lse´n C, Berglund L, Louheranta A, Rasmussen BM, Calvert GD, Maffetone A, Pedersen E, Gustafsson IB, and Storlien LH. Substituting dietary saturated for monounsaturated fat impairs insulin sensitivity in healthy men and women: the KANWU study. Diabetologia 44: 312–319, 2001.
44. Wiegman CH, Bandsma RHJ, Ouwens M, van der Sluijs FH, Havinga R, Boer T, Reijngoud DJ, Romijn JA, and Kuipers F. Hepatic VLDL production in ob/ob mice is not stimulated by massive de novo lipogenesis but is less sensitive to the suppressive effects of insulin. Diabetes 52: 1081–1089, 2003.
45. Wolkowicz PE, Urthaler F, Forrest C, Shen H, Durand J, Wei CC, Oparil S, and Dell'Italia LJ. 2-Tetradecylglycidic acid, an inhibitor of carnitine palmitoyltransferase-1, induces myocardial hypertrophy via the AT1 receptor. J Mol Cell Cardiol 31: 1405–1412, 1999.

# Chapter 7

# Induction of hepatic lipogenic gene expression upon pharmacological inhibition of glucose-6-phosphate translocase is independent of liver X receptor alpha

Aldo Grefhorst[1*], Marijke Schreurs[1*], Maaike H. Oosterveer[1], Rick Havinga[1], Louis M. Havekes[2,3], Johannes A. Romijn[4], Andreas W. Herling[5], Dirk-Jan Reijngoud[1], Folkert Kuipers[1]

[1]Laboratory of Pediatrics, University Medical Center Groningen
[2]TNO Prevention and Health, Leiden
[3]Departments of General Internal Medicine and Cardiology, Leiden University Medical Center
[4]Department of Endocrinology and Diabetes, Leiden University Medical Center
[5]Aventis Pharma Germany, Frankfurt, Germany
[*]Contributed equally to this study

**In preparation**

## Abstract

In mammals, hepatic expression of lipogenic genes is regulated by the coordinate action of thetranscription factors sterol-regulatory element-binding protein-1c (SREBP-1c), carbohydrate responsive element binding protein (ChREBP) and liver X receptor (LXR). The "master-switch" LXR controls not only transcription of *Srebp-1c* and *Chrebp* but also ChREBP activity. Treatment of mice with S4048, a pharmacological inhibitor of glucose-6-phosphate translocase, results in increased hepatic triglyceride concentrations associated with markedly enhanced transcription of lipogenic genes. We used C57BL/6J OlaHsd mice as well as LXRα -/- mice and their wild-type littermates to investigate which lipogenic transcription factor is critical for S4048-induced *de novo* lipogenesis and hepatic steatosis. S4048-treatment resulted in similar induction of hepatic steatosis and lipogenic gene expression in all strains of mice, *i.e.*, does not require the presence of LXRα. Expression of the ChREBP target gene pyruvate kinase was significantly increased, but expression of *Srebp-1c* and its target gene glucokinase was not affected or even decreased by S4048. Nuclear translocation of ChREBP was not affected, probably related to concomitantly increased AMPK activity. These data strongly indicate involvement of ChREBP but not of SREBP-1c and LXRα in S4048-induced *de novo* lipogenesis and hepatic steatosis.

## Introduction

In fed conditions, liver and muscle store excess glucose as glycogen, but this storage capacity is limited (1). A certain amount of glucose is therefore broken down in the glycolytic pathway to yield pyruvate and, after passing the tricarboxylic acid cycle, acetyl-CoA moieties that can be used for production of fatty acids and triglycerides (TGs) in a process called *de novo* lipogenesis (DNL). Hepatic transcription of genes encoding for enzymes involved in DNL is tightly controlled by three transcription factors, *i.e.*, sterol-regulatory element-binding protein-1c (SREBP-1c) (2), carbohydrate responsive element binding protein (ChREBP) (3,4), and liver X receptor (LXR) (5,6).

SREBP-1c, a basic-helix-loop-helix-leucine-zipper transcription factor bound in inactive form to the ER membrane, is known to facilitate transcription of many genes involved in DNL (2), including acetyl-CoA carboxylase (ACC), fatty acid synthase (FAS), and acyl-CoA synthase (ACS) upon its activation. Both transcription and activation of SREBP-1c itself is tightly regulated by insulin (7).

ChREBP binds as a heterodimer with Mlx (8) to the carbohydrate response element (ChoRE) composed of two E-box (5'-CACGTG-3') or E-box-like sequences present in promoters of target genes. Upon increasing intracellular levels of the glucose metabolite xylulose-5-phosphate (Xu5P), protein phosphatase-2A (PP2A) becomes active and dephosphorylates ChREBP. Translocation of ChREBP into the nucleus is enhanced upon dephosphorylation of Ser196. Dephosporylation of Thr666 enhances the binding activity of ChREBP to DNA (9). AMP-activated protein kinase (AMPK) phosphorylates ChREBP on Ser196 and protein kinase A (PKA) phosphorylates ChREBP on both Thr666 and Ser196 and can thus inhibit ChREBP-mediated gene transcription (10). Activity of AMPK is increased upon elevated energy-usage (*e.g.*, exercise) (11). Remarkably, most genes regulated by SREBP-1c also are regulated by ChREBP (12), *i.e.*, *Fas, Acc* and *Acs*. Expression of the gene encoding pyruvate kinase (PK) is regulated by ChREBP, but not by SREBP-1c (10). In contrast, expression of the gene encoding glucokinase (GK) is regulated by SREBP-1c, but not by ChREBP (13).

LXR has been identified as an oxysterol-activated nuclear receptor (14-16) that, after ligand-binding, forms a heterodimer with the retinoid X receptor (RXR). The LXR/RXR heterodimer binds to a LXR response element (LXRE), resulting in adaptation of gene transcription (17). LXR controls expression of various genes involved in DNL, in part via stimulation of *Srebp-1c* transcription (5,18,19), but also by direct effects on transcription of *Fas* (20). In experiments with SREBP-1c -/- mice, it was shown that pharmacological LXR activation increased *Acc* expression independent of SREBP-1c (21). The promoter region of the ACC-gene lacks an LXRE, suggesting indirect, SREBP-1c-independent LXR-effects. Recently, it was shown that LXR also regulates mRNA levels of ChREBP (22). Moreover, it was speculated that ChREBP activity was mediated by LXR via effects on AMPK (22).

S4048 is a pharmacological inhibitor of glucoss-6-phosphate (G6P) translocase (G6PT) and, when given to animals, provides a model of glycogen storage disease type I (GSDI). GSDI patients have a defect in the glucose-6-phosphatase (G6Pase) enzyme complex, consisting of G6PT and G6P hydrolase (G6PH). As a result of this defect, the patients do not only show increased hepatic glycogen levels, but also massively increased DNL (23). Treatment of rats with S4048 resulted in elevated hepatic G6P levels (24) and increased lipogenesis (25), resulting in hepatic steatosis. Because Xu5P is an intermediate in the pentose phosphate pathway that is markedly enhanced upon increasing G6P levels (26), the data gathered so far strongly suggest a role of ChREBP in the S4048-induced lipogenesis, but the exact roles of the other lipogenic transcription factors have remained unclear. In the present study, we therefore questioned which lipogenic transcription factor(s) is critically involved in S4048-induced DNL and hepatic steatosis.

## Material and methods

### *In vivo experiments*

Male C57BL/6J OlaHsd mice (Harlan, Horst, The Netherlands) and LXRα -/- mice and their wild-type littermates on a mixed C57BL/6J Sv129/OlaHsd background were housed in a light- and temperature controlled facility and were fed a commercially available lab chow (RMH-B, Hope Farms BV, Woerden, The Netherlands) and had free access to water. The mice received humane care and experimental procedures were in accordance with local guidelines for use of experimental animals. S4048 was infused to the mice via a permanent catheter in the right atrium of the heart (27) from which the entrance was attached to the skull. The mice were allowed a recovery period of at least five days after surgery. Mice were kept in metabolic cages during the experiment and the preliminary fasting period, allowing frequent collection small tail blood samples under conscious and unrestrained conditions (28). After nine hours of fasting, the mice were infused for six hours with S4048 (a generous gift of Aventis Pharma, Frankfurst, Germany) (5.5 mg S4048/ml PBS with 6% DMSO, 0.135 ml/h). Blood glucose levels were measured in a small tail blood sample that was taken every hour during the experiment. After the six hours of infusion, the mice were killed by cardiac puncture and the liver was immediately removed, weighed and freeze clamped. The liver was powdered and stored in separate portions until later analyses.

### *Hepatic analyses*

Hepatic concentrations of TG, free cholesterol and total cholesterol were measured using commercial kits (Roche Diagnostics, Mannheim, Germany, and Wako Chemicals, Neuss, Germany) after lipid extraction according to Bligh and Dyer (29). Phospholipid content of the liver was determined according to Böttcher *et al.* (30) after lipid extraction. Protein concentrations in livers were determined according to Lowry *et al.* (31) using bovine serum albumin (Pierce, Rockford, IL) as standard. Hepatic glycogen and G6P levels were determined as described by Bergmeyer (32).

### *Pharmacological LXR activation*

Male C57BL/6J mice received 10 mg/kg of the LXR agonist T0901317 (kindly donated by Organon Laboratories, Oss, The Netherlands) or its solvent by gavage daily for 4 days. T0901317 was dissolved in DMSO and Chremophor (both Sigma, St. Louis, MO, USA) in 5% mannitol/water, to a final concentration of 2.5 mg/ml. On the morning of the fifth day, the liver was quickly removed, weighed and frozen in separate portions for RNA isolation.

Table 7.1. Primers and probes used for realtime-PCR analysis.

| Gene | | Sequences (5' to 3') | GenBank™ accession no. |
|---|---|---|---|
| *ß-Actin* | Forward | AGCCATGTACGTAGCCATCCA | NM 007393 |
| | Reverse | TCTCCGGAGTCCATCACAATG | |
| | Probe | TGTCCCTGTATGCCTCTGGTCGTACCAC | |
| *Pk* | Forward | CGTTTGTGCCACACAGATGCT | NM 013631 |
| | Reverse | CATTGGCCACATCGCTTGTCT | |
| | Probe | AGCATGATCACTAAGGCTCGACCAACTCGG | |
| *Acc1* | Forward | GCCATTGGTATTGGGGCTTAC | NM 133360 |
| | Reverse | CCCGACCAAGGACTTTGTTG | |
| | Probe | CTCAACCTGGATGGTTCTTTGTCCCAGC | |
| *Acc2* | Forward | CATACACAGAGCTGGTGTTGGACT | NM 133904 |
| | Reverse | CACCATGCCCACCTCGTTAC | |
| | Probe | CAGGAAGCCGGTTCATCTCCACCAG | |
| *Fas* | Forward | GGCATCATTGGGCACTCCTT | NM 007988 |
| | Reverse | GCTGCAAGCACAGCCTCTCT | |
| | Probe | CCATCTGCATAGCCACAGGCAACCTC | |
| *G6pt* | Forward | GAGGCCTTGTAGGAAGCATTG | NM 008063 |
| | Reverse | CCATCCCAGCCATCATGAGTA | |
| | Probe | CTCTGTATGGGAACCCTCGCCACG | |
| *G6ph* | Forward | CTGCAAGGGAGAACTCAGCAA | NM 008061 |
| | Reverse | GAGGACCAAGGAAGCCACAAT | |
| | Probe | TCGTTCCCATTCCGCTTCGCCT | |
| *Chrebp* | Forward | GATGGTGCGAACAGCTCTTCT | NM 021455 |
| | Reverse | GGCTGTGTCATGGTGAA | |
| | Probe | CCAGGCTCCTCCTCGGAGCCC | |
| *Srebp-1c* | Forward | GGAGCCATGGATTGCACATT | AF286470 |
| | Reverse | CCTGTCTCACCCCCAGCATA | |
| | Probe | CAGCTCATCAACAACCAAGACAGTGACTTCC | |
| *Gk* | Forward | CCTGGGCTTCACCTTCTCCTT | NM 010292 |
| | Reverse | GAGGCCTTGAAGCCCTTGGT | |
| | Probe | CACGAAGACATAGACAAGGGCATCCTGCTC | |

*RNA isolation and measurement of mRNA levels by Real Time-PCR (Taqman)*

mRNA expression levels in liver was measured by realtime-PCR as described before (6). PCR results were normalised to *β-actin* mRNA levels. The sequences of the primers and probes used are listed in table 7.1.

*Nuclear translocation of ChREBP*

Hepatic nuclear extracts of livers were made according to Itoh *et al*. (33). In short, powdered livers were homogenized with pre-chilled glass douncers in a cytosolic lysis buffer containing 10 mM Hepes, pH 7.5; 1.5 mM $MgCl_2$; 10 mM KCl; and protease inhibitors (Complete, Roche Diagnostics). The homogenate was centrifuged 5 min 5,000 rpm at 4ºC. The centrifugation procedure was repeated with the received supernatant. The supernatant thus received contained the cytosolic fraction. The pellet from the first centrifugation step was dissolved in a nuclear extract buffer containing 50 mM Tris HCl, pH 7.2; 140 mM NaCl; 2 mM EDTA; 1% N-P450; and protease inhibitors (Complete, Roche Diagnostics), and incubated for 30 minutes on ice followed by centrifugation at 15,000 rpm at 4ºC for 5 min. The supernatant retrieved is the nuclear fraction. Protein content was determined using BCA-kit (Pierce) and equal amounts of protein were used to determine ChREBP by Western blotting, using an antibody raised in rabbit (Novus Biologicals, Littleton, CO).

*Hepatic insulin signaling experiment*

After 5:45 hours of S4048-infusion, two C57BL/6J mice in each group (vehicle and S4048) received an i.p. injection of 200 µl water containing 50 mU insulin (Actrapid, Novo Nordisk, Bagsvaerd, Denmark), 2.7 µg somatostatin (UCB, Breda, The Netherlands), 10% glucose and 1% bovine serum albumine (Sigma-Aldrich, St. Louis, MO). Fifteen minutes after the injection, the mice were killed by cardiac puncture and the liver was immediately removed, weighed and freeze clamped until later analysis.

Hepatic lysates were made in buffer (30 mM Tris.Cl pH 7.4; 2.5 mM EDTA pH 8.0; 150 mM NaCl; 1.3 M glycerol; 0.5 mM $Na_3VO_4$; 5 mM NaF; 5 mM $MgCl_2$; and protease inhibitors (Complete, Roche Diagnostics)) and cleared by centrifugation. Protein content was determined using BCA-kit (Pierce) and equal amounts of protein were used to determine PKB-Ser473 and αAMPK-Thr172 by Western blotting, using antibodies against protein kinase B-Ser473P (PKB-Ser473P) and αAMPK-Thr172P raised in rabbit (Cell signaling, Beverly, MA).

*Statistics*

All values represent mean ± standard deviation for the number of animals indicated. Statistical analysis was assessed by Mann-Whitney U test. Level of significance was set at $p<0.05$. Analyses were performed using SPSS for Windows software (SPSS, Chicago, IL, USA).

## Results

*ChREBP but not SREBP-1c is involved in S4048-induced DNL and hepatic steatosis*

Previous experiments from our laboratory (24,25) showed that pharmacological inhibition of G6PT with S4048 resulted in severe hepatic steatosis in rats. In the present study, conscious, unrestrained mice were infused during 6 hours with S4048. In S4048-treated C57BL/6J OlaHsd mice, blood glucose levels were significantly reduced within 1 hour (figure 7.1). At the end of the 6-hour infusion, blood glucose levels were 64% lower in the treated mice compared to untreated mice. In livers of S4048-treated mice, concentrations of glycogen, G6P and TGs were increased compared to control mice (table 7.2). Hepatic cholesterol and phospholipid levels were not affected.

In the livers of S4048-treated mice, expression of genes encoding enzymes involved in DNL, *i.e.*, *Fas*, *Acc1* and *Acc2*, was markedly increased compared to control mice (figure 7.2), suggesting that enhanced DNL contributes to S4048-induced hepatic steatosis in mice. Expression of the genes encoding the G6Pase enzyme complex, G6PT and G6PH, was also increased upon G6PT inhibition. Compared to control mice, hepatic mRNA levels of *Chrebp* and *Pk* in S4048-treated mice were increased by 90% and 400%, respectively. Taken together, this strongly suggests that S4048-induced hepatic steatosis is related to ChREBP-induced DNL, because *Pk* gene expression is regulated by ChREBP but not by SREBP-1c (10). Moreover, upon S4048-infusion, expression of *Srebp-1c* was not affected and mRNA level of its target gene *Gk* was even reduced by 70% (figure 7.2). This suggests that SREBP-1c is not involved in S4048-induced hepatic steatosis, because *Gk* expression is regulated by SREBP-1c and not by ChREBP (13).

To investigate whether ChREBP protein nuclear translocation was affected upon S4048-infusion, we determined the cytosolic and nuclear ChREBP protein levels by Western blotting. Figure 7.3 shows that most of the ChREBP protein is located in the cytosol and that G6PT inhibition, surprisingly, does not affect the subcellular translocation of ChREBP.

Table 7.2. Hepatic parameters of C57BL/6J OlaHsd mice treated with 30 $mg \cdot kg^{-1} \cdot h^{-1}$ glucose-6-phosphate translocator inhibitor S4048 or vehicle.

| | Vehicle | S4048 |
|---|---|---|
| Liverweight (% of body weight) | 5.2 ± 2.2 | 5.1 ± 0.5 |
| Proteins (mg/g liver) | 194 ± 20 | 222 ± 33 |
| Triglycerides (nmol/mg liver) | 25.7 ± 6.9 | 60.3 ± 22.6 * |
| Free cholesterol (nmol/mg liver) | 8.1 ± 1.5 | 8.2 ± 1.6 |
| Cholesterylester (nmol/mg liver) | 1.9 ± 0.7 | 2.5 ± 1.7 |
| Phospholipids (nmol/mg liver) | 37.7 ± 11.8 | 40.3 ± 5.8 |
| Liver glycogen (nmol/mg liver) | 16.1 ± 3.4 | 254.8 ± 85.4 * |
| Liver G6P (nmol/g liver) | 21.4 ± 15.0 | 574.9 ± 133.7 * |

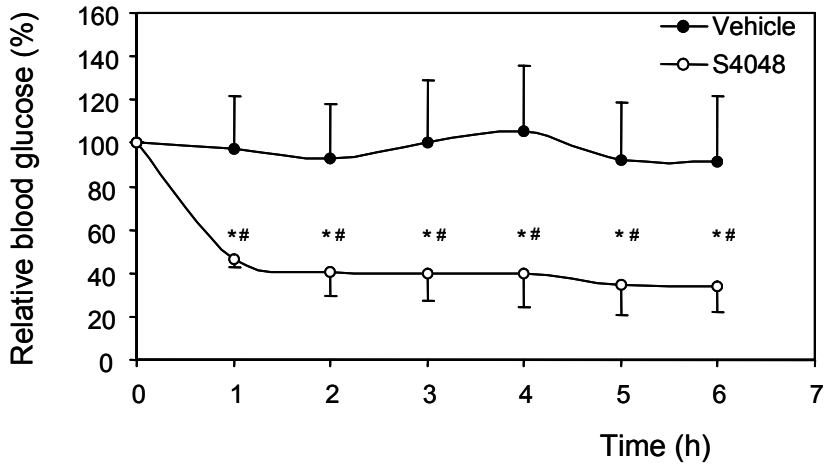


Figure 7.1. Relative blood glucose levels in C57BL/6J OlaHsd mice during of 30 $mg \cdot kg^{-1} \cdot h^{-1}$ glucose-6-phosphate translocase inhibitor S4048 or vehicle. Data are mean ± S.D.; n=7; *, $p<0.05$ S4048 vs. vehicle; #, $P<0.05$ vs. t=0.

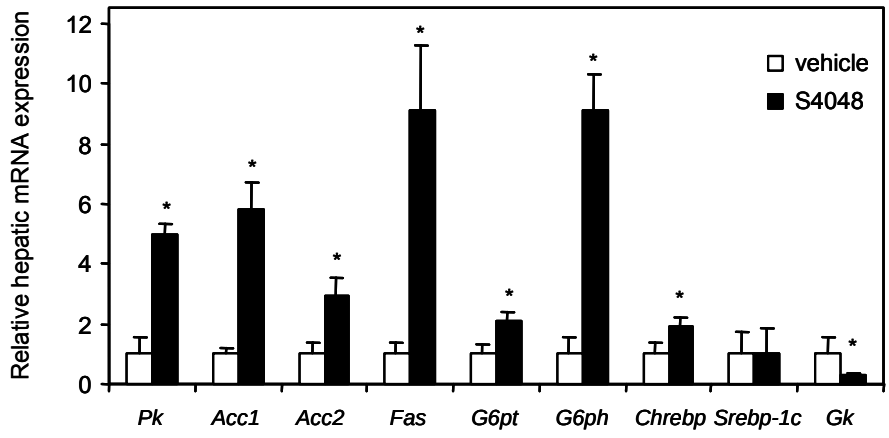


Figure 7.2. Changes in hepatic gene expression patterns upon treatment with 30 $mg \cdot kg^{-1} \cdot h^{-1}$ glucose-6-phosphate translocase inhibitor S4048. Results were normalized to *β-actin* mRNA levels, data from untreated mice defined as '1'. *Pk*, pyruvate kinase; *Acc*, acetyl-CoA carboxylase; *Fas*, fatty acid synthase; *G6pt*, glucose-phosphate translocase; *G6ph*, glucose-6-phosphate hydrolase; *Chrebp*, carbohydrate responsive element binding protein; *Srebp-1c*, sterol-regulatory element-binding protein-1c; *Gk*, glucokinase. Data are mean ± S.D.; n=5; *, $p<0.05$.

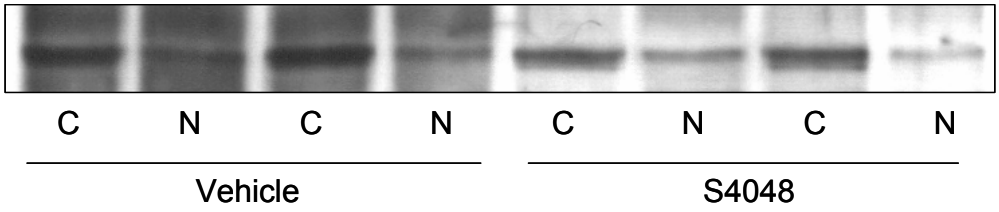


Figure 7.3. ChREBP Western blots of cytosolic (C) and nuclear (N) liver extracts of mice treated with 30 $mg \cdot kg^{-1} \cdot h^{-1}$ glucose-6-phosphate translocase inhibitor S4048 or vehicle.

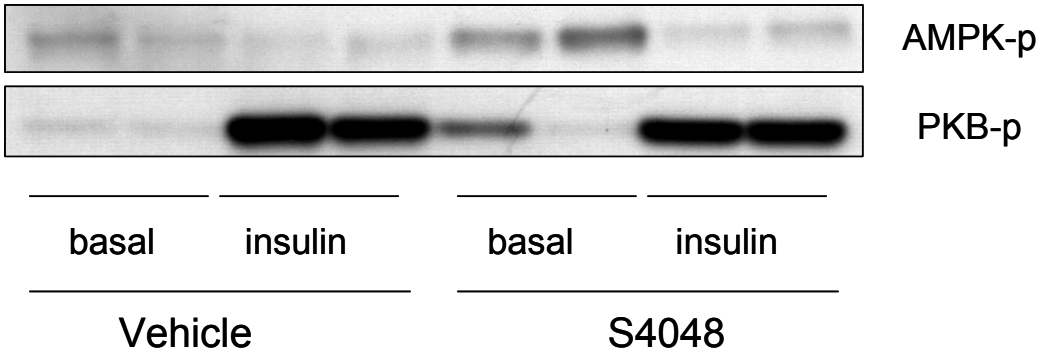


Figure 7.4. Hepatic AMPK-phosphorylation and PKB-phosphorylation Western blots of mice treated with 30 $mg \cdot kg^{-1} \cdot h^{-1}$ glucose-6-phosphate translocase inhibitor S4048 or vehicle, with or without injection of insulin. Each lane represents an individual mouse.

*Increased AMPK-phosphorylation upon S4048-treatment*

To test whether AMPK activity was changed and whether insulin could suppress this activation, as reported by Witters and Kemp (34), hepatic AMPK phosphorylation was determined by Western blotting in livers from control and S4048-treated mice with or without insulin injection (figure 7.4). Remarkably, in livers of mice not treated with insulin, the phosphorylation at Thr172 of the α-subunit of AMPK was clearly increased by S4048-treatment mice. Phosphorylation subsequently decreased to the same extent in control and S4048-treated mice. Moreover, insulin-induced phosphorylation and activation of PKB, the main transducer of insulin-effects on lipid and glucose metabolism (35), was not affected in the S4048-induced fatty livers.

*Pharmacological LXR* activation *regulates expression of the ChREBP target gene Pk*

Treatment of C57BL/6J mice with the pharmacological LXR ligand T0901317 for 4 days resulted in increased hepatic mRNA levels of *Pk* (figure 7.5). Pharmacological LXR activation did not affect *Chrebp* mRNA levels. Taken together, these results show that LXR-induced DNL might, in part, be mediated via ChREBP.

*S4048-induced de novo lipogenesis and hepatic steatosis is independent of LXRα*

To test whether S4048-induced hepatic steatosis is dependent on LXRα, the isoform most likely involved in regulation of lipogenic gene expression, LXRα -/- mice and their wild-type littermates were treated with S4048. Infusion of S4048 resulted in hypoglycemia in all mice with no differences between the knockouts and the wild-type littermates (figure 7.6). After 6 hours of infusion, blood glucose levels were decreased by 45% and 43% in LXRα +/+ and LXRα -/- mice, respectively. Hepatic glycogen, G6P and TG levels increased upon S4048-

infusion in both knockouts and wild-types (table 7.3), although hepatic TG levels upon S4048-treatment remained somewhat lower in the LXRα +/+ mice. The hepatic cholesterylester content was not affected by S4048 in the wild-types, but rose 3.4-fold in the LXRα -/- mice.

To test whether LXRα deficiency affected S4048-induced transcription of lipogenic genes, we measured hepatic gene expression by realtime RT-PCR (figure 7.7). Expression of *Pk*, *Acc1*, *Acc2* and *Fas* was induced by S4048 with no differences between LXRα -/- and LXRα +/+ mice. Thus, S4048-induced expression of lipogenic genes is independent of LXRα. In both type of mice, S4048-infusion induced transcription of *G6pt*, *G6ph* and *Chrebp*. *Srebp-1c* mRNA levels were lower in LXRα -/- mice compared to the wild-types, and its expression decreased even more upon S4048-infusion. mRNA levels of *Gk* were not affected upon S4048-infusion in either type of mice.

Comparable with the C57BL/6J OlaHsdmice, translocation of ChREBP protein was not affected by S4048 (figure 7.8): there was also no difference between LXRα +/+ and LXRα -/- mice in this respect.

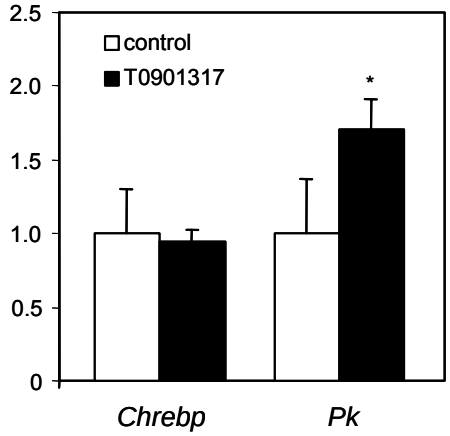


Figure 7.5. Changes in hepatic gene expression patterns upon treatment with the synthetic liver X receptor ligand T0901317. Results normalized to *β-actin* mRNA levels, data from untreated mice defined as '1'. *Pk*, pyruvate kinase; *Chrebp*, carbohydrate responsive element binding protein. Data are mean ± S.D.; n=3; *, p<0.05.

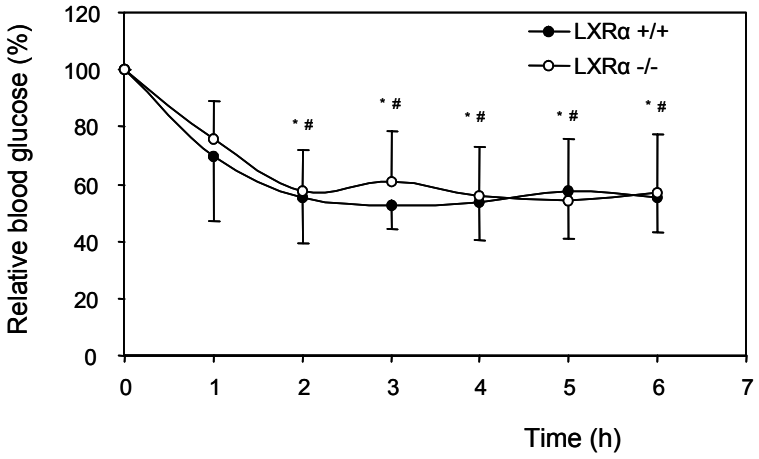


Figure 7.6. Relative blood glucose levels in LXRα +/+ and LXRα -/-mice during infusion with 30 $mg \cdot kg^{-1} \cdot h^{-1}$ glucose-6-phosphate translocase inhibitor S4048. Data are mean ± S.D.; n=6; *, p<0.05 vs. t=0 in LXRα +/+ mice; #, p<0.05 vs. t=0 in LXRα -/- mice.

Table 7.3. Hepatic parameters of LXRα +/+ and LXRα -/-mice treated with or without 30 mg·kg$^{-1}$·h$^{-1}$ glucose-6-phosphate translocater inhibitor S4048.

| | LXRα +/+ | | LXRα -/- | |
|---|---|---|---|---|
| | control | S4048 | Control | S4048 |
| Liverweight (% of body weight) | 4.6 ± 0.4 | 4.6 ± 0.0 | 4.54 ± 0.2 | 4.3 ± 0.3 |
| Proteins (mg/g liver) | 180 ± 14 | 264 ± 15 * | 186 ± 20 | 257 ± 27 * |
| Triglycerides (nmol/mg liver) | 18.1 ± 11.0 | 38.1 ± 2.5 * | 24.7 ± 5.6 | 71.2 ± 15.3 * |
| Free cholesterol (nmol/mg liver) | 7.4 ± 0.6 | 8.6 ± 1.4 | 7.2 ± 0.4 | 7.6 ± 0.3 |
| Cholesterylester (nmol/mg liver) | 1.1 ± 0.1 | 1.9 ± 0.4 | 0.9 ± 0.4 | 3.1 ± 0.3 * |
| Phospholipids (nmol/mg liver) | 44.0 ± 3.7 | 45.2 ± 3.7 | 39.5 ± 3.5 | 45.1 ± 5.0 |
| Liver glycogen (nmol/mg liver) | 78.8 ± 26.2 | 183.0 ± 6.1 * | 101.6 ± 53.0 | 336.0 ± 40.1 * |
| Liver G6P (nmol/g liver) | 262.5 ± 66.0 | 998.8 ± 288.9 * | 340.7 ± 136.8 | 624.5 ± 50.6 * |

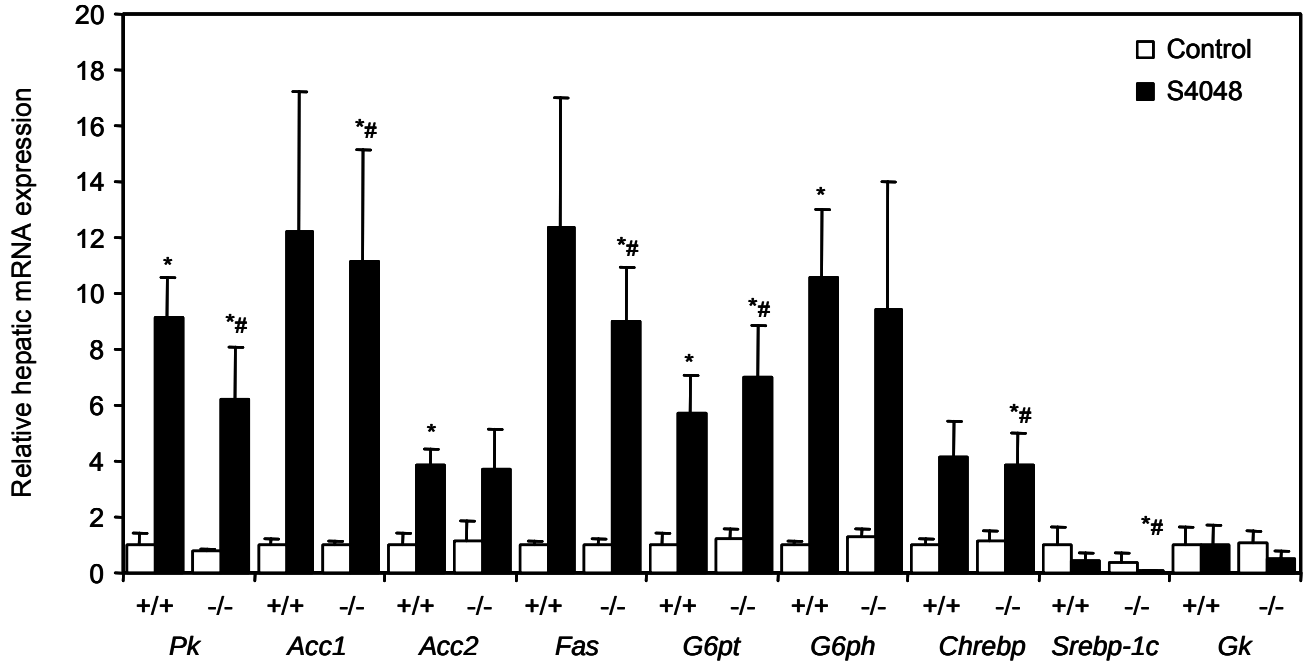


Figure 7.7. Changes in hepatic gene expression patterns in LXRα +/+ and LXRα -/- mice upon treatment with 30 mg·kg$^{-1}$·h$^{-1}$ glucose-6-phosphate translocase inhibitor S4048. Results were normalized to *β-actin* mRNA levels, data from untreated mice defined as '1'. *Pk*, pyruvate kinase; *Acc*, acetyl-CoA carboxylase; *Fas*, fatty acid synthase; *G6pt*, glucose-phopshate translocase; *G6ph*, glucose-6-phosphate hydrolase; *Chrebp*, carbohydrate responsive element binding protein; *Srebp-1c*, sterol-regulatory element-binding protein-1c; *Gk*, glucokinase. Data are mean ± S.D.; n=7 (control mice); n=3 (S4048-treated mice); *, p<0.05 S4048 *vs.* control; #, P<0.05 *vs.* control LXRα +/+ mice.

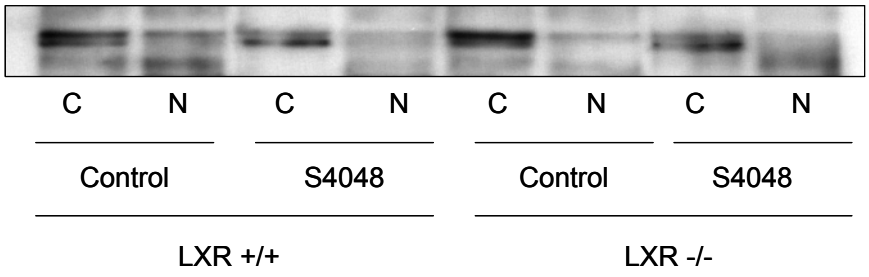


Figure 7.8. ChREBP Western blots of cytosolic (C) and nuclear (N) liver extracts of LXRα +/+ and LXRα -/- mice treated with or without 30 $mg \cdot kg^{-1} \cdot h^{-1}$ glucose-6-phosphate translocase inhibitor S4048.

## Discussion

The regulation of hepatic lipid metabolism, and especially of DNL, is regulated by several transcription factors, including SREBP-1c, ChREBP and LXR. Numerous studies have addressed the roles of SREBP-1c and LXR in control of DNL and development of hepatic steatosis (2,36,37). Other studies have focussed on the interplay between these two factors (5,6,21). So far, few studies have addressed the role of ChREBP in control of DNL (9,12,13) and only very recently it was shown that LXR regulates ChREBP activation and transcription (22). The present study indicates that pharmacological inhibition of G6PT with S4048 in C57BL/6J OlaHsd mice, resulting in increased hepatic G6P and glycogen levels, induces DNL exclusively via ChREBP. Because *Gk* expression was not increased upon S4048-infusion, SREBP-1c is probably not involved in S4048-induced hepatic steatosis. Moreover, LXRα does also not play a role: S4048-treatment had comparable hepatic effects in LXRα +/+ and LXRα -/- mice. Surprisingly, nuclear ChREBP translocation was not increased upon S4048-infusion. This is probably due to changes in phosphorylation state upon S4048-treatment. In livers of both control and S4048-treated mice, insulin decreased AMPK phosphorylation via its effects on PKB.

In previous experiments in rats, blood glucose levels of S4048-treated animals were 60% of that of control rats. (24). More drastic hypoglycemic effects were seen in the C57BL/6J mice (figure 7.1): 6 hours of S4048-infusion resulted in a 64% decrease of the blood glucose levels. The S4048-mediated increases of hepatic TG, G6P and glycogen concentrations were also more pronounced in C57BL/6J mice (table 7.2) than in rats (25). Compared to control rats, hepatic G6P, glycogen and TG levels increased 3-, 2.8-, and 4.6-fold respectively upon S4048-infusion in rats. In C57BL/6J mice, these increases were 27-, 16-, and 2.4-fold, respectively. The differences between S4048-mediated effects in rats and C57BL/6J mice could be due to the increased metabolic flux in mice compared to rats. Our laboratory used stable isotopes from intermediates in hepatic glucose metabolism to study in vivo hepatic glucose fluxes. The flux through G6Pase was 39.9 ± 3.8 $\mu mol \cdot kg^{-1} \cdot min^{-1}$ in Wistar rats (24) whereas this was 228 ± 16 $\mu mol \cdot kg^{-1} \cdot min^{-1}$ in C57BL/6J mice (38). When the G6Pase flux is higher, inhibition of this flux will lead to more drastic effects, *i.e.*, more strongly increased hepatic G6P and glycogen levels after 6 hours of S4048-infusion. In the LXRα +/+ and LXRα -/- mice on a mixed C57BL/6J Sv129/OlaHsd background, however, blood glucose levels decreased only by 44% after 6 hours of S4048-infusion (figure 7.6). The elevations of hepatic G6P, glycogen and TG were also less severe in these mice (table 7.3), indicating lower hepatic glucose flux rates. Indeed, previous studies showed that hepatic G6Pase flux in Sv129 mice was ~70% of that of C57BL/6J mice (39).

Because SREBP-1c and ChREBP control transcription of largely the same genes, it is hard to distinguish effects of both transcription factors on lipogenic gene expression *in vivo*. However, *Pk* expression is regulated by ChREBP but not by SREBP-1c (10) and *Gk* expression is regulated by SREBP-1c but not by ChREBP (13). Focussing on changes in the expression of these two genes in C57BL/6J OlaHsd mice upon S4048 treatment (figure 7.2), it is evident that G6PT inhibition and hence increased G6P levels resulted in enhanced hepatic transcriptional activity of ChREBP but not of SREBP-1c. The fact that levels of the Xu5P precursor G6P were clearly increased upon S4048-infusion also indicates a role for ChREBP. Furthermore, the decreased *Gk* expression upon S4048 infusion could be the result of SREBP-1c mediated effects of insulin (40): it was shown in rats that S4048-infusion resulted in significantly reduced plasma insulin levels (24). Of course, studies with SREBP-1c -/-, ChREBP -/- and/or SREBP-1c -/- ChREBP -/- double knockout mice should be performed to investigate the roles of ChREBP and SREBP-1c in S4048-induced *de novo* lipogenesis. Using the LXRα +/+ and LXRα -/- mice, it was already possible to exclude a role for LXRα in S4048-induced *de novo* lipogenesis. Effects of S4048 on hepatic gene expression and hepatic TG levels did not differ between LXRα +/+ and LXRα -/- mice (figure 7.7 and table 7.3).

So far, the data suggested a role for ChREBP in S4048-induced DNL and we therefore measured ChREBP protein nuclear translocation in C57BL/6J OlaHsd mice as well as in LXRα +/+ and LXRα -/- mice. (figures 7.3 and 7.8). However, no effects of S4048 were seen in either of the three types of mice. Figures 3 and 8 show clearly that ChREBP is predominantly present in the cytosol, as was already shown by Dentin *et al.* (41). The fact that the amount of ChREBP within the nucleus was not changed does not necessarily mean less active ChREBP because it is the dephosphorylation of ChREBP at Thr666 within in the nucleus that enhances its binding to the DNA (10). The phosphorylation state of Ser196 mediates its localization in the cytosol or nucleus (10). Until phospho-specific ChREBP antibodies are available, Western blotting techniques cannot be used to study the effects of S4048 on active ChREBP within the nucleus. In the future, studies with primary hepatocytes and stable cell-lines should be used to study the effects of S4048 on subcellular ChREBP protein localization and DNA-binding.

In the present study, we could not confirm the suggested role of ChREBP in LXR-induced hepatic DNL (22): pharmacological LXR activation nor LXRα deficiency affected hepatic *Chrebp* mRNA levels (figures 7.5 and 7.7). On the other hand, increased *Chrebp* mRNA levels upon S4048-infusion (figures 7.2 and 7.7) did not translate into increased ChREBP protein levels (figures 7.3 and 7.8). The effects of LXR activation on *Pk* mRNA levels (figure 7.5) are therefore presumably mediated by the ChREBP phosphorylation/dephosphorylation state. As mentioned, more advanced ChREBP antibodies and/or *in vitro* experiments should be used to study the effects of S4048 on ChREBP in more detail.

Using Western blotting techniques, we noticed increased phosphorylation of the α-subunit of AMPK upon S4048-treatment (figure 7.4), reflecting increased activity of this kinase. AMPK is known to regulate, at least, the phosphorylation of ChREBP on Thr666, thus reducing its binding to DNA (10). Activity of AMPK is enhanced upon increased AMP and/or decreased ATP levels, thus upon increased energy expenditure (11). In the present hepatic steatotic model, enhanced hepatic AMPK activity could be the result of the increased production of fatty acyl-CoA from fatty acids. This process, mediated by ACS, uses ATP and produces AMP (42). Expression of *Acs* is regulated by both SREBP-1c and ChREBP (7,12). Because insulin reduces AMPK-activity (34), we injected mice with insulin. In control and S4048-treated mice, insulin injection reduced AMPK phosphorylation. Moreover, the key-regulator of insulin signaling, PKB, was also showed increased phosphorylation upon insulin injection, with no difference between S4048-treated and control mice.

PKA is known to phosphorylate ChREBP at both Thr666 and Ser196 (10), suggesting that subcellular ChREBP localisation is presumably regulated by PKA and not by AMPK. Like AMPK, PKA activity is also increased upon increasing energy usage. Thus, enhanced AMPK and/or PKA activity might provide a mechanism to shut off ChREBP-induced DNL.

In conclusion, the present studies strongly suggest that ChREBP, but not SREBP-1c and LXRα, is involved in induction of DNL and development of hepatic steatosis upon pharmacological inhibition of G6PT. Hence, increased DNL in GSDI patients (23) might also be due to effects on ChREBP activity and/or transcription, suggesting that ChREBP might be an important target for future pharmacological interventions in these patients.

## References

1. Bollen, M, Keppens, S, Stalmans, W. Specific features of glycogen metabolism in the liver. Biochem J 336: 19-31, 1998
2. Horton, JD, Goldstein, JL, Brown, MS. SREBPs: activators of the complete program of cholesterol and fatty acid synthesis in the liver. J Clin Invest 109: 1125-1131, 2002
3. Kabashima, T, Kawaguchi, T, Wadzinski, BE, Uyeda, K. Xylulose 5-phosphate mediates glucose-induced lipogenesis by xylulose 5-phosphate-activated protein phosphatase in rat liver. Proc Natl Acad Sci USA 100: 5107-5112, 2003
4. Yamashita, H, Takenoshita, M, Sakurai, M, Bruick, RK, Henzel, WJ, Shillinglaw, W, Arnot, D, Uyeda, K. A glucose-responsive transcription factor that regulates carbohydrate metabolism in the liver. Proc Natl Acad Sci USA 98: 9116-9121, 2001
5. Schultz, JR, Tu, H, Luk, A, Repa, JJ, Medina, JC, Li, L, Schwendner, S, Wang, S, Thoolen, M, Mangelsdorf, DJ, Lustig, KD, Shan, B. Role of LXR in control of lipogenesis. Genes Dev 14: 2831-2838, 2000
6. Grefhorst, A, Elzinga, BM, Voshol, PJ, Plösch, T, Kok, T, Bloks, VW, van der Sluijs, FH, Havekes, LM, Romijn, JA, Verkade, HJ, Kuipers, F. Stimulation of lipogenesis by pharmacological activation of the liver X receptor leads to production of large, triglyceride-rich very low density lipopoprotein particles. J Biol Chem 277: 34182-34190, 2002
7. Hegarty, BD, Bobard, A, Hainault, I, Ferré, P, Bossard, P, Foufelle, F. Distinct roles of insulin and liver X receptor in the induction and cleavage of sterol regulatory element-binding protein-1c. Proc Natl Acad Sci USA 102: 791-796, 2005
8. Ma, L, Tsatsos, NG, Towle, HC. Direct role of ChREBP/Mlx in regulating hepatic glucose-response genes. J Biol Chem 280: 12019-12027, 2005
9. Uyeda, K, Yamashita, H, Kawaguchi, T. Carbohydrate responsive element-binding protein (ChREBP): a key regulator of glucose metabolism and fat storage. Biochem Pharmacol 63: 2075-2080, 2002
10. Kawaguchi, T, Takenoshita, M, Kabashima, T, Uyeda, K. Glucose and cAMP regulate the L-type pyruvate kinase gene by phosphorylation/dephosphorylation of the carbohydrate response element binding protein. Proc Natl Acad Sci USA 98: 13710-13715, 2001
11. Hardie, DG, Hawley, SA. AMP-activated protein kinase: the energy charge hypothesis revisited. Bioessays 23: 1112-1119, 2001
12. Ishii, S, Iizuka, K, Miller, BC, Uyeda, K. Carbohydrate response element binding protein directly promotes lipogenic enzyme gene transcription. Proc Natl Acad Sci USA 101: 15597-15602, 2004
13. Iizuka, K, Bruick, RK, Liang, G, Horton, JD, Uyeda, K. Deficiency of carbohydrate response element-binding protein (ChREBP) reduces lipogenesis as well as glycolysis. Proc Natl Acad Sci USA 101: 7281-7286, 2004
14. Lehmann, JM, Kliewer, SA, Moore, LB, Smith-Oliver, TA, Oliver, BB, Su, J-L, Sundseth, SS, Winegar, DA, Blanchard, DE, Spencer, TA, Willson, TM. Activation of the nuclear receptor LXR by oxysterols defines a new hormone response pathway. J Biol Chem 272: 3137-3140, 1997
15. Willy, PJ, Umesono, K, Ong, ES, Evans, RM, Heyman, RA, Mangelsdorf, DJ. LXR, a nuclear receptor that defines a distinct retinoid response pathway. Genes Dev 9: 1033-1045, 1995
16. Teboul, M, Enmark, E, Li, Q, Wikström, AC, Pelto-Huikko, M, Gustafsson, J-Å. OR-1, a member of the nuclear superfamily that interacts with the 9-cis-retinoic acid receptor. Proc Natl Acad Sci USA 92: 2096-2100, 1995
17. Glass, CK. Differential recognition of target genes by nuclear receptor monomers, dimers, and heterodimers. Endocrine Rev 15: 391-407, 1994
18. Repa, JJ, Liang, G, Ou, J, Bashmakov, Y, Lobaccaro, J-MA, Shimomura, I, Shan, B, Brown, MS, Goldstein, JL, Mangelsdorf, DJ. Regulation of mouse sterol regulatory element-binding protein 1c gene (SREBP-1c) by oxysterol receptors, LXRα and LXRβ. Genes Dev 14: 2819-2830, 2000

19. Yoshikawa, T, Shimano, H, Amemiya-Kudo, M, Yahagi, N, Hasty, AH, Matsuzaka, T, Okazaki, H, Tamura, Y, IIzuka, Y, Ohashi, K, Osuga, J-I, Harada, K, Gotoda, T, Kimura, S, Ishibashi, S, Yamada, N. Identification of liver X receptor-retinoid X receptor as an activator of the sterol regulatory element-binding protein 1c gene promoter. Mol Cell Biol 21: 2991-3000, 2001
20. Joseph, SB, Laffitte, BA, Patel, PH, Watson, MA, Matsukuma, KE, Walczak, R, Collins, JL, Osborne, TF, Tontonoz, P. Direct and indirect mechanisms for regulation of fatty acid synthase gene expression by liver x receptors. J Biol Chem 277: 11019-11025, 2002
21. Liang, G, Yang, J, Horton, JD, Hammer, RE, Goldstein, JL, Brown, MS. Diminished hepatic response to fasting/ refeeding and liver X receptor agonists in mice with selective deficiency of sterol regulatory element-binding protein-1c. J Biol Chem 277: 9520-9528, 2002
22. Cha, J-Y, Repa, JJ. The nuclear oxysterol receptor LXR is a master regulator of hepatic lipogenesis (Abstract). Diabetes 54: suppl 1, 2004
23. Bandsma, RHJ, Rake, JP, Visser, G, Neese, RA, Hellerstein, MK, van Duyvenvoorde, W, Princen, HMG, Stellaard, F, Smit, GPA, Kuipers, F. Increased lipogenesis and resistance of lipoproteins to oxidative modification in two patients with glycogen storage disease type Ia. J Pediatr 140: 256-260, 2002
24. van Dijk, TH, van der Sluijs, FH, Wiegman, CH, Baller, JFW, Gustafson, LA, Burger, H-J, Herling, AW, Kuipers, F, Meijer, AJ, Reijngoud, D-J. Acute inhibition of hepatic glucose-6-phosphate does not affect gluconeogenesis but directs gluconeogenic flux toward glycogen in fasted rats. J Biol Chem 276: 25727-25735, 2001
25. Bandsma, RHJ, Wiegman, CH, Herling, AW, Burger, H-J, ter Harmsel, A, Meijer, AJ, Romijn, JA, Reijngoud, D-J, Kuipers, F. Acute inhibition of glucose-6-phosphate translocator activity leads to increased de novo lipogenesis and development of hepatic steatosis without affecting VLDL production in rats. Diabetes 50: 2591-2597, 2001
26. Veech, RL. A humble hexose monophosphate pathway metabolite regulates short- and long-term control of lipogenesis. Proc Natl Acad Sci USA 100: 5578-5580, 2003
27. Kuipers, F, Havinga, R, Bosschieter, H, Toorop, GP, Hindriks, FR, Vonk, RJ. Enterohepatic circulation in the rat. Gastroenterology 88: 403-411, 1985
28. van Dijk, TH, Boer, TS, Havinga, R, Stellaard, F, Kuipers, F, Reijngoud, D-J. Quantification of hepatic carbohydrate metabolism in conscious mice using serial blood and urine spots. Anal Biochem 322: 1-13, 2003
29. Bligh, EG, Dyer, WJ. A rapid method of total lipid extraction and purification. Can J Biochem Physiol 37: 911-917, 1959
30. Böttcher, CFJ, van Gent, CM, Pries, C. A rapid and sensitive sub-micro-phosphorus determination. Anal Chim Acta 24: 203-204, 1961
31. Lowry, OH, Rosenbrough, NJ, Farr, AL, Randall, RJ. Protein measurement with Folin reagent. J Biol Chem 193: 265-275, 1951
32. Bergmeyer, HU. In Methods of Enzymatic Analysis. Academic Press New York, 1974,
33. Itoh, M, Adachi, M, Yasui, H, Takekawa, M, Tanaka, H, Imai, K. Nuclear export of glucocorticoid receptor is enhanced by c-Jun N-terminal kinase-mediated phosphorylation. Mol Endocrinol 16: 2382-2392, 2002
34. Witters, LA, Kemp, BE. Insulin activation of acetyl-CoA carboxylase accompanied by inhibition of the 5'-AMP-activated protein kinase. J Biol Chem. 267: 2864-2867, 1992
35. Saltiel, AR, Kahn, CR. Insulin signalling and the regulation of glucose and lipid metabolism. Nature 414: 799-806, 2001
36. Shimomura, I, Bashmakov, Y, Horton, JD. Increased levels of nuclear srebp-1c associated with fatty livers in two mouse models of diabetes mellitus. J Biol Chem 274: 30028-30032, 1999
37. Browning, JD, Horton, JD. Molecular mediators of hepatic steatosis and liver injury. J Clin Invest. 114: 147-152, 2004
38. Grefhorst, A, van Dijk, TH, Hammer, A, van der Sluijs, FH, Havinga, R, Havekes, LM, Romijn, JA, Groot, PH, Reijngoud, D-J, Kuipers, F. Differential effects of pharmacological liver X receptor activation on hepatic and peripheral insulin sensitivity in lean and ob/ob mice. Am J Physiol Endocrinol Metab 289: E829-E838, 2005
39. Goudriaan, JR, Dahlmans, VEH, Teusink, B, Ouwens, DM, Febbraio, M, Maassen, JA, Romijn, JA, Havekes, LM, Voshol, PJ. CD36 deficiency increases insulin sensitivity in muscle, but induces insulin resistance in the liver in mice. J Lipid Res 44: 2270-2277, 2003
40. Kim, S-Y, Kim, H, Kim, T-H, Im, S-S, Park, S-K, Lee, I-K, Kim, K-S, Ahn, Y-H. SREBP-1c mediates the insulin-dependent hepatic glucokinase expression. J Biol Chem 279: 30823-30829, 2004
41. Dentin, R, Benhamed, F, Pégorier, J-P, Foufelle, F, Viollet, B, Vaulont, S, Girard, J, Postic, C. Polyunsaturated fatty acids suppress glycolytic and lipogenic genes through the inhibition of ChREBP nuclear translocation. J Clin Invest 115: 2843-2854, 2005
42. Coleman, RA, Lee, DP. Enzymes of triacylglycerol synthesis and their regulation. Prog Lipid Res 43: 134-176, 2004

# Chapter 8

# The role of lipogenic transcription factors in diabetic dyslipidemia

Aldo Grefhorst, Folkert Kuipers

Laboratory of Pediatrics, University Medical Center Groningen

**In preparation**

## Abstract

Diabetes mellitus type 2 is associated with hepatic fat accumulation (hepatic steatosis) and dyslipidemia, the latter a major risk factor for the development of diabetes-associated coronary heart disease. The components of diabetic dyslipidemia are elevated plasma triglyceride (TG) levels, low concentrations of high density lipoprotein (HDL) cholesterol and the presence of small, dense low density lipoprotein (LDL) particles. An increased production of large, TG-rich very low density lipoprotein (VLDL) particles is considered a major cause of all aspects of diabetic dyslipidemia. In this review, we will discuss the role of transcription factors that (indirectly) control the actions of insulin, glucose and lipids on hepatic fatty acid and TG metabolism and hence on VLDL production. Key "lipogenic" transcription factors that regulate expression of genes encoding enzymes and transporters involved in hepatic lipid and glucose metabolism are sterol-regulatory element-binding protein-1c (SREBP-1c), carbohydrate responsive element binding protein (ChREBP), and liver X receptor (LXR). However, only speculative data exist about their roles in controlling (insulin sensitivity of) VLDL secretion. Thus, only well-conducted *in vivo* studies, *i.e.* with knockout mice and pharmacological ligands, will give proper information about the role of lipogenic gene transcription in (insulin sensitivity of) VLDL production and hence diabetic dyslipidemia.

## The metabolic syndrome, diabetes and dyslipidemia

Related to the increased incidence of obesity in the Western world, the combination of metabolic abnormalities collectively referred to as the metabolic syndrome shows a rapidly increasing prevalence. Components of the metabolic syndrome are hyperglycemia, insulin resistance, central obesity, dyslipidemia, and hypertension. According to the various guidelines (WHO 1999, European Group for the Study of Insulin Resistance 1999, and the ATP-III 2001) a person that has at least three of these components has attracted the metabolic syndrome (1). The guidelines agree that insulin resistance and/or diabetes mellitus type 2 are core components of the metabolic syndrome.

Diabetes mellitus type 2 is characterized by elevated blood glucose levels as a result of absent or decreased secretion of insulin by the pancreatic B-cells. In general, dysfunctional B-cells are a consequence of decreased sensitivity of the body for insulin (insulin resistance), for which the pancreas firstly compensated for by enhancing its insulin production. Insulin stimulates uptake of glucose by the peripheral tissues, *i.e.*, muscle and adipose tissue, and inhibits hepatic glucose production (HGP). Patients with diabetes mellitus type 1 have elevated blood glucose levels because their pancreas does not produce insulin. In these patients, administration of exogenous insulin can lower blood glucose levels to normal values. In diabetes mellitus type 2 patients, however, liver and peripheral tissues are insensitive to the actions of insulin and exogenous insulin will not have the desired metabolic effects.

Diabetes mellitus type 2 is also associated with hepatic fat accumulation (hepatic steatosis) (2) and dyslipidemia, the latter a well-known risk factor for the development of cardiovascular disease (3). Studies have shown that patients with diabetes mellitus type 2 have a markedly increased risk for heart attacks (4,5). The components of diabetic dyslipidemia are increased plasma triglyceride (TG) levels, low concentrations of high density lipoprotein (HDL) cholesterol and the presence of small, dense low density lipoprotein (LDL) particles. An increased production of large, TG-rich very low density lipoprotein (VLDL) particles is considered a major cause of all aspects of diabetic dyslipidemia (6). In general, it is thought that diabetic patients secrete more large VLDL particles (7) and that insulin is not able to suppress the production rate of the large VLDL particles.

In this review, we will discuss the role of proteins that are able to regulate gene transcription (transcription factors) that can (indirectly) control the actions of insulin, glucose or lipids on fatty acid and TG metabolism and eventually VLDL production.

## Whole-body fatty acid and triglyceride homeostasis

TG molecules are the most energy-dense molecules in mammalian physiology and consist of three fatty acids esterified to a glycerol backbone. Normally, a surplus of (dietary) energy is incorporated into TG and stored in adipose tissue. Upon fasting, the adipose TG store is used to deliver energy in the form of free fatty acids (FFA) to maintain whole-body energy balance. Transport of dietary and de novo synthesized lipids from the liver to the peripheral tissues (*i.e.*, adipocytes), and from the adipocytes back to the liver is important in this balance. The liver plays a crucial role because it can synthesize, store, secrete and oxidize fatty acids.

Because TGs are very hydrophobic, they need to be transported in blood as lipoproteins, together with cholesterol, phospholipids and proteins. The core of a lipoprotein contains TG and esterified cholesterol whereas the surface consits of phospholipids and free cholesterol. Embedded in the lipoprotein surface are the so-called apolipoproteins, proteins are needed for stabilisation of the particle and solubility of the core lipids (8). Moreover, apolipoproteins act as ligands for receptors and are required for the actions of specific enzymes (8).

### *Triglyceride-rich lipoproteins*

In the enterocytes, dietary TGs are incorporated into lipoproteins called chylomicrons. Apolipoprotein B (apoB) is the main protein of TG-containing lipoproteins (chylomicrons and VLDL). In the surface of chylomicrons, a truncated form of apoB is present, consisting of only 48% of the N-terminal part and is therefore called apoB48. Editing of the apoB100 mRNA into apoB48 mRNA is regulated by the apoB editing complex-1 (apobec1) (9). In the circulation, the TG content of these particles is lipolysed primarily by lipoprotein lipase (LPL) secreted by muscle and adipose tissue. ApoC-III inhibits the actions of LPL while apoC-II enhances its lipolytic actions. The released fatty acids can be taken up and are reesterified into TGs (*e.g.*, in adipocytes) or used as an energy source (*e.g.*, in muscle). As a result of lipolysis, chylomicrons are depleted of TGs, become smaller and are referred to as chylomicron remnants. Both chylomicrons and chylomicron remnants are cleared by the liver upon binding to the LDL receptor, the LDL receptor related protein (LRP) or hepatic lipase (HL) (10).

TG transport from the liver to peripheral tissues induces their incorporation into VLDL particles. VLDL-TGs are lipolyzed by LPL in a similar way as chylomicrons and the fatty acids are taken up by the peripheral tissues. Upon lipolysis, the TG content of the VLDL particle becomes depleted and, as a result, the particle size decreases and the relative cholesterol concentration increases. The cholesterol-dense VLDL remnant particles are called intermediate density lipoprotein (IDL) or LDL particles, depending on their size and density. With increasing VLDL particles size, the ratio of TG over phospholipid will also increase (11) and the resulting LDL particle will contain relatively more cholesterol: small, dense LDL particles. It is known that small, dense LDL particles are associated with increased cardiovascular risk (3,12).

### *Reverse fatty acid flux*

β-oxidation of fatty acids is considered the primary source of the energy and reducing equivalents (ATP, NADH) needed for *de novo* synthesis of glucose (gluconeogenesis) during fasting. Moreover, ß-oxidation generates ketone bodies, an additional fuel source for the brain when glucose levels are low. In the ß-oxidation process, fatty acyl-CoA's are broken down into shorter chains by a series of dehydrogenases. For this process, FFAs are released from the adipose stores after lipolysis of TG by triglyceride hydrolase (TGH) (also called adipose TG lipase (ATGL) (13)) and hormone sensitive lipase (HSL) (14) and carried by serum albumin to the liver. Insulin inhibits lipolysis in peripheral tissues. Thus, upon fasting, when insulin levels are low, the insulin-mediated inhibition of lipolysis is absent and FFAs are released into the circulation, taken up by the liver and partly used in the ß-oxidation process and partly reesterified to form TG. This latter process gives rise to the fasting induced hepatic steatosis (15).

## Assembly of very low density lipoproteins

### *Lipidation of apolipoprotein B*

Production of VLDL is considered a two-step process that takes place in two distinct parts of the liver cell (figure 8.1). Firstly, the apoB molecules become co-transcriptionally lipidated to form a small pre-VLDL particle in the rough endoplasmic reticulum (ER), a process catalyzed by the microsomal triglyceride transfer protein (MTTP) (16). When insufficient lipid is available, the apoB translocation is halted and the protein is degraded. The pre-VLDL particle is transported in Sar1/COPII vesicles to the smooth ER where the second step will take place. It is known that the ADP ribosylation factor-1 (ARF1) can control the formation of VLDL. It is thought that, because ARF1 is part of the COPI secretory complex involved in transport from the ER to the Golgi apparatus, it is able to influence the sorting procedure of pre-VLDL from the rough to the smooth ER (17).

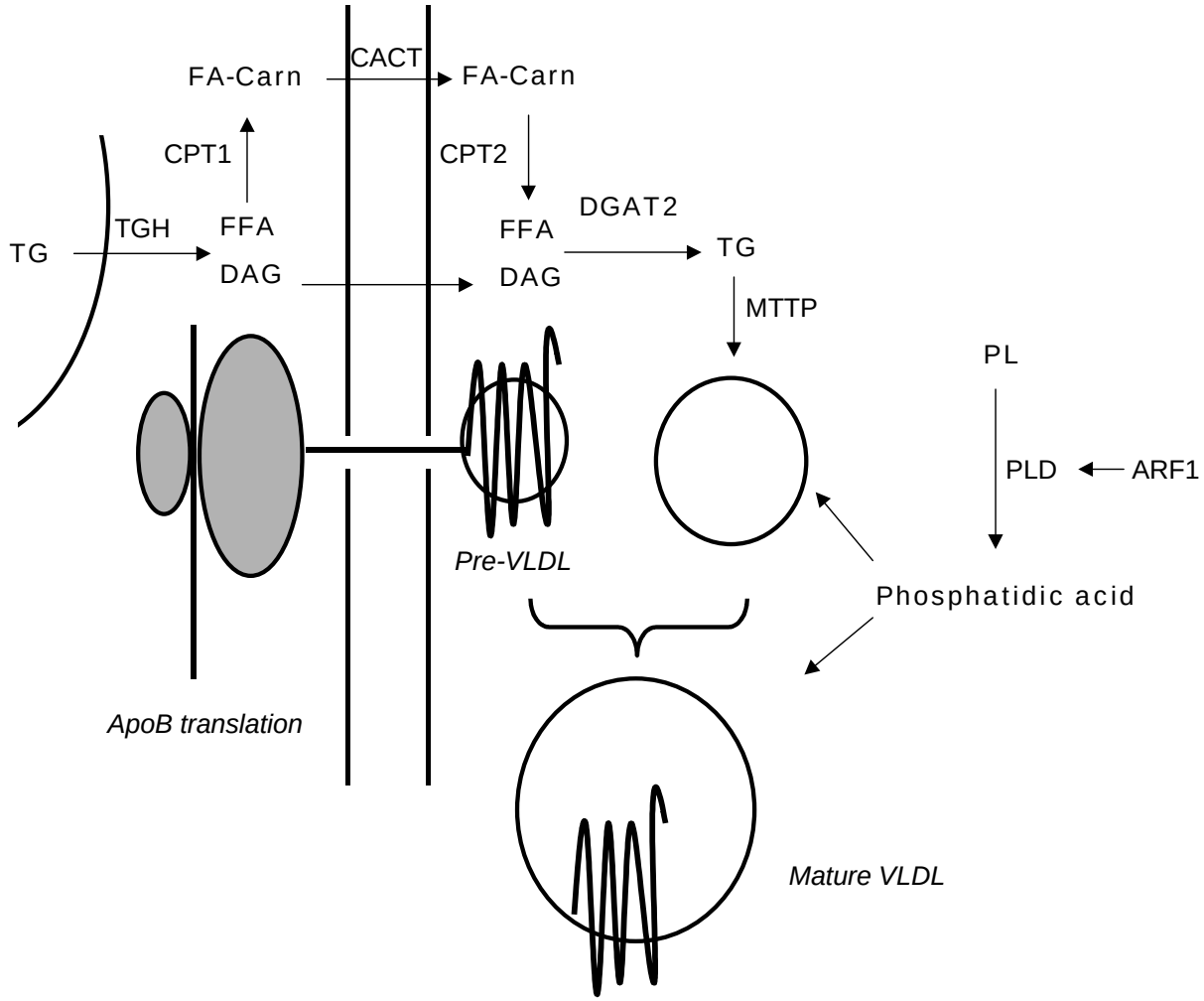


Figure 8.1. Schematic representation of VLDL assembly and secretion, located in the endoplasmic reticulum (left part of the figure) and its membrane. ARF1, ADP ribosylation factor-1; CACT, carnitine acylcarnitine translocase; CPT, carnitine palmitoyl transferase; DAG, diacylglycerol; DGAT2, diacylglycerol acyltransferase; FA, fatty acid; FFA, free fatty acid; MTTP, microsomal triglyceride transport protein; PL, phospholipid; PLD, phospholipase D; TG, triglyceride; TGH, triglyceride hydrolase.

*Lipidation of pre-VLDL particles*

In the second step of VLDL assembly, the pre-VLDL particle is further lipidated and transported to the cellular membrane. This second step again involves the action of MTTP but also that of phospholipase D (PLD), the enzyme controlling conversion of phosphatidylcholine into phosphatidic acid, a TG precursor needed in VLDL assembly (18). Activation of PLD is regulated by ARF1 and recent data show that overexpression of ARF1 not only resulted in increased pre-VLDL translocation to the smooth ER, but, as a result, also in enhanced lipidation of pre-VLDL (17).

*Amount vs. size of VLDL particles*

The amount and size of VLDL particles depends on lipidation of apoB and pre-VLDL in the first and second step, respectively. Depending on the lipidation of the pre-VLDL particle, the liver can secrete VLDL particles that vary in size. The large VLDL particles ($VLDL_1$) and the smaller $VLDL_2$ particles are thought to be secreted via seperate pathways by the liver and to follow seperate routes within the VLDL-IDL-LDL pathway (reviewed by Taskinen (6)). In general, it is thought that diabetic patients secrete more $VLDL_1$ particles (7). Major issues that need to be resolved are whether insulin regulates lipidation of pre-VLDL rather than the assembly of pre-VLDL. And if this is the case, how insulin regulates VLDL lipidation and hence secretion. We will first briefly review how insulin controls sorting of apoB towards lipidation or degradation.

## Direct effects of insulin on apoB degradation and VLDL assembly

*Effects of insulin on hepatic lipid metabolism are predominantly mediated via the phosphatidylinositol-3-kinase pathway*

Upon binding of insulin to the insulin receptor (a member of the tyrosine kinase receptor family), the receptor autophosphorylates and activates two distinct downstream signaling pathways: the phosphatidylinositol-3-kinase (PI3K) pathway and the MAP kinase/ERK kinase (MEK) pathway. The PI3K-pathway is mainly of relevance for the metabolic processes discussed in this review and will therefore be discussed.

Upon autophosphorylation of the insulin receptor, a downstream insulin receptor substrate (IRS) will be phosphorylated. Phosphorylated IRS has an increased affinity for the p85 subunit of PI3K. Activated PI3K will start the production of the second messenger phosphatidylinositol 2,4,5-trisphosphate (PIP3) from the phospholipid PI4,5P2 (PIP2). This second messenger activates, amongst others, protein kinase B (PKB) via phosphorylation, the protein involved in regulation of many steps in insulin-mediated hepatic glucose and lipid metabolism. For instance, PKB phosphorylates and hence inhibits activity of glycogen synthase kinase-3β (GSK3β), an inhibitor of glycogen synthase (GS). Thus, via its actions on PKB and GSK3, insulin stimulates conversion of glucose into glycogen (19). Nowadays, the PKB-mediated phosphorylation of a member of the forkhead transcription factor family, FoxO1, is intensively studied (20,21). Phosphorylation of FoxO1 blocks induction of expression of various genes involved in gluconeogenesis. In peripheral tissues, PKB stimulates the translocation of vesicles containing the glucose transporter-4 (GLUT4) to the membrane (22,23). Via this route, insulin stimulates peripheral glucose uptake.

*Direct effects of insulin*

Insulin regulates VLDL assembly in various ways. ApoB protein secretion is largely dependent on its intracellular degradation (24): increased or decreased apoB mRNA levels do not translate into similar changes in apoB protein secretion. Elegant *in vitro* studies showed

that insulin is able to inhibit VLDL production via acceleration of the apoB degradation (25). This process mediated by PI3K (26) but probably independent of PKB (27). Via this route, insulin affects the number of VLDL particles secreted. On the other hand, insulin inhibits transcription of the gene encoding for MTTP (28,29), probably via activation of the transcription factor sterol regulator element binding protein-1c (SREBP-1c) (30). The role of SREBP-1c in insulin-mediated lipid metabolism will be discussed later in this review. Activation of PLD, important in the lipidation of VLDL, is prevented when PIP2 levels are low, thus under conditions of high insulin (26,31).

Taken together, these data show that insulin impairs the production of large $VLDL_1$ particles via its effects on MTTP and PLD. Thus, the overall effect of insulin is the secretion of less and smaller VLDL particles. We recently confirmed this effect of insulin *in vivo* in mice in which we measured the VLDL-TG production rate under hyperinsulinemic, euglycemic conditions (32): VLDL-TG production rate decreased during hyperinsulinemia, partly due to the secretion of smaller particles.

Because a VLDL particle contains a single apoB molecule, the amount of apoB secreted directly reflects the number of VLDL particles produced. As discussed, the amount of apoB secreted by the liver depends, in part, on its lipidation (33). Therefore, one can imagine that, when the amount of TG available for VLDL is increased to a larger extent than the amount of apoB, the size of VLDL particles will increase. Moreover, insulin regulates whole-body energy balance, including TG storage and fatty acid fluxes via its inhibitory effects on peripheral lipolysis. Thus, insulin might also affect VLDL secretion via its effects on hepatic lipid availability.

## VLDL production and hepatic lipid availability

### *Sources of fatty acids*

TGs are needed for lipidation of both the apoB and the pre-VLDL particle (33). The fatty acids that constitute the hepatic TG pool originate from three sources: from (i) the diet, (ii) the peripheral (adipose) stores, and (iii) *de novo* lipogenesis. Fatty acids taken up by the hepatocyte are not directly used for VLDL production but first esterified and stored as a cytoplasmic lipid droplet (33,34). Utilization of TG from this pool for VLDL assembly requires hydrolysis followed by re-esterification.

### *De novo lipogenesis*

During *de novo* lipogenesis, fatty acids are made out of acetyl-CoA moieties (figure 8.2). The source of acetyl-CoA may be the glycolytic breakdown of glucose via pyruvate, a process in which pyruvate kinase (PK) is thought to be a major regulator (35). When glucose is taken up in the hepatocyte by the glucose transporter 2 (GLUT2), it is rapidly phosphorylated into glucose-6-phosphate (G6P) by glucokinase (GK). Then, G6P can either be used for production of glycogen, a process mediated by GS, or G6P can enter the glycolytic pathway to yield pyruvate, as mentioned above. The reverse pathway, *de novo* synthesis of glucose, is called gluconeogenesis. Herein, one G6P molecule is produced from two pyruvate molecules via intermediates such as oxaloacetate, phosphoenolpyruvate (PEP) and fructose 1,6-bisphosphate (for an exhaustive review, see (36)). The conversion of oxaloacetate into PEP is controlled by PEP carboxykinase (PEPCK), an enzyme considered rate-controlling in gluconeogenesis. The last step in gluconeogenesis, dephosphorylation of G6P, is controlled by the glucose-6-phosphatase complex.

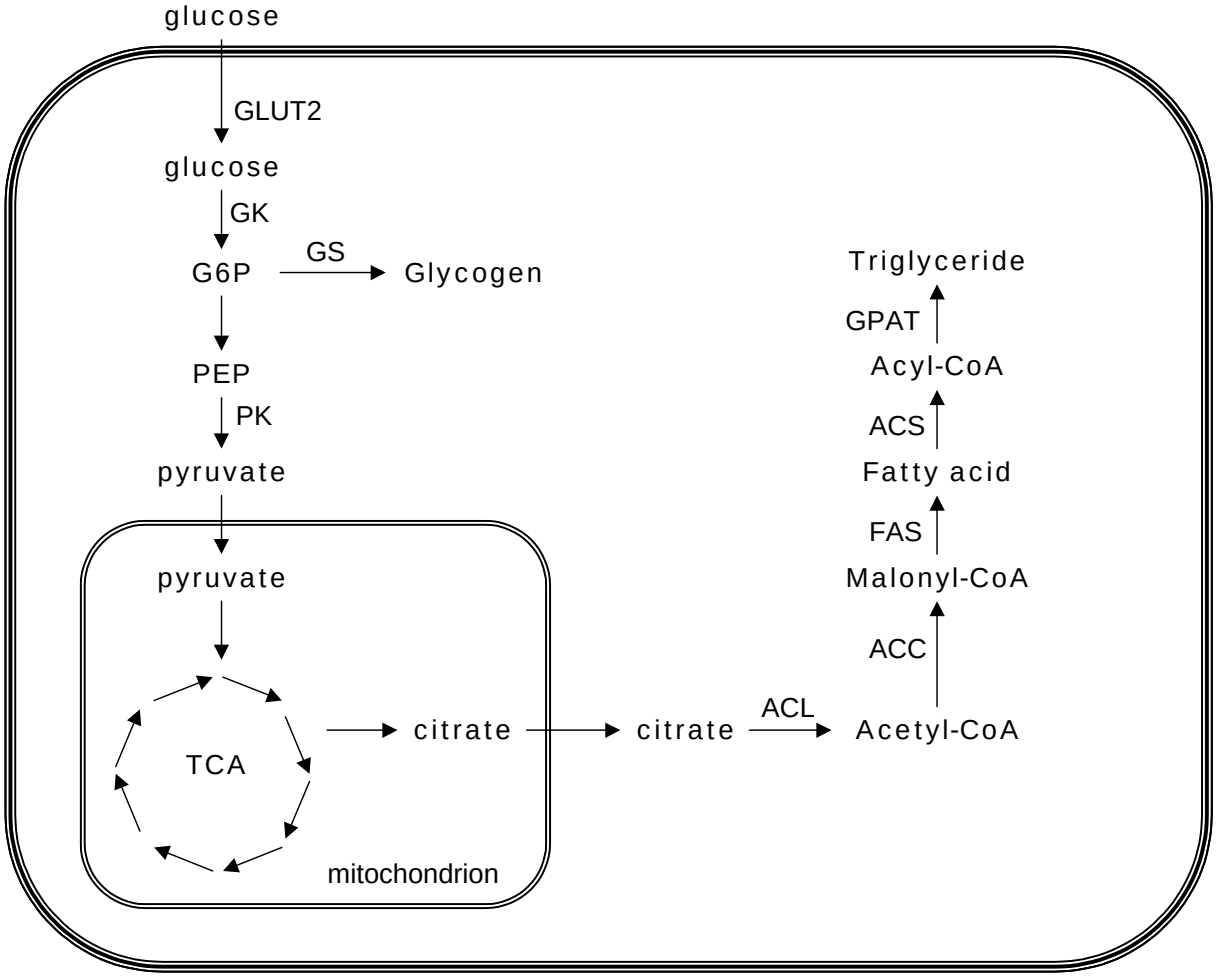


Figure 8.2. Schematic representation of the interplay between hepatic glucose and triglyceride metabolism. ACC, acetyl-CoA carboxylase; ACL, ATP citrate lyase; ACS, Acyl-CoA synthase; FAS, fatty acid synthase; G6P, glucose-6-phosphate; GLUT2, glucose transporter-2; GPAT, glycerol-phosphate acyltransferase; GS, glycogen synthase; PEP, phosphoenolpyruvate; PK, pyruvate kinase; TCA, tricarboxylic acid cycle.

In the flux from glucose to TG, pyruvate enters the tricarboxylic acid (TCA) cycle and the citrate produced herein can be converted into acetyl-CoA by ATP citrate lyase. Two acetyl-CoA's are covalently linked to each other to form malonyl-CoA. This coupling of acetyl-CoA's is regulated by acetyl-CoA carboxylase (ACC). Two different forms of ACC have been identified: activity of ACC1 produces malonyl-CoA that is used in *de novo* lipogenesis whereas ACC2 generates malonyl-CoA that inhibits carnitine palmitoyl transferase-1 (CPT1) (37), an enzyme that has been shown to be rate-controlling for hepatic ß-oxidation (38). The two different functions of malonyl-CoA probably reflect the localization of ACC1 and ACC2 in the cytosol and anchored in the mitochondrial outermembrane, respectively (37). Upon actions of fatty acid synthase (FAS), the malonyl-CoA subunits are covalently linked to form fatty acids. The fatty acyl-CoA needed for esterification of the fatty acid into TG is generated by the actions of acyl-CoA synthase (ACS), while the subsequent esterification into TG is controlled by glycerol-phosphate acyltransferase (GPAT). More background about the role of various enzymes in TG synthesis can be found in the excellent review by Coleman *et al.* (39).

In healthy subjects fed a "normal" diet, *de novo lipogenesis* contributes only 6% to the TG found in both liver and VLDL (40). In patients with nonalcoholic fatty liver disease, however, the contribution of *de novo* lipogenesis to both TG pools was found to be increased to 26% (41). Yet, the major source of fatty acids found in hepatic and VLDL TGs originate from FFAs derived from peripheral tissues (40,41).

### *Novel aspects concerning the relationship between hepatic TG content and VLDL-TG production rate*

Although it is commonly thought that the availability of TG at specific hepatocellular sites is a major determinant of number and size of the VLDL particle (33), a number of recent animal studies from our and other laboratories revealed that the hepatic TG content *per se* does not stimulate the VLDL-TG production rate. For instance, the commonly used leptin-deficient *ob/ob* mice have severe hepatic steatosis, high plasma FFA and increased hepatic *de novo* lipogenesis, but do not show an increased VLDL-TG production rate under basal conditions (42). Furthermore, hepatic steatosis associated with inhibition of glucose-6-phosphatase activity was also without effect on VLDL production (43). Acute hepatic steatosis upon inhibition of hepatic β-oxidation did not affect VLDL production nor impair hepatic insulin sensitivity (32). Various factors, apart from the accumulation of TG, might contribute to changes in VLDL production. TGs are not the sole components of VLDL: hepatic cholesterol and phospholipid availability or synthesis might also influence the secretion and assembly of VLDL. It has been suggested that *de novo* synthesis of cholesterol (44) and phospholipids (45), rather than their concentrations, are determinants of VLDL production. Moreover, both cholesterol and phospholipids are also secreted into bile by the hepatocyte. So far, it is not known whether cholesterol and phospholipids have different preferences for entry into VLDL or bile secretory pathways, but that might, in part, depend on the location of both processes in the liver and the availability of the lipids at these locations.

Studies show that in fasted conditions, the plasma FFA pool contributes the majority of fatty acids secreted by the liver in VLDL (46). Recently, its was shown in humans that fatty acids from the FFA pool are predominantly used by the liver for VLDL-TG synthesis in both fed and fasted state (47). CD36 is the fatty acid transporter in peripheral tissues. Therefore, CD36 knockout mice have an increased FFA flux to the liver (48), a condition resulting in increased hepatic TG concentrations. However, this condition is not associated with increased VLDL-TG production rates (49), thus suggesting that increased plasma FFA levels and hepatic steatosis per se do not necessary lead to increased VLDL production.

## Lipogenic transcription factors

Hepatic *de novo* lipogenesis is, to a large extent, regulated by lipogenic transcription factors. Work in various animal models suggest, but did not yet prove, an independent role for these factors in the regulation of VLDL production. Transcription and/or activation of these factors is regulated by insulin or metabolites of glucose, fatty acids and cholesterol. Very important lipogenic transcription factors that regulate expression of genes encoding for enzymes involved in hepatic lipid and glucose metabolism are SREBP-1c, carbohydrate responsive element binding protein (ChREBP), and liver X receptor (LXR).

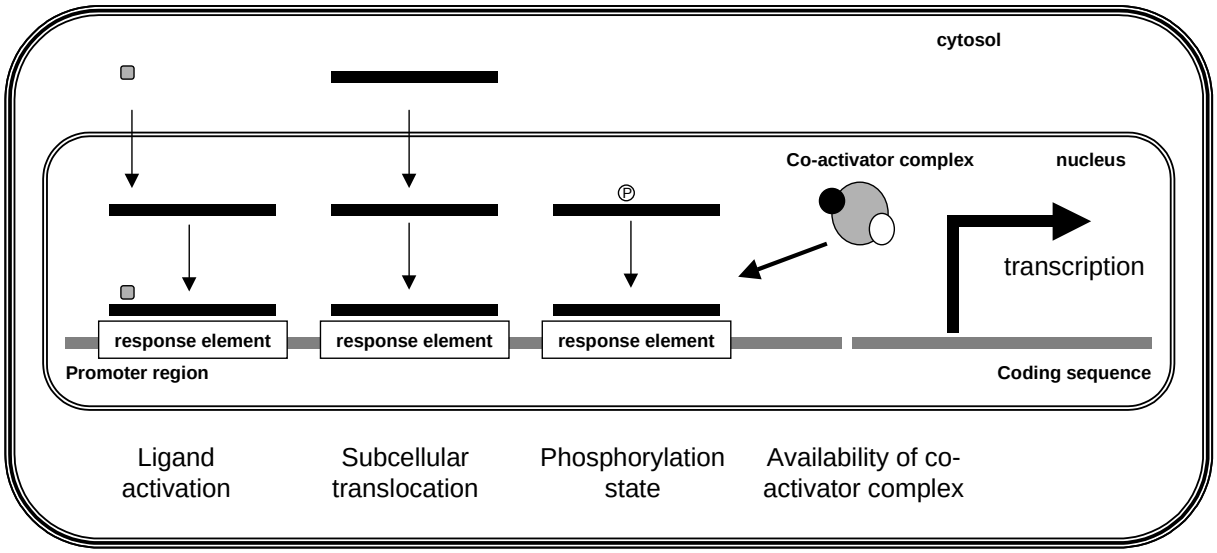


Figure 8.3. Schematic representation of different ways in which the activity of transcription factors can be regulated: via ligand activation, via subcellular translocation, via the phosphorylation state, and via availability of the co-activator complex.

*Transcription factors*

Transcription of genes by the polymerase II complex results in production of RNA. Controlling transcription of a gene is the first step in controlling the production of a protein. The promotor regions of genes contain reponse-elements that can bind certain transcription factors depending on the sequences of the elements (Figure 3). Conformational changes of a transcription factor, *i.e.*, upon binding of its ligand or upon its phosphorylation/ dephosphorylation, will change its affinity for co-activator and co-repressor complexes. These complexes consist of different proteins that can inhibit or induce activity of the polymerase-II complex and hence inhibit or induce gene transcription.

Thus, whether a transcription factor regulates transcription of a gene depends on the presence of its endogenous ligands, its phosphorylation state, its localisation (cytosolic *vs.* nuclear), the presence of specific repsonse-elements in the promotor region and the availability of the corepressor or coactivator complexes (figure 8.3).

*SREBP-1c*

SREBP-1c is a member of the basic-helic-loop-helic-leucine zipper (bHLHLZ) transcription factor family that is synthesized as an inactive precursor protein embedded in the ER membrane. Upon decreasing cellular cholesterol contents, the SREBP-1c precursor protein is translocated to the Golgi membrane, escorted by the SREBP cleavage activation protein (SCAP) (50,51). In the Golgi, the SREBP-1c isoform is cleaved to form 'mature' SREBP-1c, a process mediated by the membrane-bound serine protease site 1 protease (S1P) (52,53) and the membrane-bound zinc-metallo-protease site 2 protease (S2P) (54,55) (figure 8.4). The mature SREBP-1c translocates to the nucleus where it binds to direct repeat sterol regulatory elements (SREs; consensus sequence: 5'-TCACnCCAC-3') located in the promotor regions of several genes.

SREBP-1c induces transcription of almost all genes encoding for enzymes involved in both *de novo* fatty acid synthesis and esterification of fatty acids into TG (56). SREBP-1c knockout mice show markedly decreased mRNA levels of all of these genes (56,57). Upon fasting, when insulin levels are low, the expression of lipogenic genes is decreased. Hepatic

overexpression of SREBP-1c in mice prevented this fasting-induced effect on gene expression (58), suggesting that SREBP-1c is a key regulator of the early response of the liver to insulin. A recent study indeed confirmed that both transcription and activation of SREBP-1c is regulated by insulin (59), via a PI3K-dependent mechanism (60). The effect of insulin on nuclear translocation is, at least in part, due to the effect of reduced levels of the SCAP inhibitory protein Insig-2 (61). Additionally, insulin reduces the turnover rate of nuclear SREBP-1c (62).

The *ob/ob* mouse shows elevated liver TGs and increased blood glucose and insulin levels (63) but also increased nuclear SREBP-1c protein levels, despite severe hepatic insulin resistance (64). This suggests that SREBP-1c is very sensitive for the actions of insulin, even under conditions of reduced whole-body insulin sensitivity. This is, in part, explained by the fact that the insulin effects on glucose production are mediated via IRS1, which is downregulated in insulin-resistant animals whereas the effects of insulin on lipid metabolism are largely regulated via IRS2 (65). However, Shimomura *et al.* (66) showed that, despite IRS2-deficiency due to chronic hyperinsulinemia in *ob/ob* mice, insulin still stimulated transcription of SREBP-1c.

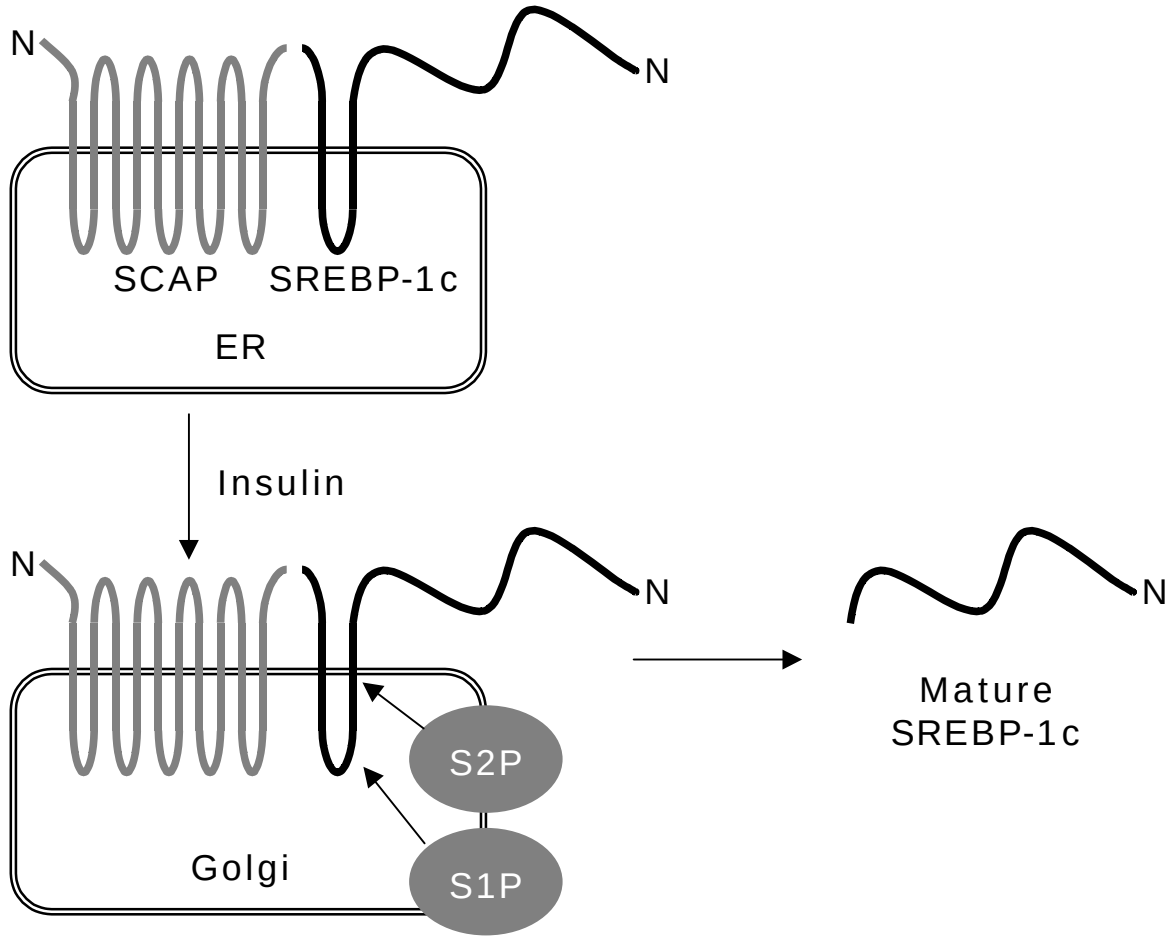


Figure 8.4. Schematic representation of SREBP-1c maturation and cleavage regulated by insulin. ER, endoplasmic reticulum; S1P, site 1 protease; S2P, site 2 protease; SCAP, SREBP cleavage activation protein; SREBP-1c, sterol-regulatory element-binding protein-1c.

In conclusion, insulin increases the nuclear activity of SREBP-1c in at least three manners: (i) via upregulation of SREBP-1c gene transcription, (ii) by stimulating production of the mature SREBP-1c form, and (iii) by decreasing the turnover rate of mature SREBP-1c. Of interest is the fact that the effects of insulin on SREBP-1c transcription and translocation are opposed by glucagon via increased intracellular cAMP levels which probably affect SREBP-1c activity via inhibition of the insulin-inhibited nuclear SREBP-1c turnover (62).

Although plasma TG levels are ~60% lower in SREBP-1c knockout mice (57), only speculative data exist about the role of SREBP-1c in the hepatic VLDL-TG production rate in basal and hyperinsulinemic states. Therefore, the precise role of SREBP-1c in the regulation of VLDL production and hence in development of diabetic dyslipidemia remains speculative. Moreover, the role of (insulin-mediated) SREBP-1c activity in the control of hepatic glucose metabolism is largely unknown, but is probably minor because lipid and glucose metabolism are controlled by insulin via distinct routes, *i.e.*, IRS2 and IRS1, respectively (65).

### *ChREBP*

When glucose is taken up by the liver and subsequently converted to G6P by GK, G6P is mainly directed into the glycogen pool or broken down in the glycolytic pathway, as mentioned before. However, when the flux through G6P is increasing, an 'escape' route called the pentose phosphate pathway becomes active (Figure 5). In this pathway, ribulose-5-phosphate is generated from G6P or from its glycolytic product fructose-6-phosphate via oxidative or non-oxidative routes, respectively (67). Via an epimerase, ribulose-5-phosphate is converted into xylulose-5-phosphate, an activator of protein phosphatase 2 A (PP2A). A few years ago, it was shown that the increased activity of PP2A upon increasing xylulose-5-P levels were associated with induced transcription of PK (68). Recently, the members of Uyeda's laboratory clearly showed that a novel transcription factor, ChREBP, is responsible for this effect (69,70).

ChREBP is a member of the bHLHLZ transcription factor family and binds to the carbohydrate reponse element (ChoRE) present in promoters of several genes, that is composed of two E-box (5'-CACGTG-3') or E-box-like sequences. The ChREBP protein probably binds as a heterodimer with Mlx (71) to its response elements. Upon increasing xylulose-5-phosphate levels, PP2A dephosphorylates ChREBP. ChREBP can be transported into the nucleus after dephosphorylation of Ser196 and dephosporylation of a second amino acid (Thr666) enhances the binding activity of ChREBP to DNA (72). ChREBP phosphorylation is regulated by AMP-activated protein kinase (AMPK) and protein kinase A (PKA) (73). The activity of AMPK becomes induced upon increasing usage of energy, *e.g.*, exercise. AMPK is considered to play a pivotal role in the control of lipid metabolism. For instance, AMPK phosphorylates and inhibits ACC1 and ACC2 (74) as well as SREBP-1c (75).

ChREBP induces transcription of various genes encoding enzymes involved in *de novo* lipogenesis (76). Remarkably, most lipogenic genes regulated by SREBP-1c are also regulated by ChREBP, *i.e.*, ACC, FAS, ACS and GPAT. Thus, glucose not only regulates lipogenic gene expression via its effects on pancreatic insulin secretion and hence insulin-mediated SREBP-1c transcription and activation, but also via ChREBP.

Treatment of rats with the pharmacological glucose-6-phosphatase inhibitor S4048 resulted in elevated hepatic G6P levels (77) and increased lipogenesis (43), a process presumably mediated via ChREBP. Upon S4048 treatment, the VLDL-TG production rate was not affected (43), but hepatic glucose production was severely decreased (77). Because the data strongly suggest a role of ChREBP in the S4048-induced lipogenesis, more experiments are needed to elucidate the role of ChREBP on the VLDL production and particle size.

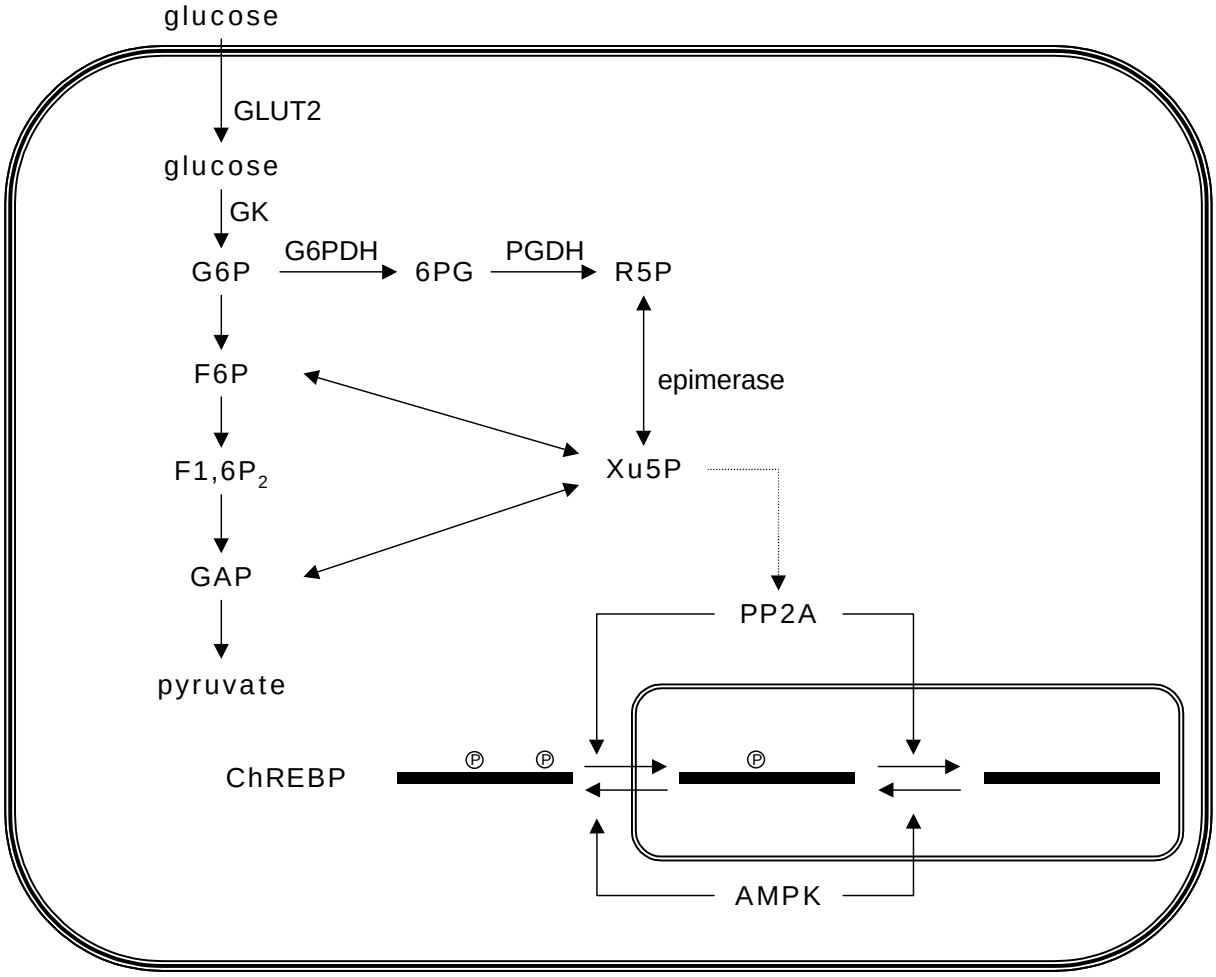


Figure 8.5. Schematic representation of hepatic ChREBP activation induced via dephosphorylation enhanced by xylulose-5-phosphate. 6PG, 6-phosphogluconate; AMPK, AMP-activated protein kinase; ChREBP, carbohydrate responsive element binding protein; $F1,6P_2$, fructose-1,6-bisphosphate; F6P, fructose-6-phosphate; G6P, glucose-6-phosphate; G6PDH, glucose-6-phosphate dehydrogenase; GAP, glyceraldehyde-3-phosphate; GK, glucokinase; GLUT2, glucose transporter-2; PGDH, 6-phosphogluconate dehydrogenase; PP2A, protein phosphatase 2A; R5P, ribulose-5-phosphate; Xu5P, xylulose-5-phosphate.

*LXR*

LXR is a member of the family of nuclear hormone receptors that needs to bind a ligand to become active and to induce or inhibit transcription of target genes. Other members of this family are the peroxisome proliferator-activated receptors (PPARs), the glucocorticoid receptor (GR) and many others (table 8.1). Two subtypes of LXR are known: LXRα is expressed mainly in the liver while LXRβ is ubiquitously expressed (78,79). Activated LXRs heterodimerize with the retinoid X receptor (RXR) and bind to the LXR response element (LXRE), consisting of two hexameric nucleotide direct repeats separated by four nucleotides (DR4; consensus sequence: 5'AGGTCAnnnnCGGTCA-3') (78,79). Oxysterols are oxygenated metabolites of cholesterol and they constitute the physiological ligands for LXR. The most potent LXR-activating oxysterols are 22(R)-hydroxycholesterol, 24(S)-hydroxycholesterol and 24(S),25-epoxycholesterol (80). The first effects of activated LXRs were seen on genes encoding proteins invloved in (reverse) cholesterol metabolism, but

pharmacological LXR activation studies showed that LXR also induces transcription of SREBP-1c (81-84), but not its translocation (59). Apart from indirect actions through SREBP-1c, LXR also directly influences transcription of *Fas* (85) and of genes encoding LPL (86) and stearoyl-CoA desaturase-1 (SCD1) (57). The latter protein is involved in the production of monounsaturated fatty acids, *i.e.*, conversion of palmitic acid (C16:0) and stearic acid (C18:0) into palmitoleic acid (C16:1) and oleic acid (C18:1), respectively (87).

We previously showed that pharmacological LXR activation resulted in severe fatty liver and with 2-fold induced VLDL-triglyceride production rate in mice (84). This increased production was completely the result of the secretion of large, TG-rich particles, a condition similar to that of diabetic dyslipidemic patients. However, studies suggested anti-diabetic effects of LXR activation (88,89), presumably via the effects of LXR on the transcription of the gluconeogenic gene *Pepck*. In contrast, *in vivo* studies on insulin sensitivity showed no differences between LXR agonist treated and untreated lean and *ob/ob* mice (90). So far, no direct data exist on the direct role of LXR on the insulin sensitivity of VLDL production.

Table 8.1. The nuclear receptor superfamily

| | |
|---|---|
| Endocrine receptors<br>Ligands: hormonal lipids | Estrogen receptor (ER) α, β<br>Progestane receptor (PR)<br>Androstane receptor (AR)<br>Glucocorticoid receptor (GR)<br>Mineralocorticoid receptor (MR)<br>Retinoid acid receptor (RAR) α, β, γ<br>Thyroid receptor (TR) α, β<br>Vitamin D receptor (VDR)<br>Ecdysone receptor (EcR)[1] |
| Adopted orphan receptors:<br>Ligands: dietary lipids | Retinoid X recptor (RXR) α, β, γ<br>Peroxisome proliferator-activated receptor (PPAR) α, β/δ, γ<br>Liver X receptor (LXR) α, β<br>Farnesoid X receptor (FXR) α, β<br>Pregnane X receptor (PXR)[2]<br>Constitutive androstane receptor (CAR) |
| Orphan receptors<br>Ligands: unknown | Steroidogenic factor 1 (SF-1)<br>Liver related hormone-1 (LRH-1)<br>DAX-1[3]<br>Short heterodimer partner (SHP)<br>TLX[4]<br>Photoreceptor cell-specific nuclear receptor (PNR)<br>NGFI-B α, β, γ[4]<br>Retinoid related orphan receptor (ROR) α, β, γ<br>Estrogen-related receptor (ERR) α, β, γ<br>RevErb α, β, γ[4]<br>Germ cell nuclear factor (GCNF)<br>TR 2,4[4]<br>Hepatocyte nuclear factor-4 (HNF-4)<br>COUP-TF α, β, γ[5] |

[1], the EcR is found in insects and is the only nonvertebrate nuclear receptor with a known ligand; [2], in humans, the rodent PXR is called steroid X receptor (SXR); [3], abbreviation of: dosage-sensitive sex reversal-adrenal hypoplasia congenita critical region on the X chromosome, gene 1; [4], no full name; [5], abbreviation of: chicken ovalbumin upstream promoter-transcription factor.

## Concluding remarks

Because the lipogenic transcription factors mentioned (SREBP-1c, ChREBP, and LXR) tightly control *de novo* lipogenesis and their activation and/or expression is controlled by insulin, carbohydrates and lipids (factors whose plasma levels are increased in type 2 diabetic subjects), one might expect that these factors play a role in the (insulin sensitivity of) VLDL production. However, proper studies relating these transcription factors with the insulin sensitivity of VLDL production have not been reported. Of course, one can question whether these factors play a huge role herein, because fatty acids produced in the *de novo* lipogenic pathway do not contribute that much to the VLDL-TG content (40,91). Only well-conduted *in vivo* studies, *i.e.* with knockout mice and pharmacological ligands, will give proper information about the role of lipogenic transcription in (insulin sensitivity of) VLDL production and hence diabetic dyslipidemia.

## References

1. Eckel, RH, Grundy, SM, Zimmet, PZ. The metabolic syndrome. Lancet 365: 1415-1428, 2005
2. Seppälä-Lindroos, A, Vehkavaara, S, Häkkinen, A-M, Goto, T, Westerbacka, J, Sovijärvi, A, Halavaare, J, Yki-Järvinen, H. Fat accumulation in the liver is associated with defects in insulin suppression of glucose production and serum free fatty acids independent of obesity in normal men. J Clin Endocrinol Metab. 87: 3023-3028, 2002
3. Carmena, R, Duriez, P, Fruchart, J-C. Atherogenic lipoprotein particles in atherosclerosis. Circulation 109 [suppl III]: III-2-III-7, 2004
4. Isomaa, B, Almgren, P, Tuomi, T, Forsén, B, Lahti, K, Nissèn, M, Taskinen, M-R, Groop, L. Cardiovascular morbidity and mortality associated with the metabolic syndrome. Diabetes Care 24: 683-689, 2001
5. Turner, RC, Millns, H, Neil, HAW, Stratton, IM, Manley, SE, Matthews, DR, Holman, RR. Risk factors for coronary artery disease in non-insulin dependent diabetes mellitus: United Kingdom prospective diabetes study (UKPDS: 23). BMJ 316: 823-828, 1998
6. Taskinen, M-R. Diabetic dyslipidaemia: from basic research to clinical practice. Diabetologia 46: 733-749, 2003
7. McEneny, J, O'Kane, MJ, Moles, KW, McMaster, C, McMaster, D, Mercer, C, Trimble, ER, Young, IS. Very low density lipoprotein subfractions in type II diabetes mellitus: alterations in composition and susceptibility to oxidation. Diabetologia 43: 485-493, 2000
8. Ginsberg, HN, Zhang, Y-L, Hernancez-Ono, A. Regulation of plasma triglycerides in insulin resistance and diabetes. Arch Med Res 36: 232-240, 2005
9. Anant, S, Davidson, NO. Molecular mechanisms of apolipoprotein B mRNA editing. Curr Opin Lipidol. 12: 159-165, 2001
10. Cooper, AD. Hepatic uptake of chylomicron remnants. J Lipid Res. 38: 2173-2192, 1997
11. Fraser, R. Size and lipid composition of chylomicrons of different Svedberg units of flotation. J Lipid Res 11: 60-65, 1970
12. Austin, MA, Krauss, RM. LDL density and atherosclerosis. JAMA 273: 115, 1995
13. Zechner, R, Strauss, JG, Haemmerle, G, Lass, A, Zimmermann, R. Lipolysis: pathway under construction. Curr Opin Lipidol 16: 333-341, 2005
14. Gilham, D, Lehner, R. The physiological role of triacylglycerol hydrolase in lipid metabolism. Rev Endo Metab Disord 5: 303-309, 2004
15. Heijboer, AC, Donga, E, Voshol, PJ, Dang, Z-C, Havekes, LM, Romijn, JA, Corssmit, EPM. Sixteen hours of fasting differentially affects hepatic and muscle insulin sensitivity in mice. J Lipid Res 46: 582-588, 2005
16. Gordon, DA, Jamil, H. Progress towards understanding the role of microsomal triglyceride transfer protein in apolipoprotein-B lipoprotein assembly. Biochim Biophys Acta 1486: 72-83, 2000
17. Asp, L, Magnusson, B, Rutberg, M, Li, L, Borén, J, Olofsson, S-O. Role of ADP ribosylation factor 1 in the assembly and secretion of apoB-100-containing lipoproteins. Arterioscler Thromb Vasc Biol 25: 566-570, 2005
18. Olofsson, SO, Asp, L, Boren, J. The assembly and secretion of apolipoprotein B-containing lipoproteins. Curr Opin Lipidol 10: 341-346, 1999
19. Saltiel, AR, Kahn, CR. Insulin signalling and the regulation of glucose and lipid metabolism. Nature 414: 799-806, 2001
20. Nakae, J, Kitamura, T, Silver, DL, Accili, D. The forkhead transcription factor Foxo1 (Fkhr) confers insulin sensitivity onto glucose-6-phosphatase expression. J Clin Invest 108: 1359-1367, 2001

21. Altomonte, J, Richter, A, Harbaran, S, Suriawinata, J, Nakae, J, Thung, SN, Meseck, M, Accili, D, Dong, H. Inhibition of foxo1 function is associated with improved fasting glycemia in diabetic mice. Am J Physiol Endocrinol Metab 285: E718-E728, 2003
22. Whiteman, EL, Cho, H, Bimbaum, MJ. Role of Akt/protein kinase B in metabolism. Trends Endocrinol Metab 13: 444-451, 2002
23. Calera, MR, Martinez, C, Liu, H, El Jack, AK, Birnbaum, MJ, Pilch, PF. Insulin increases the association of Akt-2 with Glut4-containing vesicles. J Biol Chem 273: 7201-7204, 1998
24. Sparks, JD, Zolfaghari, R, Sparks, CE, Smith, HC, Fisher, EA. Impaired hepatic apolipoprotein B and E translation in streptozotocin diabetic rats. J Clin Invest 89: 1418-1430, 1992
25. Fisher, EA, Pan, M, Chen, X, Wu, X, Wang, H, Jamil, H, Sparks, JD, Williams, KJ. The triple threat to nascent apolipoprotein B. Evidence for multiple, distinct degradative pathways. J Biol Chem 276: 27855-27863, 2001
26. Brown, A-M, Gibbons, GF. Insulin inhibits the maturation phase of VLDL assembly via a phosphoinositide 3-kinase-mediated event. Arterioscler Thromb Vasc Biol 21: 1656-1661, 2001
27. Au, CS, Wagner, A, Chong, T, Qiu, W, Sparks, JD, Adeli, K. Insulin regulates hepatic apolipoprotein B production independent of the mass or activity of Akt1/PKBα. Metabolism 53: 228-235, 2004
28. Wetterau, JR, Lin, MC, Jamil, H. Microsomal triglyceride transfer protein. Biochim Biophys Acta 1345: 136-150, 1997
29. Hagan, DL, Kienzle, B, Jamil, H, Hariharan, N. Transcriptional regulation of human and hamster microsomal triglyceride transfer protein genes. Cell type-specific expression and response to metabolic regulators. J Biol Chem 269: 28737-28744, 1994
30. Sato, R, Miyamoto, W, Inoue, J, Terada, T, Imanaka, T, Maeda, M. Sterol regulatory element-binding protein negatively regulates microsomal triglyceride transfer protein gene transcription. J Biol Chem 274: 24714-24720, 1999
31. Phung, TL, Roncone, A, de Mesy Jensen, KL, Sparks, CE, Sparks, JD. Phosphoinositide 3-kinase activity is necessary fo insulin-dependent inhibition of apolipoprotein B secretion by rat hepatocytes and localizes to the endoplasmic reticulum. J Biol Chem 272: 30693-30702, 1997
32. Grefhorst, A, Hoekstra, J, Derks, TGJ, Ouwens, DM, Baller, JFW, Havinga, R, Havekes, LM, Romijn, JA, Kuipers, F. Acute hepatic steatosis in mice by blocking β-oxidation does not reduce insulin sensitivity of very low density lipoprotein production. Am J Physiol Gastrointest Liver Physiol 289: G592-G598, 2005
33. Gibbons, GF, Wiggins, D, Brown, A-M, Hebbachi, A-M. Synthesis and function of hepatic very-low-density lipoprotein. Biochem Soc Trans. 32: 59-64, 2004
34. Gibbons, GF, Islam, K, Pease, RJ. Mobilisation of triacylglycerol stores. Biochim Biophys Acta 1483: 37-57, 2000
35. Pilkis, SJ, Granner, DK. Molecular physiology of the regulation of hepatic gluconeogenesis and glycolysis. Annu Rev Physiol 54: 885-909, 1992
36. Radziuk, J, Pye, S. Hepatic glucose uptake, gluconeogenesis and the regulation of glycogen synthesis. Diabetes Metab Res Rev 17: 250-272, 2001
37. Abu-Elheiga, L, Matzuk, MM, Abo-Hashema, KAH, Wakil, SJ. Continuous fatty acid oxidation and reduced fat storage in mice lacking acetyl-coa carboxylase 2. Science 291: 2613-2616, 2001
38. Ramsay, RR, Gandour, RD, van der Leij, FR. Molecular enzymology of carnitine transfer and transport. Biochim Biophys Acta 1546: 21-43, 2001
39. Coleman, RA, Lee, DP. Enzymes of triacylglycerol synthesis and their regulation. Prog Lipid Res 43: 134-176, 2003
40. Timlin, MT, Parks, EJ. Temporal pattern of de novo lipogenesis in the postprandial state in healthy men. Am J Clin Nutr 81: 35-42, 2005
41. Kolter, T, Proia, RL, Sandhoff, K. Combinatorial ganglioside biosynthesis. J Biol Chem 277: 25859-25862, 2002
42. Wiegman, CH, Bandsma, RHJ, Ouwens, M, van der Sluijs, FH, Havinga, R, Boer, T, Reijngoud, D-J, Romijn, JA, Kuipers, F. Hepatic VLDL production in ob/ob mice is not stimulated by massive de novo lipogenesis but is less sensitive to the suppressive effects of insulin. Diabetes 52: 1081-1089, 2003
43. Bandsma, RHJ, Wiegman, CH, Herling, AW, Burger, H-J, ter Harmsel, A, Meijer, AJ, Romijn, JA, Reijngoud, D-J, Kuipers, F. Acute inhibition of glucose-6-phosphate translocator activity leads to increased de novo lipogenesis and development of hepatic steatosis without affecting VLDL production in rats. Diabetes 50: 2591-2597, 2001
44. Isusi, E, Aspichueta, P, Liza, M, Hernández, ML, Díaz, C, Hernández, G, Martínez, MJ, Ochoa, B. Short- and long-term effects of atorvastatin, lovastatin and simvastatin on the cellular metabolism of cholesteryl esters and VLDL secretion in rat hepatocytes. Atherosclerosis 153: 283-294, 2000
45. Verkade, HJ, Fast, DG, Rusiñol, AE, Scraba, DG, Vance, DE. Impaired biosynthesis of phosphatidylcholine casuses a decrease in the number of very low density lipoprotein particles in the golgi but not in the endoplasmic reticulum of rat liver. J Biol Chem 268: 24990-24996, 1993
46. Parks, EJ, Krauss, RM, Christiansen, MP, Neese, RA, Hellerstein, MK. Effects of a low-fat, high-carbohydrate diet on VLDL-triglyceride assembly, production, and clearance. J Clin Invest 104: 1087-1096, 1999
47. Timlin, MT, Barrows, BR, Parks, EJ. Increased dietary substrate delivery alters hepatic fatty acid recycling in healthy men. Diabetes 54: 2694-2701, 2005

48. Goudriaan, JR, Dahlmans, VEH, Teusink, B, Ouwens, DM, Febbraio, M, Maassen, JA, Romijn, JA, Havekes, LM, Voshol, PJ. CD36 deficiency increases insulin sensitivity in muscle, but induces insulin resistance in the liver in mice. J Lipid Res 44: 2270-2277, 2003
49. Goudriaan, JR, den Boer, MAM, Rensen, PCN, Febbraio, M, Kuipers, F, Romijn, JA, Havekes, LM, Voshol, PJ. CD36 deficiency in mice impairs lipoprotein lipase-mediated triglyceride clearance. J Lipid Res 46: 2175-2181, 2005
50. Nohturfft, A, DeBose-Boyd, RA, Scheek, S, Goldstein, JL, Brown, MS. Sterols regulate cycling of SREBP cleaving-activating protein (SCAP) between endoplasmic reticulum and Golgi. Proc Natl Acad Sci USA 96: 11235-11240, 1999
51. Nohturfft, A, Yabe, D, Goldstein, JL, Brown, MS, Espenshade, PJ. Regulated step in cholesterol feedback localized to budding of SCAP from ER membranes. Cell 102: 315-323, 2000
52. Sakai, J, Rawson, RB, Espenshade, PJ, Cheng, D, Seegmiller, AC, Goldstein, JL, Brown, MS. Molecular identification of the sterol-regulated luminal protease that cleaves SREBPs and controls lipid composition of animal cells. Mol Cell 2: 505-514, 1998
53. Duncan, EA, Brown, MS, Goldstein, JL, Sakai, J. Cleavage site for sterol-regulated protease localized to a leu-ser bond in the lumenal loop of sterol regulatory element-binding protein-2. J Biol Chem 272: 12778-12785, 1997
54. Rawson, RB, Zelenski, NG, Nijhawan, D, Ye, J, Sakai, J, Hasan, MT, Chang, TY, Brown, MS, Goldstein, JL. Complementation cloning of s2p, a gene encoding a putative metalloprotease required for intramembrane cleavage of SREBPs. Mol Cell 1: 47-57, 1997
55. Duncan, EA, Davé, UP, Sakai, J, Goldstein, JL, Brown, MS. Second-site cleavage in sterol regulatory element-binding protein occurs at transmembrane junction as determined by cysteine panning. J Biol Chem 273: 17801-17809, 1998
56. Horton, JD, Goldstein, JL, Brown, MS. SREBPs: activators of the complete program of cholesterol and fatty acid synthesis in the liver. J Clin Invest 109: 1125-1131, 2002
57. Liang, G, Yang, J, Horton, JD, Hammer, RE, Goldstein, JL, Brown, MS: Diminished hepatic response to fasting/ refeeding and liver X receptor agonists in mice with selective deficiency of sterol regulatory element-binding protein-1c. J Biol Chem 277: 9520-9528, 2002
58. Horton, JD, Bashmakov, Y, Shimomura, I, Shimano, H. Regulation of sterol regulatory element binding proteins in livers of fasted and refed mice. Proc Natl Acad Sci USA 95: 5987-5992, 1998
59. Hegarty, BD, Bobard, A, Hainault, I, Ferré, P, Bossard, P, Foufelle, F. Distinct roles of insulin and liver X receptor in the induction and cleavage of sterol regulatory element-binding protein-1c. Proc Natl Acad Sci USA 102: 791-796, 2005
60. Fleischmann, M, Iynedjian, PB. Regulation of sterol regulatory-element binding protein 1 gene expression in liver: role of insulin and protein kinase B/cAkt. Biochem J 349: 13-17, 2000
61. Yabe, D, Komuro, R, Liang, G, Goldstein, JL, Brown, MS. Liver specific mRNA for insig-2 down-regulated by insulin: implications for fatty acid synthesis. Proc Natl Acad Sci USA 100: 3155-3160, 2003
62. Yellaturu, CR, Deng, X, Cagen, LM, Wilcox, HG, Park, EA, Raghow, R, Elam, MB. Posttranslational processing of SREBP-1 in rat hepatocytes is regulated by insulin and cAMP. Biochem Biophys Res Commun. 332: 174-180, 2005
63. Bandsma, RHJ, Grefhorst, A, van Dijk, TH, van der Sluijs, FH, Hammer, A, Reijngoud, D-J, Kuipers, F. Enhanced glucose cycling and suppressed de novo synthesis of glucose-6-phosphate result in a net unchanged hepatic glucose output in ob/ob mice. Diabetologia 47: 2022-2031, 2004
64. Shimomura, I, Bashmakov, Y, Horton, JD. Increased levels of nuclear srebp-1c associated with fatty livers in two mouse models of diabetes mellitus. J Biol Chem 274: 30028-30032, 1999
65. Taniguchi, CM, Ueki, K, Kahn, CR. Complementary roles of IRS-1 and IRS-2 in the hepatic regulation of metabolism. J Clin Invest 113: 718-727, 2005
66. Shimomura, I, Matsuda, M, Hammer, RE, Bashmakov, Y, Brown, MS, Goldstein, JL. Decreased IRS-2 and increased SREBP-1c lead to mixed insulin resistance and sensitivity in livers of lipodystrophic and ob/ob mice. Mol Cell 6: 77-86, 2000
67. Veech, RL. A humble hexose monophosphate pathway metabolite regulates short- and long-term control of lipogenesis. Proc Natl Acad Sci USA 100: 5578-5580, 2003
68. Decaux, JF, Antoine, B, Kahn, A. Regulation of the expression of the L-type pyruvate kinase gene in adult rat hepatocytes in primary culture. J Biol Chem 264: 11584-11590, 1989
69. Kabashima, T, Kawaguchi, T, Wadzinski, BE, Uyeda, K. Xylulose 5-phosphate mediates glucose-induced lipogenesis by xylulose 5-phosphate-activated protein phosphatase in rat liver. Proc Natl Acad Sci USA 100: 5107-5112, 2003
70. Yamashita, H, Takenoshita, M, Sakurai, M, Bruick, RK, Henzel, WJ, Shillinglaw, W, Arnot, D, Uyeda, K. A glucose-responsive transcription factor that regulates carbohydrate metabolism in the liver. Proc Natl Acad Sci USA 98: 9116-9121, 2001
71. Ma, L, Tsatsos, NG, Towle, HC. Direct role of ChREBP/Mlx in regulating hepatic glucose-response genes. J Biol Chem 280: 12019-12027, 2005
72. Uyeda, K, Yamashita, H, Kawaguchi, T. Carbohydrate responsive element-binding protein (ChREBP): a key regulator of glucose metabolism and fat storage. Biochem Pharmacol 63: 2075-2080, 2002

73. Kawaguchi, T, Takenoshita, M, Kabashima, T, Uyeda, K. Glucose and cAMP regulate the L-type pyruvate kinase gene by phosphorylation/dephosphorylation of the carbohydrate response element binding protein. Proc Natl Acad Sci USA 98: 13710-13715, 2001
74. Park, H, Kaushik, VK, Constant, S, Prentki, M, Przybytkowski, E, Ruderman, NB, Saha, AK. Coordinate regulation of malonyl-CoA decarboxylase, sn-glycerol-3-phosphate acyltransferase, and acetyl-CoA carboxylase by AMP-activated protein kinase in rat tissues in response to exercise. J Biol Chem 277: 32571-32577, 2002
75. You, M, Matsumoto, M, Pacold, CM, Cho, WK, Crabb, DW. The role of AMP-activated protein kinase in the action of ethanol in the liver. Gastroenterology 127: 1798-1808, 2004
76. Ishii, S, Iizuka, K, Miller, BC, Uyeda, K. Carbohydrate response element binding protein directly promotes lipogenic enzyme gene transcription. Proc Natl Acad Sci USA 101: 15597-15602, 2004
77. van Dijk, TH, van der Sluijs, FH, Wiegman, CH, Baller, JFW, Gustafson, LA, Burger, H-J, Herling, AW, Kuipers, F, Meijer, AJ, Reijngoud, D-J. Acute inhibition of hepatic glucose-6-phosphate does not affect gluconeogenesis but directs gluconeogenic flux toward glycogen in fasted rats. J Biol Chem 276: 25727-25735, 2001
78. Teboul, M, Enmark, E, Li, Q, Wikström, AC, Pelto-Huikko, M, Gustafsson, J-Å. OR-1, a member of the nuclear superfamily that interacts with the 9-cis-retinoic acid receptor. Proc Natl Acad Sci USA 92: 2096-2100, 1995
79. Willy, PJ, Umesono, K, Ong, ES, Evans, RM, Heyman, RA, Mangelsdorf, DJ. LXR, a nuclear receptor that defines a distinct retinoid response pathway. Genes Dev 9: 1033-1045, 1995
80. Lehmann, JM, Kliewer, SA, Moore, LB, Smith-Oliver, TA, Oliver, BB, Su, J-L, Sundseth, SS, Winegar, DA, Blanchard, DE, Spencer, TA, Willson, TM. Activation of the nuclear receptor LXR by oxysterols defines a new hormone response pathway. J Biol Chem 272: 3137-3140, 1997
81. Schultz, JR, Tu, H, Luk, A, Repa, JJ, Medina, JC, Li, L, Schwendner, S, Wang, S, Thoolen, M, Mangelsdorf, DJ, Lustig, KD, Shan, B. Role of LXR in control of lipogenesis. Genes Dev 14: 2831-2838, 2000
82. Repa, JJ, Liang, G, Ou, J, Bashmakov, Y, Lobaccaro, J-MA, Shimomura, I, Shan, B, Brown, MS, Goldstein, JL, Mangelsdorf, DJ: Regulation of mouse sterol regulatory element-binding protein 1c gene (SREBP-1c) by oxysterol receptors, LXRα and LXRβ. Genes Dev 14: 2819-2830, 2000
83. Yoshikawa, T, Shimano, H, Amemiya-Kudo, M, Yahagi, N, Hasty, AH, Matsuzaka, T, Okazaki, H, Tamura, Y, IIzuka, Y, Ohashi, K, Osuga, J-I, Harada, K, Gotoda, T, Kimura, S, Ishibashi, S, Yamada, N. Identification of liver X receptor-retinoid X receptor as an activator of the sterol regulatory element-binding protein 1c gene promoter. Mol Cell Biol 21: 2991-3000, 2001
84. Grefhorst, A, Elzinga, BM, Voshol, PJ, Plösch, T, Kok, T, Bloks, VW, van der Sluijs, FH, Havekes, LM, Romijn, JA, Verkade, HJ, Kuipers, F. Stimulation of lipogenesis by pharmacological activation of the liver X receptor leads to production of large, triglyceride-rich very low density lipopoprotein particles. J Biol Chem 277: 34182-34190, 2002
85. Joseph, SB, Laffitte, BA, Patel, PH, Watson, MA, Matsukuma, KE, Walczak, R, Collins, JL, Osborne, TF, Tontonoz, P. Direct and indirect mechanisms for regulation of fatty acid synthase gene expression by liver X receptors. J Biol Chem 277: 11019-11025, 2002
86. Zhang, Y, Repa, JJ, Gauthier, K, Mangelsdorf, DJ. Regulation of lipoprotein lipase by the oxysterol receptors, LXRα and LXRβ. J Biol Chem 276: 43018-43024, 2001
87. Miyazaki, M, Ntambi, JM. Role of stearoyl-coenzyme A desaturase in lipid metabolism. Prostaglandins Leukot Essent Fatty Acids 68: 113-121, 2003
88. Cao, G, Liang, Y, Broderick, CL, Oldham, BA, Beyer, TP, Schmidt, RJ, Zhang, Y, Stayrook, KR, Suen, C, Otto, KA, Miller, AR, Dai, J, Foxworthy, P, Gao, H, Ryan, TP, Jiang, X-C, Burris, TP, Eacho, PI, Etgen, GJ. Antidiabetic action of a liver X receptor agonist mediated by inhibition of hepatic gluconeogenesis. J Biol Chem 278: 1131-1136, 2003
89. Laffitte, BA, Chao, LS, Li, J, Walczak, R, Hummasti, S, Joseph, SB, Castrillo, A, Wilpitz, DC, Mangelsdorf, DJ, Collins, JL, Saez, E, Tontonoz, P. Activation of liver X receptor improves glucose tolerance through coordinate regulation of glucose metabolism in liver and adipose tissue. Proc Natl Acad Sci USA 100: 5419-5424, 2003
90. Grefhorst, A, van Dijk, TH, Hammer, A, van der Sluijs, FH, Havinga, R, Havekes, LM, Romijn, JA, Groot, PH, Reijngoud, D-J, Kuipers, F. Differential effects of pharmacological liver X receptor activation on hepatic and peripheral insulin sensitivuty in lean and ob/ob mice. Am J Physiol Endocrinol Metab 289: E829-E838, 2005
91. Donnelly, KL, Smith, CI, Schwarzenberg, SJ, Jessurun, J, Boldt, MD, Parks, EJ. Sources of fatty acids stored in liver and secreted via lipoproteins in patients with nonalcoholic fatty liver disease. J Clin Invest. 115: 1343-1351, 2005

# Chapter 9

# Summary and general discussion

World-wide prevalences of nonalcoholic fatty liver diseases, such as nonalcoholic steatohepatitis (NASH), and diabetes mellitus type 2 have and will increase markedly during the coming years (1-4). The hallmark of the fatty liver is an excessive accumulation of triglycerides (TGs) and various human studies showed that tis fat accumulation is associated with insulin resistance and diabetes mellitus type 2 (5-10). The increasing prevalence of these conditions are a result of the prevailing sedentary life-style, characterized by high food consumption and low physical activity (11). The metabolic syndrome, often referred to as a readout of the sedentary life-style in Western societies, comprises a cluster of metabolic abnormalities, among which obesity and insulin resistance are key features (5,12,13).

Although the condense summary of human data suggest a strong association between increased hepatic TG concentrations and insulin resistance, only a few basal studies on metabolic and cellular processes involved have been published. The primary research question addressed in this thesis was therefore whether increased hepatic TG concentrations induced by any cause, by definition, lead to (hepatic) insulin resistance.

Metabolism of the energy-bearing molecules glucose, fatty acids and TGs is closely linked in the liver and insulin plays a pivotal role in this interaction. In the liver, glucose is stored as glycogen, but this organ is also capable to produce glucose. Energy needed for *de novo* glucose production (gluconeogenesis) can be generated by hepatic oxidation of fatty acids (β-oxidation). On the other hand, the liver can convert glucose into fatty acids and TGs (*de novo* lipogenesis) and subsequently secrete TGs in very low density lipoprotein (VLDL) particles. In fed conditions, when blood glucose levels rise, the blood glucose lowering hormone insulin is secreted by the pancreas. Insulin inhibits hepatic glucose production (HGP), enhances conversion of glucose into glycogen, stimulates *de novo* lipogenesis, and inhibits gluconeogenesis and VLDL secretion.

Defects in the actions of insulin on lipid and glucose metabolism are thought to result in various hallmarks of insulin resistance, the metabolic syndrome and diabetes mellitus type 2. The work described in this thesis addresses the (patho)physiological effects of hepatic steatosis on these metabolic pathways in several animal models. The models used were the leptin-deficient *ob/ob* mouse, pharmacological activation of the liver X receptor, pharmacological inhibition of β-oxidation, and pharmacological inhibition of glucose-6-phosphatase.

## The *ob/ob* mouse

Leptin-deficient *ob/ob* mice are obese, hyperinsulinemic, hyperglycemic, have hepatic steatosis, and are a commonly employed animal model of diabetes mellitus type 2. In the studies described in chapter 2, we used novel stable isotope techniques to quantify the hepatic glucose fluxes and metabolic clearance rate (MCR) of glucose in *ob/ob* mice compared to wild-type, lean littermates. These studies showed that HGP did not differ between *ob/ob* and lean mice, despite higher plasma insulin levels in the *ob/ob* mice. Because the elevated plasma insulin levels did not suppress HGP, the hepatic steatosis of *ob/ob* mice is by definition associated with decreased insulin sensitivity of hepatic glucose metabolism. Previous experiments of our laboratory showed that hyperinsulinemia did not suppress the VLDL production rate in *ob/ob* mice (14). Thus, the *ob/ob* mouse is an useful animal model of hepatic steatosis associated with insulin resistance of both hepatic glucose and lipid metabolism. In the studies described in chapter 4, insulin sensitivity of glucose metabolism was studied in more detail in *ob/ob* mice. For this, we used the ‘golden standard’ to determine insulin sensitivity: the hyperinsulinemic euglycemic clamp. In this technique, mice receive an infusion with insulin to achieve a stable, relatively high plasma concentration of the hormone.

Upon the hyperinsulinemia thus created, blood glucose will start to decrease. To maintain euglycemia, a glucose solution is also infused. The infusion rate of the latter solution can be adjusted so that euglycemic conditions are met. The glucose infusion rate is a measure of the insulin sensitivity of, in this case, the mouse. Addition of [U-$^{13}$C]-glucose to the solutions allowed us to calculate HGP and MCR. Hyperinsulinemia suppressed HGP by 94% in lean mice but by only 48% in *ob/ob* mice. This underscores insulin resistance of hepatic glucose metabolism in *ob/ob* mice. Moreover, hyperinsulinemia increased MCR 5.5-fold in lean mice, whereas no increase was seen in *ob/ob* mice, indicating insulin resistance of peripheral glucose metabolism.

In conclusion, hepatic steatosis in *ob/ob* mice is associated with decreased insulin sensitivity of hepatic glucose and lipid metabolism. Concerning glucose metabolism, *ob/ob* mice are also insulin resistant in the periphery. Because plasma FFA levels are elevated in *ob/ob* mice, peripheral lipid metabolism (*e.g.*, insulin-mediated suppression of lipolysis) is probably also affected. Although *ob/ob* mice are commonly used in diabetic and obesity research, one should carefully interpret results gathered with these animals because leptin deficiency is not a normal cause of obesity, hepatic steatosis and insulin resistancein humans. Only few families are known that are homozygous for a mutation in the leptin gene (15,16). In general, monogenetic obesity in humans is scarce (17). A monogenic animal model of obesity and/or hepatic steatosis is therefore probably not the best model to study hepatic steatosis. On the other hand, because *ob/ob* mice are commonly used, detailed and physiologically-relevant information about this model is available.

For the latter reason, we used *ob/ob* mice in the studies described in chapter 5 to assess the metabolic consequences of the iminosugar derivative N-(5'-adamantane-1'-yl-methoxy)-pentyl-1-deoxynojirimycin (AMP-DNM), a novel inhibitor of glucosylceramide transferase. When administered to *ob/ob* mice, AMP-DNM normalised elevated tissue glucosylceramide levels and improved insulin sensitivity of both peripheral tissues and the liver. Because ceramide levels were not affected, these data strongly suggest that ceramide metabolites may be involve din the link between increased fatty acids and insulin resistance.

## Pharmacological activation of the liver X receptor

The liver X receptor (LXR) is a member of the 48-member superfamily of nuclear receptors that can activate or inhibit transcription of genes upon their activation by, in most cases, a small-molecular ligand. Oxysterols are oxygenated metabolites of cholesterol and are considered the endogenous ligands of LXR. The synthetic LXR ligands T0901317 and GW3965 are useful tools in LXR-related research. Upon activation, LXR stimulates transcription of various genes, *i.e.*, those encoding enzymes involved in the transport of cholesterol from the peripheral tissues to the liver and in secretion of cholesterol into bile and subsequently the feces (18). Clinical application of synthetic LXR ligands is hampered by the fact that LXR also stimulates transcription of genes encoding enzymes involved in *de novo* lipogenesis. Administration of synthetic LXR ligands to rodents results in severe hepatic steatosis (19). In the studies described in chapter 3, T0901317-induced hepatic steatosis was accompanied by a more than 2-fold induction of VLDL production. The secretion of large, TG-rich VLDL particles completely accounted for this increase. It is known that large VLDL particles will finally be converted in the very atherosclerotic small, dense low density lipoprotein (LDL) particles. In the studies described in chapter 4, hyperinsulinemic euglycemic clamp techniques and stable isotopes were used to study the effects of LXR activation on glucose metabolism and insulin sensitivity. GW3965-induced hepatic steatosis was not associated with reduced insulin sensitivity of hepatic glucose metabolism: in LXR-

ligand treated mice, HGP was suppressed by 86% and hepatic glucose fluxes were not affected. In *ob/ob* mice, in contrast, LXR activation resulted in slightly improved insulin sensitivity of peripheral glucose metabolism. This improvement was mainly due to effects of the LXR ligand on adipose tissue.

In conclusion, LXR-induced hepatic steatosis is not associated with decreased insulin sensitivity of hepatic glucose metabolism. So far, no studies have been performed to investigate the effects of LXR activation on insulin sensitivity of lipid metabolism, *e.g.*, peripheral lipolysis and hepatic VLDL production. The studies described in chapter 4 were among the first to show that hepatic steatosis per se does not lead to (hepatic) insulin sensitivity. Moreover, the studies from chapters 3 and 4 and those of others (19) were among the first to show that clinical use of pharmacological broad-acting LXR ligands as anti-atherosclerotic or anti-diabetic drugs, is hampered by their undesirable side effects. Potential application of LXR modulators in diabetes treatment will require the development of gene- and/or organ-specific compounds.

## Pharmacological inhibition of β-oxidation

In fasted conditions, dietary glucose supply is absent. In this condition, the body largely depends on the liver for maintaining euglycemia because only the liver (and the kidney to a small extent) is capable to produce glucose. For this, glycogen is broken down into glucose, but gluconeogenesis is also facilitated. Fatty acid β-oxidation, acoording the textbook biochemistry, yields the energy needed for gluconeogenesis. With low insulin levels, lipolysis of peripheral (adipose) TGs is enhanced and the free fatty acids (FFAs) thus generated are transported to the liver. Fatty acids are broken down in the β-oxidation process localised to hepatic mitochondria. Transport of fatty acids over the mitochondrial membranes, controlled by carnitine palmitoyl transferase (CPT) -1 and –2, is considered rate-limiting in the β-oxidation processes. In the studies described in chapter 6 we showed that pharmacological CPT1 inhibition with tetradecylglycidic acid (TDGA) resulted in severe microvesicular hepatic steatosis and hypoglycemia upon fasting. VLDL production rates did not differ between the TDGA-treated and control mice and hyperinsulinemic euglycemic clamps equally suppressed VLDL production in control and treated mice. Moreover, hepatic intracellular insulin signaling was not affected upon TDGA treatment. In conclusion, hepatic steatosis due to pharmacological inhibition of β-oxidation is not associated with reduced insulin sensitivity of hepatic lipid metabolism.

In humans, most fatty livers show large lipid droplets, referred to as macrovesicular steatosis. Only few clinical fatty liver diseases are microvesicular, *i.e.*, fatty livers due to disturbances in β-oxidation. For instance, medium chain acyl-CoA dehydrogenase (MCAD) deficiency, assumed to be the most common inherited disorder of fatty acid metabolism (20) is associated with microvesicular fat accumulation. Upon fasting, MCAD deficient patients develop lethargy which may proceed into coma or sudden death (20). It is not known whether this syndrome is associated with insulin resistance.

## Pharmacological inhibition of glucose-6-phosphatase

In the past, our laboratory has performed detailed studies with S4048, a pharmacological inhibitor of glucose-6-phosphate translocase (G6PT). G6PT is an enzyme of the glucose-6-phosphatase (G6Pase) complex and its inhibition leads to a condition similar to glycogen storage disease type I (GSDI). In rats, inhibition of G6Pase resulted in increased *de novo*

lipogenesis and hepatic steatosis (21,22). Remarkably, the VLDL production rate was not affected in S4048-treated animals (22). The studies described in chapter 7 showed that S4048 treatment also resulted in hepatic steatosis in mice. This condition was not associated with decreased intracellular hepatic insulin signaling, *i.e.*, phosphorylation of protein kinase B (PKB) upon insulin injection. Although it was expected that the transcription factor carbohydrate responsive element binding protein (ChREBP) was involved in the development of hepatic steatosis, the translocation of this transcription factor to the nucleus was not enhanced. The increased phosphorylation and activity of AMP-activated protein kinase (AMPK) upon S4048 treatment might, in part, be responsible for this phenomenon. However, expression of genes encoding proteins involved in *de novo* lipogenesis was clearly increased upon S4048-treatment, in a LXR-independent fashion.

It is known that liver enlargement in GSDI patients is not solely the result of glycogen accumulation, but also of increased TG levels due to enhanced *de novo* lipogenesis (23). To study the role of ChREBP in S4048-induced hepatic steatosis and its role in the livers of GSDI patients, more experiments should be performed, especially with ChREBP knockout mice (24).

## Overall conclusion

From the studies described in this thesis, it is clear that hepatic TG accumulation per se does not necessarily negatively interfere with insulin sensitivity of hepatic glucose and lipid metabolism. However, one should be aware that all studies described, except those with the *ob/ob* mice, were conducted in mice with "short-term" hepatic steatosis. Moreover, all fatty livers were the result of manipulation of *de novo* lipogenesis and/or β-oxidation. Various research groups have performed studies with other mouse models of hepatic. For instance, hepatic steatosis in CD36 knockout mice is due to increased FFA flux to the liver and associated with decreased insulin sensitivity (25,26). In addition, decreased hepatic TG levels in hormone sensitive lipase (HSL) knockout mice resulted in improved insulin sensitivity (27). Comparison of these latter studies with the ones described in this thesis strengthens the overall conclusion that hepatic steatosis in mice is not always associated with insulin resistance. Upon prolonged fasting, for instance during the night, humans also develop hepatic steatosis as a result of increased FFA flux from peripheral tissue to the liver. So far, it has not been reported that this "daily fatty liver" is associated with insulin resistance. Also in mice, 16-h fasting did not show an effect on insulin sensitivity of HGP, despite increased hepatic TG levels (28).

### *Properties of the fat droplets*

In the future, more studies should be done to precisely determine the effects lipid droplet-associated factors. First, the size of the fat droplets within the cells, *i.e.*, the metabolic differences between macro- and microvesicular hepatic steatosis, might play a role. At first sight, one could argue that because larger fat droplets use more cytosolic space, they can harm more of the intracytosolic processes, for instance insulin signaling. Smaller droplets, as seen in livers of patients with β-oxidation disorders, use less cytosolic space and leave the intracellular organelles more intact. However, microvesicular hepatic steatosis implies a more severe disease than macrovesicular steatosis (reviewed by Fromenty and Pessayre (29)). The reason for this is probably the fact that the main cause of microvesicular hepatic steatosis, impairment of mitochondrial β-oxidation, is a severe condition itself, with clinical features such as hypoglycemia, hyperammonemia, brain disorders and eventually death.

Secondly, different sources of fatty acids within the droplets might have different effects. As described above, there are differences in (hepatic) insulin sensitivity in animals with hepatic steatosis due to high fat diets and hepatic steatosis due to enhanced *de novo* lipogenesis and/or reduced β-oxidation. The localisation of the lipids within the liver might play a role herein. In the periportal zone dietary fatty acid accumulation co-localises with processes involved in gluconeogenesis and β-oxidation. Glycolysis and lipogenesis are presumably located predominantly in the perivenous zone (30). It is of importance to notice that diabetes-associated steatosis is predominantly present in the perivenous zones of the liver.

Thirdly, as already discussed, the duration of the hepatic steatosis and duration of adverse effects might be related. *Ob/ob* mice, for instance, have a life-long hepatic steatosis and also suffer from the adverse effects of this condition. Considering this, the effects of hepatic TG concentrations seen in the CD36 and HSL knockout mice (25-27) might also be the result of life-long fat accumulation. As mentioned in the introduction of this thesis, inflammation is the major factor in the transition of simple hepatic TG accumulation towards fibrosis and cirrhosis (31). Adipose tissue and tissues with excessive TG concentrations are intrinsically inflammatory active, and thus longer existing hepatic steatosis might, via inflammatory molecules, disturb intra- and extrahepatic insulin sensitivity.

The structure of the fatty acids (saturated, monounsaturated, and polyunsaturated) could differentially affect hepatic metabolism and insulin sensitivity, This is, of course, closely related to the source of the fatty acids. Various studies have shown that polyunsaturated fatty acids (PUFAs) are healthier: they suppress activity of the major lipogenesis regulatory factor sterol-regulatory element-binding protein-1c (SREBP-1c), antagonize LXR and improve plasma TG profiles (32). Moreover, PUFAs reduce *de novo* lipogenesis via inhibition translocation and activation of ChREBP (33). Studies with monounsaturated fatty acids also showed less negative effects compared to saturated fatty acids (34).

### *Extrahepatic regulation*

Next to the intrahepatic aspects mentioned, other organs might also play roles in the (lack of) association between hepatic steatosis and insulin resistance, for instance, via the adipocyte-derived hormones leptin and adiponectin. Deficiency of leptin is associated with both obesity and insulin resistance (14-16;35). Low plasma adiponectin levels are associated with the development of insulin resistance (36). Administration of adiponectin to mice resulted in decreased liver TG concentrations and increased insulin sensitivity (37). Next to these hormones, the brain can also influence hepatic insulin-mediated effects (38-40). In conclusion, complex interactions between endocrine, metabolic, and transcriptional pathways are involved in TG-induced hepatic insulin resistance, as recently discussed by Den Boer *et al.* (41).

### *What does lead to what?*

The question that remains unsolved is whether hepatic steatosis is caused by insulin resistance, or that hepatic steatosis predisposes for insulin resistance. The majority of studies described in this thesis started with the assumption that insulin resistance is a result of hepatic steatosis, or, in other words, that fatty acids, TGs and/or their metabolites and derivatives interfere with insulin signaling. However, this seemed be true in *ob/ob* mice only. In other studies, in which endogenous fatty acid fluxes were manipulated, hepatic TG concentration showed a negative correlation with the insulin sensitivity (25-27,42). More studies focussing on the role of fatty acid derivatives ceramide and glycosphingolipid will be necessary to gain insight about their role in mediating peripheral and hepatic insulin signaling and insulin sensitivity.

The two "hits" hypothesis (43) suggests that hepatic steatosis is due to reduced (peripheral) insulin sensitivity. Upon decreased insulin sensitivity, insulin-mediated suppression of lipolysis is hampered and, as a result, more fatty acids are directed to the liver. As a result, these fatty acids are stored upon esterification as TGs but will also enhance β-oxidation via activation of peroxisome proliferator activated receptor α (PPARα). Finally, this will result in enhanced gluconeogenesis and HGP. In the future, experiments need to be performed with rodents upon a high fat diet to study the time-course of development of insulin resistant. Everybody agrees that obesity and hepatic steatosis upon enhanced caloric intake and reduced physical activity is truly associated with insulin resistance and type 2 diabetes mellitus in humans (2-4,11,44,45). In the experiments with mice upon a high fat diet, the questions that need answers are (i) whether different diets, *i.e.*, different fatty acid compositions, cause more or less insulin resistant, and (ii) whether hepatic steatosis firstly affects peripheral or hepatic insulin sensitivity resistance In studies with non-diabetic patients with NAFLD, it became clear that NAFLD is associated with reduced insulin sensitivity of the periphery, not of the liver. For instance, hyperinsulinemia suppressed HGP in both NAFLD and control subjects, but insulin-enhanced glucose disposal was severely in the NAFLD subjects compared to controls (46) Using the hyperinsulinemic clamp technique, Marchesini *et al.* (9) also demonstrated a reduction of insulin-mediated glucose disposal in NAFLD.

In conclusion, fatty liver per se is not associated with reduced insulin sensitivity of hepatic glucose and lipid metabolism. Factors related with duration, inflammatory grade, fatty acid composition, and size of the fat droplets might influence severity of the fatty liver and its association with other clinical symptoms, for instance insulin resistance and diabetes mellitus type 2.

## References

1. Clark, JM, Brancati, FL, Diehl, AM. The prevalence and etiology of elevated aminotransferase levels in the United States. Am J Gastroenterol 98: 960-967, 2003

2. Zimmet, P, Shaw, J, Alberti, GMM. Preventing type 2 diabetes and the dysmetabolic syndrome in the real world: a realistic view. Diabet Med 20: 693-702, 2003

3. Zimmet, P, Alberti, KGMM, Shaw, J. Global and societal implications of the diabetes epidemic. Nature 414: 782-787, 2001

4. King, H, Aubert, RE, Herman, WH. Global burden of diabetes, 1995-2025. Prevalence, numerical estimates, and projections. Diabetes Care 21: 1414-1431, 1998

5. Marceau, P, Biron, S, Hould, F-S, Marceau, S, Simard, S, Thung, SN, Kral, JG. Liver pathology and the metabolic syndrome X in severe obesity. J Clin Endocrinol Metab 84: 1513-1517, 1999

6. Marchesini, G, Brizi, M, Morselli-Labata, AM, Bianchi, G, Bugianesi, E, McCullough, AJ, Forlani, G, Melchionda, N. Association of nonalcoholic fatty liver disease with insulin resistance. Am J Med 107: 450-455, 1999

7. Cortez-Pinto, H, Camilo, ME, Baptista, A, De Oliveira, AG, De Moura, MC. Non-alcoholic fatty liver: another feature of the metabolic syndrome? Clin Nutr 18: 353-358, 1999

8. Sanyal, AJ, Campbell-Sargent, C, Mirshahi, F, Rizzo, WB, Contos, MJ, Sterling, RK, Luketic, VA, Shiffman, ML, Clore, JN. Nonalcoholic steatohepatitis: association of insulin resistance and mitochondrial abnormalities. Gastroenterology 120: 1183-1192, 2001

9. Marchesini, G, Brizi, M, Bianchi, G, Tomassetti, S, Bugianesi, E, Lenzi, M, McCullough, AJ, Natale, S, Forlani, G, Melchionda, N. Nonalcoholic fatty liver disease. A feature of the metabolic syndrome. Diabetes 50: 1844-1850, 2001

10. Seppälä-Lindroos, A, Vehkavaara, S, Häkkinen, A-M, Goto, T, Westerbacka, J, Sovijärvi, A, Halavaare, J, Yki-Järvinen, H. Fat accumulation in the liver is associated with defects in insulin suppression of glucose production and serum free fatty acids independent of obesity in normal men. J Clin Endocrinol Metab 87: 3023-3028, 2002

11. Dowse, G, Zimmet, P. The thrifty genotype in non-insulin dependent diabetes. BMJ 306: 532-533, 1993

12. Executive summary of the third report of the National Cholesterol Education Program (NCEP) Expert Panel on detection, evaluation and treatment of high blood cholesterol in adults (Adult Treatment Panel III). JAMA 285: 2486-2497, 2001

13. Alberti, KG, Zimmet, PZ. Definition, diagnosis and classification of diabetes mellitus and its complications. Part 1: diagnosis and classification of diabetes mellitus provisional report of a WHO consultation. Diabet Med 15: 539-553, 1998

14. Wiegman, CH, Bandsma, RHJ, Ouwens, M, van der Sluijs, FH, Havinga, R, Boer, T, Reijngoud, D-J, Romijn, JA, Kuipers, F. Hepatic VLDL production in *ob/ob* mice is not stimulated by massive de novo lipogenesis but is less sensitive to the suppressive effects of insulin. Diabetes 52: 1081-1089, 2003
15. Montague, CT, Farooqi, IS, Whitehead, JP, Soos, MA, Rau, H, Wareham, NJ, Sewter, CP, Digby, JE, Mohammed, SN, Hurst, JA, Cheetman, CH, Early, AR, Barnett, AH, Prins, JB, O'Rahilly, S. Congenital leptin deficiency is associated with severe early-onset obesity in humans. Nature 387: 903-908, 1997
16. Farooqi, IS, Matarese, G, Lord, GM, Keogh, JM, Lawrence, E, Agwu, C, Sanna, V, Jebb, SA, Perna, F, Fontana, S, Lechler, RI, DePaoli, AM, O'Rahilly, S. Beneficial effects of leptin on obesity, T cell hyporesponsiveness, and neuroendocrine/metabolic dysfunction of human congenital leptin deficiency. J Clin Invest 110: 1093-1103, 2002
17. Farooqi, IS, O'Rahilly, S. Monogenic obesity in humans. Annu Rev Med. 56: 443-458, 2005
18. Repa, JJ, Mangelsdorf, DJ. The liver X receptor gene team: Potential new players in atherosclerosis. Nature Med 8: 1243-1248, 2002
19. Schultz, JR, Tu, H, Luk, A, Repa, JJ, Medina, JC, Li, L, Schwendner, S, Wang, S, Thoolen, M, Mangelsdorf, DJ, Lustig, KD, Shan, B. Role of LXR in control of lipogenesis. Genes Dev 14:2831-2838, 2000
20. Roe CR, Ding J. Mitochondrial fatty acid oxidation disorders. In: The metabolic & molecular bases of inherited disease. Scriver CR, Beaud*et al*, Sly WS, Valle D, Eds. New York, McGraw-Hill, 2001, p. 2297-2326
21. van Dijk, TH, van der Sluijs, FH, Wiegman, CH, Baller, JFW, Gustafson, LA, Burger, H-J, Herling, AW, Kuipers, F, Meijer, AJ, Reijngoud, D-J. Acute inhibition of hepatic glucose-6-phosphate does not affect gluconeogenesis but directs gluconeogenic flux toward glycogen in fasted rats. J Biol Chem 276: 25727-25735, 2001
22. Bandsma, RHJ, Wiegman, CH, Herling, AW, Burger, H-J, ter Harmsel, A, Meijer, AJ, Romijn, JA, Reijngoud, D-J, Kuipers, F. Acute inhibition of glucose-6-phosphate translocator activity leads to increased de novo lipogenesis and development of hepatic steatosis without affecting VLDL production in rats. Diabetes 50: 2591-2597, 2001
23. Bandsma, RHJ, Rake, JP, Visser, G, Neese, RA, Hellerstein, MK, van Duyvenvoorde, W, Princen, HMG, Stellaard, F, Smit, GPA, Kuipers, F. Increased lipogenesis and resistance of lipoproteins to oxidative modification in two patients with glycogen storage disease type Ia. J Pediatr 140: 256-260, 2002
24. Iizuka, K, Bruick, RK, Liang, G, Horton, JD, Uyeda, K. Deficiency of carbohydrate response element-binding protein (ChREBP) reduces lipogenesis as well as glycolysis. Proc Natl Acad Sci USA 101: 7281-7286, 2004
25. Goudriaan, JR, Dahlmans, VEH, Teusink, B, Ouwens, DM, Febbraio, M, Maassen, JA, Romijn, JA, Havekes, LM, Voshol, PJ. CD36 deficiency increases insulin sensitivity in muscle, but induces insulin resistance in the liver in mice. J Lipid Res 44: 2270-2277, 2003
26. Goudriaan, JR, den Boer, MAM, Rensen, PCN, Febbraio, M, Kuipers, F, Romijn, JA, Havekes, LM, Voshol, PJ. CD36 deficiency in mice impairs lipoprotein lipase-mediated triglyceride clearance. J Lipid Res 46: 2175-2181, 2005
27. Voshol, PJ, Haemmerle, G, Ouwens, DM, Zimmermann, R, Zechner, R, Teusink, B, Maassen, JA, Havekes, LM, Romijn, JA. Increased hepatic insulin sensitivity together with decreased hepatic triglyceride stores in hormone-sensitive lipase-deficient mice. Endocrinology 144: 3456-3462, 2003
28. Heijboer, AC, Donga, E, Voshol, PJ, Dang, Z-C, Havekes, LM, Romijn, JA, Corssmit, EPM. Sixteen hours of fasting differentially affects hepatic and muscle insulin sensitivity in mice. J Lipid Res 46: 582-588, 2005
29. Fromenty, B, Pessayre, D. Inhibition of mitochondrial beta-oxidation as a mechanism of hepatotoxicity. Pharmacol Ther 67:101-154, 1995
30. Jungermann, K. Zonation of metabolism and gene expression in liver. Histochemistry 103: 81-91, 1995
31. Jansen, PLM. Nonalcoholic steatohepatitis. Neth J Med 62: 217-224, 2004
32. Ou, J, Tu, H, Shan, B, Luk, A, DeBose-Boyd, RA, Bashmakov, Y, Goldstein, JL, Brown, MS. Unsaturated fatty acids inhibit transcription of the sterol regulatory element-binding protein-1c (SREBP-1c) gene by antagonizing ligand-dependent activation of LXR. Proc Natl Acad Sci USA 98: 6027-6032, 2001
33. Dentin, R, Benhamed, F, Pégorier, J-P, Foufelle, F, Viollet, B, Vaulont, S, Girard, J, Postic, C. Polyunsaturated fatty acids suppress glycolytic and lipogenic genes through the inhibition of ChREBP nuclear translocation. J Clin Invest 115: 2843-2854, 2005
34. Vessby, B, Uusitupa, M, Hermansen, K, Riccardi, G, Rivellese, AA, Tapsell, LC, Nälsén, C, Berglund, L, Louheranta, A, Rasmussen, BM, Calvert, GD, Maffetone, A, Pedersen, E, Gustafsson, I-B, Storlien, LH. Substituting dietary saturated for monounsaturated fat impairs insulin sensitivity in healthy men and women: The KANWU study. Diabetologia 44: 312-319, 2001
35. Garg, A, Misra, A. Hepatic steatosis, insulin resistance, and adipose tissue disorders. J Clin Endocrinol Metab 87: 3019-3022, 2002
36. Berg, AH, Combs, TP, Du, X, Brownlee, M, Scherer, PE. The adipocyte-secreted protein Acrp30 enhances hepatic insulin action. Nature Med 7: 947-953, 2001
37. Xu, A, Wang, Y, Keshaw, H, Xu, LY, Lam, KSL, Cooper, GJS. The fat-derived hormone adiponectin alleviates alcoholic and nonalcoholic fatty liver diseases in mice. J Clin Invest 112: 91-100, 2003

38. Pocai, A, Lam, TKT, Gutierrez-Juarez, R, Obici, S, Schwartz, GJ, Bryan, J, Aguilar-Bryan, L, Rossetti, L. Hypothalamic $K_{ATP}$ channels control hepatic glucose production. Nature 434: 1026-1031, 2005
39. Buettner, R, Patel, R, Muse, ED, Bhanot, S, Monia, BP, McKay, R, Obici, S, Rossetti, L. Severe impairment in liver insulin signaling fails to alter hepatic insulin action in conscious mice. J Clin Invest 115: 1306-1313, 2005
40. Okamoto, H, Obici, S, Accili, D, Rossetti, L. Restoration of liver insulin signaling in Insr knockout mice fails to normalize hepatic insulin action. J Clin Invest 115: 1314-1322, 2005
41. den Boer, M, Voshol, PJ, Kuipers, F, Havekes, LM, Romijn, JA. Hepatic steatosis: a mediator of the metabolic syndrome. Lessons from animal models. Arterioscler Thromb Vasc Biol 24: 644-649, 2004
42. Division of Vascular and Connective Tissue Research, TNO Prevention and Health. Annual Report 2001
43. Day, CP, James, OF. Steatohepatitis: a tale of two "hits"? Gastroenterology 114: 842-845, 1998
44. Kahn, BB, Flier, JS. Obesity and insulin resistance. J Clin Invest 106: 473-481, 2000
45. Haffner, S, Taegtmeyer, H. Epidemic obesity and the metabolic syndrome. Circulation 108: 1541-1545, 2003
46. Bugianesi, E, Gastaldelli, A, Vanni, E, Gambino, R, Cassader, M, Baldi, S, Ponti, V, Pagano, G, Ferrannini, E, Rizzetto, M. Insulin resistance in non-diabetic patients with non-alcoholic fatty liver disease: sites and mechanisms. Diabetologia 48: 634-642, 2005










# Nederlandse samenvatting

Het toenemend vóórkomen van overgewicht gaat hand in hand met een toename in het vóórkomen van diabetes mellitus type 2 op steeds jongere leeftijd. Patiënten met diabetes mellitus type 2 hebben een verhoogd bloedglucose als gevolg van het feit dat de alvleesklier geen of onvoldoende insuline produceert. Deze situatie wordt voorafgegaan door een afgenomen insulinegevoeligheid van het lichaam, een conditie die insulineresistentie wordt genoemd. Insulineresistentie is onderdeel van het 'metabool syndroom', een verzameling van factoren die ieder op zich een verhoogde kans geven op het krijgen van hart- en vaatziekten. Componenten van het metabool syndroom, naast insulineresistentie, zijn onder andere overgewicht, een verhoogde bloeddruk en een verstoord plasma lipid profiel (teveel 'slecht' LDL-cholesterol en te weinig 'goed' HDL-cholesterol).

De lever is belangrijk in de regulering van het metabolisme van zowel koolhydraten (bijvoorbeeld glucose) als lipiden (bijvoorbeeld vetzuren). De lever kan glucose opslaan als glycogeen maar tevens glucose produceren en uitscheiden in de circulatie. Daarnaast is de lever in staat glucose om te zetten in triglycerides, energierijke moleculen die bestaan uit drie vetzuren gekoppeld aan glycerol. De lever kan vetzuren ook verbranden, hetgeen energie oplevert voor de gluconeogenese (de productie van glucose uit verschillende andere stoffen, zoals melkzuur en aminozuren). Tenslotte scheidt de lever triglycerides (en cholesterol) uit in de circulatie in zogenaamde 'very low density lipoprotein' (VLDL) deeltjes.

Insuline is het bloedglucose-verlagende hormoon dat door de alvleesklier wordt uitgescheiden als reactie op toegenomen bloedglucose concentraties na een maaltijd. Insuline remt de glucoseproductie door de lever en stimuleert de opname van glucose door met name spieren en vetweefsel. In de lever stimuleert insuline de omzetting van glucose in glycogeen, vetzuren en triglycerides. Daarnaast onderdrukt insuline de uitscheiding van triglyceride-rijke VLDL-deeltjes. In het vetweefsel remt insuline de omzetting van de triglycerides in vetzuren en zorgt daarmee voor een daling van de hoeveelheid vrije vetzuren in het bloed. In gevaste toestand, wanneer de insulineconcentratie laag is, is de remming van de triglyceride-afbraak afgenomen waardoor meer vrije vetzuren de lever bereiken. Deze vetzuren worden, zoals al vermeld, deels verbrand om aan de energiebehoefte van het lichaam te voldoen en deels in de lever opgeslagen in de vorm van triglycerides.

Het continue transport van vetzuren en triglycerides dat (mede) wordt gereguleerd door insuline is van groot belang voor de energiehuishouding van het lichaam. Veranderingen in dit transport gaan gepaard met veranderingen in de triglyceride concentratie van de lever. Verhoogde hepatische triglyceride concentraties (vette lever of hepatische steatose) zijn geassocieerd met diverse klinische aandoeningen en kunnen een voorloper zijn van ernstige aantastingen van de lever, zoals cirrose. Uit klinische studies is naar voren gekomen dat hepatische steatose is geassocieerd met insulineresistentie en diabetes mellitus type 2.

In de studies beschreven in dit proefschrift werd met behulp van diermodellen het effect van hepatische steatose op (insulinegevoeligheid van) het glucose- en vetmetabolisme in de lever onderzocht. Op deze manier is getracht de onderliggende moleculaire processen die ten grondslag liggen aan de verminderde insulinegevoeligheid bij hepatische steatose op te helderen.

## *Ob/ob* muizen

Leptine is een hormoon dat door het vetweefsel wordt geproduceerd en onder andere het verzadigingsgevoel reguleert. *Ob/ob* muizen zijn leptine-deficiënt en eten derhalve meer dan gewone muizen. *Ob/ob* muizen zijn in vergelijking met gewone muizen zwaarder en hebben een hoger bloedglucose en meer triglycerides in hun bloed. Daarnaast hebben *ob/ob* muizen een hepatische steatose en zijn ze in ernstige mate insulineresistent. Onduidelijk was of de verhoogde bloedglucoses een gevolg zijn van een verhoogde hepatische glucoseproductie en/of een afgenomen glucose opname. In hoofdstuk 2 is gebruik gemaakt van stabiele isotopen om de glucose fluxen in de lever en de glucoseklaring te vergelijken tussen *ob/ob* en normale, slanke muizen. De netto hepatische glucoseproductie in *ob/ob* muizen verschilde niet met die van de controle muizen: de verhoogde glucosespiegels bleken primair het gevolg van een afgenomen glucoseklaring. Het feit dat de hepatische glucoseproductie, ondanks verhoogde insulinespiegels, niet verschilde tussen *ob/ob* muizen en slanke muizen duidt echter wel op hepatische insulineresistentie van de *ob/ob* muizen.

Het glucosemetabolisme en de insulinegevoeligheid in *ob/ob* muizen is in hoofdstuk 4 in meer detail onderzocht. De 'gouden standaard' voor het vaststellen van insulinegevoeligheid is de hyperinsulinemische euglycemische clamp. Hierbij krijgen wakkere, vrij bewegende muizen een intraveneuze infusie met insuline. Als gevolg hiervan stijgen de insulineconcentraties en door deze 'hyperinsulinemie' zal de bloedglucose concentratie dalen. Om een normale bloedglucose te handhaven (euglycemie) wordt een tweede oplossing met glucose geïnfundeerd. De hoeveelheid glucose die geïnfundeerd moet worden om euglycemie te handhaven is een maat voor de insulinegevoeligheid van de muis. Wordt aan de hyperinsulinemische euglycemische clamp een kleine hoeveelheid [U-$^{13}$C]-glucose toegevoegd, dan is het mogelijk om de hepatische en perifere insulinegevoeligheid te meten. De hepatische gevoeligheid is de mate van onderdrukking van de glucoseproductie onder invloed van hyperinsulinemie, de perifere gevoeligheid de toename van de glucoseklaring.

In *ob/ob* muizen leidde hyperinsulinemie tot een 48% onderdrukking van glucoseproductie door de lever, terwijl dit percentage in de normale muizen 94% was. Dit onderstreept de insulineresistentie van het hepatische glucosemetabolisme in *ob/ob* muizen. Daarnaast bleek dat hyperinsulinemie leidde tot een vijfvoudige toename van de glucoseklaring in de slanke muizen terwijl er geen effect viel waar te nemen in de *ob/ob* muizen.

De *ob/ob* muizen zijn dus een goed model voor insulineresistentie van het hepatische glucosemetabolisme in associatie met een hepatische steatose. Eerdere experimenten in het laboratorium Kindergeneeskunde hebben daarnaast insulineresistentie van het hepatische lipid metabolisme in *ob/ob* muizen aangetoond.

Ceramide en glycosphingolipiden hebben, net als triglycerides, vetzuren als bouwstenen. Er is gesuggereerd dat ceramide en/of glycosphingolipiden ook betrokken zijn bij de insulineresistentie geassocieerd aan de hepatische steatose in *ob/ob* muizen. De aandacht gaat daarbij vooral uit naar de glycosphingolipiden omdat zij samen met de insulinereceptor in grote concentraties aanwezig zijn in het celmembraan in zogenaamde 'rafts'. In de studies beschreven in hoofdstuk 5 is onderzocht of behandeling van *ob/ob* muizen met AMP-DNM, een nieuwe farmacologische remmer van de omzetting van ceramide in glycosphingolipiden, effect had op de insulinegevoeligheid. Het bleek dat zowel de perifere als de hepatische insulinegevoeligheid verbeterde na AMP-DNM behandeling. Omdat de ceramide concentraties van de weefsels niet veranderden na behandeling terwijl de glycosphingolipid concentraties daalden, kan geconcludeerd worden dat niet ceramide maar glycosphingolipiden betrokken zijn bij insulineresistentie.

## Farmacologische activering van de liver X receptor

De liver X receptor (LXR) is een transcriptiefactor: een eiwit dat de transcriptie van genen reguleert. Oxysterolen zijn metabolieten van cholesterol en zij kunnen door middel van binding aan LXR de activiteit van LXR stimuleren en daarmee dus ook de transcriptie van diverse genen beïnvloeden. Cholesterol reguleert via deze oxysterolen zijn eigen stofwisseling want LXR stimuleert de transcriptie van genen betrokken bij het 'reverse cholesterol transport': transport van cholesterol van plaatsen waar het kwalijke gevolgen kan hebben (zoals atherosclerotische plaques in bloedvaten) via de lever naar de darm en de feces. Uit experimenten met synthetische LXR liganden blijkt dat LXR tevens de transcriptie stimuleert van genen betrokken in de productie van vetzuren en triglycerides, zowel direct als indirect. De indirecte stimulering verloopt via 'sterol-regulatory element-binding protein-1c' (SREBP-1c), een belangrijke regulator van de vetzuur en triglyceride synthese in de lever. Farmacologische LXR activering heeft dus niet alleen positieve effecten (toename van het 'reverse cholesterol transport'), maar als bijwerking leververvetting. In de studies beschreven in hoofdstuk 3 is onderzocht of LXR-geïnduceerde hepatische steatose leidt tot veranderingen in de VLDL-productie. Het geven van de synthetische LXR ligand T0901317 gedurende vijf dagen aan muizen resulteerde in een meer dan tweevoudige toename van de VLDL-triglyceride productie. De uitscheiding van grote, triglyceride-rijke VLDL deeltjes kon deze toename volledig verklaren. Uit de literatuur is bekend dat grote VLDL deeltjes meer atherosclerotische eigenschappen hebben dan kleine VLDL deeltjes.

Ondanks het feit dat hepatische steatose en de uitscheiding van grote VLDL deeltjes, samen met insulineresistentie, karakteristiek zijn voor het metabool syndroom, zijn onlangs enkele studies gepubliceerd waarin synthetische LXR-liganden anti-diabetische eigenschappen worden toegedicht. We onderzochten de effecten van farmacologische LXR activering op glucose metabolisme en insulinegevoeligheid in meer detail en hiertoe werden normale, slanke muizen en *ob/ob* muizen gedurende 10 dagen behandeld met de synthetische LXR ligand GW3965. Hoofdstuk 4 beschrijft de experimenten met de hyperinsulinemische euglycemische clamp in combinatie met stabiele isotopen. In normale muizen veranderde de insulinegevoeligheid en het hepatische glucosemetabolisme niet na farmacologische LXR activering. In behandelde *ob/ob* muizen werd wel een lichte verbetering van de insulinegevoeligheid waargenomen, maar dit bleef nog ver achter bij de insulinegevoeligheid in normale muizen. LXR activering bleek weinig tot geen effect te hebben op de glucose fluxen in de levers van *ob/ob* muizen, maar de glucoseklaring onder hyperinsulinemische condities was wel verbeterd in deze muizen. Uit metingen van de genexpressie bleek dit effect vooral gelokaliseerd te zijn in het vetweefsel.

Concluderend kan gesteld worden dat de marginale anti-diabetische effecten van synthetische LXR liganden in *ob/ob* muizen het gevolg zijn van een lichte toename in de glucose opname door het vetweefsel. Opvallend is dat LXR activering leidt tot hepatische steatose die niet gepaard gaat met een afgenomen insulinegevoeligheid.

## Farmacologische remming van de β-oxidatie

Om onder niet-gevoede omstandigheden aan de energiebehoefte te voldoen is het lichaam afhankelijk van vetzuurverbranding door de lever, een proces dat β-oxidatie wordt genoemd en plaats vindt in de mitochondria. Verbranding van vetzuren levert de energie die nodig is voor de synthese van glucose uit diverse substraten zoals lactaat (gluconeogenese). Carnitine palmitoyl transferase-1 (CPT1) transporteert vetzuren over de mitochondriale membranen en is derhalve cruciaal in de eerste stappen van de β-oxidatie. Farmacologische remming van CPT1 met behulp van tetradecylglycidic acid (TDGA) heeft tot gevolg dat vetzuren in de lever minder snel verbrand worden en in sterkere mate opgeslagen worden als triglyceride. Behandeling van muizen met TDGA tijdens vasten resulteert dan ook in microvesiculaire hepatische steatose, zoals vermeld in hoofdstuk 6. In muizen met een TDGA-geïnduceerde hepatische steatose werd de insulinegevoeligheid van de VLDL-productie onderzocht, wederom met behulp van de hyperinsulinemische euglycemische clamp. Tevens werd de intracellulaire insuline signaleringscascade onderzocht. De hepatische steatose had geen invloed op de insulinegevoeligheid: insuline onderdrukte nog steeds de VLDL-productie en stimuleerde de intracellulaire signaleringscascade.

Kortom, de acute TDGA-geïnduceerde hepatische steatose is niet geassocieerd met een afgenomen insulinegevoeligheid van het vetmetabolisme in de lever. Daarnaast bewijst deze studie dat de hoeveelheid lever triglyceride niet per se de VLDL-productie hoeft te beïnvloeden. In andere studies in ons laboratorium, onder andere met *ob/ob* muizen, is dit eveneens aangetoond.

## Farmacologische remming van glucose-6-fosfaat translocase

Naast SREBP-1c en LXRα is de 'carbohydrate responsive element binding protein' (ChREBP) een derde factor die transcriptie stimuleert van genen betrokken bij de synthese van vetzuren en triglycerides. Opvallend is dat de activiteiten van ChREBP en SREBP-1c elkaar grotendeels overlappen en dat LXRα naar alle waarschijnlijkheid zowel de transcriptie van SREBP-1c als de activiteit van ChREBP positief beïnvloedt. In de lever wordt de activiteit van ChREBP gestimuleerd door xylulose-5-fosfaat, een metaboliet van glucose. Eerdere experimenten van ons laboratorium toonden aan dat ratten die waren behandeld met S4048, een remmer van het enzym glucose-6-fosfaat translocase, een hepatische steatose ontwikkelden in combinatie met toegenomen glucose-6-fosfaat concentraties in de lever. In de studies beschreven in hoofdstuk 7 is in muizen onderzocht welke transcriptie factor (SREBP-1c, LXRα of ChREBP) betrokken is bij de S4048-geinduceerde transcriptie van 'lipogene' genen. Analyse van de genexpressies na S4048-infusie toonde aan dat niet SREBP-1c, maar ChREBP hiervoor verantwoordelijk was. De sterk toegenomen glucose-6-fosfaat concentraties in de lever wezen hier eveneens op. Infusie van S4048 bij LXRα-knockout muizen resulteerde eveneens in een sterke toename van de expressie van de lipogene genen.

Geconcludeerd kan worden dat remming van glucose-6-fosfatase resulteerde in een toename van glucose-6-fosfaat en dat dit de activiteit van ChREBP beïnvloedde. ChREBP, en niet SREBP-1c of LXRα, was vervolgens betrokken in de daarop volgende inductie van de expressie van lipogene genen. Patiënten met glycogeen stapelings ziekte type I (GSDI) hebben een defect in het glucose-6-fosfatase eiwit en tevens een verhoogde hepatische lipogenese. Een verhoogde ChREBP activiteit is naar alle waarschijnlijkheid in GSDI-patiënten de oorzaak van de hepatische steatose.

## De rol van transcriptiefactoren in diabetische dyslipidemie

In dit proefschrift is een aantal factoren naar voren gekomen dat van invloed is op de expressie van genen betrokken bij het vetzuur en triglyceride metabolisme: LXR, SREBP-1c en ChREBP. Omdat deze factoren een grote rol spelen in het hepatische vetmetabolisme en hun activiteit en/of transcriptie wordt geactiveerd door vetten, glucose en insuline (factoren die in hoge concentraties voorkomen in diabetische patiënten), lijkt het niet meer dan logisch om te onderzoeken wat hun rol is in diabetes en daaraan gerelateerde verstoringen in het vetmetabolisme. Hoofdstuk 8 geeft een overzicht van wat bekend is over de rol van de drie factoren in de aan diabetes gerelateerde verstoring in plasma lipiden profielen (diabetische dyslipidemie). Opvallend is dat zeer weinig bekend is over het relatieve belang van LXR, SREBP-1c en ChREBP in het bepalen van de insulinegevoeligheid van het glucose- en vetmetabolisme in de lever. Over de effecten van de transcriptiefactoren op de (insulinegevoeligheid van de) VLDL-productie is derhalve ook weinig bekend. Onderzoek met farmacologische activatoren, manipulaties met voedingsmiddelen en het gebruik van muizen die deficient zijn voor één of meer van de genoemde transcriptiefactoren zijn dan ook zeer gewenst om meer hierover te weten te komen.

## Algemene conclusie

Aan de hand van de studies in dit proefschrift kan geconcludeerd worden dat de hoeveelheid triglycerides in de lever op zich weinig zegt over de mate van hepatische insulinegevoeligheid: zowel de LXR- als de TDGA-geïnduceerde hepatische steatose zijn niet geassocieerd met een afname van de hepatische insulinegevoeligheid. Andere factoren zijn naar alle waarschijnlijk belangrijke determinanten voor het wel of niet optreden van insulineresistentie. Te denken valt bijvoorbeeld aan de oorsprong van de triglycerides, de duur van de hepatische steatose, de locatie van de triglycerides in de lever en de grootte van de vetdruppels in de cellen. Hoofdstuk 5 laat daarnaast zien dat ook andere vetzuur-bevattende lipiden, zoals de glycosphingolipiden, insulineresistentie kunnen induceren.

Uit klinische studies is gebleken dat obesitas, hepatische steatose, insulineresistentie en diabetes mellitus type 2 zeer nadrukkelijk met elkaar geassocieerd zijn. Daarom is verder fysiologisch onderzoek naar onderliggende moleculaire processen aan te raden. Te denken valt bijvoorbeeld aan onderzoek naar de rol van de genoemde transcriptiefactoren, de effecten van een dieet met veel vetten (oorzaak nummer één van diverse metabole problemen in de Westerse samenleving) en de effecten van duur en ‘type’ van de hepatische steatose. Technieken die hierbij een rol kunnen spelen zijn de al genoemde hyperinsulinemische euglycemische clamp en het gebruik van stabiele isotopen om de hepatische glucose, vetzuur en triglyceride fluxen te meten. Qua analytische bepalingen valt in dit kader te denken aan het meten van de veranderingen in genexpressie met behulp van RT-PCR en micro-arrays, maar omdat het belangrijk is om verder te kijken dan de genen, is het ook aan te raden veel aandacht te besteden aan het kwantificeren van de fosforylerings status van (signaal-transductie-) eiwitten, het meten van de daadwerkelijke enzym activiteiten en de concentraties van metabolieten en eindproducten in het hepatische vet- en glucosemetabolisme. Kortom, een volledige integratie van het toepassen van hightech *in vivo* technieken naast het meten van verschillende specifieke parameters zal in de (nabije) toekomst meer informatie over de daadwerkelijke rol van hepatische vetstapeling in de insulinegevoeligheid opleveren. Tevens zal meer informatie over de rol van (hepatische) lipiden in de modulering van insulinegevoeligheid bijdragen aan de ontwikkeling van dieetgerelateerde en farmacologische strategieën voor de behandeling en/of preventie van insulineresistentie.

# Dankwoord

De afgelopen vier jaar (en een beetje) heb ik met heel veel plezier gewerkt aan de studies die beschreven staan in dit proefschrift. Mijn plezier in het werk kwam niet alleen door het boeiende onderwerp, maar vooral ook door de goede sfeer op het laboratorium kindergeneeskunde. Mocht ik de afgelopen jaren wat hebben geleerd, dan is het wel dat werk in het algemeen en wetenschap in het bijzonder gebaat is bij een goede, prettige en motiverende samenwerking tussen collega's.

De grote initiator voor, tijdens en zelfs na mijn promotieonderzoek is niet geheel toevallig tevens de man die grotendeels verantwoordelijk is voor het creëren van die prettige sfeer op het laboratorium kindergeneeskunde: Folkert Kuipers. Zonder zijn rustige maar honderd procent gedreven inzet voor alles wat met wetenschapsbeoefening te maken heeft was dit proefschrift nooit geworden wat het nu is. Aan de ene kant wees hij mij op nieuwe studies, of schoof mij deze in de schoenen, en aan de andere kant wist hij in no-time altijd net die mooie zin te vinden waar ik niet op kon komen. Folkert, bedankt voor al je vertrouwen. Wie weet ga ik de met sigarenlucht doordrenkte correcties nog missen in de VS.

Aansluitend moet ik bij deze (nogmaals) mijn excuses maken bij Louis Havekes en Hans Romijn voor het feit dat ik toch de voorkeur gaf aan Groningen. Louis en Hans, ik ben blij dat jullie als mede-promotores willen optreden, wat gezien jullie wezenlijke bijdragen aan meerdere hoofdstukken van dit proefschrift niet meer dan vanzelfsprekend is!

Volgens mij is Theo van Dijk dé man van het *in vivo* glucose metabolisme in Nederland! Helaas moet hij dat zelf nog even meer doorhebben. Ik heb het geluk gehad veel met hem samen te mogen werken. Als men ons tegen kwam op ADL08 met de muisjes gezellig op tafel, soepje erbij, kopje koffie en de Sudoku's, zullen niet velen hebben gedacht dat er baanbrekende *in vivo* technieken werden ontwikkeld of uitentreuren toegepast. Theo, laat ik eens eerlijk zijn: zonder jou geen 'clamp' of 'MIDA' en dus ook een veel dunner proefschrift. Eén woord is dus op zijn plaats: bedankt!

Bij *in vivo* experimenten kun je in ons laboratorium niet om Rick Havinga heen, maar dat blijkt helemaal niet erg te zijn. Rick, zonder jouw operatieskills, het gevraagd en ongevraagd meedenken bij experimenten was dit boekje een droom gebleven danwel een nachtmerrie geworden. PS. De Havinga-Kuipers roddeluurtjes zal ik nog gaan missen in Dallas!

Onderzoek doe je niet alleen maar als team. Ik vond het erg prettig (en zeer productief) om als kersverse AIO door mede-AIO's op gang te worden geholpen. Baukje, ik had me geen betere start van mijn wetenschappelijke carrière kunnen bedenken dan onze gezamenlijke LXR experimenten. Bedankt voor die fantastische vliegende start. Robert, ook jouw hulp bij experimenten en het theoretisch en praktisch meedenken had ik, achteraf gezien, niet kunnen missen. Daarnaast ben de overige mede-energie AIO's veel dank verschuldigd voor de prettige samenwerking op diverse fronten. Terry, Maaike en Marijke, bedankt voor de uren gezelschap op ADL08, de hulp bij de experimenten en analyses en jullie motiverende aanwezigheid. Dat wordt een aantal mooie proefschriften!

Ik heb het geluk gehad te mogen werken met zowel één van de beste geneeskunde als wel Life Science studenten. Jildou en Annelies, ik heb stiekem veel van jullie geleerd. Succes met jullie verdere carrières. Vergeet de wetenschap niet, want mensen zoals jullie zijn er volgens mij voor geknipt.

Ik ben blij om nog steeds (in de wandelgangen) te vernemen dat Y2.117 AIO-kamer nummer 1 is en blijft! Coen, Janine, Thierry, Antonella, Anja, Alberto en Laura: bedankt!, merci!, grazie!, ¡gracias! voor de fantastische sfeer, het beantwoorden van telefoontjes, de goede gesprekken en het meedenken in al die jaren! En natuurlijk, ook de 'andere' AIO's, postdocs en stafleden van zowel Kindergeneeskunde als MDL maakten de afgelopen tot wat

ze waren: meer dan geslaagd! Bedankt (in volstrekt willekeurige volgorde) Leonie, Jelske, Tineke, Jaap, Torsten, Christian, Frans, Esther, Hester, Niels, Jan Peter, Anniek (2x), Yan, Renate, Jenny, Titia, Martijn, Axel, Jannes, Krzysztof, Hans, Marieke, Jacqueline, Rebekka, Sandra, Ekkehard, Anna, Ewa, Gloria, Han (2x), Klaas-Nico, Thomas, Uwe, Frans, Henkjan, Edmond, Karin, Dirk-Jan (zou ik nog zonder hem naar een congres durven?), Feike, Klary, Marion en Roel.

Analisten zijn de kurk waarop een goed laboratorium drijft. Zonder mijn met een gouden strotje gezegende 'overbuurman' Renze, de PCR-o-fiel Fjodor, Anke, Vincent, Henk, Nicolette, Janny, Juul, Frank, Albert, Mariska, Janette, Fiona, Lisette, Kyrjon, Manon, Hermi, Pim (2x), Klaas, Theo ↑, Trijnie, Fettie, Jenny, Janneke (2x), Marius, Marianne, Karloes en Desiree zou het een ontzettende puinhoop worden in de laboratoria van Kindergeneeskunde, MDL, metabole ziekten en proteomics.

We hebben nog meer vrienden in Leiden. Bedankt Margriet en Peter voor jullie ondersteuning in de afgelopen jaren. Tot slot een staande ovatie voor de verzorgers van de hoofdpersonen in dit proefschrift: de dierverzorgers van ADL08. Harm, Ralph, Diana en Natasha, bedankt voor jullie goede zorgen!

Tot zover het werk… Laten we niet vergeten dat dingen buiten het werk vaak veel belangrijker zijn. Al sinds het begin van mijn Groningse loopbaan mag ik me gelukkig prijzen met een fantastische groep vrienden. Van de ene kant uit de groep ex-Dizkartianen verenigd in Nevadí (die naam zien we ook niet vaak meer, hè). Zonder hen was Groningen nooit zo leuk geweest dat ik er nog wel wat jaartjes tegenaan wilde gooien. Bedankt! Arnout, ik ben blij je als vriend (uit deze groep) mijn paranimf wilt zijn. Laten we maar eens een lange woensdagavond proosten dat de vriendschap nog lang mag blijven duren en dat de afstand Heiligerlee en Dallas geen belemmering zal zijn.

Daarnaast de zeven medefarmaceuten! Ik vind het telkens weer fantastisch om te zien dat elke 'farmaboy' op geheel eigen wijze met farmacie bezig is. Mannen, ik prijs me gelukkig met zo'n groep waarin ik niet alleen mijn eigen wetenschappelijk gezwets kwijt kan, maar ook nog eens verneem hoe het er aan toe gaat in apotheek, ziekenhuis en industrie.

Ronald, broertje, ik vind het fantastisch dat je mijn paranimf wilt zijn! Op de ons eigen nuchtere manier laten we toch regelmatig aan elkaar blijken hoe gesteld we op elkaar zijn. Dat ik dat nu nog eens extra kan bestendigen tijdens mijn promotie maakt het alleen maar beter op!

Mijn ouders hebben me altijd zo opgevoed dat ik gedurende het bewandelen van mijn eigen weg toch het beste uit mezelf kan halen. Vaders, moeder, met jullie nuchtere maar natuurlijke manier van opvoeden hebben jullie zeer nadrukkelijk aan de wieg gestaan van dit proefschrift. Bedankt in het vertrouwen, de kansen en de vrijheid!

Er is iemand in mijn leven die me meer lief is dan wie of wat dan ook. Maaike, ik ben blij dat je onvoorwaardelijk in mij blijft geloven en zelfs zo gek bent om je studie minimaal een jaar in de ijskast te leggen om met mij mee te gaan naar het grote onbekende Amerika. Waaraan zou ik al dit geluk te danken hebben? Trouwens, had ik je vandaag al gezegd…

En dan is het nu tijd voor een drankje… Mocht ik iemand vergeten zijn, dan drinkt die er maar één extra op mijn kosten.

Aldo

# Curriculum vitae

Aldo Grefhorst werd op 25 oktober 1974 geboren in Apeldoorn. In dezelfde plaats voltooide hij eerst de HAVO en daarna het VWO. In 1994 begon hij met de studie Farmacie aan de Rijksuniversiteit Groningen. Het afstudeeronderzoek werd uitgevoerd binnen de vakgroep Farmacokinetiek en Drug Delivery van prof. dr. D.F.K. Meijer en betrof onderzoek naar de effectiviteit van de ACE-remmer captopril bij proteïnurie in ratten met adriamycine-geïnduceerd nierfalen. In 1999 studeerde Aldo af en begon hij met de opleiding tot apotheker. Het apothekersdiploma behaalde hij in 2001.

In 2001 begon Aldo bij de vakgroep kindergeneeskunde van de medische faculteit van de Rijksuniversiteit Groningen als onderzoeker in opleiding binnen het ZonMW-project getiteld ‘Hepatic steatosis is not a benign condition: molecular pathophysiology of glucose and lipid metabolism in steatosis’ (nr. 903-39-291). Dit project is een samenwerking tussen Leiden en Groningen. Prof. dr. J.A. Romijn en prof. dr. L.M. Havekes zijn de projectleiders in Leiden en prof. dr. F. Kuipers is de projectleider in Groningen.

Vanaf februari 2006 zal Aldo als postdoc werkzaam zijn bij de afdeling Molecular Genetics van de University of Texas Southwestern Medical Center in Dallas, Texas, USA. Zijn Amerikaanse research wordt door het Ter Meulen Fonds van het Koninklijk Nederlandse Akademie voor Wetenschappen gesubsidieerd en heeft als titel ‘De rol van ‘lipogene transcriptie factoren’ in de regulatie van de insuline gevoeligheid van het glucose en vet metabolisme in de lever.’

# List of publications

**A. Grefhorst**, B.M. Elzinga, P.J. Voshol, T. Plösch, T. Kok, V.W. Bloks, F.H. van der Sluijs, L.M. Havekes, J.A. Romijn, H.J. Verkade, F. Kuipers. Stimulation of lipogenesis by pharmacological activation of the liver X receptor leads to production of large, triglyceride-rich very low density lipoprotein particles. J Biol Chem. 2002: 277: 34182-34190.

R.H.J. Bandsma, **A. Grefhorst**, T.H. van Dijk, F.H. van der Sluijs, A. Hammer, D.J. Reijngoud, F. Kuipers. Enhanced glucose cycling and suppressed de novo synthesis of glucose-6-phosphate result in a net unchanged hepatic glucose output in ob/ob mice. Diabetologia. 2004: 47: 2022-2031.

**A. Grefhorst**, J. Hoekstra, T.G.J. Derks, D.M. Ouwens, J.F.W. Baller, R. Havinga, L.M. Havekes, J.A. Romijn, F. Kuipers. Acute hepatic steatosis in mice by blocking β-oxidation does not reduce insulin sensitivity of very-low-density lipoprotein production. Am J Physiol Gastrointest Liver Physiol. 2005: 289: G592-598.

D. Duran-Sandoval, B. Cariou, F. Percevault, N. Hennuyer, **A. Grefhorst**, T.H. van Dijk, F.J. Gonzalez, J.C. Fruchart, F. Kuipers, B. Staels. The farnesoid X receptor modulates hepatic carbohydrate metabolism during the fasting-refeeding transition. J Biol Chem. 2005: 280: 29971-19979.

**A. Grefhorst**, T.H. van Dijk, A. Hammer, F.H. van der Sluijs, R. Havinga, L.M. Havekes, J.A. Romijn, P.H. Groot, D.J. Reijngoud, F. Kuipers. Differential effects of pharmacological liver X receptor activation on hepatic and peripheral insulin sensitivity in lean and ob/ob mice. Am J Physiol Endocrinol Metab. 2005: 289: E829-E838

B. Cariou, K. van Harmelen, D. Duran-Sandoval, T. van Dijk, **A. Grefhorst**, E. Bouchaert, J.C. Fruchart, F.J. Gonzalez, F. Kuipers, B. Staels. Transient impairment of the adaptive response to fasting in FXR-deficient mice. FEBS Lett. 2005: 579:4076-80.

J.M. Aerts, R. Ottenhoff, **A. Grefhorst**, A.S. Powlson, M. van Eijk, T.H. van Dijk, F. Kuipers, J. Aten, J. Groener, A. Strijland, A.K. Groen, L. Boon, M.J. Serlie, H.P. Sauerwein, T. Wennekes, H.S. Overkleeft, J.K. Sethi, S. O'Rahilly, A.J. Meijer. Pharmacological inhibition of glucosylceramide synthase enhances insulin sensitivity: a novel therapeutic approach to insulin resistance. Submitted.

P. Costet, B. Cariou, G. Lambert, F. Lalanne, B. Lardeux, A.-L. Jarnoux, **A. Grefhorst**, B. Staels, M. Krempf. Hepatic PCSK9 expression is regulated by nutritional status via insulin and sterol regulatory-element binding protein 1c. Submitted.

B. Cariou, K. van Harmelen, D. Duran-Sandoval, T.H. van Dijk, **A. Grefhorst**, G. Torpier, J.-C. Fruchart, F.J. Gonzalez, F. Kuipers, B. Staels. The farnesoid X receptor modulates adiposity and peripheral insulin resistance. Submitted

G. van Dijk, K. de Vries, **A. Grefhorst**, F. Kuipers, J. Koolhaas, B. Buwalda. Psychosocial stress and dietary fat: towards an understanding of the neurological mechanisms underlying the metabolic syndrome. Submitted

T.G.J. Derks, T.H. van Dijk, **A. Grefhorst**, G.P.A. Smit, F. Kuipers, D.-J.Reijngoud. Acute inhibition of carnitine-palmitoyltransferase 1 (CPT-1) does not affect de novo synthesis of glucose-6-phosphate (G6P) in moderately fasted mice. In preparation

T.H. van Dijk, **A. Grefhorst**, M.H. Oosterveer, F.H. van der Sluijs, B. Staels, D.-J. Reijngoud, F. Kuipers. Whole body glucose metabolism is impaired in FXR-null mice. In preparation

**A. Grefhorst**, M. Schreurs, M.H. Oosterveer, R. Havinga, L.M. Havekes, J.A. Romijn, D.-J. Reijngoud, F. Kuipers. Induction of hepatic lipogenic gene expression upon pharmacological inhibition of glucose-6-phosphate translocase is independent of liver X receptor α. In preparation.

# Colour figures

On page 54:

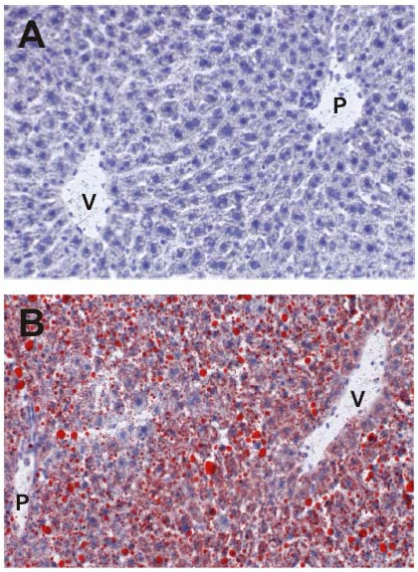


Figure 3.1. Uniform Oil-Red-O (ORO) staining for neutral fat in livers of T0901317-treated mice. No staining was observed in liver sections from male C57BL/6J mice receiving the solvent (A). Massive staining was found in liver sections from mice treated four days with 10 mg/kg of the LXR agonist T0901317 (B). V, central vein; P, portal vein. Original magnification 50x.

On page 110:

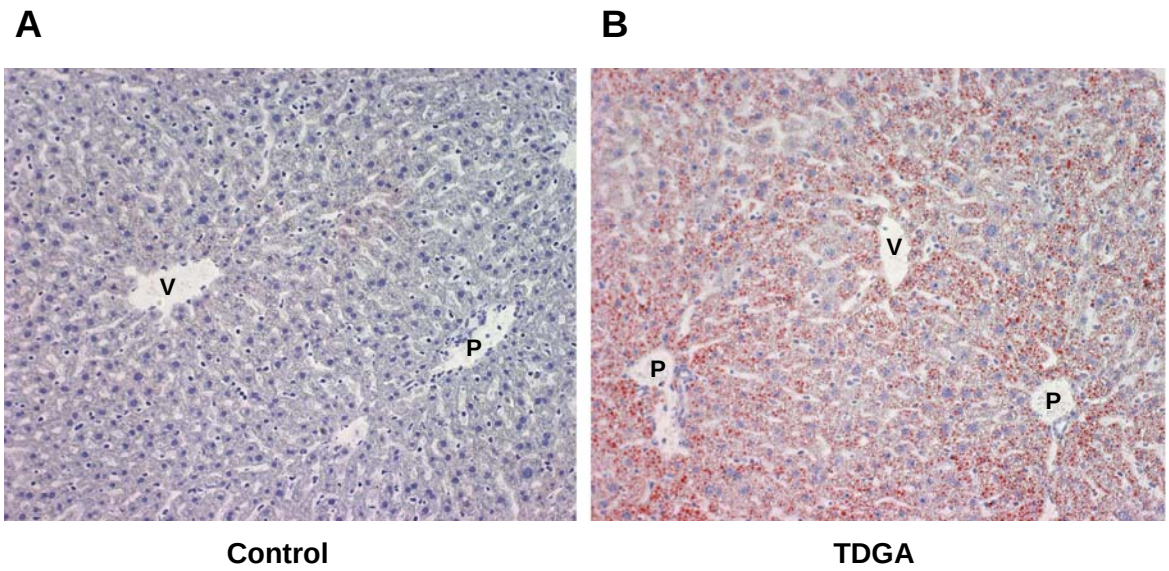


Figure 6.2. Oil-Red-O staining for neutral lipids in livers of mice treated with or without CPT1-inhibitor TDGA. V, central vein; P, portal vein.